Application of Atmospheric Cold Plasma to Improve Microbial Safety of Meat Products

by

Barun Kumar Yadav

A thesis submitted in partial fulfillment of the requirements for the degree of

Doctor of Philosophy

in

Bioresource and Food Engineering

Department of Agricultural, Food and Nutritional Science
University of Alberta

Abstract

Meat products, including ready-to-eat (RTE) ham, fresh poultry meat, and dry pet foods have been associated with several foodborne outbreaks and recalls, due to the occurrence of microbial pathogens such as *Listeria monocytogenes* and *Salmonella enterica* serovar Typhimurium. Elimination of these microbial pathogens on meat products is a challenging task. Atmospheric cold plasma (ACP) is a novel non-thermal technology that has attracted attention as an effective decontamination technique. The overall objective of this research was to evaluate the microbial inactivation efficacy of ACP for improving the high and low water activity (a_w) meat product safety, when it is integrated with other selected methods, and to study the influence of important product and process parameters on the inactivation efficacy of such integrated treatments.

In the first study, RTE ham was formulated with NaCl (1 % & 3 %) and with or without rosemary extract to evaluate the interaction effects of these ingredients with ACP treatment to achieve *L. innocua* inactivation on ham surface. Irrespective of the % NaCl and the rosemary extract content of ham, ACP treatment showed significant antibacterial effects in a short exposure time against *L. innocua* on the ham surface. The % NaCl content of ham and the presence of rosemary extract on the ham surface did not influence the antimicrobial efficacy of ACP treatment. A significant increase in lipid oxidation, product weight loss, and color changes were the major limitations of the open atmospheric cold plasma treatment. In the second study, ACP treatment was integrated with modified atmospheric packaging to achieve a higher antimicrobial efficacy, and the ham was formulated with preservatives and bacteriocins. The in-package gas composition had a significant influence on the antimicrobial efficacy of ACP. A significantly higher reduction in *L. monocytogenes* counts was observed when the in-package gas mixture contained oxygen. During 7 days of post-ACP treatment storage, the cell counts of *L. monocytogenes* were reduced to below

the detection limit. The presence of preservatives or bacteriocin in ham did not enhance the inactivation of *L. monocytogenes* during ACP treatment. This study suggested that post-ACP treatment storage time was an important parameter to achieve higher inactivation efficacy.

The underlying inactivation mechanisms were investigated in the third study, which revealed that *L. monocytogenes* cells were under high oxidative stress conditions with permeabilized membranes during post-ACP treatment storage. In the first 24 h of post-treatment storage, a significant percentage of the cell population lost their membrane integrity, but the esterase was active, which means cells were metabolically active. After 7 days of post-ACP treatment storage, a high percentage of cells lost their esterase activity and membrane integrity. During long-term post-treatment storage, cell membrane permeabilization was one of the major causes of the loss of culturability.

The potential applicability of in-package ACP treatment to inactivate *Salmonella* in low a_w pet foods was evaluated in the fourth study. The antimicrobial efficacy of ACP treatment against *Salmonella* in low a_w freeze-dried pet foods was affected by bacterial growth condition, microbial load, treatment time, post-ACP treatment storage time, and a_w, with some significant interaction effects between these parameters. *Salmonella* equilibrated to 0.13 a_w on pet food surface exhibited the greatest resistance to ACP treatment. The extended post-ACP treatment storage reduced the *Salmonella* counts below the detection limit in 0.54 a_w pet foods.

The final study focused on developing an integrated process, using sequential treatment of selected organic acids and ACP to reduce *S.* Typhimurium in fresh poultry meat. The sequential treatment of organic acids [lactic acid (LA) or gallic acid (GA)] followed by ACP led to significantly enhanced and rapid inactivation of *S.* Typhimurium. The probable mechanisms associated with the

inactivation of *S.* Typhimurium were due to the synergistically enhanced membrane permeabilization and membrane lipid oxidation. In addition, the sequential treatment of LA or GA with ACP significantly reduced the cell metabolic activity and affected the intracellular reactive oxygen species level of *S.* Typhimurium. The significantly greater inactivation of *S.* Typhimurium on poultry meat surface by the sequential combination of organic acids and ACP treatments compared to individual treatments demonstrated the potential application of this method to improve the microbial safety of fresh poultry meat. An ACP integrated organic acid misting and cooling process was designed to evaluate the simultaneous cooling and decontamination efficacies of this process for fresh meat and preliminary studies were performed.

This research shows the inactivation efficacy of the ACP integrated processes against foodborne pathogens in high and low a_w meat products. The knowledge gained in this research would help in further research and in development of ACP integrated processes for industrial application.

Preface

This thesis is an original work done by Barun Kumar Yadav at the Food Safety and Sustainability Engineering Lab at the University of Alberta under Dr. Roopesh Mohandas Syamaladevi. Thesis is written according to the guideline provided by the Faculty of Graduate Studies and Research, University of Alberta.

Chapter 3 of this thesis has been published as Yadav, B., Spinelli, A. C., Govindan, B. N., Tsui, Y. Y., McMullen, L. M., & Roopesh, M. S. (2019). Cold plasma treatment of ready-to-eat ham: Influence of process conditions and storage on inactivation of *Listeria innocua*. *Food Research International*, *123*, 276–285. https://doi.org/10.1016/j.foodres.2019.04.065

M. S. Roopesh, L. M. McMullen, Y. Y. Tsui, and B. Yadav conceptualized and designed the study and interpreted the results. B. Yadav and A. C. Spinelli together conducted microbiological experiments, collected data, and did data analysis. B. Yadav did quality and plasma characterization experiments and collected data. M. S. Roopesh, L. M. McMullen, and Govindan, B. N. helped in data analysis and interpretation. B. Yadav drafted the manuscript. M. S. Roopesh, L. M. McMullen, Govindan, B. N reviewed and edited the manuscript. M. S. Roopesh, L. M. McMullen, and Y. Y. Tsui acquired funding for the study.

Chapter 4 of this thesis has been published as Yadav, B., Spinelli, A. C., Misra, N. N., Tsui, Y. Y., McMullen, L. M., & Roopesh, M. S. (2020). Effect of in-package atmospheric cold plasma discharge on microbial safety and quality of ready-to-eat ham in modified atmospheric packaging during storage. *Journal of Food Science*, *85*(4), 1203–1212. https://doi.org/10.1111/1750-3841.15072

M. S. Roopesh, L. M. McMullen, Y. Y. Tsui, and B. Yadav conceptualized and designed the study and interpreted the results. B. Yadav and A. C. Spinelli together conducted microbial experiments and collected data. B. Yadav did quality and plasma characterization experiments and collected data. B. Yadav did data analysis. M. S. Roopesh, L. M. McMullen, and N. N. Misra helped in data analysis and interpretation. B. Yadav drafted the manuscript. M. S. Roopesh, L. M. McMullen, N. N. Misra reviewed and edited the manuscript. M. S. Roopesh, L. M. McMullen, and Y. Y. Tsui acquired funding for the study.

Chapter 5 has been prepared for submission as Yadav, B., & Roopesh, M. S. Inactivation mechanisms of *Listeria monocytogenes* during in-package atmospheric cold plasma treatment and post-treatment storage.

B. Yadav and M. S Roopesh conceptualized and designed the study. B. Yadav conducted the experiment, collected data, and performed stat analysis. B. Yadav wrote the draft manuscript. M. S Roopesh reviewed and edited the manuscript.

Chapter 6 of this thesis has been published as Yadav, B., & Roopesh, M. S. (2020). In-package atmospheric cold plasma inactivation of *Salmonella* in freeze-dried pet foods: Effect of inoculum population, water activity, and storage. *Innovative Food Science and Emerging Technologies*, *66*, 102543. https://doi.org/10.1016/j.ifset.2020.102543

B. Yadav and M. S Roopesh conceptualized and designed the experiment and methodology. Barun Yadav conducted the experiments, acquired data, and performed stat analysis. M. S Roopesh helped in results interpretation. Barun Yadav wrote the draft manuscript. M. S Roopesh reviewed and edited the manuscript.

Chapter 7 of this thesis has been published as Yadav, B., & Roopesh M.S (2022). Synergistically enhanced *Salmonella* Typhimurium reduction by sequential treatment of organic acids and atmospheric cold plasma and the mechanism study. Journal of *Food Microbiology, 104, 103976*. https://doi.org/10.1016/j.fm.2021.103976

B. Yadav and M. S Roopesh conceptualized and designed the experiment and methodology. Barun Yadav conducted the experiments, acquired data, and performed stat analysis. M. S Roopesh helped in results interpretation. Barun Yadav wrote the draft manuscript. M. S Roopesh reviewed and edited the manuscript.

I dedicated my dissertation work to my beloved father and mother

Bhagwani Yadav

&

Chandrakala Devi

Acknowledgments

I want to take this opportunity to express my immense gratitude and appreciation to all of those who directly and indirectly supported me in completing this scientific research work. First foremost, I wish to express my sincere thank you to my supervisor Dr. Roopesh Mohandas Syamaladevi. Thank you for providing me the opportunity to join your research lab in the first instance and allowing me to pursue my Ph.D. degree under your guidance. Thank you for your constant guidance and encouragement throughout my degree. Thank you for always allowing me to ask questions and opinions. I never had a second thought when it came to getting advice from you. Thank you for your constant efforts and valuable suggestions in completing my thesis work.

I would like to thank my thesis committee members, Dr. Lynn McMullen, and Dr. Ying Tsui. To Dr. Ying Tsui for always allowing me to ask questions and getting valued opinions on many occasions. Thank you for sharing your expert knowledge and stopping by my lab on many occasions to check on the experimental setup. Your approach to science beyond the lab has always inspired me, and it will stay with me forever. To Dr. Lynn for finding time out of your busy schedule to help plan and execute a research project. Thank you for providing me the opportunity to work in your lab alongside an intelligent and caring colleague. Also, I want to thank you for your time and effort in reviewing my research manuscripts and sharing your expert advice on manuscript editing and data presentation. Thank you both for all the expert advice, supports, and guidance in assisting me with my studies.

I would like to extend my thank you to my candidacy examination committee members, Dr. Marleny D. Aranda Saldana and Dr. Anastasia L. Elias, for their suggestions. Also, I am indebted to Dr. Feral Temelli for finding time to be a part of my final defense examination committee. Finally, I would like to thank Dr. Aubrey F Mendonca for agreeing to be the external examiner for

my thesis defense and for investing his time in evaluating my thesis. Thank you to Dr. Aja Reiger for her help in operating the flow cytometry.

I extend my sincerest thanks to Alberta Agriculture and Forestry, Alberta innovates, Alberta Livestock and Meat Agency, National Sciences and Engineering Research Council of Canada, and Mitacs accelerate Program for providing financial support for these projects.

My special thanks to Ana Spinelli for her help and support with the microbiological analysis to speed up my thesis work during the first year of my Ph.D. program. I would also like to thank my labmates, Amritha Jaya Prasad, Samir Subedi, Shreyak Chaplot, Alvita Mathias, Abdullahi Adam, Bina Gautam, Dr. Basheer Iqdiam, Dr. Lihui Du, Ehsan Feizollahi, Harleen Kaur Dhaliwal, Julia Bersukova, and Muhammad Faisal Arif, for their support and encouragements. My sincere thanks to my colleagues and friends, Brasathe Jeganathan, Yuan Fang, Zhiying Wang, Gautam Gaur, Bhavick Jani, Dhruv Sharma, Baltej Singh Rupal, and Sukhjit Singh, for their constant support and motivation. A special thanks to my dear friend Gurveer Kaur and Akshat Yadav for inspiring me to pursue my dream and for all the support.

I want to thank my wife, Rajani Bala. Thank you for providing me space, taking care of the baby, and moral support to complete the degree. I also would like to welcome my son Reyansh Yadav to become part of this incredible journey.

I especially would like to thank my parents, brother, and sister for their consistent emotional support and for encouraging me to follow my dream.

Table of Contents

List of Tables

List of Figures

List of Abbreviations

ACP	Atmospheric Cold Plasma
APJ	Atmospheric Plasma Jet
a_w	Water activity
CP	Cold Plasma
CFU	Colony forming unit
CDC	Centre for Disease Control
DBD	Dielectric Barrier Discharge
DNA	Deoxyribonucleic acid
DV	Daily Value
FDA	Food and Drug Administration
f	Frequency
GA	Gallic Acid
kV	kilovolt
kHz	kilohertz
LA	Lactic Acid
LED	Light Emitting Diode
MAP	Modified Atmospheric Packaging

MDA	Malondialdehyde
ND	Not Detected
OES	Optical Emission Spectroscopy
PI	Propidium iodide
PV	Peroxide Value
PBS	Phosphate Buffered Saline
RNA	Ribonucleic acid
RNS	Reactive Nitrogen Species
RONS	Reactive Oxygen and Nitrogen Species
ROS	Reactive Oxygen Species
RTE	Ready-to-Eat
TBA	Thiobarbituric acid
TSA	Tryptic Soy Agar
TSB	Tryptic Soy Broth
VSA	Vapor Sorption Analyzer

Chapter 1: General Introduction and Objectives

1.1 Introduction

Meat products are important sources of proteins, vitamins B, iron, and minerals (Boler & Woerner, 2017). Global meat consumption experienced a sharp rise by 58 % and reached 360 million tonnes, driven by population and economic growth in the past two decades (Weis, 2013; Whitnall & Pitts, 2019). Meat and meat products are ideal substrates for microbial growth, and they are highly susceptible to bacterial contamination, which can cause foodborne illnesses and outbreaks (Pothakos, Devlieghere, Villani, Björkroth, & Ercolini, 2015). Some of the major pathogens of concern associated with meat and meat products are *Campylobacter* species, *Salmonella enterica*, *Escherichia coli*, and *Listeria monocytogenes* (Heredia & García, 2018; Tack et al., 2019). Foodborne illnesses and outbreaks related to contaminated meat products, including high-moisture products like ready-to-eat (RTE) ham, fresh poultry meat, and low-moisture products like dry pet food pellets, have increased in the past years (Behravesh et al., 2010; CDC, 2012; Tack et al., 2019; Vieira & Boyer, 2019)

To ensure the safety of meat and meat-based products, the industry uses a range of decontamination strategies to eliminate microorganisms or control their growth. Some of the constituents of meat impart high sensitivity in terms of loss of sensory attributes when conventional thermal decontamination methods are used (Vinnikova, Synytsia, & Kyshenia, 2019; Zhou, Xu, & Liu, 2010). Microbial inactivation efficacies of non-thermal decontamination methods have been tested in recent years, including high pressure processing, irradiation, pulsed electric field, and atmospheric cold plasma (Albert, Braun, Saffaf, & Wiacek, 2021; Zhou et al., 2010). Among the non-thermal technologies, atmospheric cold plasma (ACP) treatment is a recent innovation to improve the safety and quality of fresh meat and RTE meat products. The unique

feature of ACP is its capability to generate a cocktail of chemically active species such as reactive oxygen and nitrogen species, while remaining at near ambient temperature, enabling its safe application to food products (Hoffmann et al., 2013; Misra and Jo, 2017). These reactive species exhibit antimicrobial properties and hence, ACP has a wide range of microbial decontamination applications on various food surfaces. The ACP treatment is a waterless decontamination approach, which leaves no chemical residue after treatments. In addition, the availability of flexible plasma generation devices and treatment modes of ACP make it easier to integrate with other conventional techniques to develop novel hurdle antimicrobial interventions.

The applicability of ACP treatment to decontaminate meat and meat products have been reported, including beef (Jayasena et al., 2015), bacon (Kim et al., 2011), pork (Fröhling et al., 2012), ham (Song et al., 2009), and chicken skin (Noriega, Shama, Laca, Díaz, & Kong, 2011). The results of these studies suggested that the antimicrobial efficacy of ACP is significantly affected by several parameters including product surface topography, water content/water activity of the product, gas medium, type of microorganism, operating power, plasma source, treatment time, and storage time. ACP treatment can result in quality changes, including lipid oxidation, product weight loss, and color change. The meat product safety during ACP treatment can be improved, and the quality changes can be controlled by optimizing ACP treatment parameters.

ACP can be integrated with other commonly used decontamination methods to achieve high antimicrobial efficacy (Chaplot et al., 2019; Cui, Wu, Li, & Lin, 2014; Trevisani et al., 2017; Kim et al., 2011). For instance, ACP integrated with mild heat, ultrasound, and organic acids showed synergistic antimicrobial effects (Liao et al., 2020). However, limited information is available on the microbial inactivation efficacy of ACP integrated treatments on meat products, including fresh poultry meat, RTE cooked ham, and dry pet foods. More research is required to understand the

influence of important parameters to achieve the highest microbial inactivation efficacy, when ACP is integrated with conventional microbial intervention methods.

A distinctive feature of ACP discharge is its ability to generate plasma inside a closed package containing food products. The reactive species inside the package can interact with the food products and these reactive species recombine into their natural state within nanoseconds to several hours. The in-package ACP treatment can also be integrated into industrial process lines as a post-package decontamination step (Misra, Yepez, Xu, & Keener, 2018).

Some common strategies for ensuring RTE cooked meat product safety include the use of preservatives and bacteriocins and modified atmosphere packaging (Horita et al., 2018). In-package ACP treatment can possibly be used along with these strategies for the decontamination of RTE meat products such as cooked ham. Previous studies reported the application of in-package ACP treatment to reduce *L. monocytogenes* on RTE meat (Rød, Hansen, Leipold, & Knøchel, 2012). During ACP treatment, the ingredients of RTE meat, including salt, essential oil, preservatives, and bacteriocins may interact with ACP reactive species, influencing the inactivation efficacy of ACP (Joshi et al., 2011; Smet et al., 2019). Also, the composition of gas used for modified atmosphere packaging also need to be considered because the gas composition can influence the ACP discharge chemistry and its microbial inactivation efficacy (Han et al., 2016; Misra et al., 2018). The ACP reactive species inside the package can have a lifetime in the nanoseconds to a few hours. These reactive species can interact with products and microbial pathogens during post-treatment storage and may lead to additional microbial inactivation and quality changes (Gavahian, Chu, Mousavi Khaneghah, Barba, & Misra, 2018; Han et al., 2016). Therefore, these factors need to be investigated to ensure maximum inactivation efficacy of in-package ACP treatment.

Low water activity (a_w) meat products, including dry pet foods, have been associated with *Salmonella* related outbreaks (Health Canada, 2012; CDC, 2012; Syamaladevi et al., 2016). *Salmonella* in low a_w foods exhibits high resistance to conventional thermal and non-thermal treatments (Finn et al., 2013; Prasad et al., 2019; Santillana Farakos et al., 2013). In-package ACP treatment can potentially reduce *Salmonella* in low a_w pet food products, attributed to the antimicrobial properties of reactive species inside the package. Product factors (e.g., a_w) and process factors (e.g., type of gas mixture inside the package, treatment and storage time) can influence the *Salmonella* reduction efficacy of in-package ACP treatment. The influence of these factors needs to be investigated to optimize the in-package ACP treatment for low a_w meat food products.

In poultry meat industry, a diverse range of organic acids are used to decontaminate fresh meat. However, stringent regulatory requirements on the maximum allowable concentration of organic acids and their short exposure time on product surfaces limit their antimicrobial effects (Dinçer & Baysal, 2004; Mani-López, García, & López-Malo, 2012; Sohaib, Anjum, Arshad, & Rahman, 2016). Several studies suggested that combining physical treatment such as UV light and irradiation with mild concentrations of food grade organic acids can synergistically enhance bacterial inactivation (Cap et al., 2020; Oliveira, Cossu, Tikekar, & Nitin, 2017). Recently, Chaplot et al. (2019) demonstrated the potential benefits of integrating ACP with peracetic acid to enhance *S.* Typhimurium inactivation on poultry meat surfaces. More information is required to understand the antimicrobial efficacy of ACP treatment integrated with different organic acids on fresh meat products. Also, the mechanisms associated with the synergistic antimicrobial efficacy of such integrated treatments need to be investigated.

1.2 Hypotheses

The ACP treatment can reduce the foodborne pathogens associated with fresh and processed meat products and can be integrated to conventional food processing operations. The microbial inactivation efficacy of ACP will depend on a number of food product and process parameters. The ACP generated reactive species can interact with meat food product components (e.g., lipids) and ingredients (e.g., preservatives), affecting their antimicrobial efficacy. In the case of low-moisture meat products like freeze-dried pet foods, the a_w of the product can influence the microbial inactivation efficacy of ACP, as the resistance of microorganisms to antimicrobial treatments is dependent on a_w of the food matrix. Process parameters including temperature, type of gas medium, and treatment mode (open atmosphere vs in-package treatment) will influence the type of ACP generated reactive species, their concentration and stability, hence the antimicrobial efficacy of ACP. Some of the ACP generated reactive species can have a lifetime of up to a few hours, so in a closed environment, they can interact with microorganisms for an extended period, causing additional microbial inactivation during storage. A sequential integrated treatment of organic acid followed by ACP will achieve higher inactivation efficacy compared to individual treatments due to their synergistic antimicrobial actions on microorganisms.

1.3 Objectives

The overall objective of this research was to evaluate the microbial inactivation efficacy of ACP for improving the high and low a_w meat product safety when it is integrated with other selected methods and to study the influence of important product and process parameters on the inactivation efficacy of such integrated treatments.

1.3.1 Specific objectives are:

1. To investigate the effect of product factors, ACP process parameters and post-treatment storage on the reduction of *Listeria innocua* on RTE ham (Chapter 3).
2. To investigate the effect of gas composition and RTE ham formulations on the inactivation of *Listeria monocytogenes* and ham quality during in-package ACP treatment and post-treatment storage (Chapter 4).
3. To understand the mechanisms of inactivation of *Listeria monocytogenes* during in-package ACP treatment and post-treatment storage (Chapter 5).
4. To investigate the inactivation efficacy of in-package ACP treatment against *Salmonella* in meat based freeze-dried pet foods (Chapter 6).
5. (a) To investigate the efficacy of ACP integrated with organic acid treatment to reduce *S.* Typhimurium in fresh poultry meat and the inactivation mechanisms. (b) To develop an ACP integrated organic acid misting and cooling process for fresh poultry meat (Chapter 7).

This research focuses on integrating ACP treatment with the most frequently used microbial intervention methods in the meat industry to enhance bacterial pathogen inactivation. *Listeria monocytogenes* were selected in this research to study their survival during in-package ACP treatment and post-treatment storage, as they can grow and survive in the environment of meat processing facilities and are associated with recalls of RTE meat. *L. innocua* was selected as a surrogate of *L. monocytogenes. Salmonella* Typhimurium has been associated with recalls of low-moisture foods, hence was selected in this study to evaluate their survival in freeze-dried pet foods during in-package ACP treatment.

Chapter 2: Literature Review

2.1 Meat and meat-based food products

Meat and meat-based food products are important sources of proteins, iron, vitamins B, and other nutrients and mineral (Boler & Woerner, 2017). People prefer to eat meat products because of their good taste, flavor, and they provide desirable high-quality proteins in a regular diet to support health. Consumption of 100 g of cooked meat offers almost 50 % of the daily value (DV) of protein based on a 2000 calories diet (Boler & Woerner, 2017). Over the past 20 years, global meat consumption has increased by 58 % and reached 360 million tonnes (Whitnall & Pitts, 2019). Population and economic growth are the major drivers of increased meat consumption. Globally, the average per capita meat consumption doubled from 23 kg in 1961 to 43 kg in 2009 (Weis, 2013). The average per capita meat consumption quantities in Europe and North America were around 80 kg and 100 kg, respectively (Hannah and Roser, 2017). However, among food commodities, meat and meat-based food products have been found to be the least trusted by consumers because of safety issues (Misra & Jo, 2017).

Meat food safety and quality issues have always been a concern for food industry, government authorities, and consumers. This challenge arises because fresh meat is perishable with a short shelf life and highly susceptible to bacterial contamination. To increase the shelf life of meat, it can be transformed into products with longer durability (Horita et al., 2018). A range of processed meat products with different nutritional compositions and sensory attributes have been manufactured and marketed in the past years. Among processed meat products, ready-to-eat (RTE) products are an important class of meat products and gained relevance in recent years, driven by consumer demand for convenient food (Brunner, van der Horst, & Siegrist, 2010; Horita et al.,

2018). However, RTE-cooked meat products can be contaminated during the preparation processes including slicing, handling, and packaging.

2.2 Foodborne illness overburden

Foodborne illness due to consumption of contaminated food is a global public health issue, with annually 600 million cases and 420,000 deaths (WHO, 2015) worldwide. Approximately 4 million (1 out of 8 individuals) cases of illnesses, 11,500 hospitalizations, and 240 deaths are reported every year in Canada because of foodborne pathogens (Public Health Agency of Canada, 2015). Food products of animal origin are one of the major sources for foodborne pathogens such as *Campylobacter* species, *Salmonella enterica*, *Escherichia coli*, and *Listeria monocytogenes* (Heredia & García, 2018). An estimated 42 % of the reported foodborne illnesses (in the USA between 1998 to 2008) was associated with foods of animal origin, in which poultry meat products accounted for 22 % (Painter et al., 2013).

2.3 Microbial challenges associated with ready-to-eat cooked ham

Raw meat used for the preparation of ready-to-eat (RTE) cooked meat is an excellent substrate for microbial growth because of its high water activity (a_w ~ 0. 99), favorable pH, (5.5-6.5), and the presence of various nutrients (Pothakos et al., 2015). The occurrence of background microorganisms in raw meat before cooking depends on the inherent species and handling processes. However, the microbiota of packaged RTE cooked meat is commonly dominated by lactic acid bacteria (*Lactobacillus*, *Leuconostoc*, and *Carnobacterium* spp.), and *Brochothrix thermosphacta*, and are very often responsible for the spoilage of RTE cooked meat products during storage (Horita et al., 2018). The contamination of RTE meat products with pathogenic microorganisms can also occur during handling, processing, and post-processing operations. Among pathogenic microorganisms associated with foodborne illnesses, *L. monocytogenes* stand

out due to high hospitalization rates (>90 %) and fatality (20-30 %) (Thomas et al., 2015). (Ricci et al., 2018). *L. monocytogenes* is typically associated with RTE meat products possibly due to post processing contamination from equipment surfaces such as slicers and conveyors belts (Beresford et al., 2001; Farber et al., 2021; Rød et al., 2012).

2.4 Microbial challenges associated with freeze-dried pet foods

Around 57 % of Canadian households own pets with 7.9 million cats (~37 % Canadian households) and 5.9 million dogs (~32 % Canadian households) living in Canadian homes (Oliveira, 2014). The ingredients of pet foods are mostly of animal origin, and these ingredients are identified as high risk due to possible *Salmonella, L. monocytogenes, and E. coli* contamination (Behravesh et al., 2010; Nemser et al., 2014). Concern over dry pet food safety has increased in the last decades because of several outbreaks and recalls related to *Salmonella* contamination (Health Canada, 2012; CDC, 2012; Kananub et al., 2020). Dry pet foods with $a_w < 0.85$ have a long shelf-life (Farakos et al., 2013). *Salmonella* can survive for an extended period of time in the low a_w environment (Beuchat et al., 2011; Finn et al., 2013). *Salmonella*-related infection can also be transmitted through direct or indirect contact with pet animals.

2.5 Microbial challenges associated with fresh poultry meat

Contamination of poultry meat with pathogenic and spoilage microorganisms has been a long-standing challenge for the industry. Poultry meat serves as a natural host for many *Salmonella* serovars (Nair & Johny, 2019). An estimated 66 million kg of poultry meat are lost every year due to microbiological spoilage in USA (Wang, Zhuang, Hinton, & Zhang, 2016). Poultry meat is estimated to cause 14 % of *Salmonella* outbreak-associated foodborne illnesses among food commodities (Vieira and Boyer, 2019). According to the Centre for Disease Control and Prevention (CDC), *Salmonella* causes about 1.35 million foodborne illnesses in USA every year.

The top 3 *Salmonella* serotypes causing salmonellosis are Enteritidis, Newport, and Typhimurium (CDC, 2021; Tack et al., 2019).

2.6 Current decontamination strategies

Various physical, chemical, and biological approaches are used to effectively reduce pathogens from food products and enhance the safety and shelf life, while ensuring minimum changes in the food quality.

2.6.1 RTE cooked meat

Some of the strategies commonly employed to control the growth of spoilage and pathogenic microorganisms in RTE cooked meat include preservatives, bacteriocins, and modified atmospheric packaging (Horita et al., 2018). The most frequently used preservatives and bacteriocins in RTE cooked meat include sodium chloride, sodium lactate, sodium diacetate, and nisin (Field et al., 2018; Horita et al., 2018; Mbandi and Shelef, 2002). Preservatives and bacteriocins in RTE cooked meat can effectively inhibit the growth of microorganisms. However, food industries are working to reduce the number of additives in RTE cooked meat. Preparation of RTE meat with fewer additives and reduced sodium is challenging because that can affect the overall sensory and microbiological properties. Alternate strategies to enhance the shelf life and microbial safety of RTE cooked meat are post-packaging decontaminations. These decontamination steps aim to reduce the microbial load and eliminate pathogens, mainly *L. monocytogenes*, if present on RTE meat products surfaces after cooking (Ahn, Lee, Knipe, & Balasubramaniam, 2014).

In-package thermal pasteurization is a primary post-packaging decontamination method, currently used in the RTE meat industry. The packaged products are dipped in hot water for 10 min (70 –

96 °C) or passed through a steam heat (> 95 °C) tunnel for a few minutes (Ahn et al., 2014; Pietrasik, Pierce, Zhang, & Mcmullen, 2012). Although thermal deccontamination is very effective for the inactivation of microorganisms in RTE meat, it can adversely affect the sensory and nutritional qualities due to overcooking, as the RTE meat previously underwent the cooking process (Horita et al., 2018). It is necessary to explore alternative approaches to decontaminate fresh and RTE-cooked meat products to preserve meat quality attributes. Recently, food science and engineering researchers have focused on developing various alternatives, including novel non-thermal processes. For example, high-pressure processing is non-thermal approaches that have been used for meat decontamination applications (Albert et al., 2021; Dinçer & Baysal, 2004; Sohaib et al., 2016). Among novel non-thermal technologies, atmospheric cold plasma (ACP) treatment for the safety and quality of fresh and RTE meat products is a recent innovation.

2.6.2 Freeze-dried pet foods

High-quality pet food treats can be produced by freeze-drying to preserve product quality with reduced lipid oxidation. Freeze drying is a low-temperature process that cannot be considered a kill step to inactivate pathogenic microorganisms. Since pathogenic bacteria, mainly *Salmonella* can survive in low a_w freeze-dried pet foods, additional measures should be considered to inactivate any of them if present, in these products after processing. In-package ACP treatment can be applied for post-process decontamination of foods, including freeze-dried pet foods and treats.

2.6.3 Fresh poultry meat

The decontamination methods commonly employed to reduce the microbial loads in fresh poultry meat include chemical disinfectants (e.g., organic acids, chlorine, hydrogen peroxide), bio-preservatives, mild thermal treatments, and irradiation (Dinçer & Baysal, 2004). In thermal

decontamination, fresh meat carcasses are subjected to spot cleaning using hot water (>74 °C), spray rinsing of the carcass with hot water or pressurized steam (>90 °C, 1137 kPa), steam vacuuming (34 - 103 kPa), and a combination of chemical solution with pressurized steam (Dinçer & Baysal, 2004; Sohaib et al., 2016). Most of the thermal treatments are validated to reduce bacterial cell counts by 1 to 3 logs effectively, but adverse effects on the overall quality of the meat products were also reported (Vinnikova et al., 2019). Changes in meat flavor, aroma, and loss of texture are common during the thermal treatment of meat; additionally, lipid oxidation is one of the significant causes of off-flavor and rancidity during subsequent storage (Barbosa-Cánovas et al., 2014). This is mainly the case in poultry meat, which contains significant amounts of fat (Vinnikova et al., 2019). In addition to thermal treatment, chemical intervention strategies such as organic acids like lactic acid, peroxyacetic acid, and citric acid to decontaminate fresh meat products are extensively used in the meat industry. However, the main limitations are the stringent regulatory restrictions on the allowable concentration of these chemical antimicrobials in meat products and the dependence of their antimicrobial efficacy on factors such as residence time, temperature, and pH limit their antimicrobial efficacy (Berdejo, Pagán, García-Gonzalo, & Pagán, 2019; Dinçer & Baysal, 2004; Mani-López et al., 2012)

2.7 Atmospheric cold plasma science and technology

2.7.1 Plasma and its classification

Plasma is the fourth state of matter. It is an ionized form of gas, containing atoms, ions, electrons, photons, various free radicals, molecules in the metastable state with net-zero electric charge, and atoms in their fundamental or excited states (Liao et al., 2017; Neyts et al., 2015). According to the thermodynamic equilibrium temperature of the constituents, plasma can be broadly categorized into thermal plasma and non-thermal plasma. The thermal plasma has an electron temperature

similar to that of heavier species. In contrast, in the case of non-thermal plasma, the lower temperature of plasma reactive species compared to electron temperature within the plasma bulk make it suitable for food and bioproduct treatments (Liao et al., 2017; Neyts et al., 2015; Zhou et al., 2020). Plasma can be induced in any neutral gas by providing sufficient energy capable of causing ionization of the gas. The latest scientific advancements in plasma physics led by innovative designs of several plasma sources have enabled plasma generation at atmospheric pressure conditions and ambient temperature, also referred to cold plasma.

2.7.2 Atmospheric cold plasma (ACP)

Cold plasma, also known as non-thermal or low-temperature plasma, is produced mainly by supplying enough energy to neutral gas to cause ionization. This is accomplished when electrons with sufficient energy collide with neutral atoms or other molecules. The most frequently used methods take advantage of the electrical breakdown of a gas (discharge gas) in the presence of an applied external electric field. Consequently, electrons and other charged particles accelerate under the externally applied electric field and transfer their energy through inelastic collision to other particles and atoms (Gaunt, Beggs, & Georghiou, 2006). The reactive plasma species generation mechanisms include electron impact processes (e.g., vibration, excitation, dissociation, attachment, and ionization), three-body neutral recombination, neutral chemistry, ion-ion neutralization, ion-molecule reactions, Penning ionization, quenching, photoemission, photo-absorption, and photo-ionization. When the discharge medium has oxygen and nitrogen as its components, various reactive nitrogen (RNS) and oxygen species (ROS), such as NO_X, hydroxyl radicals ($^{\bullet}OH$), superoxide anions ($^{\bullet}O_2^-$), ground-state atomic oxygen [$O(^3P)$], singlet oxygen molecules [$O_2(^1\Delta g)$], and ozone (O_3), are produced, which possess excellent antimicrobial properties (Misra, Yadav, Roopesh, & Jo, 2019).

2.7.3 Atmospheric cold plasma sources

The cold plasma generation sources focus on utilizing the applied electric fields to ionize the gas most efficiently for the specific application. In this regard, many designs of plasma sources have been developed and tested. As a result, the operation principle, the power supply unit, and the configuration are specific to each type of plasma source. The most frequently used plasma discharges reported for food processing applications are the corona, dielectric barrier discharge (DBD), microwave, and radiofrequency discharges. A brief introduction and working principle of the most commonly reported plasma sources for food surface decontamination application are described below.

2.7.4 Corona discharge

Corona discharges are characterized as a luminous glow localized in a space near sharp edges, tips, or thin wires in a highly non-uniform electric field (Laroque, Seó, Valencia, Laurindo, & Carciofi, 2022; Misra et al., 2019). The basic setup to generate corona discharge requires an asymmetric electrode pair, for example, a thin wire and plate or a sharp pin and plate. When the applied electric field near the electrode exceeds the gas breakdown threshold limit, the corona appears as a self-sustaining, non-luminous filamentary discharge starting at the discharge electrode and ending at the ground (Laroque et al., 2022; Misra et al., 2019).

2.7.5 Dielectric barrier discharge

A dielectric barrier discharge (DBD) system consists of two metal electrodes (a powered electrode and a ground electrode) separated by a variable gap ranging from 0.1 mm to a few centimeters (Laroque et al., 2022). In a typical DBD, one or both electrodes are covered with a dielectric material such as quartz, glass, polymer, or ceramic, and an inter-dielectric gap is occupied by working gas. When high voltage is supplied to one of the electrodes, the gas between the inter-

electrode space experiences an increased electric field, resulting in ionization of the gas. Depending on the gas mixture, operating power, and dielectric surface properties, the DBD could move into filamentary to complete diffuser discharge regime (Gaunt et al., 2006).

2.7.6 In-package cold plasma discharge

The in-package cold plasma decontamination techniques use DBD, where between the electrode gap, a sealed package filled with desired gas and food materials is placed. The plasma is generated inside the sealed package, resulting in a cocktail of chemically active antimicrobial species. These reactive species recombine into their original form within a nanosecond to a few hours and decontaminate the food inside a sealed package. A significant advantage of in-package treatment is that it prevents post-process cross contamination.

2.7.7 Atmospheric pressure plasma jet

A DBD system can also be designed in the form of two rings or coaxial electrodes separated with dielectric materials, in which a gas is forced to flow between the pair of electrodes (Laroque et al., 2022). When high voltage is applied to one of the electrodes, it ionizes the gas, and the flowing gas pushes the plasma outside the electrode region to form a plasma jet. The main difference between DBD and plasma jet from an application standpoint is that DBD plasmas are geometrically confined to inter-electrode gaps or the containment enclosure. In contrast, plasma jets allow the ionized species to be launched outside.

2.8 Antibacterial mechanisms of atmospheric cold plasma (ACP)

The atmospheric cold plasma discharge generates a cocktail of reactive species such as reactive oxygen species (ROS), reactive nitrogen species (RNS), free radicals, ions, charged particles, and metastable molecules if air is used as the plasma generating medium. The exposure of ACP to

bacteria can initiate complex biochemical reactions, resulting in physical and chemical modifications of bacterial cells. The exact mechanism through which ACP-generated reactive species inactivate bacteria is not precisely known yet. Several studies have demonstrated that bacterial inactivation by ACP is target and system dependent. ACP generated charged particles and reactive species play an important role in bacterial inactivation (Dobrynin et al., 2009; Hoffmann et al., 2013; Liao et al., 2017; Timoshkin et al., 2012). Therefore, the antibacterial effect of ACP discharge is likely due to the synergistic action of reactive species and charged particles produced by the ACP system. Depending on the type and the composition of the gas mixture used, diverse categories and amounts of chemically reactive species are generated by ACP (Al-Abduly & Christensen, 2015; Han et al., 2016). Mainly, ROS and RNS produced by plasma make a significantly higher contribution to the inactivation of bacteria. ROS and RNS are known to have strong oxidative effects on bacterial cell structures. Among ACP-generated ROS and RNS, ozone (O_3), hydrogen peroxide (H_2O_2), hydroxyl radical, and peroxynitrites are considered to exhibit high antibacterial efficacy (Toyokawa, Yagyu, Misawa, & Sakudo, 2017; Zhou et al., 2018).

The ACP-generated reactive species and charged particles cause damage to bacterial cells both at the extracellular and intracellular levels. Several authors identified that the mechanical disruption of the bacterial cell wall and oxidative damage caused to bacterial cell envelope by reactive species are the leading factors of bacterial death after ACP treatment (Dezest et al., 2017; Dobrynin et al., 2009; Laroussi & Leipold, 2004; López et al., 2019). The mechanical erosion of bacterial outer cell envelope could be due to the bombardment of charged particles or accumulation of charges on outer cell membrane, leading to the formation of pores through electrostatic disruption by a phenomenon called electroporation (Laroussi, Mendis, & Rosenberg, 2003; López et al., 2019). This level of damage to the extracellular structure enables the leakage of important intracellular

components and the diffusion of reactive species through the cell membrane, which would cause oxidative damage to the cytoplasmic membrane, lipids, proteins, and DNA. In addition to mechanical damage, neutral active species generated in plasma discharge, such as hydrogen peroxide, hydroxyl and peroxide radicals, metastable and atomic oxygen, and ozone can produce oxidative damage to various cellular structures and macromolecules (López et al., 2019). Reactive species initiate their oxidative effect primarily on polyunsaturated fatty acids of the cytoplasmic membrane (Laroussi et al., 2003; López et al., 2019). The process of lipid peroxidation initiates with subtracting H radicals from unsaturated carbon bonds of fatty acids by OH radicals (or any other reactive species capable of abstracting hydrogen from the methylene group), leading to the formation of malondialdehyde (MDA) as an end product. MDA is used as a marker for lipid peroxidation, where the presence of MDA causes DNA damage and results in cell injury or death (Joshi et al., 2011). Thus, lipid peroxidation can compromise normal cell viability by modifying cell membrane properties.

2.9 Factors affecting the antimicrobial efficacy of ACP

The antibacterial effect of ACP is dependent on various processing parameters, including treatment time, gas composition, relative humidity, post-treatment storage time, substrate factors, and target microorganisms (Dobrynin et al., 2009; Liao et al., 2017). Thus, by tailoring the process parameters involved in plasma generation, many mechanisms may act separately or synergistically. For an efficient application and ACP integration with other microbial inactivation methods, a detailed understanding of the system parameters, substrate characteristics, environmental conditions, and product associated characteristics and matrices is required.

2.10 Decontamination of meat products by ACP

Meat-based food products are excellent sources of essential nutrients, vitamins, and proteins in human diets and provide an ideal medium for the growth of microorganisms. In recent years, several foodborne illnesses and product recalls have been reported associated with fresh poultry meat, RTE cooked ham, and meat-based pet food products. The potential of ACP to enhance meat food safety was previously reported (Misra & Jo, 2017; Rød et al., 2012). For instance, the potential application of ACP to decontaminate fresh foods (Ziuzina, Patil, Cullen, Keener, & Bourke, 2014), fresh meat products (Misra & Jo, 2017), RTE meat (Rød et al., 2012), beef (Yong et al., 2017), pork (Kim, Yong, Park, Choe, & Jo, 2013), and dry foods (Choi, Yang, Park, & Chun, 2018; Kim & Min, 2018) was studied. An excellent feature of the ACP is its low-temperature, high efficacy of bacterial inactivation, no water use, and lack of any chemical residues, making it ideal for food safety applications. Product shelf-life extension is another important global issue to support food security and minimize waste. Cold plasma can be applied for bacterial inactivation on food products to increase shelf life. Recently, several studies reported in-package plasma treatment of foods, including grape tomatoes (Min et al., 2018), Romaine lettuce (Min, Roh, Niemira, et al., 2017), and chicken fillets (Wang, Zhuang, Lawrence, & Zhang, 2018). The results demonstrated that cold plasma could be used to decontaminate foods inside the sealed package and extend the shelf life of products, while keeping the quality of the product intact. A list of recent studies on atmospheric cold plasma decontamination of meat-based food products is presented in Table 2.1. However, the data show high variability in the antimicrobial efficacy of ACP treatment, which is greatly influenced by the type of bacteria, physiological state of microorganisms, food matrix, treatment conditions, gas medium, and post-treatment storage time. These variabilities make it difficult to compare ACP efficacies reported in different studies.

Table 2.1: Application of atmospheric cold plasma for inactivation of microorganisms on meat products

Products	Organisms	Plasma source	Process parameters	Maximum log reduction	Reference
Bacon	*L. monocytogenes* *E. coli* *S.* Typhimurium	APP jet	Power: 125 W Gas: He + O_2 (10 lpm + 10 sccm) Time: 90 s	2.6 log CFU/g 3 log CFU/g 1.73 log CFU/g	(Kim et al., 2011)
Pork loin	*E. coli* *L. monocytogenes*	DBD	Power: 3 kV, 30 kHz Gas: He + O_2 (0.7 % + 0.3 %) Time: 10 min	0.55 log cycles 0.59 log cycles	(Kim et al., 2013)
	E. coli *L. monocytogenes*		Voltage: 3 kV, 30 kHz Gas: He 100 % Time: 10 min	0.34 log cycles 0.43 log cycles	
Membrane filters	*L. innocua*	APP jet	Voltage: 8.0 kV f: 38.5 kHz He + O_2 (1:5) Time: 10 s	2.23 log CFU/cm^2	(Noriega et al., 2011)
Skin of Chicken breasts	*L. innocua*	APP jet	Voltage: 16.0 kV f: 30 kHz He + O_2 (1:5) Time: 8 min	0.40 log CFU/cm^2	

Table 2.1 Continued: Application of atmospheric cold plasma for inactivation of microorganisms on meat products

Products	Organisms	Plasma source	Process parameters	Maximum log reduction	Reference
RTE bresaola	*L. innocua*	In-package DBD	Power: 62 W (60 s) Gas: He + O_2 (70 % + 30 %)	0.8 log CFU/g	(Rød et al., 2012)
RTE ham	*S.* Typhimurium *L. monocytogenes*	DBD Open Atmospheric	Power: 10 kV, 10 kHz Gas: Air Time: 20 min	1.14 log steps 1.02 log steps	(Lis et al., 2018)
Dry cured Beef product pastirma	Stapylococcus aureus *L. monocytogenes*	APP jet	Voltage: 25 kV f: 25 kHz Gas: He + O_2 (50 % + 50 %) Time: 5 min	0.85 log CFU/cm^2 0.83 log CFU/cm^2	(Gök et al., 2019)
Fresh beef	*S.* Enteritidis	APP jet PAW 0.05 % PALA 0.10 %PALA 0.15 % PALA 0.20 % PALA	Voltage: 19.2 kV Time: 40 s Hold time 10 min	0.24 log CFU/mL 1.01 log CFU/mL 1.1 log CFU/mL 2.67 log CFU/mL 4.82 log CFU/mL	(Qian et al., 2019)

PAW: Plasma Activated Water; PALA: Plasma Activated Lactic Acid

2.11 ACP integrated decontamination approaches to improve meat product safety

One of the ways to apply ACP for food decontamination is to integrate it with existing food processing operations. For instance, previous studies reported the improved antimicrobial efficacy of sequential treatment of ACP and some of the common organic acids used in the meat industry i.e., peracetic acid and citric acid treatments for fresh meat decontamination (Chaplot et al., 2019) for commercial applications.

2.11.1 ACP integrated treatments to improve RTE meat safety

The most common strategies applied to control the growth of spoilage and pathogenic microorganisms in RTE cooked meat include preservatives, bacteriocins, vacuum or modified atmosphere packaging (MAP), and post-packaging thermal treatment (Horita et al., 2018). However, several studies reported that ACP treatment could be successfully employed as an alternate post-packaging decontamination technique (Misra and Jo, 2017; Rød et al., 2012). For example, Rød et al. (2012) showed that in-package ACP treatment of RTE meat with MAP (30 % O_2 + 70 % argon) gas resulted in a maximum 1.6 log reduction in *L .innocua* cell counts. Other studies reported that the ACP treatment of ham using air as working gas had a limited antibacterial effect; however, after 14 days of post-treatment storage in 70 % CO_2 + 30 % N_2 increased the inactivation level to 2.55 log (Lis et al., 2018). The previous studies did not address the influence of RTE meat constituents such as preservatives, bacteriocins, and antioxidants on the overall inactivation efficacy of ACP. Therefore, it is necessary to understand the interaction effects of ACP to inactivate bacteria on the surface of RTE foods formulated with preservatives or bacteriocins to develop ACP based integrated approach. More studies are required to understand the important process and product factors influencing the decontamination efficacy when ACP is

integrated with these industrially used processes. Studies on the integration of ACP treatment with other microbial intervention methods will help the future development of ACP technology.

2.11.2 ACP integrated decontamination for poultry meat

Combining multiple decontamination methods can be effective in reducing the microbial load with minimal changes in product quality attributes (Horita et al., 2018; Sohaib et al., 2016). However, limited number of studies are available on understanding the antimicrobial efficacy of treatments combining ACP and other decontamination methods on fresh meat products (Chaplot et al., 2019; Cui, Wu, Li, & Lin, 2017; Matan, Nisoa, & Matan, 2014; Trevisani et al., 2017). For example, integrated treatments of ACP with peracetic acid (PAA) resulted in a 5.3 log reduction of *Salmonella* cell counts on the poultry meat surface compared to 1.3 and 2.3 log reductions when PAA and ACP treatment were used alone, respectively (Chaplot et al., 2019). Similarly, Cui et al. (2017) reported additional reductions of more than 2 log in *L. monocytogenes* cell counts on pork loin surface after sequential treatment of lemongrass oil followed by nitrogen ACP jet. Another study reported that ACP combined with sodium dodecyl sulphate (SDS) and lactic acid (LA) reduced the *E. coli* population on egg surface to below the limit of detection (Trevisani et al., 2017). The results of these studies demonstrated the potential benefits of treatments combining ACP with other decontamination methods. However, more data are needed to develop integrated treatment using ACP and antimicrobials such as organic acids. To optimize the process parameters, more understanding on the main mechanisms associated with the improved decontamination efficacy of ACP integrated treatments is required.

2.11.3 Simultaneous cooling and decontamination of fresh meat by ACP integrated treatments

Cooling of the meat products is one of the major processing steps employed in the meat processing industries to control microbial growth and reduce quality changes. ACP integrated cooling can possibly decontaminate and reduce the temperature of food products simultaneously. Temperature plays a vital role in plasma chemistry, and it can influence the generation and degradation of reactive oxygen and nitrogen species (RONS) including, ozone, hydroxyl radicals, and nitrous oxide (NO_X). It is important to understand the plasma chemistry and concentration of reactive species at cooling temperatures (Park, Choe, & Jo, 2018).

Product weight loss is one of the major economic losses during air cooling (Zhang, Mao, Li, Luo, & Hopkins, 2019). A significant weight loss in poultry meat was reported after 6 min of ACP treatment (Chaplot et al., 2019). Water misting during or before cooling can possibly reduce the loss of product weight. In a combined organic acid and ACP treatment, the organic acid solution can be applied as a mist, that can increase the dispersibility of acid on the meat surface. Misting can also increase the relative humidity around the plasma discharge region. Many earlier studies reported that the ACP treatment in a high relative humidity environment significantly increased bacterial inactivation (Dobrynin et al., 2009; Liao et al., 2017). Recently, Jiang et al. (2017) showed that aerosolization of H_2O_2 solution through plasma discharge region resulted in 4 log reduction in the bacterial population on spinach surface after 45 s treatment and 30 min dwell time.

2.12 Conclusions

There are limited studies focussing on evaluating the microbial inactivation efficacy on meat products, when ACP is integrated with other processing and decontamination approaches. Further

research is required to understand the influence of various product and process parameters and their interactions on the microbial inactivation efficacies of ACP and ACP-based integrated processes for different types of meat products. This research gap is addressed in Chapters 3, 4, 6, and 7, where the inactivation efficacies of ACP-based integrated processes were evaluated, against important pathogens related to RTE ham, freeze-dried pet foods and fresh poultry meat. Chapter 5 addressed the research gap of understanding the underlying microbial reduction mechanisms during in-package ACP treatment and post-treatment storage of RTE ham.

Chapter 3: Cold Plasma Treatment of Ready-To-Eat Ham: Influence of Process Conditions and Storage on Inactivation of *Listeria innocua*

3.1 Introduction

In recent years, consumer diet preferences have significantly shifted towards the ready-to-eat (RTE), fresh, minimal processed, high nutritional foods with natural color, texture, and flavor. However, fresh and RTE foods are susceptible to contamination with pathogenic microorganisms such as bacteria and viruses. Foodborne illness, as a result of eating contaminated foods is a global public health issue, with the annual worldwide poll arising at an alarming 600 million cases and 420,000 deaths (WHO, 2015). Every year in Canada, approximately 4 million (1 out of 8 people) cases of sickness, 11,500 hospitalizations and 240 deaths are reported because of foodborne illnesses (Health Canada, 2016). A major outbreak of foodborne illness due to the consumption of sliced roast beef contaminated with *L. monocytogenes* occurred in Canada in 2008, which resulted in 42 death and an estimated loss of nearly $242 million CAD to the food industry and governments due to product recall and health related expenses (Thomas et al., 2015). The number of outbreaks caused by *L. monocytogenes* have increased in many European countries (Food & Authority, 2015). Contaminated RTE food products, notably meat and seafoods have been identified as high-risk products (Kim, Jayasena, Yong, & Jo, 2016). Surface contamination of RTE meat may occur during post-processing as *L. monocytogenes* can survive in the processing environment and they can be transferred to product from equipment surfaces such as slicers (Rød, Hansen, Leipold, & Knøchel, 2012). Treatments including thermal, high pressure processing and antimicrobial additives are used for post-package control of microorganisms on the surface of cooked products (Jiang & Xiong, 2015). However, each of these processes has its own drawbacks. For instance, thermal treatments can impact the quality of the products (Pietrasik et al., 2012).

Atmospheric cold plasma is an emerging non-thermal technology, which offers a great opportunity for decontamination of food surfaces including RTE ham (Misra et al., 2017) Plasma is the fourth state of matter and defined as the partially ionized gas consisting of mostly free radicals, photons, positive and negative ions, free electrons, quanta of electromagnetic radiation and atoms in natural and excited states that possess a net neutral charge (Pignata, D'Angelo, Fea, & Gilli, 2017). The plasma discharge can be generated from a dielectric barrier system, and restricts the temperature of the ionized gas to room temperature and is termed as "cold plasma" (Moisan et al., 2001). Plasma discharge produces various antimicrobial reactive elements including positive and negative charged particles, free radicals, UV photons, ozone, superoxide, hydroxyl radicals, and nitric oxides (Laroussi & Leipold, 2004; Surowsky, Schlüter, & Knorr, 2014). The type of reactive species produced by plasma discharge depends on the gas, in which plasma is generated. Various aspects of modes of antimicrobial actions of cold plasma for destruction of bacteria, viruses, fungi, and biofilms have been discussed previously (Laroussi, 2002; Misra & Jo, 2017; Niemira, 2012; Pignata et al., 2017; Scholtz, Pazlarova, Souskova, Khun, & Julak, 2015). RTE ham can be treated by cold plasma while the product is inside a package. Rød, Hansen, Leipold, & Knøchel (2012) reported inactivation effect of atmospheric plasma against *L. innocua* on RTE meat (bresaola) inside the package. Song et al. (2009) found that the atmospheric plasma significantly reduced *L. monocytogenes* cells on ham and cheese surfaces, but the inactivation efficacy was influenced by treatment time, input power and type of food surface. Noriega et al. (2011) demonstrated the potential efficacy of atmospheric plasma against *L. innocua* on membrane filter, chicken skin and meat. However, more studies are required to understand the impact of different product and process factors on the effectiveness of cold plasma treatment to reduce bacteria on RTE ham.

Rosemary extract is commercially used in RTE cooked ham products to control the growth of *L. monocytogenes*. It prevents the lipid oxidation of RTE ham during processing and post treatment storage. The addition of preservatives could impact the effect of plasma on inactivation of *L. monocytogenes*. However, very limited research data are available regarding the effect of intrinsic (e.g., preservatives) and extrinsic factor (e.g., temperature) on the resistance of *L. monocytogenes* to cold plasma treatment. In this study, ham was formulated with different concentrations of NaCl to determine the impact on efficacy of plasma on reduction of *L. innocua* in response to sodium reduction strategies proposed by Health Canada (2015). The objectives of this study were to (1) determine the influence of temperature, presence of antioxidants, and salt concentration of ham on the antimicrobial efficacy of cold plasma treatment; and (2) determine the influence of post-treatment storage on the survival of *L. innocua.*

3.2 Materials and methods

3.2.1 Bacterial strain and growth conditions

Listeria innocua ATCC 33090 was used in this study as a surrogate for *L. monocytogenes*. For the preparation of the culture, the strain was streaked from a -80 °C stock culture onto Tryptic Soy Agar (TSA) (Difco, Becton–Dickinson, Sparks, MD, USA), followed by inoculation into TS broth (TSB) and incubated overnight at 37 °C. Fresh broth was inoculated with 1 % (v/v) of the overnight culture and incubated at 8 °C until the culture reached an OD_{600} nm between 0.9 and 1.0. The culture was centrifuged at 5311 × *g* for 3 min, the supernatant discarded, and the cell pellet was resuspended in 1 mL of saline solution (0.85 % NaCl).

3.2.2 Preparation of ham

Cooked ham with a final sodium chloride (salt) concentration of 1 (w/w) or 3 % (w/w) was prepared according to Liu et al. (2014). The formula of ham consisted of ground pork, ice (20 % of meat weight), sodium tripolyphosphate (0.63 % of meat weight), sodium erythorbate (0.1 % of meat weight), dextrose (3.1 % of meat weight), Prague powder containing 6 % $NaNO_2$ and 94 % NaCl (0.46 % of meat weight), and NaCl (0.82 or 3.36 % of meat weight for 1 or 3 % NaCl in the final product). After production and cooling, the ham was cut into 2 mm-thick slices with a surface area of 50 cm^2, vacuum packaged, and stored at 0 °C until use. A rosemary extract (NatureGuard™, Newly Weds Foods, Edmonton, AB, Canada) solution in 0.5 % ethanol was prepared at a concentration of 10 g/L as described by Teixeira, Repková, Gänzle, & McMullen (2018).

For sample preparation, the sliced ham was opened aseptically, and slices were cored to obtain pieces of meat with a surface area of 1 cm^2. The samples were placed on a sterile glass slide in sterile petri dish and 10 µL of rosemary extract solution (10 g/L) was added to achieve a volumetric concentration exceeding 5-fold of the minimum inhibitory concentration (MIC) against *L. innocua*. For control samples only 0.5 % ethanol solution was added as solvent control. The addition of 10 µL rosemary extract as described above produced a final surface concentration of ~ 102 µg/cm^2. The samples were then inoculated with 10 µL of *L. innocua* cells suspension to achieve a 10^7 cfu/cm^2 final mean cell counts on ham surface. After each inoculation procedure, samples were dried for 5 min at 23 °C in the biosafety cabinet.

3.2.3 Cold plasma (CP) equipment

A Dielectric Barrier Discharge (DBD) system (PG 100-3D, Advanced Plasma Solutions, Malvern, PA, USA) was used to treat the samples with cold plasma. The experimental setup of plasma generation system and accessories to acquire plasma characteristics are presented in (Figure 3.1). Preliminary experimentation was done to determine the parameters used for cold plasma treatment. The DBD system used a frequency of 3,500 Hz and duty cycle of 70 %. The gap between the high voltage electrode and ground electrode was maintained at ~ 5 mm throughout all the experiments to obtain uniform plasma. The high voltage electrode was connected to the input power supply of a transformer with 250 - 300 W, which produced a high pulsating voltage output of 0-28 kV with 0- 2A current output.

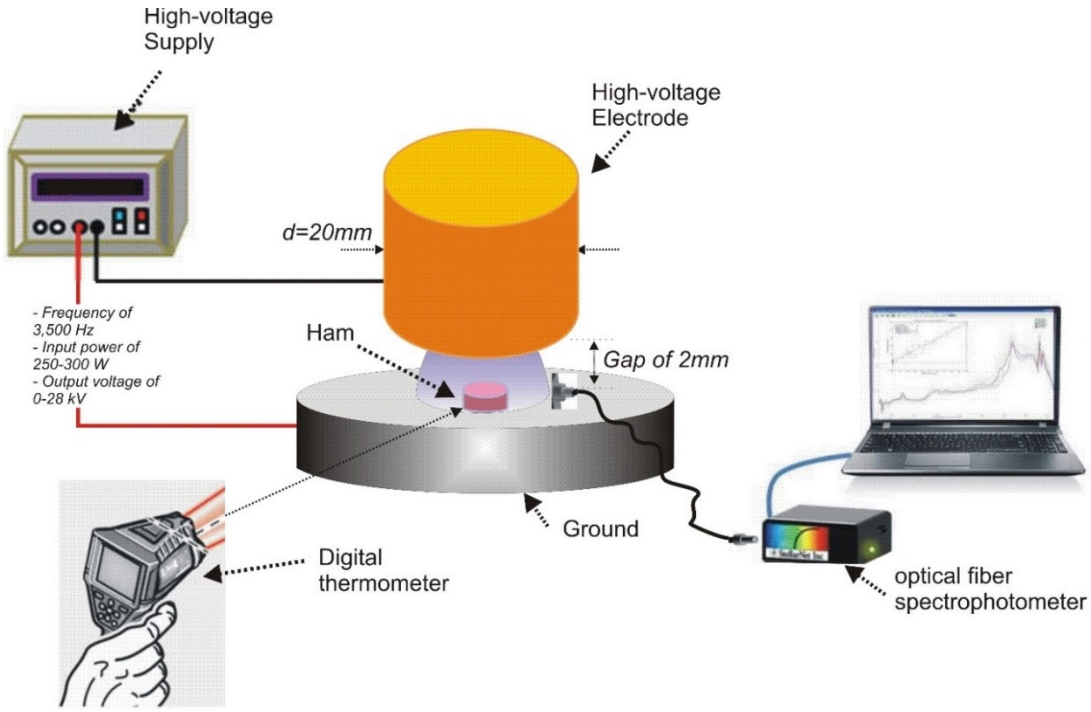

Figure 3.1: Cold plasma treatment system for treatment of ham.

3.2.4 Cold plasma treatment of ham

For cold plasma treatments, ham samples were placed on top of a glass slide on a steel platform. The gap between vertical high voltage electrode and the top surface of the ham was kept at ~2 mm for all experiments. The diameter of high voltage electrode was 20 mm, and the outer surface of the electrode was covered with 5 mm dielectric layer. The steel platform acted as a ground electrode during the plasma discharge (Figure 3.1). For treatments at 4 °C, the plasma system was placed in a refrigerator at 4 °C. The samples were subjected to direct atmospheric plasma exposure for selected times and after treatment, the slide with ham was placed in a sterile petri dish, the lid was sealed with PARAFILM, and samples were stored for 6 and 24 h at 4 °C.

3.2.5 Microbial enumeration

Surviving cells of *L. innocua* were enumerated immediately (0 h) after cold plasma treatment and after storage for 6 and 24 h at 4 °C. Untreated samples were prepared to determine the initial cell counts. Samples were transferred aseptically into a 50 mL falcon tube containing 1 mL of 0.1 % peptone water. Tubes containing sample were vortexed for 60 s to detach cells from ham surface, and 0.1 mL of aliquots were transferred into a sterile 1.5 mL Eppendorf tube and serially diluted in 0.1 % peptone water. Surviving cells after cold plasma treatment and storage were enumerated by plating 0.1 mL aliquots of appropriate dilution on nonselective tryptic soy agar (TSA). Plates were incubated at 37 °C for 48 h. Results were expressed as a log reduction $\log_{10}(N/N_o)$, where N is the number of CFU (colony-forming unit) after treatment and N_o is the number of CFU of the bacteria on samples not exposed to cold plasma treatment, which was determined for each experiment.

Two sets of experiments were performed to investigate the inactivation effect of plasma against *L. innocua* on ham. In the first set, the effect of NaCl concentration (1 or 3 %) in ham on inactivation of *L. innocua* by plasma was investigated at 23 °C and 4 °C. Based on the first set of experiment results, 1 % NaCl ham was selected to investigate the effect of the presence of rosemary extract on plasma inactivation of *L. innocua* at 23 °C and 4 °C. For both experiments samples were exposed to atmospheric plasma for 0, 30, 60, 90, 120, and 180 s. In the second experiment, samples (described above) treated with cold plasma at either 4 or 23 °C for 60 or 180 s were additionally stored for 0, 6 or 24 h at 4 °C.

3.2.6 Effect of atmospheric cold plasma treatment on lipid oxidation by TBARS

Lipid oxidation of 1 % NaCl ham with rosemary extract (10 g/L) or without rosemary extract was determined using the thiobarbituric acid (TBA) assay modified from Bedinghaus & Ockerman (1995) and the results were expressed as malonaldehyde (MDA) mg equivalent/kg ham. Briefly, 0.4 g of ham was homogenized (Polytron® PT 10-35GT, Kinematica AG, Luzern, Switzerland) in a 5 mL of 20 % trichloroacetic acid containing 1.6 % phosphoric acid, using for 120 s at 15×1000 rpm. The homogenate was centrifuged (Allegra 25R centrifuge, Beckman coulter Inc. IN, USA) at 5311 × *g* for 5 min at 4 °C. One mL aliquot of the supernatant was transferred into 15 mL falcon tube containing 1 mL of freshly prepared 20 mM TBA solution in distilled water. The tubes were vortexed for 20 s, placed in boiling water bath at 95 °C for 35 min, and cooled by placing on ice for 10 min. To measure fluorescence, duplicate aliquots of 200 µL of each sample was transferred to a 96 well plate. The fluorescence intensity was measured with a spectrophotometer (Variskon flash, Thermo Electron Corporation, Nepean, ON, Canada) at excitation and emission wavelength of 535 nm and 553 nm, respectively.

3.2.7 Water content and water activity determination

The water content of 1 % NaCl ham without plasma treatment was measured using oven drying method and weight loss in the sample as a result of plasma treatment was measured using an analytical balance. The water loss of plasma treated samples were calculated on dry basis. The water activity (a_w) of treated sample was measured using a water activity meter (Aqualab, Meter group Inc., Pullman, WA, USA). To evaluate the change in water content and a_w, and to confirm the drying of ham samples during cold plasma treatment, water desorption isotherm of ham samples at 25 °C was generated by using a vapor sorption analyzer (VSA) (Decagon device, Meter group Inc. Pullman, WA, U.S.A.) in the water activity range 0.98 to 0.90 (Syamaladevi, Tang, & Zhong, 2016). The sample (approximately 0.8 g) was exposed to a set range of relative humidity values inside the VSA (0.98 to 0.90) until an equilibrium water content was reached. The equilibrium water content and corresponding water activity values were recorded at each equilibrium point. Further, the water content and water activity values obtained after plasma treatments were determined and compared with those obtained from VSA (desorption isotherm).

3.2.8 Color measurement

The change in surface color of 1 % NaCl ham with or without rosemary extract was measured using Chroma Meter CR-410 (Konica Minolta sensing Inc., Osaka, Japan) with D_{65} and 10° standard observers. CIE color parameters lightness (L*), red-green (a*), and yellow-blue (b*) of the sample were determined. Each sample reading was taken at three different locations in triplicate and averaged for all measurements of plasma treated ham.

3.2.9 Cold plasma diagnostics

The dielectric barrier plasma discharge system generates several reactive species in excited states. The determination of all the active species present in plasma can be very difficult, but some of the important chemical reactive species in plasma can be identified by capturing the optical spectrum of emitted light from excited plasma species. A spectrophotometer (Black comet C-25, StellarNet Inc., Tampa, FL, USA) coupled to an optical fiber and controlled by spectra viz software was used to capture the optical emission spectroscopy. The light emitted by excited plasma species between the electrode gap was captured using optical fiber (UV-Vis, diameter 600 μm) by placing it 5 mm away from the electrode to avoid arcing. The spectrophotometer used a slit width of 25 μm, a concave grating of 40 mm and 590 grooves/mm, signal to noise ratio of 1000:1, integration time limit of 1 ms to 65 s, and a wavelength detection range 190-1000 nm. The set integration time was 1000 ms and the set values of number of scans to average was 3 to obtain stable spectra. The spectra were further averaged and analyzed for identification of reactive species.

3.2.10 Ozone, nitrous oxides, and hydrogen peroxide estimation

The atmosphere between the two electrodes during plasma treatment was analyzed using Dräger short term detector tube (Dräger Safety AG & CO, Lubeck, Germany). These tubes contain a specific chemical reagent that changes color after getting in contact with specific gases. The tube was connected to Dräger Accuro detector pump (Dräger Safety AG & CO, Lubeck, Germany) to collect gas sample. The ozone, nitrous gases and hydrogen peroxide tubes had a gas measuring range from 30-300 ppm, 50-1000 ppm and 0.1-3 ppm, respectively. These gases were measured according to the manufacture's instruction after plasma treatment for 160-180 s. This method was selected because of the ease of use recommended by previous studies (Klockow & Keener, 2009).

Briefly, to ensure that ozone, nitrous gases and hydrogen peroxide content fall within the measurement range of Dräger detector tubes, smaller volumes of gas samples i.e., 10 mL for ozone, and 200 mL for nitrous gases and hydrogen peroxide were collected into the tubes connected with Dräger Accuro detector pump. The final concentrations of ozone, nitrous gases and hydrogen peroxide were then calculated based on the instruction provided by the manufacturer.

3.2.11 Temperature measurement

The temperature of ham samples and electrode surface were determined before and immediately after plasma treatments using an Imaging IR thermometer (FLIR TG165, systems Inc, Wilsonville, OR, USA). Inbuilt laser pointer trigger was used to orient with the help of crosshair function of thermometer to pinpoint temperature measurement at selected locations.

3.2.12 Statistical analysis

All the experiments were performed in triplicates. Data for logarithmic microbial counts obtained from incomplete split-split plot experiment were subject to analysis of variance using generalized linear mixed effects procedure of SAS® software (Proc Glmmix; SAS Institute, Cary, NC, USA 2011). The treatment factors % NaCl (1 and 3 %), rosemary extract (with or without), temperature (4 and 23 $^{\circ}$C) and treatment/storage times were used as fixed effects. Main (individual effect of each treatment factor) and interaction effect (two-way interactions of individual treatment factors) among fixed factors were tested. The random effects in the model included the main effect of replications and its two-way interaction with time as well as temperature. Data were unbalanced (unequal levels of rosemary for treatment factors), hence the Kenward-Roger approximation was used to adjust the denominator degrees of freedom and the estimated standard errors for main and interaction effects. The level of significance used in the test was $P \leq 0.05$. To control for the Type

I error rate in posthoc multiple pairwise comparisons of treatment group mean, the Tukey's honest significant difference test was used.

3.3 Results and discussion

3.3.1 Microbial inactivation during cold plasma treatment

To understand the impact of cold plasma on inactivation of *L. innocua*, experiments were designed to assess the effect of NaCl (1 % and 3 %), treatment temperature (4 and 23˚C), treatment times and rosemary extract (with or without) in inactivation of *L. innocua* on ham. The initial count of *L. innocua* on ham surface was ~ 7 log CFU/cm^2. Statistical analysis revealed that interaction effects were not significant. Only the main effect of time was significant. An increase in treatment time from 30 to 60 s increased the inactivation but an additional 30 or 60 s of cold plasma treatment did not change the inactivation of *L. innocua* (Figure 3.2). Plasma treatment for 180 s resulted in a significantly higher log reduction of 1.43 CFU/cm^2 of *L. innocua* (Figure 3.2). The observed effect of treatment time on *L. innocua* inactivation in the present study was consistent with prior reports that used atmospheric plasma to inactivate *L. monocytogenes* inoculated on tomato and strawberry surfaces and reported higher lethality after 180 s; whereas, an increased treatment time from 30 to 120 s did not significantly reduce the counts (Ziuzina et al., 2014). Similarly, Rød et al. (2012) reported that inactivation effect of in-packaged modified atmospheric plasma treatment of *L. innocua* on RTE meat bresaola was significantly influenced by treatment time and gas compositions inside package. They observed a reduction in *L. innocua* counts ranging from 0.8 to 1.6 log CFU/g after multiple plasma treatments (20 s, 60 W) at 10 min intervals inside the package filled with (30 % O_2 + 70 % Ar). Song et al. (2009) observed a higher and rapid inactivation of *L. monocytogenes* on smooth cheese surface (up to 8 log CFU/g) in comparison to rough and porous

surface of ham (0.25 to 1.73 log CFU/g). They suggested that the porous structure of ham could be supporting many attachment and migration sites for *L. monocytogenes* and potentially protecting cells from exposure to plasma.

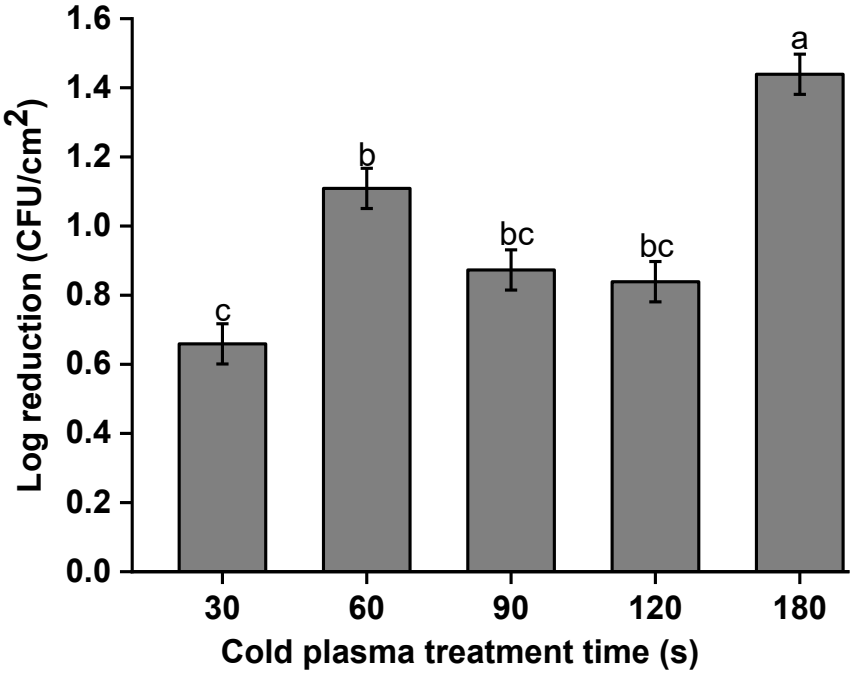

Figure 3.2: Effect of plasma treatment time on inactivation of *L. innocua* inoculated on RTE ham. Columns with different letters indicate a significant difference in reduction of *L. innocua*. Data are shown as least square means ± standard error (n = 68) of triplicate independent experiments of different level of salt, rosemary extract, and temperature.

Cold plasma treatment temperature or % NaCl did not result in significant differences in lethality (Figure 3.3 A&B). Temperature plays an important role in plasma chemistry, and it influences the generation and degradation of RONS, including ozone, hydroxyl radicals and NO_X. In a closed air plasma reactor, the generation of ozone (O_3) rapidly decreased by 25 times, when plasma processing temperature increased from 25 °C to 225 °C because the degradation rate of O_3

increased (Park, Choe, & Jo, 2018). Ozone has powerful oxidation potential and it has antibacterial effect against microorganisms (Guzel-Seydim, Greene, & Seydim, 2004). In this study, the plasma processing temperature did not significantly affect the inactivation level of *L. innocua* on ham (Figure 3.3 A&B). It could be due to rapid diffusion of generated O_3 and other reactive gas into surrounding open atmosphere.

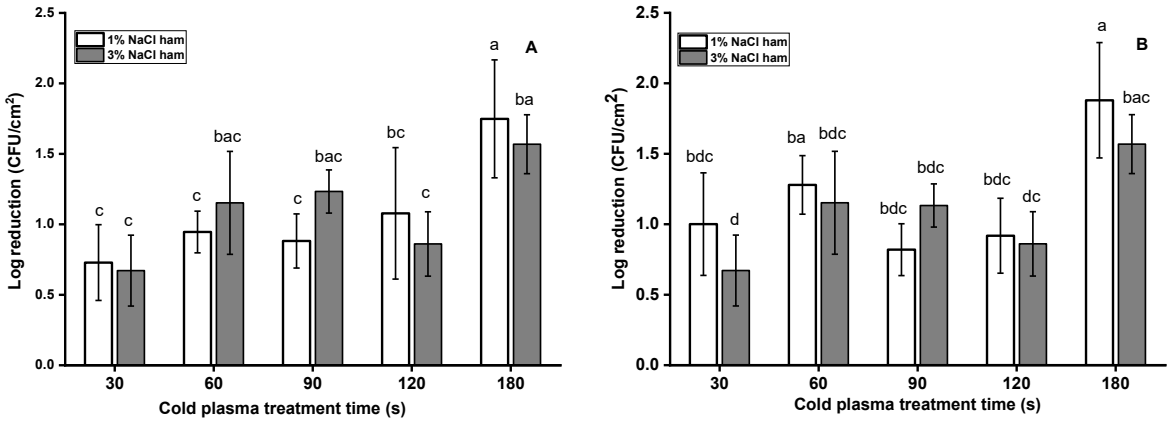

Figure 3.3: Effect of treatment temperature on inactivation of *L. innocua* after 0-180 s cold plasma treatment on ham surface with 1 % NaCl or 3 % NaCl at 23 ºC (A), and at 4 ºC (B). Data are shown as least square means ± standard deviations of triplicate independent experiments (n = 3). Treatment mean with different letters are significantly different (P< 0.05)

The similarity in inactivation of *L. innocua* on 1 % NaCl and 3 % NaCl ham is consistent with prior reports that used atmospheric plasma to treat yeast cells and reported less inactivation effect in saline solution compared to water (Ryu et al., 2013). Ryu et al. (2013) did experiments in aqueous solutions, thus it is possible that the osmotic shock to the cells in water was responsible for the lethality of the cells and not the plasma treatment. To the author's knowledge, this is the

first study to report the effect of plasma treatment on a ham formulated with different salt concentrations.

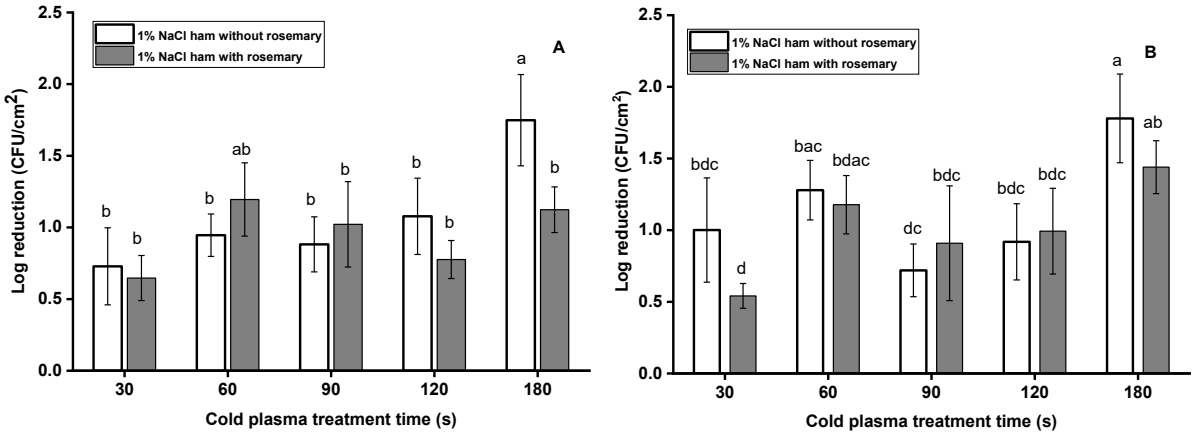

Figure 3.4: Effect of treatment temperature on log mean cell count reduction of *L. innocua* after 0-180 s cold plasma treatment on 1 % NaCl ham with and without rosemary extract at 23 °C (A), and at 4 °C (B). Data are shown as least square means ± standard deviations of triplicate independent experiments (n = 3). Treatment means with different letters are significantly different ($P < 0.05$)

Rosemary extract is used commercially in RTE ham to inhibit the growth of *L. monocytogenes* and to prevent lipid oxidation during post packaged storage (Ojeda-Sana, van Baren, Elechosa, Juárez, & Moreno, 2013; Zhang, Kong, Xiong, & Sun, 2003). In the concentration range 1 to 10 g/L, rosemary extract exhibited inhibitory antimicrobial activity against *L. monocytogenes* (Teixeira et al., 2018). The effect of rosemary extract on 1 % NaCl ham surface on the lethality of plasma treatment at treatment temperatures 23 °C and 4 °C were compared to a 1 % NaCl ham surface without rosemary extract (Figure 3.4 A&B). Cell counts of untreated ham samples with rosemary were comparable to cell counts of untreated control samples without rosemary (data not shown). Presence of rosemary extract on ham surface slightly changed the inactivation effect of plasma treatment, but the effect was not consistent for all treatment times (Figure 3.4 A&B). The

constituents of meat products, such as fat, may protect bacteria against the inhibitory effect of spice extract (Zhang et al., 2003). Other reason of reduced inactivation effect of plasma could be due to the free radical scavenging effects of rosemary extract that limit the antimicrobial effect of plasma treatment. These reduced inactivation effects were significant for plasma treatment for 180 s at 23 °C (Figure 3.4 A)). Further investigation is needed to understand the interaction between plasma reactive species and rosemary extract or NaCl and inactivation mechanism of *Listeria*.

3.3.2 Effect of storage

Storage after cold plasma treatment had very little impact on the reduction of *L. innocua* population on ham (Table 3.1 & 3.2). The maximum observed reductions were obtained after 6 h storage but they were similar to reductions after 24 h on 1 % NaCl ham without rosemary exposed to cold plasma for 180 s at 23 °C (Table 3.1). Reactive species produced by plasma induce damage to the bacterial cell membrane, leading to the sublethal injuries of cells after plasma treatment (Liao et al., 2017). In combination with plasma treatment, post-plasma treatment storage at 4 °C may have delayed the recovery of sublethal injured cells and resulted in reduced counts of *L. innocua*. Han et al. (2016) performed a cell recovery model to assess the effect of plasma treatment time, in combination with refrigerated storage and reported a treatment time dependent behaviour of cell recovery after refrigerated storage. A similar trend was observed in this study, where cold plasma treatment of ham for 180 s and stored for 6 h resulted in reduced counts of *L. innocua* compared to samples treated for 60 s and stored for 6 h (Table 3.1). The effect of post-plasma treatment storage on microbial inactivation in in-packaged system has been widely reported (Mins et al., 2017; Wang., Zhuang, & Zhang, 2016; Ziuzina et al., 2014).

Table 3.1: Mean cell log reductions of *L. innocua* on ham formulated with 1 % NaCl (with and without rosemary extract) or 3 % NaCl and exposed to cold plasma treatment for 60 or 180 s at 23 °C and stored at 4 °C for 0, 6, or 24 h.

Treatment time (s)	Treatment temperature (°C)	Storage time (h)	Log N/No		Log N/No
			1 % NaCl ham		3 % NaCl ham
			With rosemary	Without rosemary	Without rosemary
60	23	0	1.2 ± 0.2^{c}	0.9 ± 0.1^{cC}	1.1 ± 0.3^{C}
60	23	6	1.5 ± 0.3^{c}	0.8 ± 0.4^{dC}	1.6 ± 0.5^{ABC}
60	23	24	1.0 ± 0.3^{c}	1.1 ± 0.4^{cC}	0.9 ± 0.0^{C}
180	23	0	1.1 ± 0.1^{c}	1.6 ± 0.3^{bcABC}	1.6 ± 0.2^{ABC}
180	23	6	1.3 ± 0.3^{bc}	2.2 ± 0.4^{aA}	2.0 ± 0.4^{AB}
180	23	24	1.3 ± 0.2^{bc}	1.9 ± 0.3^{abAB}	1.2 ± 0.2^{BC}

Lower case $^{a-d}$ indicate significantly different ($p<0.05$) mean log reduction of *L. innocua* on 1 % NaCl ham with or without rosemary extract; capital letters $^{A-D}$ indicate significantly different ($P<0.05$) mean log reduction of *L. innocua* on 1 % NaCl and 3 % NaCl ham without rosemary extract. Across the column effect of treatment time and storage and between the rows effect of % NaCl or rosemary.

The plasma inactivation efficacy depends on the duration of post-plasma treatment storage, as extended storage allows the diffusion of reactive species in food. A 24 h post-treatment storage time facilitated the extended action of plasma reactive species on bacterial cells by retaining generated reactive species within a closed container, promoting diffusion of long-lived species (e.g. O_3, H_2O_2, and NO_2) inside the food product tissue (Ziuzina et al., 2014). However, a significant increase in the lethality during extended post-treatment storage of 24 h in comparison to 6 h was not observed in this study (Table 3.1 & 3.2). This is likely due to the open atmospheric

treatment condition that allowed the reactive species to diffuse in the surrounding environment, preventing the continuous exposure to *L. innocua* on ham.

Table 3.2 Mean log reductions of *L. innocua* on ham formulated with 1 % NaCl (with and without rosemary extract) or 3 % NaCl and exposed to cold plasma treatment for 60 or 180 s at 4 °C and stored at 4 °C for 0, 6, or 24 h.

Treatment time (s)	**Treatment temperature (°C)**	**Storage time (h)**	**Log N/No**		**Log N/No**
			1 % NaCl ham		**3 % NaCl ham**
			With rosemary	**Without rosemary**	**Without rosemary**
60	4	0	1.1 ± 0.2^{b}	1.2 ± 0.2^{abABC}	1.1 ± 0.1^{BC}
60	4	6	1.3 ± 0.2^{ab}	1.6 ± 0.3^{abAB}	1.1 ± 0.2^{BC}
60	4	24	1.3 ± 0.4^{ab}	1.7 ± 0.4^{abBC}	0.9 ± 0.1^{C}
180	4	0	1.4 ± 0.2^{ab}	1.7 ± 0.5^{abAB}	1.4 ± 0.3^{BC}
180	4	6	1.4 ± 0.2^{ab}	1.9 ± 0.2^{aA}	1.3 ± 0.2^{ABC}
180	4	24	1.6 ± 0.5^{ab}	1.8 ± 0.5^{abAB}	0.9 ± 0.1^{C}

Lower case $^{a-d}$ indicate significantly different ($p<0.05$) mean log reduction of *L. innocua* on 1 % NaCl ham with or without rosemary extract; capital letter $^{A-D}$ indicate significantly different ($P<0.05$) mean log reduction of *L. innocua* on 1 % NaCl and 3 % NaCl ham without rosemary extract. Across the column effect of time and storage and between the rows effect of % NaCl or rosemary.

During storage, salt concentration as a main effect had a significant effect ($p<0.01$) on the inactivation of *L. innocua* on ham; and there was a significant two-way interaction ($p<0.001$) between NaCl concentration and treatment temperature. When samples were treated for 180 s at 23 °C, the observed log reductions of *L. innocua* were not significantly different in ham formulated with 1 % NaCl than those in ham formulated with 3 % NaCl (Table 3.1). Regardless of storage

time or the presence of rosemary, the log reduction of *L. innocua* on ham formulated with 1 % NaCl, was greatest when samples were treated at 4 °C (log reduction of 1.49 CFU/cm^2), whereas treatment of ham with 3% NaCl at 4 °C resulted in significantly lower reductions (0.96 log CFU/cm^2) in *L. innocua*. Presence of NaCl in water reduced the antimicrobial effects of plasma during direct treatment, possibly by altering the dynamics of reactive species generated by atmospheric plasma (Kang et al., 2014). Hydroxyl radicals produced by plasma can interact with Cl^- ions of NaCl, and forming ($OHCl^-$) bonds, which prevent free movement of hydroxyl radicals and limit their accessibility to fungal spores in solutions, causing less damage to spores (Kang et al., 2014). In another study, Ryu et al. (2013) demonstrated that the inactivation of yeast in saline (145 mM NaCl) was less compared to water when treated with Ar plasma jet. In the present study, lethality of plasma against *L. innocua* on ham was significantly influenced by % NaCl in ham after post plasma treatment storage. This could be due to reduced antimicrobial activity of reactive species generated by plasma on 3 % NaCl ham compared to 1 % NaCl ham, leading to less damage to *L. innocua* cells on 3 % NaCl ham. After 24 h post-plasma treatment storage at 4 °C, the observed log reduction in *L. innocua* on 3 % NaCl ham without rosemary treated for 180 s was significantly lower compared to 1 % NaCl ham (Table 3.2). Although data are significantly different, the differences are very small and may not be biologically relevant. The hypothesis of this study was that the presence of rosemary extract would result in a synergistic effect on microbial inactivation during storage after plasma treatment. Rosemary extract is a well-known antioxidant and has been used commercially in ham to provide inhibitory action against microorganism growth during storage (Zhang et al., 2003). Although the presence of rosemary extract had a significant effect ($p<0.05$) on the log reduction of *L. innocua* regardless of treatment

temperature, NaCl concentration, or storage time, the difference over all treatments was ~0.2 log CFU/cm^{2,} which is not biologically relevant. No significant synergistic effects of rosemary extract with cold plasma treatment were observed on reducing *L. innocua* population during post-treatment storage. It could be that the rosemary extract scavenges the free radicals produced by plasma and limits the antimicrobial effects of the plasma treatment.

3.3.3 Effect of plasma treatment on lipid oxidation

TBARS assay was used to determine the effect of plasma treatment time on lipid oxidation of ham samples (with or without rosemary). TBARS values of 1 % NaCl ham, with or without rosemary extract (10 g/L) treated with plasma were significantly higher than those of untreated samples (Figure 3.5). This result is similar to that of Jayasena et al. (2015), who found that the TBARS values of plasma treated beef and pork were increased with increasing plasma treatment time. Similarly, Kim, Yong, Park, Choe, & Jo (2013) and Rød et al. (2012) reported that plasma treatment of ready-to-eat meat and pork loin exhibited higher TBARS values than untreated samples. The observed increase in lipid oxidation of plasma treated meat could be due to the highly oxidative nature of plasma reactive species such as reactive oxygen species, super oxide, free radical, hydrogen peroxide, and reactive nitrogen species. These reactive oxygen species act as precursors of hydroperoxide production and initiate lipid oxidation (Kim et al., 2013; Min & Ahn, 2005). However, Albertos et al. (2017) and Jung et al. (2017) reported no significant effect on lipid oxidation after atmospheric plasma treatment of meat batter and fresh mackerel fillets. These differences might be induced by the type of plasma system used to treat the sample and the dynamic nature of plasma reactive species (Attri et al., 2015; Jung et al., 2017).

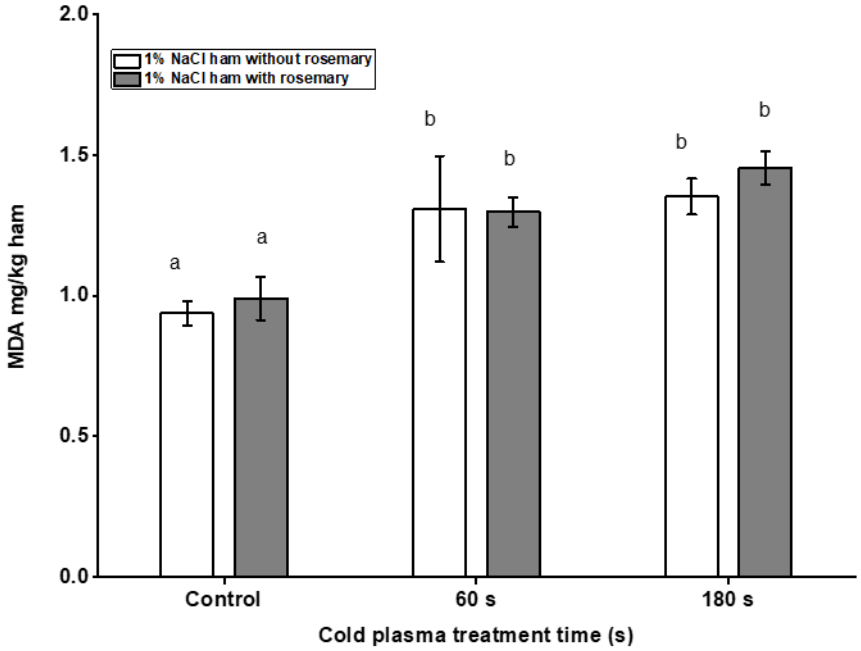

Figure 3.5. Lipid oxidation in 1 % NaCl ham samples without rosemary (white column) and with rosemary (grey column) extract after plasma exposure at 23 ºC. Columns with different letters indicate a significant difference in lipid oxidation. Data are shown as least square means ± standard deviations of triplicate (n = 3) independent experiment.

3.3.4 Effect of plasma treatment on color parameters

Among all quality parameters, consumers consider meat color as an indicator of freshness and quality of meat. Moreover, meat appearance has direct influence on the acceptance of meat, and it influences the consumer preference to purchase (Jayasena et al., 2015). The impact of plasma treatment on color parameters of ham samples with 1 % NaCl (with or without rosemary) is presented in (Table 3.3). The results showed that after plasma exposure, the L* (brightness) and b*(yellow-blue) values of ham sample (with or without rosemary) were not significantly changed compared to the untreated control sample. Whereas the a* (red-green) values of ham samples (with or without rosemary) were significantly lower than those of untreated samples. These results are in concurrence with the cold plasma treatment effect on surface color change reported on pork loin

and fresh chicken breast by Jayasena et al. (2015); Kim et al. (2016) and Wang, Zhuang, Hinton, & Zhang (2016). Similar results were reported by Wang et al. (2016) who found that the cold plasma treatment did not significantly change the L* values of chicken breast fillets. There were no significant differences in color parameter L*, a*, and b* values of pork meat after exposure to argon, helium, and nitrogen gas vacuum cold plasma for the duration of 5 and 10 min (Ulbin-Figlewicz, Brychcy, & Jarmoluk, 2013).

Table 3.3: Color parameters (L*, a*, and b*) of 1 % NaCl ham samples after plasma treatment at 23 ºC

Time (sec)	**With Rosemary**			**Without rosemary**		
Color parameter	**L***	**a***	**b***	**L***	**a***	**b***
Control	91.70±0.1[a]	1.18±0.1 [a]	-0.20±0.10 [a]	91.76±0.26 [a]	1.15±0.07 [a]	-0.18±0.05 [a]
30	91.78±0.1[a]	1.05±0.1 [a]	-0.13±0.04 [a]	91.60±0.63 [a]	0.98±0.08 [b]	-0.21±0.03 [a]
60	91.73±0.4[a]	0.96±0.0 [b]	-0.06±0.02 [a]	91.99±0.75 [a]	0.88±0.05 [b]	-0.24±0.09 [a]
90	91.68±0.1[a]	0.93±0.0 [b]	-0.04±0.00 [a]	91.74±0.42 [a]	0.94±0.02 [b]	-0.18±0.04 [a]
120	91.84±0.1[a]	0.97±0.0 [b]	-0.07±0.07 [a]	91.80±0.21 [a]	0.88±0.02 [b]	-0.12±0.02 [a]
180	91.61±0.5[a]	0.95±0.0 [b]	-0.06±0.12 [a]	92.19±0.26 [a]	0.97±0.04 [b]	-0.22±0.02 [a]

Values (mean ± standard deviation of three independent treatment) followed by lower case letter in the same column represents significant differences ($P \leq 0.05$).

3.3.5 Effect of plasma treatment on water content and water activity

A significant decrease in water content of ham during cold plasma treatment at all the treatment times (Figure 3.6) were observed, resulting from drying of the samples. For instance, the water content decreased from 0.642 to 0.316 kg water/kg ham (equivalent to 1.793 to 0.462 kg water/kg dry mass) after 180 s treatment (Figure 3.6). The water activity values of ham also decreased during

cold plasma treatments, but the change in a_w values were small i.e., from 0.95 to a minimum of 0.92. The desorption process in ham using vapor sorption analyser (VSA) was examined since the change in water contents was considerably higher compared to the change in a_w during cold plasma treatments.

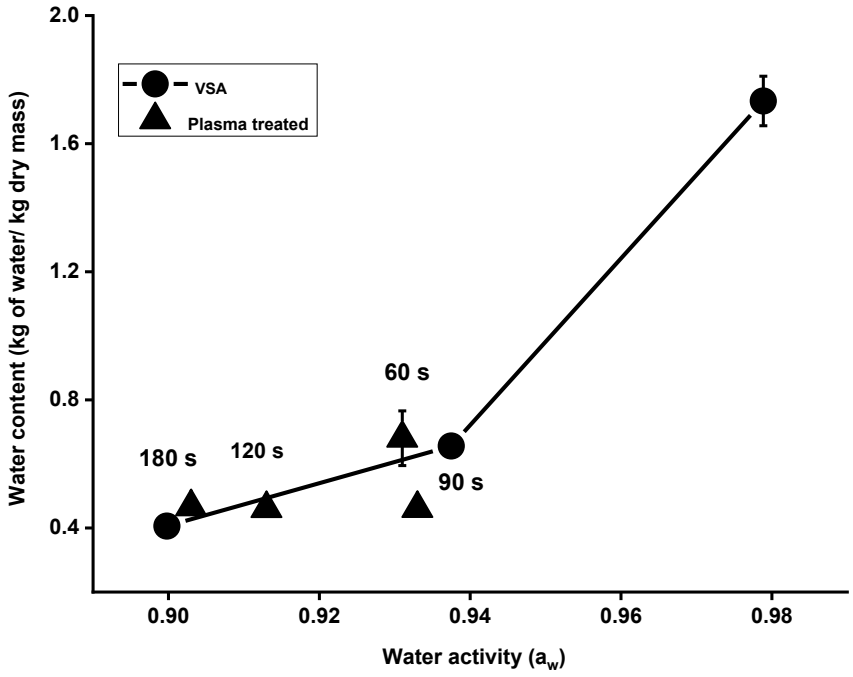

Figure 3.6: Water content and water activity of 1 % NaCl ham samples without rosemary extract treated with plasma at 23 ºC (triangles with corresponding plasma treatment time) and water desorption isotherm (equilibrium water contents and water activity) of untreated ham obtained by vapor sorption analyser (VSA) at 25 °C (circle with line).

It was necessary to understand the water desorption property of ham and confirm that the water activity values were equivalent to the decreased water contents in ham. The ham samples were equilibrated at selected water activities inside the VSA to determine corresponding water contents at 25 °C. An important assumption was made regarding the existence of a pseudo water vapour

equilibrium at the interface of ham and air above the surface during cold plasma treatment of ham, especially for longer duration, although cold plasma treatment is a dynamic process. The water content values of ham at selected equilibrated water activity values during desorption process were very close to those of ham after cold plasma treatment, especially after treatment for 120 and 180 s treatments (Figure 3.6), which confirmed drying of the samples during cold plasma treatments. Water in meat can be classified into three components; bound water (1 %), entrapped or immobilised water (85 %), and free water (Warner, 2017). The water tightly bound to macromolecules (bound water) is not affected by plasma treatment (Albertos et al., 2017). Albertos et al. (2017) reported that the plasma treatment significantly decreased the entrapped water content in the dense myofibrillar network and consequently increased the extramyofibrillar water content (free water) of fish. They suggested that plasma treatment could change the fish microstructure, resulting in the release of trapped immobilised water. In the present study, a considerable decrease in water content was observed with a small change in a_w during cold plasma treatment. This is probably due to the release of entrapped water from the dense myofibrillar network to extramyofibrillar water (free water) during cold plasma treatment (Albertos et al., 2017). This released water likely maintained the available water in ham and hence the observed a_w values after plasma treatments were similar to the a_w of untreated ham (Figure 3.6).

3.3.6 Plasma diagnostics

Optical emission spectra of excited plasma species discharge were obtained at atmospheric condition over the spectral range 200-900 nm (Figure 3.7). Majority of the peaks were obtained in the near UV region of the spectra (Figure 3.7). The observed dominant peak in the wavelength region 300 to 450 nm of air plasma (Figure 3.7) shows vibrational band of neutral and ionic

emission of nitrogen molecule (Fridman, 2012). The OH peak around 300 nm was also identified (Cullen et al., 2014). The peaks associated with optical transition of oxygen atom are observed at low intensities around 780 nm. Most of the reactive oxygen species are beyond the detection of optical spectrum, it might be due to relatively long half-life of active oxygen species, which tends to lose energy due to particle collision, quenching its energy before detectable light emission (Ziuzina, Patil, Cullen, Keener, & Bourke, 2013).

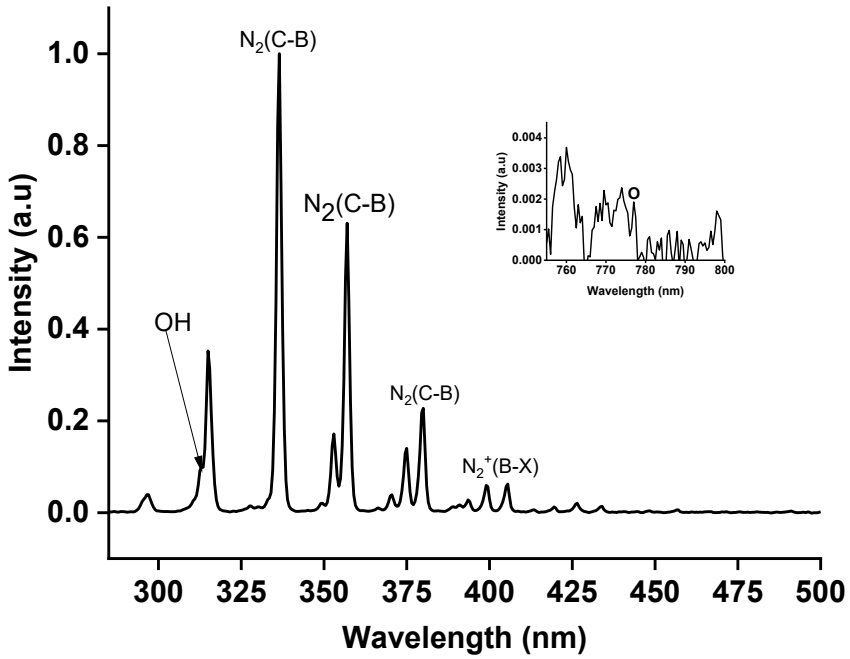

Figure 3.7: Optical emission spectra of atmospheric air DBD plasma generated at 28 kV.

3.3.7 Ozone, nitrous oxides, and hydrogen peroxide concentration after plasma treatments

The atmosphere between the electrodes was also analyzed to quantify the generated concentrations of ozone, nitrous gases and hydrogen peroxide. Reportedly these gases have strong antimicrobial activity against microorganisms and have been utilized in industry for commercial applications (Hertwig, Reineke, Rauh, & Schlüter, 2017; Misra, Ziuzina, Cullen, & Keener, 2013). Dielectric

barrier discharge is generally recognized as one of the most efficient methods to produce ozone (Misra et al., 2013). The high electromagnetic field between the discharge gap splits off the oxygen molecules in air into unstable singlet oxygen, which in turn combines with O_2 to from ozone (Chang & Wu, 1997). Also, this highly reactive oxygen interacts with air humidity, and it can result in the formation of various reactive species, including hydrogen peroxide and nitrous gases (Lee et al., 2015; Moiseev et al., 2014). In this experiment, the gas samples were collected from the electrode gap during the treatments because these reactive species have very short life in open atmosphere. A maximum ozone concentration of 833.3 ppm was recorded during the plasma treatment duration of 150-180 s. Ozone has powerful oxidation potential, with a redox potential of 2.07 and it has antibacterial effect against a number of microorganisms including gram-positive and gram-negative microorganisms (Seydim et al., 2004). The measured concentrations of nitrous gases, and hydrogen peroxide during plasma treatment times of 150-180 s were 106.6 ppm and 2.8 ppm respectively. Lee et al. (2015) reported that among all reactive species, hydrogen peroxide is one of the most stable reactive species and responsible for spore inactivation with highest intracellular concentration.

3.3.8 Effect of plasma treatment on ham and electrode surface temperature

The surface temperatures of ham before, during, and after plasma treatments and the electrode surface after plasma treatment for 180 s are presented in Figure 3.8. Plasma treatment increased the ham surface temperature from 21.0 °C to 26.1 °C and 25.1 °C, during and after treatments, respectively (Table 3.4). The maximum measured electrode surface temperature was 29 °C (Tbale 3.4) after 180 s treatment. No significant difference in ham surface temperature was observed with increased duration of treatment ($P > 0.05$). The plasma treatment can be considered as a non-

thermal treatment since the temperature increase was negligible during the process and it possibly did not influence the microbial inactivation rate.

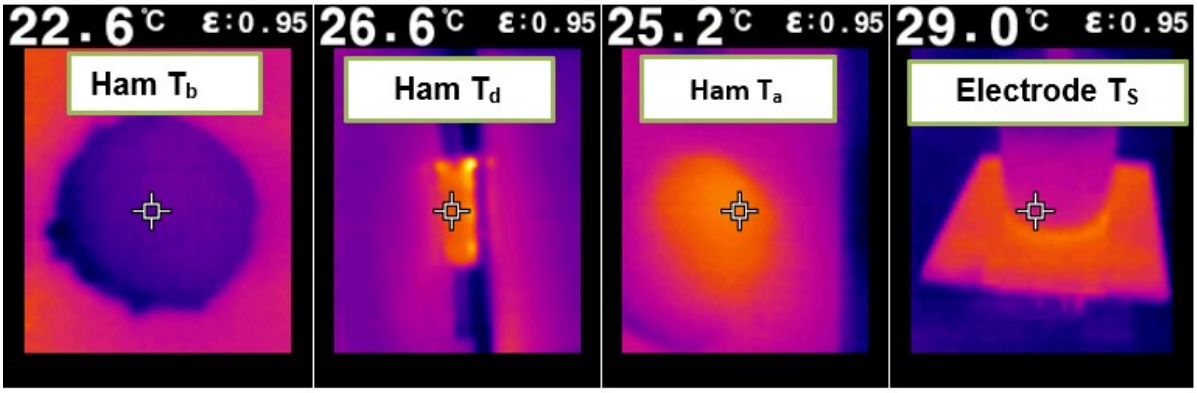

Figure 3.8: Surface temperatures of ham before plasma treatment (T_b) (a), during treatment (T_d) for 180 s (b) and after 180 s plasma treatment (T_a) (c) and the surface temperature of the electrode after 180 s plasma treatment (T_s).

Table 3.4: Ham surface temperature before (T_b), during (T_d), and after cold plasma treatments (T_a) and electrode surface temperature at the end of treatment (T_s).

Treatment time (s)	**Temperature T °C**			
	Before treatment (T_b)	**During treatment (T_d)**	**After treatment (T_a)**	**Electrode surface (T_s)**
30	21.8±0.7	24.0±0.5	23.1±0.2	25±0.8
60	21.8±0.8	23.9±1.1	23.6±0.8	26.5±0.6
90	22.1±0.7	25.0±0.7	24.3±0.6	27.3±1.3
120	21.9±0.8	25.3±1.2	24.5±0.3	27.9±1.2
180	21.7±0.8	26.1±1.6	25.1±0.9	28.5±0.9

Values (Mean ± standard deviation of three independent treatments).

3.4 Conclusions

This study evaluated the inactivation effect of atmospheric cold plasma treatment of RTE ham containing different NaCl concentrations and rosemary extract at 23 °C and 4 °C for control of *L. innocua*. Plasma treatment time and post plasma treatment storage had a significant effect on the inactivation of *L. innocua* on RTE ham. However, no significant inactivation effect of plasma against *L. innocua* on ham with 3 % NaCl and 1 % NaCl ham were observed for the same treatment time. Similarly, cold plasma treatment in the presence of rosemary extract did not significantly influence the inactivation of *L. innocua* at both treatment temperatures, except for 180 s plasma exposure at 23 °C. Among quality parameters, lipid oxidation, color, and water loss of 1 % NaCl ham were investigated after cold plasma treatment. This finding demonstrated that the concentration of thiobarbituric acid reactive substance (TBARS) was significantly increased after a 60 s cold plasma treatment. However, no significant differences in surface color parameters L* and b* values were observed after plasma treatment, except the significant increase in a* value. In the present study, a significant decrease in ham water content after cold plasma treatments was observed. Drying, oxidation, and flavor changes of meat products during open atmospheric cold plasma treatment could be a challenge for future scale-up of this technology.

Chapter 4: Effect of In-Package Atmospheric Cold Plasma Discharge on Microbial Safety and Quality of Ready-to-Eat Ham in Modified Atmospheric Packaging during storage

4.1 Introduction

Listeria monocytogenes is a foodborne pathogen that causes infections with a high hospitalization rate (>90 %) and a fatality of 20-30 % (Hernandez-Milian & Payeras-Cifre, 2014; Thomas, Murray, et al., 2015). Ready-to-eat (RTE) products, particularly meat and seafood, have been identified as "high risk" for *Listeria* contamination (Health Canada, 2011; Zhu, Du, Cordray, & Ahn, 2005). According to the Center for Disease Control and Prevention, the reported incidence of listeriosis has remained unchanged in the past 10 years (CDC, 2014), despite strict guidelines that were put in place to control *L. monocytogenes* (Ricci et al., 2018). In RTE cooked meat, the surface contamination with *L. monocytogenes* may occur during the post-processing steps since *Listeria* survive in processing facilities and can be transferred to products from equipment surfaces such as slicers and conveyor belts (Beresford, Andrew, & Shama, 2001; Rød, Hansen, Leipold, & Knøchel, 2012). In food products, where the contamination is mainly on the product surface, surface decontamination techniques can be used to reduce the risk of the presence of *L. monocytogenes*.

Atmospheric cold plasma (ACP) is an emerging novel non-thermal surface decontamination technology. The decontamination effects of ACP discharge are due to the generation of cocktails of reactive species, including reactive oxygen species (ROS), reactive nitrogen species (RNS), UV photons, positive and negative charges, and free radicals, all of which have tremendous potential to injure and kill bacteria, spores and other pathogenic organisms (Misra et al., 2018; Surowsky,

Schlüter, et al., 2014). The concentration of these reactive species in plasma is dependent on process parameters, including applied voltage, gas composition, temperature, relative humidity, duration of treatment, and post-treatment storage (Chizoba, Sun, & Cheng, 2017; Park et al., 2018). Several studies have reported the potential antimicrobial action of ACP against a range of microorganisms on different surfaces (Liao et al., 2017; Yong et al., 2017). However, decontamination of RTE meat products using ACP has rarely been investigated. Previous studies reported inactivation of *L. monocytogenes* on RTE meat, including ham surface (Song et al., 2009; Chapter 3), beef jerky (Yong et al., 2017), fresh pork (Fröhling et al., 2012) and RTE meat bresaola (Rød et al., 2012). Recently, a number of studies reported in-package plasma treatment of foods including grape tomatoes (Min et al., 2018), bulk Romaine lettuce (Min, Roh, Niemira, et al., 2017), and chicken fillets (Wang et al., 2018). The results demonstrated that cold plasma could be used to decontaminate foods inside the sealed package while keeping the quality of the product intact.

Modified atmosphere packaging (MAP) is extensively used in the food industry to extend shelf life and preserve sensory quality. The most commonly used gases in MAP of meat include; oxygen, nitrogen, and carbon dioxide, together with a trace amount of helium, argon, and carbon monoxide (Misra & Jo, 2017; Phillips, 1996). Frequently, mixtures of these gases, with specific percentages, are used for meat and meat products. In most cases, cooked meats are stored in 70 % N_2 + 30 % CO_2 (Farber, 2016). Apart from MAP, other important strategies used for ensuring RTE cooked meat product safety include use of preservatives and bacteriocins. Preservatives and bacteriocins, including sodium nitrite, sodium lactate, sodium diacetate, carnocylin A, and leucocin A can inhibit *L. monocytogens* growth (Balay et al., 2018; Field et al., 2018; Horita et al., 2018; Mbandi

& Shelef, 2002). A hurdle approach, combining food reformulation (e. g., use of preservatives or bacteriocins), MAP, and non-thermal post-packaging decontamination, can enhance the microbial safety and quality of cooked RTE meat products (Horita et al., 2018). However, among non-thermal post-packaging decontamination strategies, application of ACP along with ham reformulation on quality and safety of RTE meat has not been reported. It is important to understand the interaction effect of ACP to inactivate *L. monocytogenes* on the surface of ham formulated with preservatives or bacteriocins to develop ACP-based hurdle approach. Hence, the objectives of this study were to investigate the efficacy of ACP to inactivate *L. monocytogenes* on the surface of ham formulated with or without preservatives or bacteriocins. An additional objective was to observe the changes in color and lipid oxidation as a function of gas composition used in MAP, treatment time, and post-plasma treatment storage.

4.2 Materials and methods

4.2.1 Preparation and formulation of ham

Curing ingredients, preservatives, and bacteriocin (wt/wt kg of lean meat) were mixed in lean meat to prepare cooked control ham, ham with preservatives, and bacteriocin. Lean meat mixed with other ingredients was cooked according to Liu, Miller, Basu, & McMullen. (2014). The formulation of control ham consisted of lean meat, ice (16.71 % of meat weight), sodium triphosphate (0.50 % of meat weight), and sodium chloride (0. 21 % or 0.98 % of meat weight), Prague powder/curing ingredient ((0.33 % of meat weight (6 % sodium nitrite, 94 % NaCl)), sodium erythorbate (0.08 %), and dextrose (2.45 % of meat weight). For ham with preservatives, sodium diacetate (0.1 % of meat weight), and sodium lactate (1.40 % of meat weight) were added, keeping all other ingredients the same as the control ham except reduced sodium chloride

concentration (0.21 % of meat weight). A partially purified culture ferment (0.05 %) from *Carnobacterium maltaromaticum* UAL 307 (containing 3 bacteriocins including carnocyclin A, piscicolin 126, and carnobacteriocin BM1) was added to prepare ham with bacteriocins. The cooked hams were placed on ice for 10 min and kept at 4 °C for overnight cooling. After overnight cooling, the cooked ham was sliced (2 mm thick, surface area 50 cm^2) with a sterilized slicer, vacuum-packed, and stored at 0 ºC until use.

4.2.2 Cultivation of bacterial strains and growth condition

Five strains of *L. monocytogenes* (FSL J C1-056; FSL J1- 177; FSL R2-499; FSL N1-227; FSL N3-013) were selected in this study. Strains were streaked from -80 °C stock cultures and propagated on TS agar, incubated at 37 °C for 48 h to isolate individual colonies. Individual colonies were picked, transferred to 1 mL tryptic soy broth (TSB), and incubated overnight at 37 °C. After overnight growth, a 1 % inoculum was transferred into TSB and incubated in an orbital shaker at 25 °C (200 RPM) for 24 h. To create the 5-strain cocktail of *L. monocytogenes*, 1 mL of each culture was mixed and centrifuged at 5311 × *g* for 10 min, and the supernatant was discarded. The cell pellet was resuspended in 1 mL of 0.85 % NaCl and kept at 25 °C until use (within 1 h).

4.2.3 Inoculation and modified atmosphere packaging

Vacuum-packed cooked ham was opened and cored to obtain samples with a surface area of 1 cm^2. Each sample was inoculated with 10 µL of cells (final concentration 10^8 CFU/cm^2) suspended in 0.85 % NaCl and the control samples were inoculated with the same volume of 0.85 % NaCl. After inoculation, samples were held in a biosafety hood for 10 min on a sterile tray. Using forceps, each inoculated ham sample was aseptically transferred to 76.2 µm thick, nylon and polypropylene coextruded vacuum bags (Unipac Packaging Products Ltd., Edmonton, AB, Canada). Packages

containing ham samples were packaged in different atmospheres (MAP1: 20 % O_2 + 40 % N_2 + 40 % CO_2, MAP2: 50 % CO_2 + 50 % N_2, MAP3: 100 % CO_2) using a gas flush packaging machine (Model C200; Multivac, Kansas City, MO, USA). The final gas volume per package averaged approximately 20 cm^3.

4.2.4 Plasma system and treatment

For in-package ACP treatment, a dielectric barrier discharge (DBD) plasma system (PG 100-3D, Advanced plasma solutions, Malvern, PA, USA) with a voltage output in the range 0-30 kV at 3.5 kHz was used. The distance between the high voltage electrode (2.5 cm diameter) and a ground electrode was equal to the height of the polyethylene package (approx. 8 mm) with ham sample. ACP was generated inside each package at 30 kV under atmospheric pressure with selected gas compositions (MAP1, MAP2, and MAP3). These gases were used as plasma generating media. For ACP treatment, the packaged ham samples were directly placed between the electrodes (i.e. within the plasma discharge region). Between the ham and top electrode, the polythene bag and gas act as additional barriers. The inoculated packaged ham samples were exposed to ACP for selected durations (1 to 10 min) at room temperature (23 ± 2 °C). Prior to ACP treatment, inoculated samples were held inside the packages for approximately 1 h and sealed packaged samples were stored at 4 °C for 18 h to achieve a uniform time interval between inoculation and packaging and between packaging and ACP treatment. All experiments were performed in triplicate.

4.2.5 Microbial enumeration

Cell counts of *L. monocytogenes* of ACP treated and control ham samples were monitored after 1 h, 24 h, and 7 days of storage at 4 °C. Un-inoculated packaged samples were also prepared and

stored under the same conditions as treated samples for each experiment to verify the absence of contamination prior to the experiment and after storage. Packaged samples were opened aseptically inside the biosafety hood and the samples were transferred into 50 mL falcon tubes containing 1 mL of 0.5 % peptone water. Falcon tubes containing ham samples were vortexed for 60 s to detach cells from ham sample, prior to serial dilution. Aliquots of 0.1 mL of appropriate dilutions were plated on PALCAM agar for estimation of uninjured cells and TSA to estimate total viable cell counts. Plates were incubated at 37 °C for 48 h prior to enumeration. Counts were converted to $\log_{10}$ CFU/cm^2 for statistical analysis.

4.2.6 Determination of lipid oxidation

To investigate the effect of in-package plasma exposure on ham quality, un-inoculated ham samples were exposed to ACP for 5 min or 10 min, followed by 24 h and 7 days of post-treatment storage at 4 °C. Untreated controls samples were stored under the same environmental conditions as treated samples. Lipid oxidation was measured using thiobarbituric acid (TBA) assay modified from the method described in Chapter 3 of this thesis, and the results were represented as malonaldehyde (MDA) mg equivalent/kg of ham. A detailed description of experimental procedure can be found in Chapter 3, section 3.6 of this thesis.

4.2.7 Determination of color parameters

The color of ACP treated, and stored ham samples were measured using a chromameter CR-410 (Konika Minolta sensing Inc., Osaka, Japan). The chroma meter measuring head consisted of D_{65} lighting source, 8 mm aperture, and a 10° standard observer angle. The Hunter lab color parameters L*, a* and b* values were recorded.

4.2.8 Optical emission spectroscopy

The optical emission spectrum of ACP discharge within the packages was acquired with an enhanced UV sensitivity black comet concave grating spectrometer (Black comet C-25, StallerNet Inc., Tampa, FL, USA). The UV enhanced CCD detector had a signal to noise ratio of 1000:1 and was recorded over a wavelength range of 190-850 nm. The emitted light was collected via coupled optical fiber (F600-UV-ViS-SR, Stellernet Inc., Tampa, FL, USA) with a diameter of 40 μm, spectral range 190-850 nm, and a numerical aperture of 0.22. The optical fiber was placed perpendicular to the plasma discharge and facing centrally towards the package to allow the light to pass through the center of the curvature of the polythene bag filled with gas. The set integration time was 1000 ms, and each spectrum was averaged and scanned 5 times using Spectra viz software. To reduce the error, 10 spectra were collected for each treatment condition and the data were normalized and averaged for peak identification.

4.2.9 Measurements of ozone, nitrous gas, and hydrogen peroxide concentration

Gas phase concentration of ozone, nitrous gas and hydrogen peroxide inside the packages were measured after plasma treatment. A Dräger short-term detector tube (Dräger Safety AG & CO, Lubeck, Germany), an ozone 10/a Dräger tube (CH 21 001 Dräger Safety AG & CO, Lubeck, Germany), a nitrous fume 50/a Dräger tube (81 01 921) and a hydrogen peroxide 0.1/a Dräger tube (81 01 041) were used to detect the respective gas concentrations along with a Dräger Accuro detector following the manufacturer's instruction. The final concentration of respective gases was calculated according to Klockow & Keener (2009) and manufacturer's guidelines.

4.2.10 Statistical analysis

Data on the response variables i.e., logarithmic cell counts, lipid oxidation, and changes in color parameter were subjected to analysis of variance using a generalized linear mixed-effects procedure of SAS® University edition (Proc Glmmix; SAS studio 3.71, Cary, NC, USA). The fixed effects were treatment factors including ham formulation (presence or absence of preservatives or bacteriocins), packaged gas composition (MAP1, MAP2 and MAP3), ACP treatment time, and post ACP treatment storage time. The level of significance reported in the test was P-value ≤ 0.05 using Tukey's honest test.

4.3 Results

4.3.1 Characterization of ACP discharge

Optical emission spectroscopy was conducted to capture the dominant plasma reactive species, in the UV/VIS wavelength (190-850 nm) region. Figure 4.1 shows the emission spectra of MAP1 (20 % O_2 + 40 % N_2 + 40 % CO_2), MAP2 (50 % CO_2+50 % N_2), and MAP3 (100 % CO_2) of in-package ACP discharge, which exhibited strong emission from excited nitrogen species in the UV region, and weak emission spectrum of hydroxyl (OH) and oxygen species.

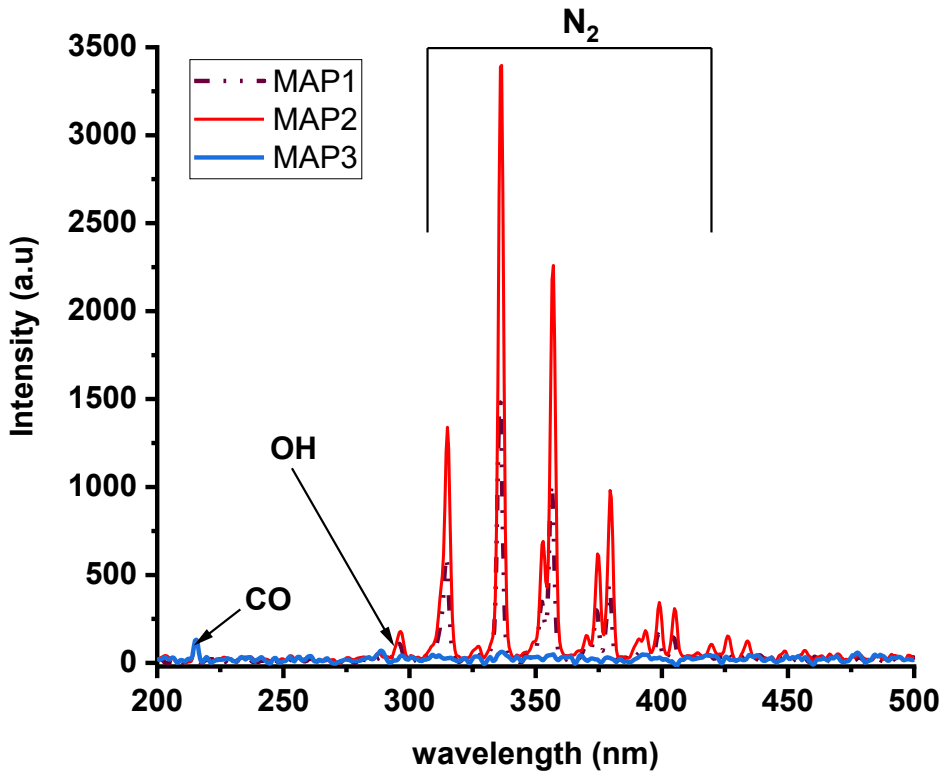

Figure 4.1: Optical emission spectra of atmospheric in-package plasma discharge at 30 kV, 3.5 kHz, and 0.2 mA. Data are shown as an average of three independent spectra.

Analysis of the three distinct spectra obtained from the generated plasma discharge in MAP1, MAP2, and MAP3, indicated that the strong peaks obtained in near-UV and visible regions corresponding to strong emission from N_2 and N_2^+ excited species were strongly influenced by the percentage of gases used. Further analysis of the emission spectrum of MAP3 showed that the obtained peaks corresponding to 231, 269, 311, 365.5, 354.5, 388, 399, 425, 437, 480, and 490 nm were possibly due to carbon dioxide positive and negative excited species. However, the intensity of these peaks was very low in the of MAP3.

4.3.2 Gaseous phase concentration of major long-life reactive species after ACP treatment

The concentration of ozone, hydrogen peroxide, and nitrous gases was measured inside the sealed package immediately after ACP treatments as functions of treatment time and gas compositions (Table 4.1). For MAP1, after 2 min of plasma exposure, the ozone concentration reached the highest values of detection limit (1500 ppm) of the present setup, whereas the concentrations of hydrogen peroxide and nitrous gases were only 150 ppm and 1000 ppm, respectively. For MAP2 and MAP3, generated ozone concentration was under the detection limit (< 3 ppm) and 70 ppm, respectively, even after a longer treatment time of 10 min. Similarly, the hydrogen peroxide and nitrous gas concentrations were under the detection limit after 10 min of ACP treatment for MAP2 and MAP3. Table 4.1 shows the lifetime of generated reactive gas in terms of measured active concentrations corresponding to 10 min ACP treatment at room temperature of 23 ± 2 °C.

Table 4.1: Ozone, hydrogen peroxide, and nitrous gas concentration after plasma treatments in gaseous phase

MAP	Treatment time	Gaseous phase concentration (ppm)		
		Ozone	**Hydrogen peroxide**	**Nitrous gas**
MAP1	0 min	ND*	ND*	ND*
	2 min	> 1500	10.0 ± 3.0	2063 ± 118.4
	5 min	> 1500	> 15	2983 ± 175.5
	10 min	> 1500	> 15	4233 ± 275.3
MAP2	0 min	ND*	ND*	ND*
	2 min	ND*	ND*	ND*
	5 min	ND*	ND*	ND*
	10 min	ND*	ND*	ND*
MAP3	0 min	ND*	ND*	ND*
	2 min	9.6 ± 2.0	ND*	ND*
	5 min	29.3 ± 3.0	ND*	ND*
	10 min	70.6 ± 7.0	ND*	ND*

(MAP1: 20 % O_2 + 40 % N_2 + 40 % CO_2), (MAP2: 50% CO_2 + 50 % N_2); (MAP3: 100 % CO_2)

ND*: Not detected

4.3.3 Effect of ACP treatment time and gas composition on *L. monocytogenes* inactivation

All ham samples were inoculated with an average of 8 log CFU/cm^2 *L. monocytogenes* cells. A mixed model ANOVA was used to assess the effect of three different ham formulations, i.e. control ham, ham with preservatives, and ham with bacteriocins, on the reduction of *Listeria* cell count after ACP treatment with selected gas compositions and treatment time. ACP treatment time, ham formulation, and in-package gas composition influenced the reduction of *L. monocytogenes* counts on the ham surface (Figure 4.2A-C). Data for counts on PALCAM agar were similar to those obtained for TSA agar (data not shown). The combined effect of ACP treatment time and gas composition (MAP) was evaluated on three ham formulations, control ham (absence of preservatives or bacteriocins) (Figure 4.2A), ham with preservatives (Figure 4.2B), and ham with bacteriocins (Figure 4.2C). Significant interactions between treatment time and gas compositions, ($P < 0.\ 05$) and between gas and ham groups ($P < 0.05$) were observed.

A significant difference in total cell counts of *Listeria* was found among the ham formulations (F value (2, 106) = 17.1; $P < 0.05$), among the gas compositions (F value (2, 106) = 118.8; $P < 0.05$), and among the treatment time (F value (4, 106) = 44.4; $P < 0.05$). ACP treatment with MAP1 was significantly more effective to reduce *Listeria* cell counts compared to MAP2 and MAP3, when control hams or hams formulated with preservatives or bacteriocins were tested. For MAP1, 5 min ACP treatment significantly reduced the *L. monocytogenes* cell counts in comparison to 1, 2, or 3 min treated samples, irrespective of ham formulation (Figure 4.2A-C). For MAP2 or MAP3, ACP treatment time had no significant effect on the reduction of total cell counts of *Listeria* on ham with preservatives (Figure 4.2B).

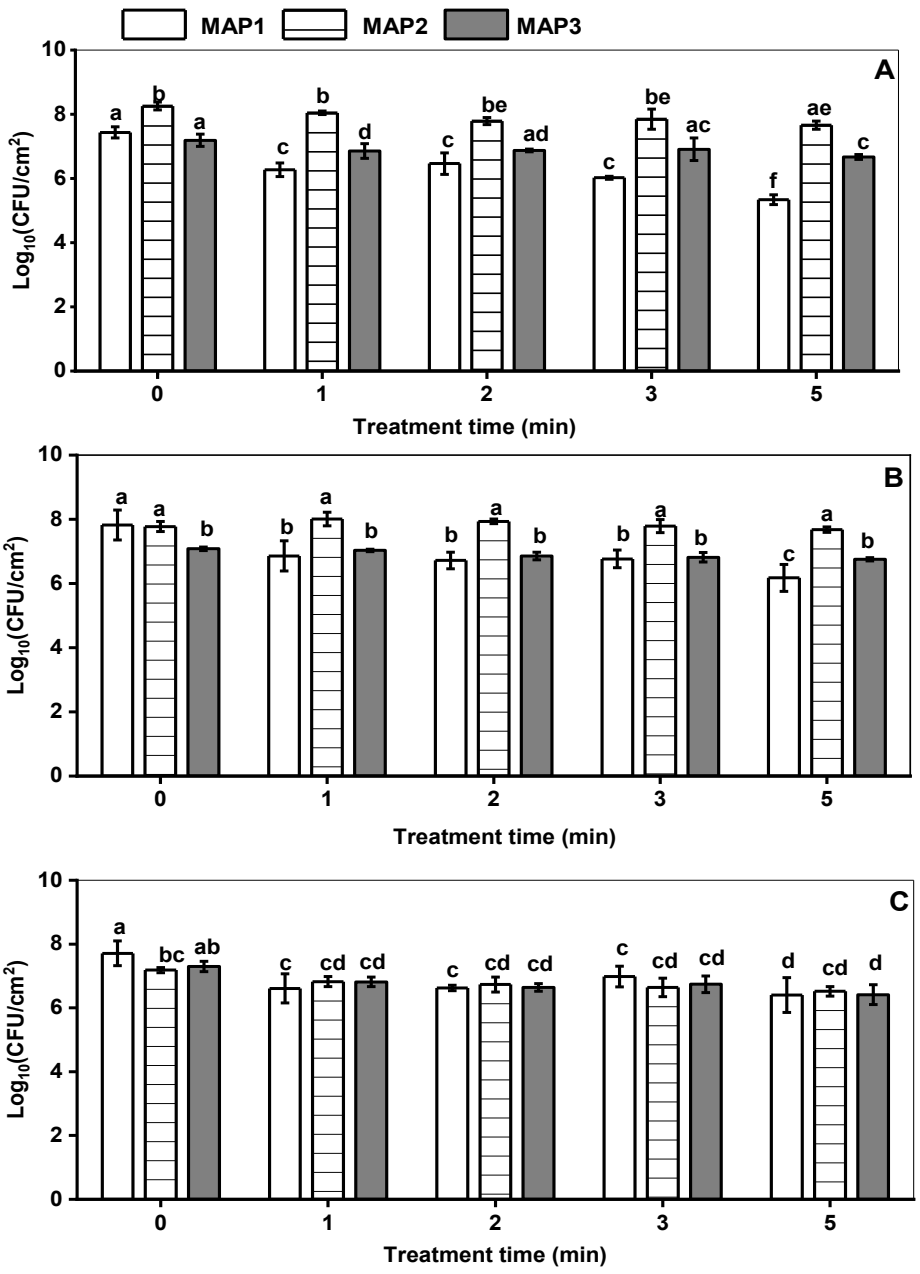

Figure 4.2: Effects of ACP treatment time and gas composition on mean cell counts of *L. monocytogenes* inoculated onto ham. A: Control ham; B: ham with preservatives: C: ham with bacteriocins. Surviving cells were enumerated on non-selective TSA after 1 h of post-ACP treatment storage at 4 °C. MAP1 (20 % O_2 + 40 % N_2 + 40 % CO_2): white solid column, MAP2 (50 % CO_2 + 50 % N_2): hatched column, MAP3 (100 % CO_2): solid grey column. Data are shown as means ± standard deviations (n=3). Treatment means are compared across the panel i.e., *L. monocytogenes* cell counts on ham type compared within a time and gas composition; Treatment means with different letters are significantly different ($P < 0.05$).

For ham with bacteriocins, the reduction of *L. monocytogenes* during ACP treatment was lower compared to those for the control ham and ham with preservatives. Maximum log reductions of 2.1, 0.5, and 0.6 CFU/cm^2 were observed on the control ham after 5 min of ACP treatment in MAP1, MAP2, and MAP3, respectively (Figure 4.2A).

4.3.4 Effect of post-treatment storage on inactivation of *L. monocytogenes*

Post-treatment storage in MAP decreased the counts of *L. monocytogenes* on control ham (without preservatives and bacteriocin), depending on the treatment time and in-package gas composition used ($P < 0.05$) (Figure 4.3A-B). During 7 days of storage, gas composition had a significant effect on the reduction of *L. monocytogenes* cell counts (Figure 4.3B). There was a significant two-way interaction between treatment time and post-treatment storage (7 days). ACP treatment of control ham for 5 min followed by 24 h and 7 days of storage resulted in significantly greater reduction in *Listeria* population in MAP1, with log reductions of 1.9 and 3.2 CFU/cm^2, respectively. ACP treatment of control ham for 10 min followed by 7 days post-treatment storage reduced the *L. monocytogenes* cell counts to below the detection limit (> 6 log reduction; limit of detection 1 log CFU/cm^2) (Figure 4.3B). For MAP2 and MAP3, 10 min ACP treatment in combination with 24 h and 7 days post-treatment storage had < 1.2 log CFU/cm^2 reductions (Figure 4.3A-B). Based on this finding, MAP1 was selected for further inactivation studies with different ham formulations, as ACP treatment with MAP1 showed higher efficacy against *L. monocytogenes*.

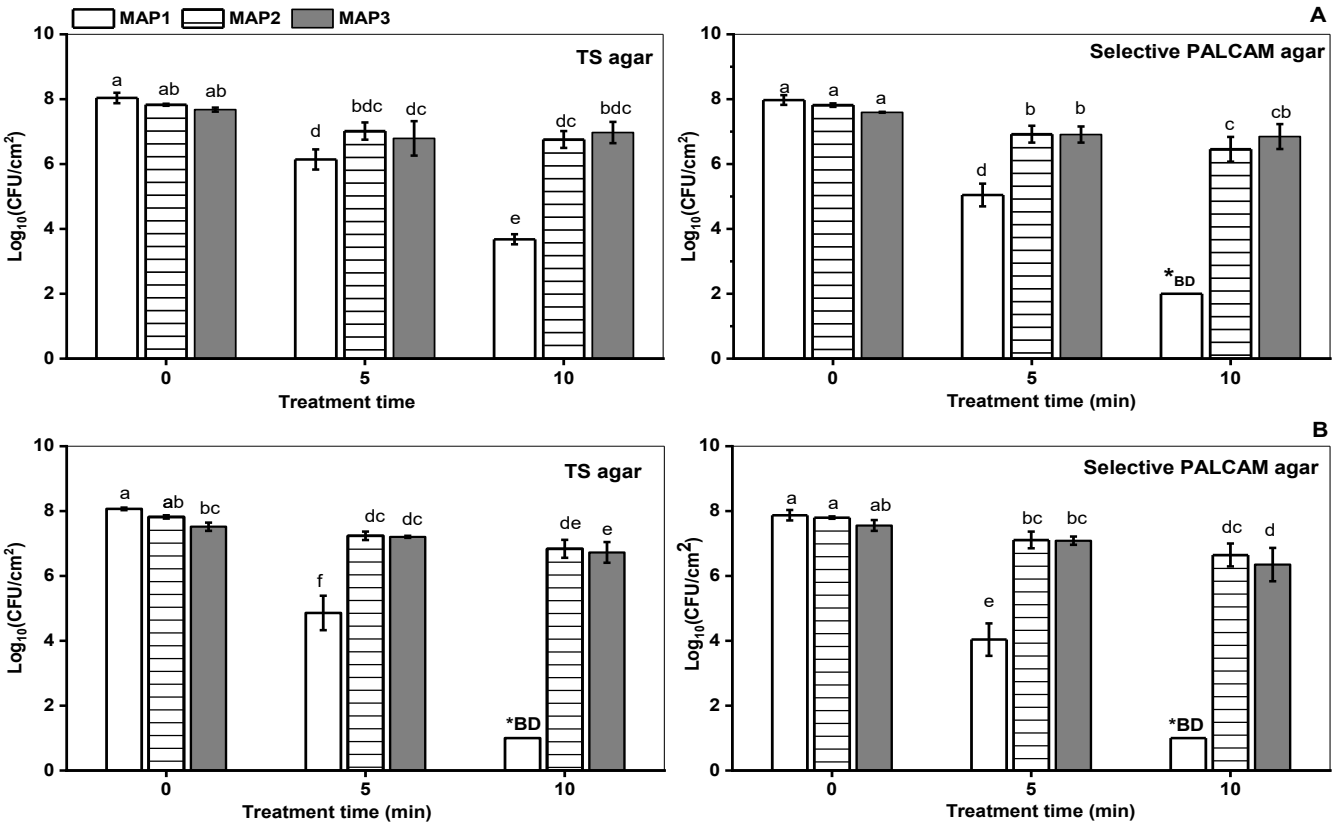

Figure 4.3: Effect of ACP treatment time and gas composition on mean cell counts of *L. monocytogenes* inoculated onto control ham after 24 h and 7 days of post-ACP treatment refrigerated storage at (4 °C). Surviving cells were enumerated on non-selective TSA and selective PALCAM agar. A: Stored at 4 °C for 24 h after ACP treatment. B: Stored at 4 °C for 7 days after ACP treatment. MAP1 (20 % O_2 + 40 % N_2 + 40 % CO_2): MAP2 (50 % CO_2 + 50 % N_2): MAP3 (100 % CO_2). Data are shown as means ± standard deviations (n=3). Treatment means with different letters are significantly different ($P < 0.05$). *BD: Below the limit of detection; For 24 h, 2 log (CFU/cm^2) and for 7 days storage, 1 log (CFU/cm^2) were considered as the detection limits.

Next, the effect of ham formulation (ham with preservatives or bacteriocins) in combination with ACP treatment and extended storage on the reduction of counts of *L. monocytogenes* using MAP1 was evaluated. There was no significant interaction ($P > 0.05$) between storage time and type of ham formulation. Ham formulation had no significant ($P > 0.05$) effect on the reduction of *L. monocytogenes*. After 10 min of ACP treatment using MAP1 with 7 days post-treatment storage, *L. monocytogenes* cell counts significantly reduced to below the detection limit (i.e., > 6 log reduction) irrespective of type of ham (data not shown). For ham with preservatives, ACP treatment time for 5 min with 7 days post-treatment storage using MAP1 reduced *L. monocytogenes* cell counts by ~ 3.0 log CFU/cm^2, which is comparable to reduction observed on the control ham. For ham with bacteriocins, the inactivation effect was slightly higher (~ 3.7 log CFU/cm^2) in comparison to that on the control ham or on ham with preservatives. Irrespective of the ham formulation, inactivation efficacy of in-package ACP treatment strongly correlated with treatment time and the presence of oxygen in the gas mixture; while the inactivation effect could be further increased with extended post-treatment storage.

Selective PALCAM agar media was used for the estimation of uninjured cells after in-package ACP treatment of ham (Figure 4.3A-B). The *L. monocytogenes* cells grown on PALCAM agar media were below the limit of detection (> 6 log reduction) after 10 min in-package ACP treatment of control ham using MAP1 followed by 24 h post-treatment storage (Figure 4.3A). However, the log reduction in *L. monocytogenes*, grown on TS agar media was ~4 log after 10 min in-package ACP treatment of control ham using MAP1 followed by 24 h post-treatment storage (Figure 4.3A). Further, the *L. monocytogenes* cell counts grown on TSA media were below the limit of detection after 10 min in-package ACP treatment of control ham using MAP1, followed by 7 days of post-

treatment storage (Figure 4.3B). Consequently, it may be assumed that a large number of *L. monocytogenes* cells were injured during 10 min ACP treatment, and these injured cells were inactivated during 24 h and 7 days of post-treatment storage (Figure 4.3A-B).

4.3.5 Effect of ACP treatment on lipid oxidation

To investigate the effect of ham formulation, plasma treatment time, post-treatment storage, and in-package gas composition on lipid oxidation of ham samples, TBARS method was used to estimate the lipid oxidation equivalent to mg MDA/kg of ham. ACP treatment time and gas composition had a significant effect on lipid oxidation in comparison to untreated ham samples and their influence on lipid oxidation of ham was dependent on each other as there was a significant two-way interaction between them when the samples were treated in MAP1 or MAP3 (Figure 4.4A-B). In the case of MAP2, the ACP treatment time did not significantly affect the lipid oxidation of samples compared to untreated control samples (Figure 4.4A). The increase in ACP treatment time from 5 to 10 min did not significantly increase lipid oxidation of samples regardless of the gas composition (Figure 4.4A-B). For instance, a 5 or 10 min plasma treatment using MAP1 and subsequent post-treatment storage of 24 h resulted in 0.50±0.05 and 0.59±0.01 mg MDA/ kg of ham, respectively in comparison to the untreated ham with 0.17±0.13 mg MDA/kg of ham. Based on this finding and taking the consideration of gas composition effect on *Listeria* inactivation, MAP1 was selected for further analysis of lipid oxidation on ham samples with preservative or bacteriocin, as ACP treatment using MAP2 or MAP3 had only little effect on lipid oxidation.

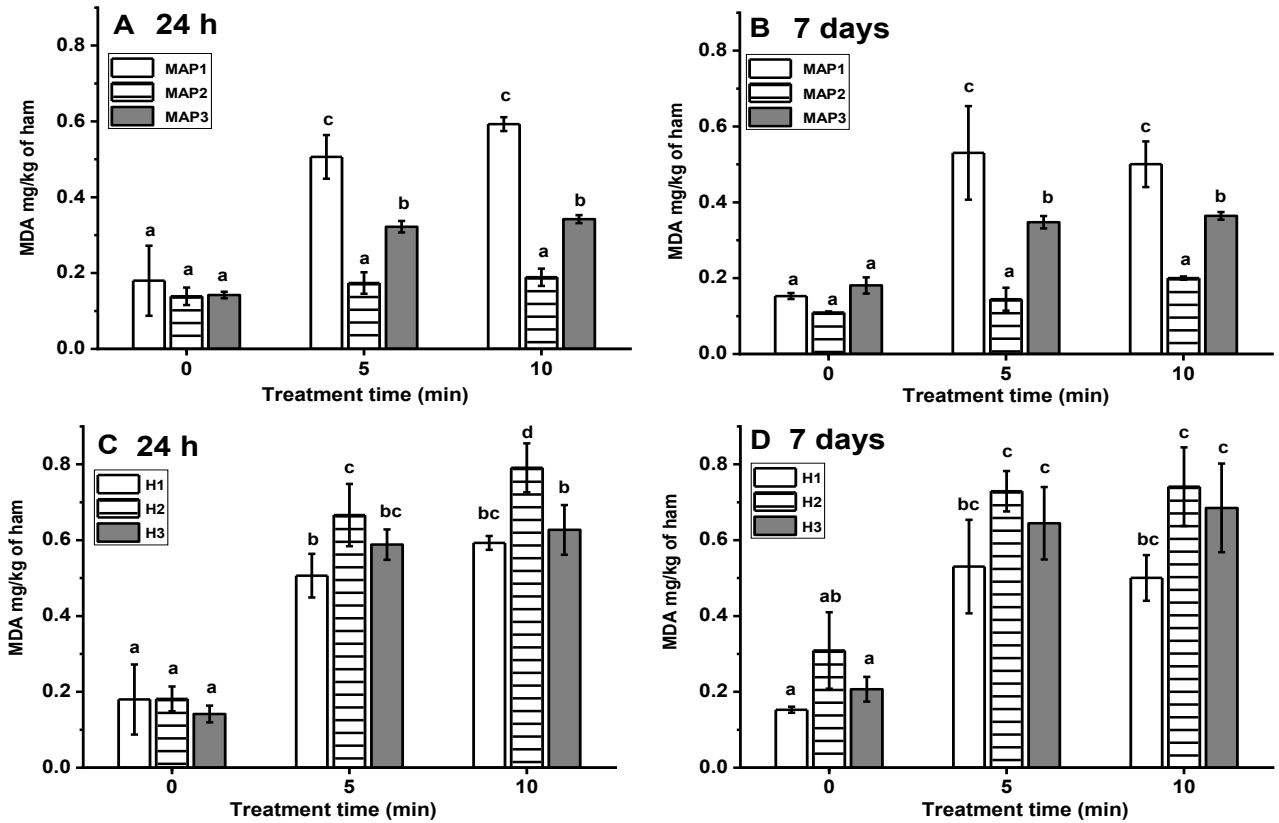

Figure 4.4: Effect of in-package ACP treatment on lipid oxidation values of ham after post-ACP treatment storage at 4 °C. Panels A and B present the malondialdehyde equivalent lipid oxidation values of control ham after in-package ACP discharge in three different gas mixtures, MAP1 (20 % O_2 + 40 % N_2 + 40% CO_2), MAP2 (50 % CO_2 + 50 % N_2), and MAP3 (100% CO_2). Panels C and D present the malondialdehyde equivalent lipid oxidation values of three different ham groups (H1: control ham, H2: ham with preservatives, and H3: ham with bacteriocins), exposed to ACP discharge in MAP1 (20 % O_2 + 40 % N_2 + 40 % CO_2). Data are presented as means ± standard deviations (n=3). Treatment means with different letters are significantly different ($P < 0.05$).

The treatment time had a significant effect on lipid oxidation of samples irrespective of ham formulation, compared to untreated control samples (Figure 4.4C-D). ACP treated ham with preservatives showed significantly higher TBARS after 24 h post-treatment storage compared to control ham or ham with bacteriocins (Figure 4.4C). The TBARS of ACP treated control ham and ham with bacteriocins were comparable (Figure 4.4C-D). No significant two-way interactions between post-treatment storage time and gas composition or post-treatment storage time and ham formulation were observed. No significant differences in TBARS were observed between the ham storage for 24 h or 7 days post-treatment, for all the gas composition and ham formulations used in this study.

4.3.6 Effect of ACP treatment on color parameters

Table 4.2 shows the changes in color parameters L*, a*, and b* values of control ham samples after ACP treatment and subsequent post-treatment storage. ACP treatment time and gas composition significantly influenced the color parameter values of the surface of ham after 24 h post-treatment storage. For MAP1 and MAP3, the L* and b* values of ACP treated ham surface significantly increased compared to untreated ham after 24 h storage. Regardless of packaged gas composition, post-treatment storage of 7 days significantly changed the L* and b* values of ham surface compared to ham samples after 24 h storage (Table 4.2). In contrast to L* and b* values of ham surface, a* values of ACP treated ham surface were significantly decreased in MAP1 and MAP3 after 24 h of post-treatment storage. Following 7 days post-treatment storage, a* values of ACP treated ham surface did not significantly change compared to 24 h storage ham samples. Regardless of the storage, ACP treatment of ham in MAP2 did not significantly influence the color parameter values of ham surfaces in comparison to untreated samples.

Table 4.2: Effect of ACP treatment time and gas composition on color parameters (L*, a* and b*) of control ham (without preservatives or bacteriocins) samples after 24 h or 7 days of post-plasma treatment storage at 4 °C.

		Color parameters					
		24 h storage			**7 days storage**		
MAP	**Treatment time (min)**	**L***	**a***	**b***	**L***	**a***	**b***
MAP1	0	90.80^{xAa}	1.89^{xAa}	0.36^{xAa}	88.21^{yAa}	1.90^{xAa}	-0.29^{yAa}
	5	91.84^{xAb}	0.92^{xAb}	0.88^{xAb}	89.60^{yAb}	1.07^{xAb}	0.84^{yAb}
	10	92.05^{xAb}	0.91^{xAb}	1.14^{xAc}	89.75^{yAb}	1.04^{xAb}	0.72^{yAb}
MAP2	0	88.11^{xBa}	1.71^{xBa}	-0.65^{xBa}	87.35^{yBa}	1.76^{xAa}	-0.22^{yBa}
	5	87.96^{xBa}	1.34^{xBa}	-0.61^{xBa}	86.84^{yBa}	1.25^{xAa}	-0.10^{yBb}
	10	87.95^{xBa}	1.32^{xBa}	-0.57^{xBa}	86.80^{yBa}	1.10^{xAa}	-0.04^{yBb}
MAP3	0	90.26^{xCa}	1.95^{xBa}	0.03^{xAa}	90.00^{yAa}	1.92^{xAa}	$-0.20y^{Aa}$
	5	90.75^{xCb}	1.17^{xBb}	0.46^{xAb}	91.24^{yAa}	1.11^{xAb}	0.80^{yAb}
	10	90.82^{xCb}	1.21^{xBb}	0.37^{xAb}	91.66^{yAb}	1.01^{xAb}	0.81^{yAb}
	SEM	0.21	0.11	0.09	0.34	0.09	0.14

Data are shown as means of triplicate independent experiments. Lower case letters $^{a, b}$ represent significantly different ($P < 0.05$) means of color parameters, among treatment times within a MAP type. Capital letters $^{A, B}$ represent significantly different means of color parameters, among MAP types. Lower case $^{x, y}$ represents significantly different color parameters, between storage groups. SEM: standard error mean (n=27), (MAP1: 20 % O_2 + 40 % N_2 + 40 % CO_2), (MAP2: 50 % CO_2 + 50 % N_2); MAP3: (100 % CO_2).

MAP1 gas composition was selected to evaluate the effect of ham formulation on color parameter values of ACP treated ham surface after 24 h or 7 days storage. Presence of preservatives or bacteriocins in ham did not significantly influence the color parameter values of ACP treated ham surfaces after 24 h or 7 days post-treatment storage in comparison to control ham surface (data not shown)

4.4 Discussion

The ACP discharge produces cocktails of reactive species, and the interaction of these reactive species cause irreversible damage to cell membrane (Liao, Liu, et al., 2017). The antimicrobial effect of ACP is the result of various factors, including oxidative stress caused by ROS and RNS, disruption of surface and cells wall structure of microorganisms by electrostatic burst and etching action, alteration in membrane permeability and finally oxidative damage of RNA and DNA (Han et al., 2016; Joshi et al., 2011; Liao et al., 2017). The present study demonstrated that the inactivation efficacy of ACP discharge against *L. monocytogenes* on ham surface strongly depended on the MAP gas composition and ACP treatment time and the interaction between them. A modified atmosphere containing oxygen at ambient concentration (MAP1) resulted in highest inactivation of *L. monocytogenes* in comparison to atmospheres containing no oxygen or a very trace amount as an impurity (MAP2 and MAP3) (Figure 4.2A-C). The influence of higher oxygen concentration on ACP inactivation efficacy has previously been reported (Han et al., 2016; Laroussi & Leipold, 2004). Plasma discharge in a process gas mixture containing oxygen produces highly reactive oxygen species such as ozone (O_3), hydrogen peroxide, nitrous gases, singlet oxygen, superoxides and hydroxyl radicals (Table 4.1 and Figure 4.1). The presence of oxygen in the package atmosphere enhanced the production of hydrogen peroxide and reactive nitrogen species (RNS) during ACP treatment (Table 4.1).

The production of RNS was reported in the plasma discharge with air as the gas (Moiseev et al., 2014). Combined effect of ROS with RNS can result in enhanced antibacterial effect of ACP in comparison to either group alone (Boxhammer et al., 2012). This enhanced antibacterial effect is attributed to the production of peroxynitrites, a strong antibacterial agent, generated by secondary reaction of generated ROS and RNS, during ACP discharge (Brisset & Hnatiuc, 2012). A more detailed discussion on ROS and RNS can be found in Arjunan, Sharma, & Ptasinska (2015). The use of a gas composition for MAP that could diminish the generation of either ROS or RNS may not have the best antibacterial efficacy. In this study, MAP1 with a higher oxygen and nitrogen concentration, led to greater ROS and RNS production in comparison to MAP2 or MAP3 with little or no oxygen concentrations. The generated concentrations of reactive RONS including ozone, nitrous gas, and hydrogen peroxide were dependent on treatment time (Table 4.1). Longer treatment times generated higher concentrations of reactive species. Accumulation of these reactive species in the confined environment could severely damage the cells of *L. monocytogenes* and led to reduced cell counts after longer ACP exposure (Figure 4.2A-C) using MAP1, regardless of ham formulation. However, increasing plasma treatment time from 1 to 2 or 3 min did not significantly reduce the *L. monocytogenes* cell counts on the surface of the ham (Figure 4.2A-C) irrespective of ham formulation and gas composition. This could be due to the presence of ACP resistant sub-populations of *L. monocytogenes*. This requires further investigation to understand if populations of *L. monocytogenes* can be resistant to ACP treatment.

The bacteriocin preparation used in this study included carnocyclin A, piscicolin 126 and carnobacteriocin BM1 from *C. maltromaticum* ATCC PTA-5313 (Martin-Visscher et al., 2008). Carnocylin A is a 60-residue circular bacteriocin with compelling antilisterial activity (Balay et al., 2018; Martin-Visscher, Gong, Duszyk, & Vederas., 2009). Total cell counts of *L.*

monocytogenes on untreated control ham, ham with preservatives, and ham with bacteriocins were comparable, which means that the presence of preservatives or bacteriocins in ham samples did not exhibit their own antimicrobial activity at the time of inoculations. When MAP1 was used, in-package ACP treatment significantly reduced the cell counts of *L. monocytogenes* on ham surfaces, irrespective of ham formulation (Figure 4.2A-C). The initial cell counts of *L. monocytogenes* grown on non-selective TSA or selective PALCAM agar were similar for all ham formulations (data not shown). Overnight storage prior to ACP treatment did not result in changes in numbers of *L. monocytogenes* on the surface of the ham. In this study, presence of preservatives or bacteriocins did not significantly influence the ACP treatment efficacy to inactivate *L. monocytogenes* inoculated on different types of ham surface. With this finding, it can be speculated that there was no significant interactive effect of ACP discharge with preservatives or bacteriocins to inactivate *L. monocytogenes* on ham surface.

To achieve complete inactivation of *L. monocytogenes* after ACP treatment, an extended post-treatment storage was required (Dezest et al., 2017). The observed reduction in cell counts of *L. monocytogenes* was > 6 log after 10 min ACP treatment followed by 7 days of storage (Figure 4.3A-D). Han et al. (2016) used a cell recovery model to predict the impact of ACP treatment, in combination with refrigerated storage and proposed a treatment time dependent response of cell recovery after post-treatment refrigerated storage. A similar effect was observed in this study where ACP treatment of 10 min and 24 h or 7 days of post-treatment storage resulted in greater reductions in *L. monocytogenes* cells compared to samples treated for 5 min and stored for 24 h or 7 days (Figure 4.3A-B). The lethal effect of post-treatment storage on the microbial survival was documented by others (Han et al., 2016; Misra et al., 2018; Rød et al., 2012). Along with ACP treatment, post-treatment storage at 4 °C may have resulted in lower counts due to the presence of

reactive species in MAP1. The extended storage may promote the prolonged action of plasma reactive species on bacterial cells due to the confinement of the generated reactive species within the package, enhancing the diffusion of long-lived species into the food matrix and bacterial cells, and starting chain reactions in bacterial cells leading to cell damage (Ziuzina et al., 2014).

Among all the evaluated gas compositions, MAP1 resulted in highest lipid oxidation in all ham samples. Presence of 20 % O_2 in MAP1 led to the formation of various ROS and RNS during ACP discharge (Table 4.1). Due to the high oxidative nature of ozone, it causes irreversible degradation to the fatty acid compounds in ham cell membrane and cellular protein (Cho et al., 2014). Ozone is identified as a potential initiator of free radical derived oxidation reactions in food, particularly in lipids, where it decomposes fatty acids (Cho et al., 2014). Moreover, ozone is highly unstable and degrades very rapidly into diatomic form (Sekhon et al., 2010). Apart from ozone, other plasma reactive species such as hydroxyl radicals, singlet oxygen, superoxide anion and hydrogen peroxide also cause lipid oxidation, either directly or act as a precursor (Amaral, Solva, & Lannes, 2018). Long duration or high voltage plasma exposure induces lipid oxidation in dairy and meat fat (Sarangapani, Keogh, Dunne, Bourke, & Cullen, 2017). The oxidation of lipids by ACP proceeds from criegee mechanism and the typical by-products of oxidation includes carboxylic acid, ozonised, aldehydes, and hydroperoxides (Sarangapani et al., 2017). In the case of MAP2 and MAP3, the measured concentrations of ozone, hydrogen peroxide and nitrous gases were either below the limit of detection or lower than that found in MAP1 (Table 4.1), and this could account for the lower lipid oxidation in ham samples stored in MAP2 and MAP3, compared to those stored in MAP1 after ACP treatments.

Consumers consider meat color as an indicator of freshness and quality of meat, Moreover, meat appearance has direct influence on the acceptance of meat, and it influences the consumer

preference to purchase a meat product. The decreased a* and increased b* values of packaged ACP treated ham samples could be associated with the oxidation of myoglobin and oxymyoglobin to metmyoglobin by ROS, including ozone and hydrogen peroxide (Cho et al., 2014; Jayasena et al., 2015). The higher greenish color of ACP treated meat could be due to the reaction between generated hydrogen peroxide and myoglobin (Fröhling, Durek, et al., 2012). Jung et al. (2017) reported higher concentration of nitrite in ACP treated meat. The generated nitrite by ACP could react with myoglobin to form nitrimyoglobin and induce green color or decreased a* values (Yong, Han, Kim, Suh, & Jo, 2018). Jayasena et al. (2015) and Kim et al. (2013) treated pork loin with DBD plasma and reported a significant decrease in a* values during post-treatment storage. However, they did not observe any notable changes in b* values. In this study, the values of a* and b* of ACP treated ham in MAP1 were significantly different compared to MAP2 or MAP3 (Table 4.2). This could be due to the higher concentrations of ozone, hydrogen peroxide, and nitrous gas in MAP1 compared to MAP2 or MAP3 (Table 4.1). Similar to this finding, Fröhling et al. (2012) reported that ACP treatment of fresh pork induced a slight increase in L* values. Whereas, Jung et al. (2017) reported that the direct plasma exposure to meat batter formulated with pork, water, and sodium chloride (80:20:1, w/w/w) had no effect on L* values. Also, the a* values of meat batter were significantly increased and b* values were significantly decreased with the increase in ACP treatment time (Jung et al., 2017). However, it is difficult to compare observed color parameters of different studies as they used different processing and storage conditions.

4.5 Conclusions

This study investigated the effect of in-package gas composition in combination with ACP treatment time and post-treatment storage on the inactivation of *L. monocytogenes* on control ham, ham with preservatives, and ham with bacteriocin. Regardless of the type of ham, plasma treatment

with MAP1 (20 % O_2 + 40 % N_2 + 40 % CO_2) reduced the cell counts of *L. monocytogenes* by 2 log (CFU/cm^2), and the cell counts were further reduced to below the limit of detection (> 6 log reduction) after 7 days of post-treatment storage at 4 °C. The presence of preservatives or bacteriocin in ham did not enhance the inactivation of *L. monocytogenes* after ACP treatment. Lipid oxidation of ACP treated ham was significantly influenced by gas composition. Irrespective of the type of ham, ACP treatment with MAP1 significantly increased lipid oxidation. The findings of this study demonstrated that the post-treatment storage is required to completely inactivate *L. monocytogenes* after ACP treatment. However, the selection of specific gas composition inside the package is crucial to achieve the required level of microbial inactivation. This study will help to select optimized process and storage conditions for in-package ACP treatment to reduce *L. monocytogenes*.

Chapter 5: Inactivation Mechanisms of *Listeria monocytogenes* During In-Package Atmospheric Cold Plasma Treatment and Post-treatment Storage

5.1 Introduction

Listeria monocytogenes is a foodborne pathogen that causes an estimated 178 cases of foodborne listeriosis annually in Canada (Health Canada, 2016). Although listeriosis is a rare foodborne disease, it is linked to a disproportionately high level of hospitalization (>90 %) and fatality (20-30 %) (Hernandez-Milian and Payeras-Cifre, 2014; Thomas et al., 2015). Ready-to-eat (RTE) products, particularly meat and seafood, have been identified as "high risk" for *Listeria* contamination (Health Canada, 2011; Zhu et al., 2005). According to the Center for Disease Control and Prevention (CDC), the reported incidences of listeriosis have remained unchanged in the past 10 years (CDC, 2014), despite the strict guidelines (Ricci et al., 2018). *L. monocytogenes* is typically associated with RTE meat products as post-processing contamination can happen from equipment surfaces such as slicers and conveyors belts (Beresford et al., 2001; Rød et al., 2012). In-package ACP treatment can be used as a post-processing decontamination step for RTE meat safety.

In recent years, several studies investigated the potential use of atmospheric cold plasma (ACP) as a decontamination technology to control *Listeria* on different food surfaces (Liao et al., 2017). Cold plasma is an ionized gas composed of electrons, ions, charged particles, and free radicals. The ACP discharge generates cocktails of short and long-lived reactive species including reactive oxygen species (ROS), reactive nitrogen species (RNS), which have shown tremendous antimicrobial potential to injure and inactivate bacteria on food surfaces (Lee et al., 2017; Misra and Jo, 2017). Previous studies reported inactivation of *L. monocytogenes* on RTE meat, including ham surface (Song et al., 2009; Chapter 3), beef jerky (Yong et al., 2017), fresh pork (Fröhling et

al., 2012), and RTE meat bresaola (Rød et al., 2012). Some studies recently reported that ACP treatment could be successfully employed as an alternate post-packaging decontamination technique for RTE meat products (Misra and Jo, 2017; Rød et al., 2012). For example, Rød et al. (2012) showed that in-package ACP treatment of RTE meat with MAP (30 % O_2 + 70 % argon) gas resulted in a maximum 1.6 log reduction in *L .innocua* cell counts. In addition, some of these studies reported a significant increase in decontamination effects during post-treatment storage after in-package ACP treatments (Han et al., 2016; Lis et al., 2018). Han et al. (2016) investigated the storage effects on the inactivation of *L. monocytogenes* cells suspended in PBS solution after in-package ACP treatment. They conducted in-package ACP treatment using air as the plasma generating gas for 1 min. They reported 4.26 and 6.02 log CFU/mL reduction of *L. monocytogenes* after 1 h and 24 h post-treatment storage, respectively. In our previous study, we evaluated the effect of in-package ACP treatment on the reduction of *L. monocytogenes* at ham surface during post-treatment storage of 24 h and 7 days. The results showed an additional 3 log reduction in *L. monocytogenes* cells after 7 days storage compared to 24 h for samples exposed to ACP for 10 min (Chapter 4 of this thesis).

The plate counting method used for microbial inactivation efficacy evaluation does not consider the different physiological states of bacteria. Numerous studies have reported that the physical treatments, including ACP, can induce bacteria to exist in a viable but non-culturable (VBNC) state or result in sublethal injury of bacteria (Ramamurthy et al., 2014; Schottroff et al., 2018). Bacteria in VBNC or sublethally injured states are alive; however, the culture-based microbiological techniques can lead to underestimation of microbial cell number, which can survive the ACP treatment and post-treatment storage (Schottroff et al., 2018). A better understanding of the physiological states of *L. monocytogenes* on the ham surface after in-package

ACP treatments and the following post-treatment storage is necessary to develop ACP-based decontamination processes and storage conditions.

Flow cytometry is an excellent tool for microbiological analysis, as it enables the evaluation of morphological and physiological changes in bacteria at a single-cell level. With the use of appropriate fluorescence dye, it is feasible to classify cells into three different categories; intact, metabolically active, and permeabilized cell mixtures (Fröhling and Schlüter, 2015; Lang et al., 2018). Recently, the potential application of flow cytometry to asses the bacterial physiological status after ACP treatments was demonstrated (Carré et al., 2018; Fröhling et al., 2012; Fröhling & Schlüter, 2015; Surowsky et al., 2014). In this study, the influence of post-ACP treatment storage on membrane integrity, esterase activity, and oxidative stress of *L. monocytogenes* were investigated by flow cytometry.

5.2 Materials and methods

5.2.1 Ham sample preparation

Ham samples was prepared as described in Chapter 4 section 4.2.1 of this thesis. Specifically, the ingredients consisted of ice (16.71 % of meat weight), sodium triphosphate (0.50 % of meat weight), sodium chloride (0. 21 % of meat weight), Prague powder/curing ingredient ((0.33 % of meat weight (6 % sodium nitrite, 94 % NaCl)), sodium erythorbate (0.08 %), and dextrose (2.45 % of meat weight). The cooked ham was transferred on ice for 10 min and stored at 4 °C for overnight cooling. After overnight cooling, the cooked ham was sliced (2 mm thick, surface area 50 cm^2) with a sterilized slicer, vacuum-packed, and stored at °C until use.

5.2.2 Bacterial culture preparation

L. monocytogenes strain (FSL J1- 177) was streaked from –80 °C stock cultures and streaked on tryptic soy (TS) agar plates, incubated at 37 °C for 48 h to obtain isolated individual colonies. After overnight growth, a 1 % inoculum was transferred into TS broth and incubated in an orbital shaker at 25 °C (200 RPM) for 24 h. It was centrifuged at 5311 × *g* for 1 min, and the supernatant was discarded. The cell pellets were resuspended in 1 mL of 0.85 % NaCl and kept at 25 °C until use (within 1 h).

5.2.3 Packaging and inoculation

Vacuum-packed cooked ham was opened and cored to obtain samples with a surface area of 1 cm^2. Each sample was inoculated with 10 µL of cells (final concentration of 10^8 CFU/cm^2), suspended in 0.85 % NaCl. The control samples were inoculated with the same volume of 0.85 % NaCl. After inoculation, samples were held in a biosafety cabinet for 10 min on a sterile tray. Using forceps, each inoculated ham sample was aseptically transferred in 76.2 µm thick, nylon and polypropylene coextruded vacuum bags (Unipac Packaging Products Ltd., Edmonton, AB, Canada). The ham samples were packaged in modified atmosphere packages with 20 % O_2 + 40 % N_2 + 40 % CO_2, using a gas flush packaging machine (Model C200; Multivac, Kansas City, MO). The final gas volume per package averaged approximately 20 cm^3.

5.2.4 Cold plasma treatment

For in-package ACP treatment, a dielectric barrier discharge (DBD) plasma system (PG 100-3D, Advanced plasma solutions, Malvern, PA, USA) was used as described in chapter 4 section 4.2.4 of this thesis. The inoculated ham samples were exposed to ACP for 2.5, 5, 7.5, and 10 min at room temperature (22 ± 2 °C). Treated and untreated control samples were stored at 4 °C for 1 h, 24 h, and 7 days. All the experiments were performed in triplicate.

5.2.5 Total viable cell counts

L. monocytogenes cell counts on ACP treated and control ham samples were monitored after 1 h, 24 h, and 7 days of storage at 4 °C. Un-inoculated packaged samples were also prepared and stored under the same conditions as treated samples for each experiment to verify the absence of contamination before the experiment and after storage. Packaged samples were opened aseptically inside the biosafety hood and the samples were transferred into 50 mL falcon tubes containing 1 mL of 0.85 % NaCl solution. Falcon tubes containing ham samples were vortexed for 60 s to detach cells from ham sample, prior to serial dilution. Aliquots of 0.1 mL of appropriate dilutions were plated on TSA to estimate total viable cell counts. Plates were incubated at 37 °C for 48 h for colonies growth. Counts were converted to $\log_{10}$ CFU/cm^2 for statistical analysis.

5.2.6 Flow cytometry analysis

The analysis was performed using a flow cytometer (BD LSR-Fotessa, BD Biosciences, San Jose, CA, USA), equipped with a 50 mW blue Ar laser emitting at a wavelength of 488 nm and 50 mW yellow Ar laser emitting at a wavelength 561 nm to excite green (530 ± 30 nm) and red fluorescence (610 ± 15 nm), respectively. The green fluorescence of SYTO9, carboxyfluorescein (cFDA), and dichloro-dihydro fluorescein diacetate (H_2DCFDA) were received in the Y530 photomultiplier with a bandpass filter of 530 ± 30 nm and the fluorescence of propidium iodide (PI) was acquired in the Y610 photomultiplier with a bandpass filter (610 ± 15 nm). The fluorescence signals were collected on logarithmic scales and data were acquired in FACSDiva 8 software. FCS files were extracted from the FACSDiva 8 software and obtained data were analyzed using FlowJo software (Tree Star, Ashland, USA). For every stained bacteria, samples of at least 10,000 events were collected at a flow rate of approximately 250-500 events per sec. The cell density plots obtained by flow cytometry analysis were divided into four regions with

respect to green and red fluorescence intensity. The regions were manually adjusted based on green and red fluorescence intensity to include more than 95 % of cells from unstained controls as green and red fluorescence negative. The mean of percentage values obtained from three independent density plots were calculated and presented on a bar graph where x-coordinate was the treatment time and y-coordinate were the percentage of stained cells.

5.2.7 Membrane integrity

SYTO9 and propidium iodide (PI) were used to differentiate between intact and damaged cell membranes. The stock solution of 20 mM PI and 3.33 mM SYTO9 was procured from Thermo fisher and stored at -20 °C. On the day of the experiment, a fresh working solution of SYTO9 (20 µM) and PI (60 µM) was prepared in 0.85 % NaCl solution. The bacterial cells from the ham surface were harvested in 3 mL of 0.85 % NaCl solution as described in section 5.2.5. An aliquot of 150 µL of bacterial cell suspension was carefully pipetted into 5 mL tube and 25 µL of SYTO9 and PI was added into each tube to reach final concentrations of 8 µM SYTO9 and 20 µM PI. Tubes were gently vortexed and incubated in dark for 15 min. Flow cytometry reading was collected not more than 30 min after incubation.

5.2.8 Esterase activity and membrane permeabilization

Esterase activity of *L. monocytogenes* cells after post-ACP treatment storage was assessed using a membrane permeable dye 5(6)-carboxyfluorescein diacetate mixed isomers (cFDA). This dye is nonfluorescent in its native form, but extremely intense fluorescence is produced upon hydrolysis by nonspecific intracellular esterase. cFDA does not stain dead cells. The stock solution of 5(6)-carboxyfluorescein diacetate mixed isomers (cFDA) (Thermo Fisher Scientific Waltman, MA, USA) was dissolved in dimethyl sulfoxide to achieve a concentration of 1 mM.

The bacterial cells from the ham surface were harvested in 3 mL of 0.85 % NaCl solution as described in section 5.2.5. An aliquot of 150 µL of bacterial cell suspension was carefully pipetted into 5 mL tube. The cells suspension was incubated in dark with 50 µM cFDA for 15 min at 37 °C with shaking. The physiological status of cells can be measured using membrane-impermeant PI. Therefore, 20 µM PI was added after 15 min of incubation with cFDA and stored in dark at room temperature for 10 min before flow cytometry measurements.

5.2.9 Oxidative stress and membrane permeabilization

The stock solution of 6-carboxy-2',7'-dichlorodihydrofluorescin diacetate (H_2DCFDA), a membrane-permeable fluorescence dye (Thermo Fisher Scientific, Waltman, MA, USA) was dissolved in dimethyl sulfoxide to achieve a concentration of 1 mM. The bacterial cells from ham surface were harvested in 3 mL of 0.85 % NaCl solution as described in section 5.2.5. An aliquot of 150 µL of bacterial cell suspension was carefully pipetted into 5 mL tube. To assess the intracellular oxidative stress level of *L. monocytogenes*, cell suspension was incubated with 20 µM H_2DCFDA for 15 min at 37 °C with shaking. To measure the bacterial cell membrane permeabilization along with oxidative stress, membrane impermeant dye PI was added with a final concentration of 20 µM after 15 min of incubation with H_2DCFDA. Tube containing bacterial cell suspension and dye was gently vortexed and stored in dark at room temperature for an additional 10 min before flow cytometry measurements.

5.2.10 Statistical analysis

Data on the response variables were subjected to analysis of variance using a generalized linear mixed-effects procedure of SAS® University edition (Proc Glmmix; SAS studio 3.71, Cary, NC, USA). The treatment factors, ACP treatment time, and post-ACP storage time were used as fixed effects. The level of significance reported in the test was P-value ≤ 0.05 using Tukey's honest test.

5.3 Results

5.3.1 Effect of post-ACP treatment storage time on total viable cell counts

The inactivation levels of *L. monocytogenes* on the ACP treated samples after post-treatment storage of 1 h, 24 h, and 7 days at 4 °C were determined. The initial cell count of *L. monocytogenes* on the ham surface was ~8 log CFU/cm^2. The results indicated a significant decrease in *L. monocytogenes* cell counts compared to untreated control at all tested treatment times after 1 h, 24 h, and 7 days post-treatment storage at 4 °C (Figure 5.1). Both the ACP treatment time and the post-treatment storage time had significant influence on the reduction of *L. monocytogenes* on the ham surface (Figure 5.1). An increase in treatment time from 1 min to 2.5 min did not significantly reduce the cell counts, but an additional 2.5 min treatment resulted in a significant reduction in the cell counts of *L. monocytogens* (Figure 5.1). Maximum log reductions of 2.5, 3.5, and 4.9 log CFU/cm^2 in *L. monocytogenes* cell counts were observed for samples exposed to 10 min of ACP treatment, followed by 1 h, 24 h, 7 days post-treatment storage, respectively. Statistical analysis revealed that the interaction effect between ACP treatment time and post-treatment storage time was significant, which means that the reduction in *L. monocytogenes* depended on ACP treatment time and post-treatment storage time and vice versa. After 2.5 min of ACP treatment, followed by 24 h and 7 days post-treatment storage resulted in 1.6 and 2.3 log CFU/cm^2 reduction in *L. monocytogenes* population, respectively. Whereas, after 5 min ACP treatment, followed by 24 h and 7 days post-treatment storage resulted in a significantly higher reduction in *L. monocytogenes* cell counts, with log reduction of 2.3, and 3.7 log CFU/cm^2, respectively. A significantly higher reduction in cell counts of *L. monocytogenes* was observed for samples stored for 7 days, followed by 24 h and 1 h, respectively, irrespective of ACP treatment time.

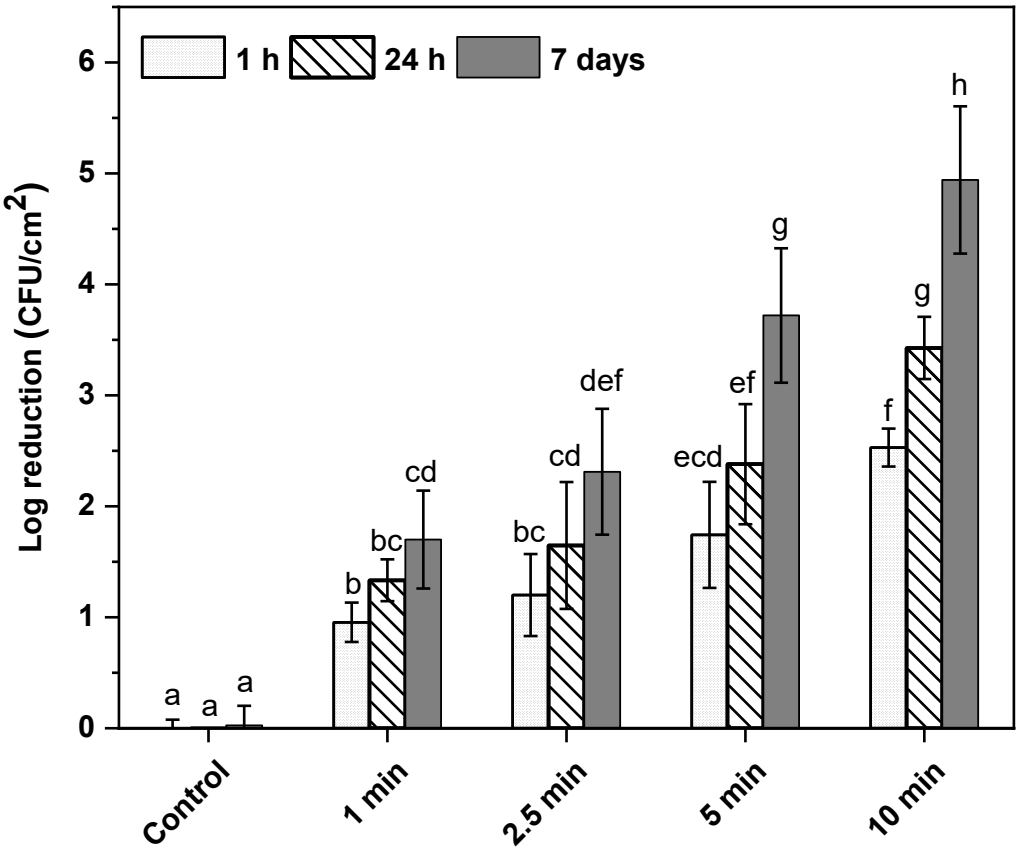

Figure 5.1: Mean cell counts of *L. monocytogenes* on ham surface after in-package ACP treatment and storage. White bar with dots represents post-treatment storage for 1 h at 4 °C; white bar with hatch lines represents post-treatment storage for 24 h at 4 °C; grey bar represents post-treatment storage for 7 days at 4 °C. Data are shown as means ± standard deviations (n=3). Treatment means with different letters are significantly different.

5.3.2 Effect of post-ACP treatment storage time on membrane integrity

The distribution of stained *L. monocytogenes* cells varied based on the ACP treatment times and post-treatment storage time (Figure 5.2A-C). The percentage of unstained (SYTO9 + PI negative) cells of untreated control samples remains greater than 62 % after 1 h, 24 h, and 7 days post-treatment storage at 4 °C (Figure 5.2A-C). The ACP treatment for 1 min followed by 1 h, 24 h, and 7 days post-treatment storage of *L. monocytogenes* on ham surface reduced the unstained cell population to 0.8, 5.8, and 1.5 %, respectively.

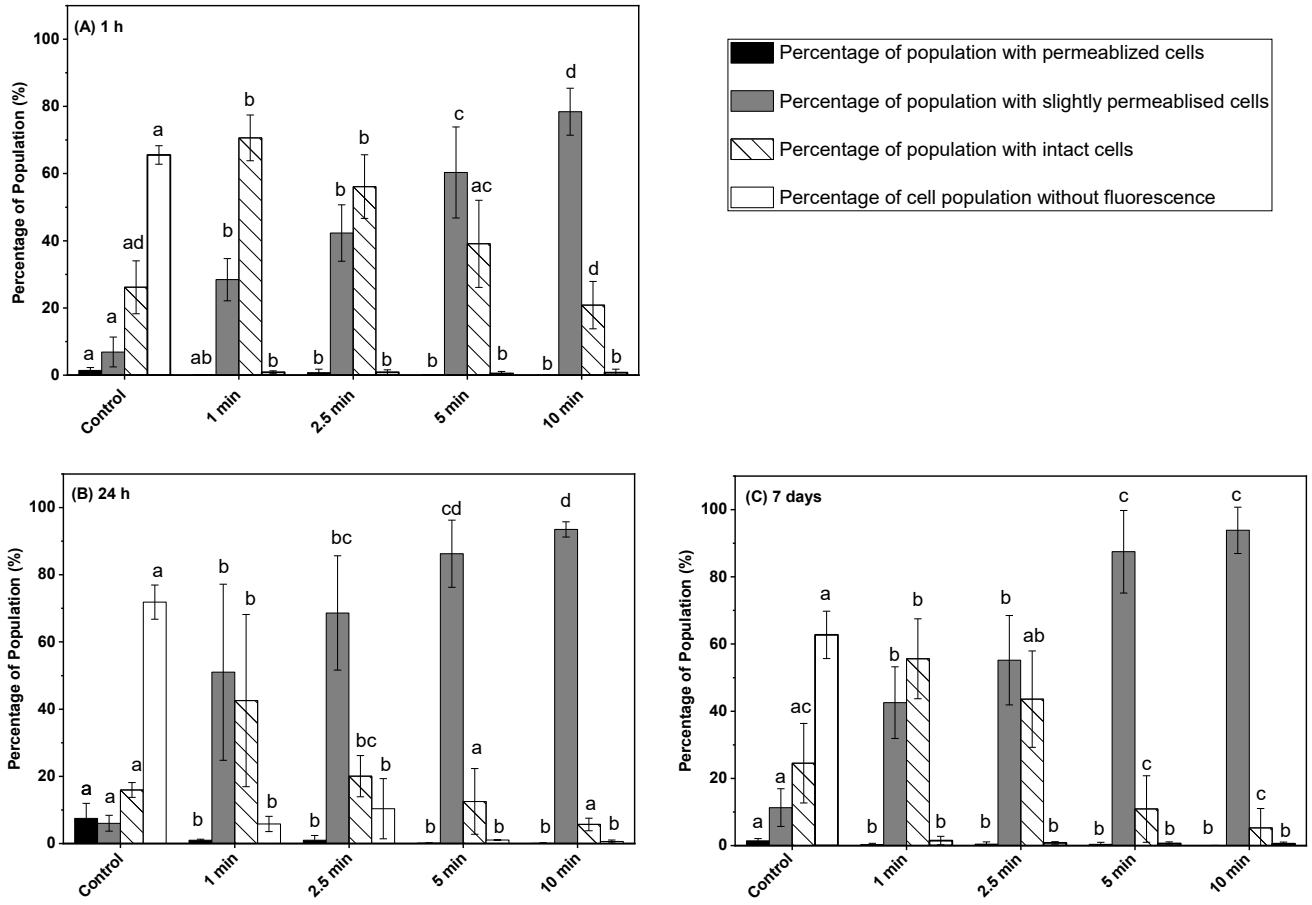

Figure 5.2: Membrane integrity measurements of *L. monocytogenes* cells on ham surface using SYTO9 and PI in combination after in-package ACP treatment storage at 4 °C for: (A) 1 h, (B) 24 h, (C) 7 days. Black bar represents permeabilized cells (PI- fluorescence); grey bar represents slightly permeabilized cells (SYTO9 + PI fluorescence); white bar with hatch lines represents intact cells (SYTO 9 fluorescence); white bar represents cells without fluorescence. Data are shown as means ± standard deviations (n=3). Treatment means with different letters are significantly different.

The percentage of *L. monocytogenes* with intact cell membranes increased from 26 % (untreated controls) to 70 % after 1 min of ACP treatment, followed by 1 h of post-treatment storage at 4 °C. During post-treatment storage of 24 h, the percentage of cells with intact membranes decreased significantly from 70 to 42 %, again it was increased to 55 % after 7 days post-treatment storage. Irrespective of post-treatment storage time, an increase in ACP treatment time from 1 to 2.5 min did not significantly change the percentage of cells with intact membrane. A significant decrease in *L. monocytogenes* cells with intact membranes was observed after 5 and 10 min ACP treatments for all the post-treatment storage times (Figure 5.2A-C). In fact, the percentage of *L. monocytogenes* with intact cell membranes remained almost below 6 % after 10 min ACP treatment followed by 24 h and 7 days post-treatment storage. The percentage of *L. monocytogenes* with the slightly permeabilized membranes (SYTO9 + PI stained) was significantly greater for all the ACP treatment times and post-treatment storage times compared to untreated controls. Regardless of post-treatment storage time, no significant difference in the percentage of cells with a slightly permeabilized membrane was observed after 2.5 min ACP treatment compared to 1 min ACP treatment. A significant increase in the percentage of *L. monocytogenes* with the slightly permeabilized cell membrane was observed after 5 min ACP treatment compared to 2.5 min for all post-treatment storage times (Figure 5.2A-C). The ACP exposure of 10 min of *L. monocytogenes* on ham surface followed by 1 h, 24 h, and 7 days post-treatment storage significantly increased the percentage of cells with slightly permeabilized membranes to 78, 93, and 93 %, respectively. Irrespective of ACP treatment time and post-treatment storage time, the percentages of *L. monocytogenes* with permeabilized cell membranes (PI stained) were lower than 1 % for all treated samples.

5.3.3 Effect of post-ACP treatment storage time on esterase activity

The impact of ACP on intracellular compounds was investigated by measuring esterase activity of *L. monocytogenes* cells after ACP treatment, followed by post-treatment storage of 1 h, 24 h, and 7 days using cFDA and PI in combination (Figure 5.3A-C). The ACP treatment time and post-treatment storage time dependent action on membrane integrity measured by SYTO9 and PI in combination was confirmed by measuring esterase activity. The percentage distribution of unstained (cFDA+ PI negative), cFDA stained, cFDA + PI stained, and PI stained cells in untreated control samples were 45.6, 24, 16.4, and 1.9 %, respectively. After 1 min of ACP treatment followed by 1 h post-treatment storage time, the percentage of unstained and intact *L. monocytogenes* with esterase activity was decreased significantly from 45.6 to 10.6 and from 24 to 14.8 %, respectively, compared to untreated control. The percentage of cells with slightly permeabilized membrane and esterase activity was increased at the same time from 16.4 to 65.6 %. The number of slightly permeabilized membranes of *L. monocytogenes* cells with esterase activity increased to the highest level of 93.9 % after 5 min ACP treatment followed by 1 h storage whereas all other fractions of the population were less than 3 % (Figure 5.3A). During the extended duration of post-treatment storage 24 h and 7 days, a significant increase in the percentage of permeabilized cells was observed compared to 1 h stored samples, whereas the percentage of slightly permeabilized cells with esterase activity decreased significantly for all tested treatment times (Figure 5.4A-C). The permeabilized cell population during 1 h to 7 days post-treatment storage increased with increase in ACP treatment time and reached 90.9 % for samples treated with 10 min ACP treatment, while the percentage of slightly permeabilized cells with esterase activity decreased at the same time from 87.3 to 1.9 %.

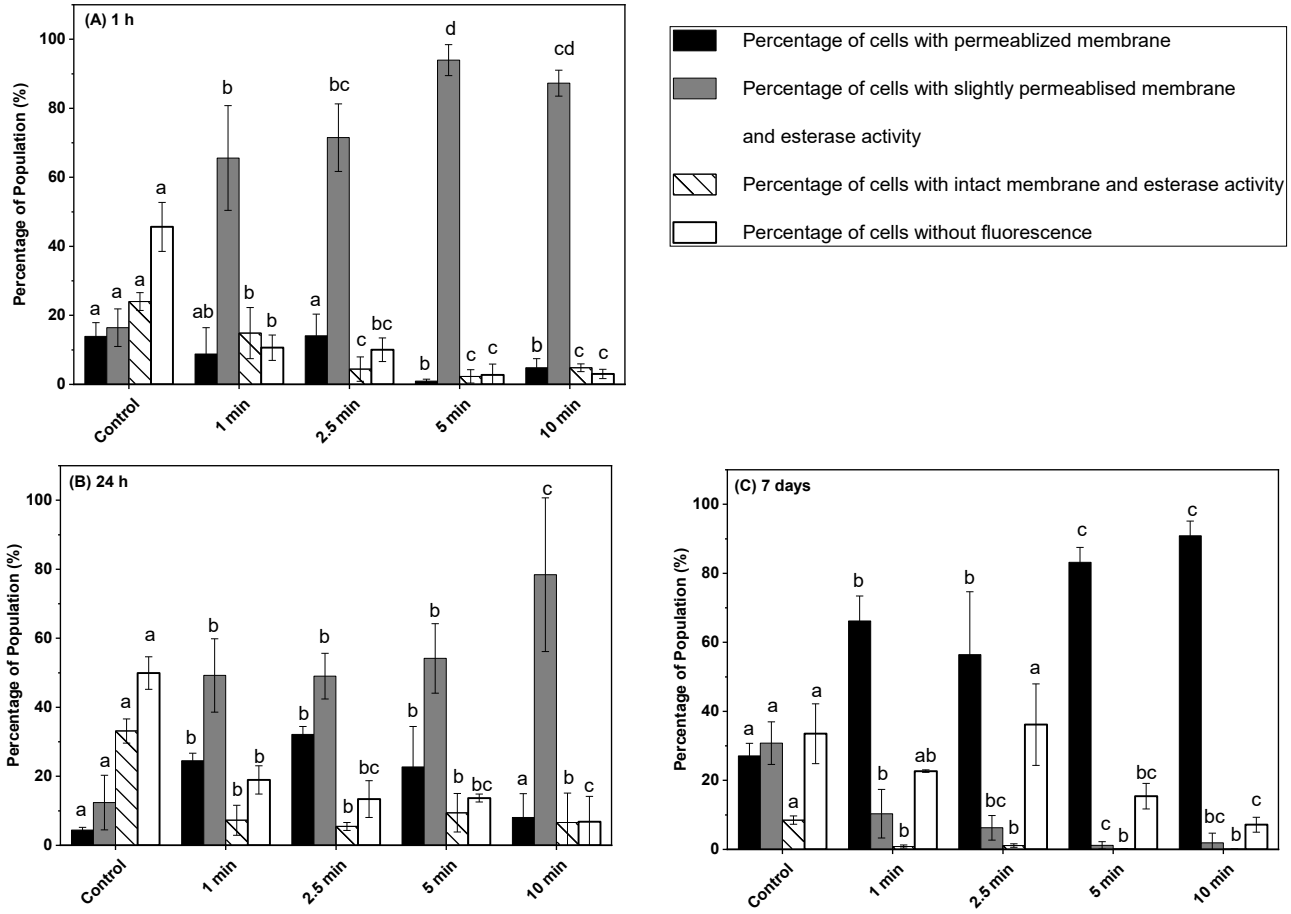

Figure 5.3: Esterase activity and membrane integrity measurements of *L. monocytogenes* cells on ham surfaces using cFDA and PI in combination after in-package ACP treatment storage at 4 °C for: (A) 1 h, (B) 24 h at 4 °C, (C) 7 days. Black bar represents permeabilized cells (PI- fluorescence); grey bar represents slightly permeabilized cells with esterase activity (cFDA + PI fluorescence); white bar with hatch lines represents intact cells with esterase activity (cFDA fluorescence); white bar represents cells without fluorescence. Data are shown as means ± standard deviations (n=3). Treatment means with different letters are significantly different.

5.3.4 Effect of post-ACP treatment storage time on oxidative stress

The impact of ACP treatment followed by post-treatment storage of 1 h, 24 h, and 7 days on intracellular oxidative stress was investigated using H_2DCFDA in combination with PI (Figure 5.4A-C). The percentage of unstained (H_2DCFDA + PI negative) cells of untreated control samples significantly decreased from 72 to 11 % after 1 min ACP treatment following 1 h post-treatment storage. At the same time, the percentage of cells with a slightly permeabilized membrane and oxidative stress increased significantly from 10 (control) to 64 %. An increase in treatment time from 1 to 2.5 min followed by 1 h post-treatment storage time did not significantly change the percentage of cells with intact membrane and oxidative stress, completely permeabilized, and a slightly permeabilized membrane with oxidative stress. During the post-treatment storage of 24 h and 7 days, a slight increase in the percentage of unstained and permeabilized cells was observed compared to 1 h stored samples, while the percentage of cells with a slightly permeabilized membrane and oxidative stress decreased (Figure 5.4A-C). Samples treated with ACP for 10 min followed by 1 h storage showed 92 % of slightly permeabilized cells with oxidative stress, whereas after 24 h and 7 days post-treatment storage decreased it to 81 % and 4 %, respectively. However, the percentage of cells with permeabilized membrane without oxidative stress increased after 24 h and 7 days post-treatment storage compared to 1 h stored samples, for all treatment times. For instance, samples exposed to 5 min ACP followed by 1 h, 24 h, and, 7 days post-treatment storage resulted in 5.3, 20.4, and 86 % of cells with permeabilized membrane, respectively. Similarly, irrespective of ACP treatment time, a slight increase in the percentage of unstained cells was observed after 24 h and 7 days post-treatment storage compared to 1 h post-treatment stored samples (Figure 5.4A-C).

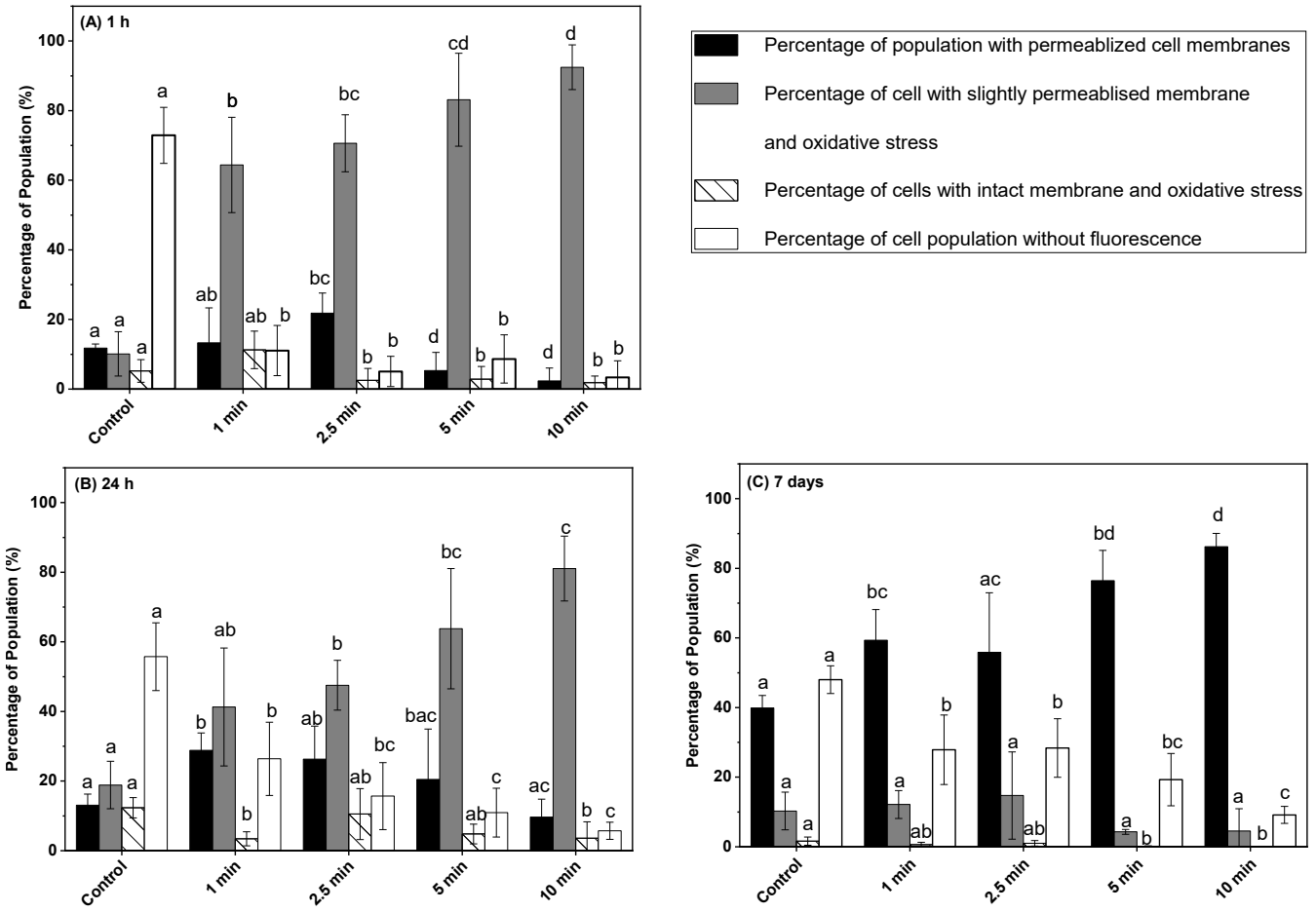

Figure 5.4: Oxidative stress and membrane integrity measurements of *L. monocytogenes* cells on ham surface using H_2DCFDA and PI in combination after in-package ACP treatment storage at 4 °C for: (A) 1 h, (B) 24 h at 4 °C, (C) 7 days. The black bar represents permeabilized cells (PI- fluorescence); grey bar represents slightly permeabilized cells with oxidative stress (H_2DCFDA + PI fluorescence); white bar with hatch lines represents intact cells with oxidative stress (H2DCFDA fluorescence); white bar represents cells without fluorescence. Data are shown as means ± standard deviations (n=3). Treatment means with different letters are significantly different.

The percentage of intact cells with oxidative stress remained lower than 10 % for all tested treatment times and it further reduced during the post-treatment storage to lower than 1 %.

5.4 Discussion

The results of this study demonstrated that the antimicrobial efficacy of in-package ACP discharge on ham surface significantly depended on ACP treatment time and post-treatment storage. The observed treatment time-dependent *L. monocytogens* inactivation on ham during post-treatment storage in this study was consistent with prior reports (Han et al., 2016; Rød et al., 2012). Han et al. (2016) used a cell recovery model to establish a relationship between ACP treatment time and post-treatment storage and reported a treatment time-dependent response of cell recovery during post-ACP treatment storage. A similar inactivation effect was observed in this study where ACP treatment of 10 min followed by 24 h and 7 days of post-ACP treatment storage showed significantly higher reduction in *L. monocytogenes* compared to samples exposed to 5 min ACP and stored for 24 h and 7 days (Figure 5.1). The additional antibacterial effects of post-ACP treatment storage was reported by several authors on a diverse range of food surfaces including ham (Lis et al., 2018; Misra & Jo, 2017; Surowsky et al., 2014; Ziuzina et al., 2020). They suggested that the post-treatment storage might promote diffusion of ACP generated reactive species in an enclosed environment, facilitating extended bactericidal action on cells.

Although the enhanced antibacterial effect of post-ACP treatment storage is well documented, only limited information is available about their mechanisms of action on *L. monocytogenes* during post-treatment storage (Han et al., 2016; Lis et al., 2018; Surowsky et al., 2014). The membrane, cell wall, and intracellular component damages are generally considered as the main reasons for microbial inactivation (Liao et al., 2017). Therefore, flow cytometry analysis was performed in this study to investigate the underlying inactivation mechanisms of *L. monocytogenes* after post-

ACP treatment storage of 1 h, 24 h, and 7 days at 4 °C. In this regard, membrane integrity, intracellular oxidative stress, and esterase activity of *L. monocytogenes* were measured by flow cytometry. The *L. monocytogenes* membrane integrity data showed a specific response trend for the ACP treatment time and post-treatment storage. Regarding membrane permeabilization, an increase in the percentage of slightly permeabilized cells and a decrease in the intact cell population after 24 h storage compared to 1 h storage indicates additional membrane damage during storage. This increase in membrane permeabilization during storage is likely due to the membrane oxidation caused by long-lived plasma reactive species, particularly hydrogen peroxide. Previously, the high concentrations of hydrogen peroxide after 6 h and 18 h of post-treatment storage were reported (Chapter 6). Hydrogen peroxide is considered as one of the major contributors to bacterial inactivation resulting in cell membrane oxidation during ACP treatment (Toyokawa et al., 2017). Similar to these findings, a significant increase in the percentage of cells with a slightly permeabilized membrane after 24 h post-treatment storage was reported for *Citrobacter freundii* in apple juice treated with ACP jet for 8 min (Surowsky, Fröhling, et al., 2014). No significant change in the percentage of slightly permeabilized cell population with increase in post-treatment storage time from 24 h to 7 days was observed, indicating irreversible damage to the cells that led to the loss of cell recovery during long-term storage. Although the percentage of a slightly permeabilized cell population was comparable for samples after 24 h and 7 days storage, a significant decrease in the number of *L. monocytogenes* cells was observed after 7 days storage compared to 24 h storage. This implies that during long term post-treatment storage, permeabilization of cells membrane is one of the major causes of the loss of culturability and a large fraction of permeabilized cells lost their ability to grow on a nutrient agar plate.

The gold standard plate counting method for inactivation efficacy evaluation does not consider the different physiological states of bacteria. The ACP treatment can induce bacteria to enter the viable but non-culturable (VBNC) state that can lead to underestimation of microbial cell numbers (Ramamurthy et al., 2014; Schottroff et al., 2018). Recently, a few studies reported the use of cFDA in combination with PI to identify metabolically active (active esterase) and damaged bacterial cell populations after ACP treatment by flow cytometry (Carré et al., 2018; Antje Fröhling & Schlüter, 2015; Surowsky et al., 2014). In this study, the esterase activity of *L. monocytogenes* cells increased in response to ACP treatment, and the maximum value was found for 10 min ACP exposed samples after 1 h storage. Similar to these findings, treatment time dependent increase in the esterase activity of *Citrobacter freundii* in apple juice in response to ACP treatment was reported immediately after ACP treatment and after 3 h post-treatment storage (Surowsky et al., 2014). A significant decrease in the esterase activity and increase in the percentage of permeabilized cells of *L. monocytogens* during subsequent post-treatment storage of 24 h and 7 days compared to 1 h storage suggests a loss of metabolic activity. This result suggests that after ACP treatment a large fraction of *L. monocytogens* cells were metabolically active during 1 h of post-treatment storage. This finding is further supported with the observed higher colony forming units of *L. monocytogens* on TSA plates in 1 h stored samples compared to 24 h and 7 days.

The ACP discharge in the presence of nitrogen, oxygen, and carbon dioxide generates various short lived and long-lived reactive oxygen and nitrogen reactive species (RONS), including ozone, hydrogen peroxide, nitrates, and nitrites that participate in microbial decontamination (Misra et al., 2018; Toyokawa et al., 2017). The ACP generated reactive species inactivate bacteria through cell membrane disruption via membrane disintegration and generation of intracellular ROS species

(Liao et al., 2017; Patange et al., 2019). In this study, the intracellular oxidative stress of *L. monocytogenes* cells after post-treatment storage was analyzed using dye exclusion methods with H_2DCFDA and the PI assays by flow cytometry. The PI stains the bacterial DNA when the cell membranes are permeabilized and H_2DCFDA reveals the oxidative stress of bacteria. The results from these combined assays revealed that higher percentage of the cell population was under a high oxidative stress environment with slightly permeabilized cell membranes in response to ACP treatments after 1 h storage. An increase in the percentage of cells with a slightly permeabilized membrane and oxidative stress after 24 h storage indicated an interactive effect of ACP generated long-lived reactive species with the bacterial cell membrane during storage. Previous studies reported the presence of a traceable amount of hydrogen peroxide, ozone, and nitrous compounds inside the package after post-treatment storage (Han et al., 2016; Chapter 6). Apart from ACP generated reactive species, oxidatively stressed bacteria generate several peroxides and superoxides inside cells that cause a series of oxidation-reduction reactions and further generate a large amount of short-lived but a high amount of hydroxyl radical species, which consequently can cause intracellular damage (Patange et al., 2019). The higher percentage of permeabilized cell population without oxidative stress (only PI stained) after 7 days of storage compared to 1 h or 24 h suggests that the bacterial cells were no longer under oxidative stress conditions and lost their membrane integrity. This finding is further supported by the lack of culturability and loss of esterase activity in *L. monocytogens* cells after an extended duration of post-treatment storage.

5.5 Conclusions

In conclusion, concerning to 1 h, 24 h, and 7 days of post ACP-treatment storage, a treatment time-dependent decrease in the cultivable *L. monocytogenes* population was observed with 5 log reduction after 10 min of treatment. Flow cytometry method highlighted the physiological states

of three bacteria sub-population distribution depending on the ACP treatment time and post-treatment storage. Flow cytometry data suggest that a very high percentage of *L. monocytogenes* cells were under high oxidative stress conditions with active esterase and slightly permeabilized membrane even after 24 h of storage. Both the flow cytometric data on esterase activity and plate count method revealed a treatment time dependent decrease in the total active bacterial population for samples after 7 days of post-treatment storage.

Chapter 6: In-package Atmospheric Cold Plasma Inactivation of *Salmonella* in Freeze-dried Pet Foods: Effect of Inoculum population, Water activity, and Storage

6.1 Introduction

Each year worldwide, foodborne illnesses affect approximately 600 million people and cause nearly 420,000 deaths (Mehlhorn, 2015; WHO, 2015). In Canada alone, every year, contaminated food causes approximately 4 million cases of foodborne diseases and 11,500 hospitalizations, including 240 deaths (Health Canada, 2016). *Salmonella* is one of the major foodborne pathogens responsible for more than one out of four hospitalization cases of all foodborne illnesses in Canada (Health Canada, 2016). *Salmonella* can be found in the intestinal track of animals. Foodborne illnesses by *Salmonella* can be associated with the consumption of contaminated food products, particularly those of animal origin. *Salmonella*-related infection can also be transmitted through direct or indirect contact with pet animals. A total of 7.5 million Canadian households (~57 %) own pets; 7.9 million cats (~37 % of Canadian households) and 5.9 million dogs (~32 % of Canadian households) live in Canadian households (Oliveira, 2014). Ingredients of pet foods are mostly of animal origin, and these ingredients are identified as high risk due to possible *Salmonella, Listeria monocytogenes, and Escherichia coli* contamination (Behravesh et al., 2010; Nemser et al., 2014). Concern over dry pet food safety has increased in the last decades because of several outbreaks and recalls related to *Salmonella* contamination (CDC, 2012; Health Canada, 2012; Kananub et al., 2020; Syamaladevi et al., 2016). Dry pet foods with $a_w < 0.85$ have long shelf-life (Santillana Farakos et al., 2013). *Salmonella* can survive for a long period of time in low a_w environment (Beuchat et al., 2011; Finn et al., 2013). Increased resistance of *Salmonella* in low a_w foods against conventional and novel decontamination methods was reported by several authors

(Finn et al., 2013; Limcharoenchat et al., 2018; Mattick et al., 2000; Prasad et al., 2019; Farakos et al., 2013).

Atmospheric cold plasma (ACP) is an emerging, green, non-thermal food decontamination technique, with an application advantage of ACP generation inside a closed food package. In-package dielectric barrier discharge (DBD) is one of the methods to generate cold plasma inside a confined food package. The decontamination effects of ACP discharge inside the food package is due to the presence of a diverse range of reactive species including free radicals, ions, and reactive oxygen and nitrogen species (RONS) (Misra et al., 2018). These reactive species possess tremendous potential to injure and inactivate several microorganisms, including bacteria, fungi, and spores (Bourke, Ziuzina, Boehm, Cullen, & Keener, 2018; Misra et al., 2019, 2018). Reactive species concentration in the ACP discharge is dependent on several process parameters including, discharge gap, gas composition, exposure time, relative humidity, substrate type, and post-treatment storage conditions (Moiseev et al., 2014; Chapter 4 of this thesis).

High-quality pet food treats are produced by freeze drying to preserve product quality and prevent lipid oxidation. Freeze drying is a low temperature drying process, which cannot be considered a kill step to inactivate pathogenic microorganisms, including *Salmonella*. Since pathogenic bacteria can survive in low a_w foods such as freeze-dried pet foods, additional measures should be considered to inactivate any of them present in these products after processing. In-package ACP treatment may be applied for post-process decontamination of foods, including freeze-dried pet foods and treats. However, limited studies have been reported regarding the potential of in-package ACP for the decontamination of low a_w foods. For instance, previous studies reported the inactivation of *Salmonella* on dry foods, including nuts (Niemira, 2012), onion flakes (Kim & Min, 2018), tempered wheat grains (Popo et al., 2019), wheat flour (Misra et al., 2015), and whole black

pepper (Hertwig, Reineke, Ehlbeck, Knorr, & Schlüter, 2015) by ACP. These studies demonstrated that ACP discharge could be used to inactivate *Salmonella* on dry foods surfaces. However, some findings indicated that the ACP treatment led to significant lipid oxidation and resulted in adverse effects on the quality of foods with high fat content, especially, meat and meat-based products (Sarangapani et al., 2017; Chapter 4 of this thesis)

To the author's best knowledge, decontamination efficacy of in-package ACP treatment for freeze-dried pet foods has not been reported before. Several products and process factors could influence the *Salmonella* inactivation in freeze-dried pet foods by in-package ACP, including treatment and post-treatment storage time, a_w, growth condition of bacteria etc. The literature survey revealed that there is a lack of information on the effects of bacterial growth conditions and initial inoculum population on inactivation of *Salmonella* by in-package ACP. Therefore, the objectives of this study were to (i) investigate the impact of initial inoculum population and inoculum growth condition on *Salmonella* inactivation on freeze-dried pet foods by in-package ACP; (ii) assess the impact of a_w and post-treatment storage on *Salmonella* inactivation on freeze-dried pet foods by in-package ACP; and (iii) evaluate the lipid oxidation in freeze-dried pet foods after ACP treatment and post-treatment storage.

6.2 Material and methods

6.2.1 Experimental design

Overall, the experimental design consisted of inoculation of freeze-dried pet food pellets using two methods, *i.e*., broth and lawn inoculation. Thereafter, the inactivation efficacy of in-package ACP treatment and post-treatment storage against *Salmonella* on samples equilibrated to target a_w were compared with untreated samples. The influence of initial inoculum population on ACP inactivation efficacy against *Salmonella*, immediately after ACP treatment and post-treatment

storage (7 or 14 days at 21±2 °C) was also evaluated. Additionally, the changes in peroxide value and thiobarbituric acid reactive substance (TBARS) value of freeze-dried pet foods at target a_w were evaluated immediately after ACP treatment and after post-treatment storage (14 days at 21±2 °C). All experiments were performed in triplicate.

6.2.2 In-package ACP discharge characterization

Optical emission spectra (OES) of ACP discharge within the packages without samples were collected to identify the major reactive species in excited states as described in chapter 4, section 4.2.8. Temperature and the gas phase concentrations of major reactive species were measured before and immediately after ACP treatment and during post-treatment storage (6 and 18 h) at 21 ± 2 °C. The temperature of the gas inside the package without pet food was measured using an imaging infrared thermometer (FLIR TG165, system Inc., Wilsonville, FL, USA). The gaseous phase concentrations of ozone (O_3), hydrogen peroxide (H_2O_2), and nitrous gases ($NO+NO_2$) were measured immediately following in-package ACP treatment without pet food, using a short-term detection tube (Dräger Safety AG & Co. Lubeck, Germany) (Chapter 4, section 4.2.9 of this thesis). A syringe needle was attached at one end of the detection tube and another end was inserted into Dräger Accuro Detection pump (Dräger Safety AG & Co., Lubeck, Germany) for the collection of a gas sample by inserting a needle into the package. A Dräger short-term detector tube 10/a (CH 21 001 Dräger Safety AG & Co. Lubeck, Germany), 50/a Dräger tube (81 01 921), and 0.1/a Dräger tube (81 01 041) were used to detect O_3, $NO + NO_2$, and H_2O_2, respectively. The final concentration of the gas was calculated in ppm, following the manufacturer's instructions.

6.2.3 Cultivation of bacterial strains and growth conditions

Frozen stock culture of *Salmonella enterica* Typhimurium ATCC13311 and *S. enterica* Senftenberg ATCC43845 was streaked on a tryptic soy agar (TSA) plate and incubated for 24 h at

37 °C. A single isolated colony from each plate was picked and transferred into 5-mL tryptic soy broth (TSB) and incubated in an orbital shaker for 24 h at 37 °C (200 RPM). Subsequently, 100 µL of culture was transferred into 5-mL TSB and incubated for 18 h (200 RPM and 37°C). To prepare broth grown two-strain cocktails of *Salmonella*, 1 mL of each culture were mixed and centrifuged at 5,311 × *g* for 10 min, and the supernatant was discarded. The harvested cell pellet was resuspended in 1 mL of 0.1 % peptone water to obtain a *Salmonella* cocktail with an initial cell population of approximately 10^9 CFU/cm^2.

The bacterial lawn was prepared according to the procedure reported by Prasad, Gänzle, & Roopesh (2019) with some modifications. Briefly, to prepare the lawn grown culture of two-strain cocktails of *Salmonella*, 100 µL of broth grown culture of each strain was evenly spread onto TSA plate and incubated for 24 h at 37 °C. The bacterial lawn was collected with 1-mL 0.1 % (w/v) peptone water and centrifuged at 9,632 × *g* for 5 min. After the supernatant was discarded, the cell pellet was resuspended in peptone water to make up to 1 mL total volume. To create two-strain cocktail of *Salmonella* with an initial cell population of 10^{10} CFU/cm^2, 1 mL of each culture was mixed together and vortexed for 15 s. Subsequently, this cocktail culture was serially diluted to obtain lower average cell populations of 10^9 CFU/cm^2 and 10^8 CFU/cm^2. The initial cell population on freeze-dried pet foods was confirmed by spread plating on TS agar media and counts were represented as log CFU/cm^2. A relatively high initial inoculum population was selected in this study. As considerable decrease in bacterial cell counts was observed during the equilibration process (up to 1.5 log) and storage (up to 1 log), depending on target a_w and initial inoculum population. This is an important consideration since a lower initial inoculum population may not allow to obtain sufficient log reductions to understand the inactivation pattern with ACP treatment time and post-treatment storage.

6.2.4 Inoculation and equilibration of pet foods

The meat constituents used to prepare pet foods includes fresh angus beef, Romney lamb, wild boar, and Yorkshire pork. Freeze-dried pet food (dog treat samples with 2 % moisture, 40 % crude protein, 1 % crude fiber, 8.5 % crude ash, and 40 % fat) was obtained from a local store. The initial a_w of the pet food was 0.24 ± 0.02, measured at 25 °C using a water activity meter (Aqualab 4TE, Meter group, Pullman, WA, USA). Packaged pet food was opened aseptically and cut to obtain a square surface with 1 cm × 1 cm and 5-mm thickness. The general inoculation and equilibration procedures used in this study were described by Prasad, Gänzle, & Roopesh (2019). Each sample was spot inoculated with 50 µL of cells, suspended in 0.1 % peptone water and the control samples were inoculated with the same volume of peptone water. With a micropipette tip, inoculum was spread on sample surfaces and kept in a biosafety hood for 1 h on a sterile plate. The inoculated samples were equilibrated to target a_w values (0.13, 0.34, and 0.54), by placing the sterile plate with samples in a sealed box filled with saturated solutions of lithium chloride ($a_{w,\ 25\ °C}$ = 0.13±0.02), magnesium chloride ($a_{w,\ 25\ °C}$ = 0.34± 0.02), and sodium chloride ($a_{w,\ 25\ °C}$ = 0.54± 0.02) for 4 days.

6.2.5 Modified atmosphere packaging

After inoculation and equilibration, pet food samples were aseptically transferred into 76.2-µm thick nylon and polypropylene coextruded vacuum bags (Univac Packaging Products Ltd., Edmonton, AB, Canada) using sterile forceps. Packages were filled with gases to mimic atmospheric air, i.e., modified atmosphere containing 78 % N_2 + 21 % O_2 + 1% CO_2, using a gas flush packaging machine (Model C200; Multivac, Kansas City, MO, USA). The average final gas volume per package was approximately 20 ± 2 cm^3.

6.2.6 Atmospheric cold plasma (ACP) system and treatment

Description of the atmospheric cold plasma (ACP) discharge system used in this study can be found in Chapter 4, section 4.2.4 of this thesis. The discharge gap between the high voltage electrode and ground electrode was equal to the height of gas filled polyethylene packages (approx. 8 mm) containing pet food samples. For in-package ACP treatment, the packaged pet food samples were directly placed on ground electrode within the plasma discharge region. The entire bottom surface of high voltage electrode was in direct contact with the package. Between the pet food sample and high voltage electrode, the polythene bag and gas acted as additional dielectric barriers. Plasma was generated inside the confined package at 30 kV for selected durations at room temperature (21±2 °C) under atmospheric pressure. Before in-package ACP treatment, samples were kept inside the package for 1 h and were stored at room temperature for 18 h to attain uniform time interval between packaging and ACP treatment.

6.2.7 Microbial enumeration

Surviving cell population of *Salmonella* on pet food samples were analysed immediately after ACP treatment and after post-treatment storage of 7 and 14 days. Uninoculated packaged samples were also prepared and stored at the same conditions as ACP-treated sample to ensure the absence of contamination by the presence of background microbiota prior to ACP treatment and after storage. ACP-treated and untreated samples were aseptically opened and transferred into 50-mL falcon tube containing 3 mL of 0.1 % peptone water and vortexed for 60 s to detach cells from samples. An aliquot of 0.1 mL was serially diluted in 0.1 % peptone water and 0.1 mL of appropriate dilutions were surface-plated on TSA in duplicate. For the determination of minimum bacterial detection limit, pet food was washed in 3 mL peptone water and 0.1-mL aliquot was spread on TSA plate. Plates were incubated at 37 °C for 24 h and subsequently, number of colony forming

units (CFU) were counted. Plates with no growth of bacteria were incubated for 48 h and checked for the presence of colonies. Counts were converted to $\log_{10}$ CFU/cm^2. The calculated value of limit of detection was 1.5 log (CFU/cm^2).

6.2.8 Determination of peroxide value and lipid oxidation

To examine the effect of in-package ACP treatment on lipid oxidation in pet food samples, uninoculated samples were equilibrated to target a_w and exposed to ACP after packaging. Peroxide value (PV) and thiobarbituric acid reactive substances (TBARS) value of treated samples were determined immediately after ACP treatment. Additionally, TBARS value was determined after 14 days of post-treatment storage at room temperature (21 ± 2 °C). Untreated control samples were also stored at the same conditions as treated samples.

Peroxide value, representing the primary lipid oxidation products was determined using peroxide test kit (07KTPR2000, MP Biomedical LLC, Irvine, ON, Canada), following manufacturer instructions. Briefly, 1.0 ± 0.05 g of hand crushed, and the thoroughly mixed dry sample was transferred into 15-mL falcon tube. Ten glass beads were placed in the tube containing 1 g sample. Then, 3 mL of peroxide preparation reagent was added and vortexed for 1 min, before placing the tube in dry heat bath at 40 °C for 10 min. After 10 min, the sample was vortexed for 15 s and placed back into the dry bath heater for another 5 min. After 15 min of heating, the warm sample was filtered through membrane filter (SKU 07DPP1000, MP Biomedical LLC, Irvine, ON, Canada), connected to a vacuum apparatus at vacuum pressure range of 16-34 kPa (SafTestTM, filtration unit, MP Biomedical LLC, Irvine, ON, Canada). A 200 µL aliquot of the filtrate was pipetted into the tube and 200 µL of preparation reagent was added to further dilute the filtrate. Subsequently, 1 mL of peroxide test kit reagent A, B, and C were dispensed into the tube and kept on a rocker for 10 min after 15 s of vortexing. After 10 min, the absorbance reading was measured

by inserting tube into MP-SaFTest analyser (MP Biomedical, LLC, 9 Goddard, Irvine, Canada). The peroxide values were expressed as meq/kg of fat in sample.

The thiobarbituric acid reactive substances (TBARS) value, representing the secondary lipid oxidation products of pet foods after in-package ACP treatment was carried out using the method reported in Chapter 3, section 3.2.6 of this thesis with little modification. Approximately 0.5 g of sample was crushed with hand and dispersed in 5 mL of 20 % trichloroacetic acid (TCA) containing 1.6 % of phosphoric acid. Solution containing the sample was homogenized for 1 min at 15 × 1000 rpm using a homogenizer (Polytron^{R} PT 10-35GT, Kinematica AG, Luzern, Switzerland). The homogenate was centrifuged at 5,311 × *g* for 5 min at 5 °C and supernatant was collected. One mL of this supernatant was mixed with 1 mL of freshly prepared 0.02 M TBA solution and vortexed for 30 s at 3,000 RPM. Then, mixture was kept in water bath for 30 min at 95 °C, and immediately cooled by placing on ice for 10 min. A 200 µL of the aliquot of the mixture was transferred into clear bottom 96-well plate in duplicate for each sample. The fluorescence intensity was measured using a spectrophotometer (Variskon flash, Thermo Electro Corporation, Nepean, ON, Canada) at excitation and emission wavelengths of 353 and 553 nm, respectively. TBARS values were calculated by dividing fluorescence intensity of sample with the slope of standard curve, and the results were presented as mg of malonaldehyde (MDA) equivalent/kg of pet food.

6.2.9 Statistical Analysis

All the experiments were performed in triplicate and data of the response variables i.e., logarithmic cell counts, peroxide value, and lipid oxidation were subjected to analysis of variance using PROC GLIMMIX effects procedure of SAS® University edition (SAS studio 3.71, Cary, NC, USA). The treatment factors including a_w, treatment time, initial inoculum population, growth condition, and

post-treatment storage were used as fixed effects. The level of significance reported in the test was P-value ≤ 0.05 using Tukey's honest test.

6.3 Results

6.3.1 Characterization of in-package ACP discharge

Optical emission spectroscopy was used to capture all dominant excited state plasma reactive species in the UV/VIS wavelength (190-850 nm) region (Figure 6.1).

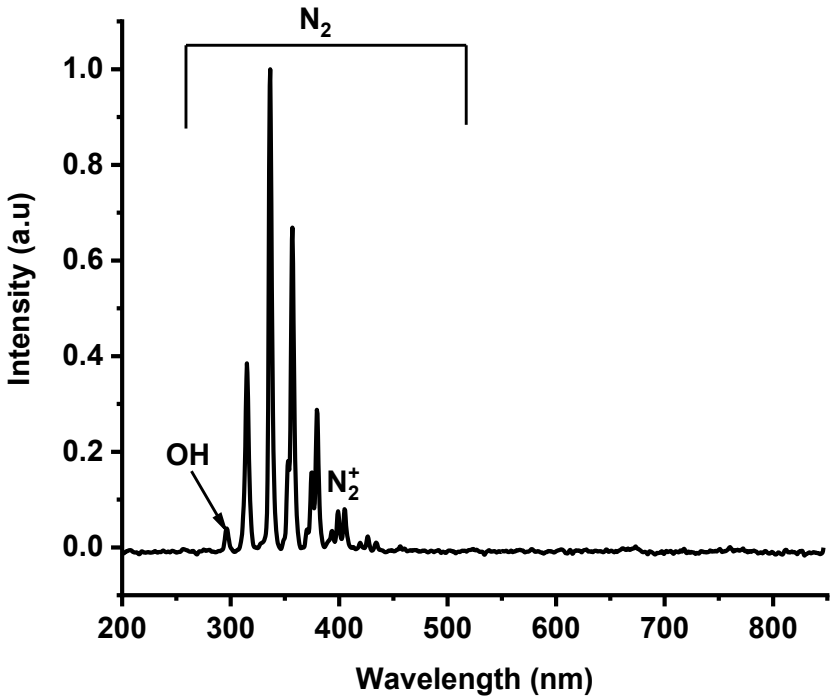

Figure 6.1: Optical emission spectra of atmospheric in-package DBD discharge with input voltage 0-30 kV at a temperature 21±2 °C. This figure shows the normalized emission intensity of plasma excited species in wavelength range 200 – 800 nm. Data are shown as a means of three independent spectra.

The emission spectra of in-package ACP discharge showed strong emission from excited nitrogen species in the UV region, and weak emission of hydroxyl (OH) and oxygen species (Thomas-Popo et al., 2019). Analysis of the spectra obtained from the generated plasma discharge indicated that

the emission intensities of ACP discharge were dominated by excited nitrogen second positive system at 316, 336.5, 357, 380, and 405 nm, and first nitrogen negative system at 391.5 nm (Misra et al., 2015; Thomas-Popo et al., 2019). The nitrogen second positive system and first negative system are mainly produced due to the electron impact excitation of molecular ground state of nitrogen. The emission peaks in the range of 280 to 310 nm (Figure 6.1) were identified as OH radicals (Thomas-Popo et al., 2019).

Table 6.1: Temperature and the gas phase concentrations of ozone, nitrous gas, and hydrogen peroxide inside the package at different ACP treatment times and post-treatment storage.

	Storage (h)					
	0	0	0	0	6	18
Treatment time	Temperature (°C)	O_3 (ppm)	$NO+NO_2$ (ppm)	H_2O_2 (ppm)		
0 s	20.6±0.6	ND	ND	ND	ND	ND
5 s	23.9±1.3	658±80	617±126	15.0±8.6	ND	ND
15 s	24.2±0.4	925±96	958±191	55.0±18.0	ND	ND
30 s	26.2±1.7	>1500	1500±250	125±25	ND	ND
1 min	28.9±1.5	>1500	2100±260	193±40	86.6±11.5	ND
2.5 min	33.0±2.0	142±25	1017±126	243±40	200±50	33.0±11.4
5 min	45.1±1.4	ND	317±76	>300	277±25	107±14
10 min	50.9±1.5	ND	ND	>300	>300	133±15

Data shown as means ± standard deviation of triplicate independent experiment.
ND: Below the limit of detection, not detected.

Peak concentrations of O_3 (>1500 ppm) and $NO+NO_2$ (2100 ppm) were reached rapidly, within 1 min of ACP treatments (Table 6.1). Thereafter, concentrations of O_3 and $NO+NO_2$ started falling very rapidly with increasing ACP treatment time. After 10 min of ACP exposure the measured concentrations values of ozone (< 0.3 ppm) and $NO + NO_2$ (< 25 ppm) reached below the lowest detection limit of the present measurement procedure (Table 6.1). The concentrations of ozone and

nitrous gases were not detected during post-treatment storage of 6 h or 18 h (data not shown). Whereas the concentration of H_2O_2 increased with an increase in ACP treatment time. After 5 min of ACP treatment, the H_2O_2 concentrations reached highest value of the detection limit (300 ppm) (Table 6.1). The hydrogen peroxide concentration was detected even after 6 and 18 h of ACP treatment (Table 6.1).

6.3.2 Effect of bacterial growth condition on *Salmonella* inactivation by ACP

For this set of experiments, pet food with a_w of 0.34 was selected, as this was close to the initial a_w value of the purchased freeze-dried pet food samples (~0.26). *Salmonella* cells was grown either in broth medium or as a lawn and inoculated on pet food samples with an average cell population of 9.2 log (CFU/cm^2) and equilibrated to a target $a_w \sim 0.34$. After equilibration and packaging, the *Salmonella* cell counts on untreated pet food samples were 8.1 log (CFU/cm^2) (Figure 6.2). In-package ACP treatment resulted in significant ($P<0.05$) reduction in *Salmonella* cell counts with increase in ACP treatment times, for broth and lawn grown cells. A significantly higher *Salmonella* reduction of 2.6 log on pet food sample inoculated with broth grown cells was observed after in-package ACP treatment for 10 min compared to 1.4 log (CFU/cm^2) reduction for lawn grown cells (Figure 6.2). Significant interaction between *Salmonella* growth condition and ACP treatment time on log reductions was observed (F value (4, 30); $P < 0.05$). Based on the above findings, *Salmonella* grown on a lawn were selected for next sets of experiments, as they showed higher resistance to ACP treatment.

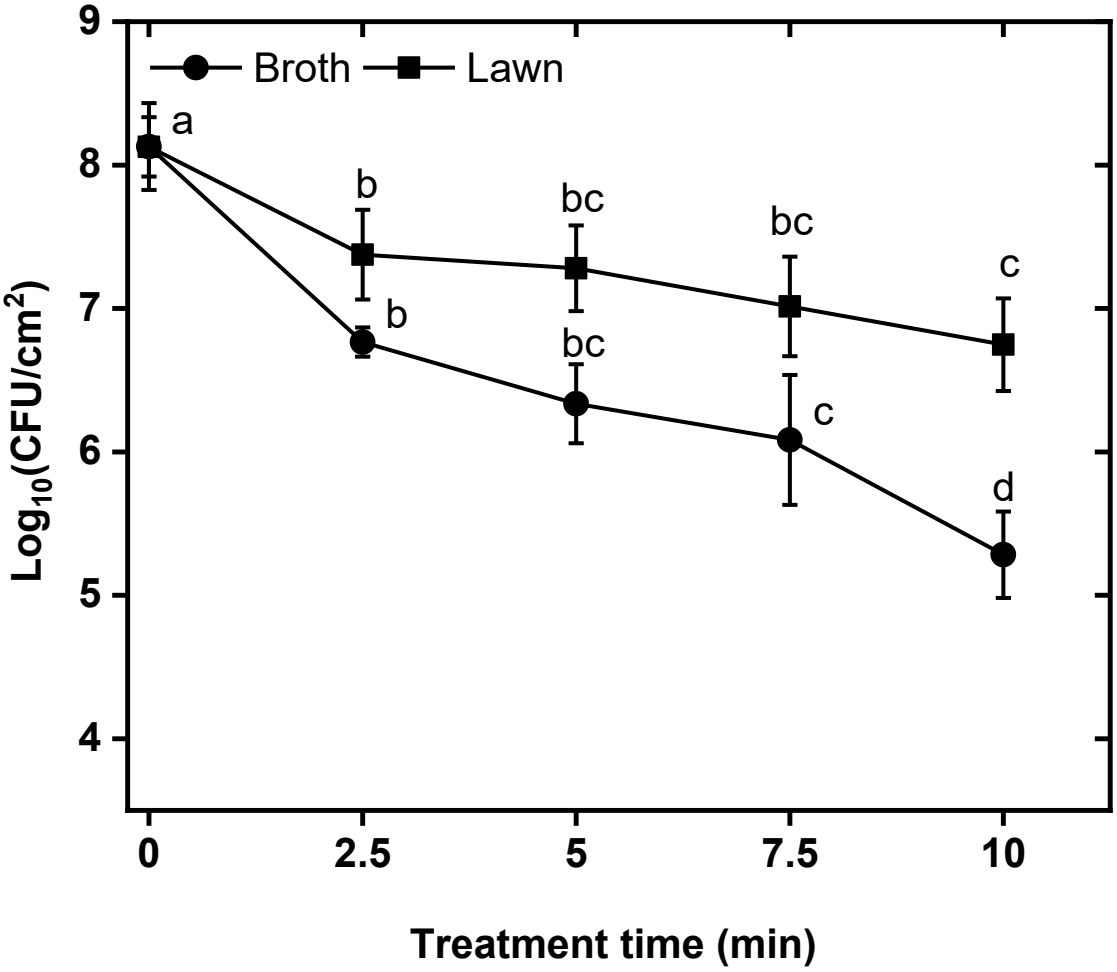

Figure 6.2: Effect of in-package ACP treatment time on mean surviving cell counts of *Salmonella* inoculated on pet food. Samples were inoculated with an initial mean cell counts of 9.2 log (CFU/cm^2). 0 min: Mean cell counts of *Salmonella* at a target a_w 0.34 after equilibration and packaging i.e., before ACP treatment. Line with black square symbols: Pet food inoculated with *Salmonella* grown as lawn. Line with black circle symbols: Pet food inoculated with *Salmonella* grown in the broth media. Data are shown as means and standard deviation of three independent experiments. Treatment means are compared along the line i.e., mean cell counts of *Salmonella* on pet food compared within treatment times; Treatment means with different letters are significantly different ($P< 0.05$) along the line.

6.3.3 Effect of initial inoculum population on inactivation of *Salmonella* by ACP

To investigate the effect of initial inoculum population on inactivation of *Salmonella* by in-package ACP, pet food samples were inoculated with average initial inoculum populations of 10.3, 9.4, and 8.5 log (CFU/cm^2) and equilibrated for 4 days to achieve a target $a_w \sim 0.34$ (Figure 6.3). After equilibration and packaging, the initial average cell populations of untreated control samples were significantly decreased to 9.2 log, 8.1 log and 7.6 log (CFU/cm^2) (Figure 6.3). A significant interaction between initial cell population and ACP treatment time (F value (8, 30) = 15.1; $P< 0.05$) on *Salmonella* cell reduction was observed. Irrespective of the treatment times, samples inoculated with lower cell population (8.5 and 9.4 log CFU/cm^2) were significantly more susceptible to ACP treatment compared to pet food samples with higher cell population. For instance, significant reductions in *Salmonella* cell population were observed on pet food samples with an initial population of 8.5 log (CFU/cm^2) after 2.5 min and longer ACP treatments (Figure 6.3). For samples inoculated with a higher initial cell population of 10.3 log (CFU/cm^2), ACP treatment did not reduce *Salmonella* cells significantly, even after 10 min of ACP treatment (Figure 6.3). After 10 min of ACP treatment, maximum log reductions of 0.2, 1.6, and 3.3 log (CFU/cm^2) were observed on pet food samples compared to untreated samples, with initial cell populations of 10.3, 9.4 and 8.5 log (CFU/cm^2), respectively (Figure 6.3).

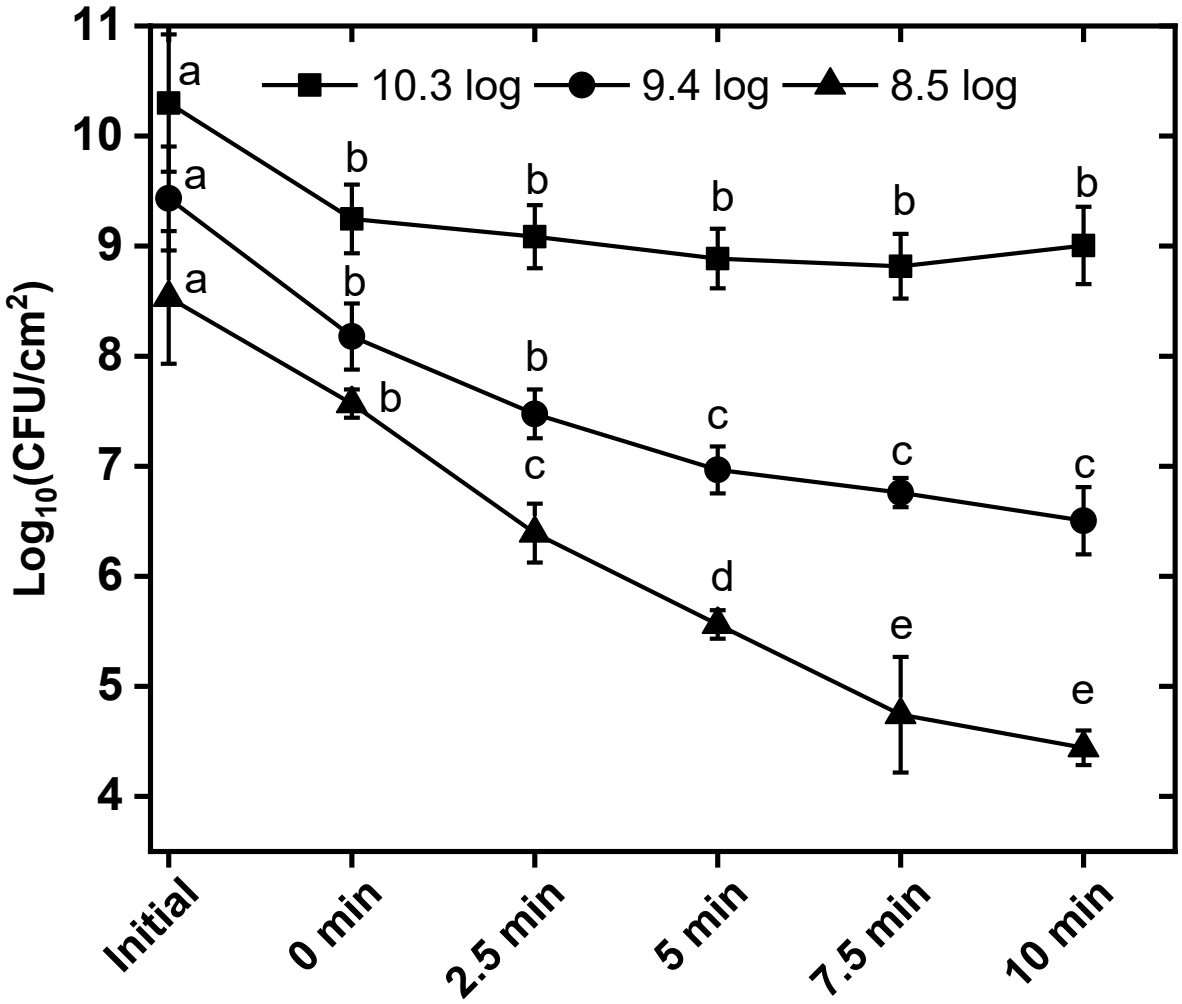

Figure 6.3: Effect of in-package ACP treatment time on mean surviving cell counts of *Salmonella* inoculated on pet food. Initial: Mean inoculum *Salmonella* cell counts before the equilibration. 0 min: Mean *Salmonella* cell counts at target a_w of 0.34 after equilibration and packaging i.e., before ACP treatment. Pet food inoculated with mean *Salmonella* cell counts of 10.3 log (CFU/ cm^2) (Square symbols), 9.4 log (CFU/ cm^2) (Circle symbols), and 8.5 log (CFU/ cm^2) (Tringle symbols). Data shown as means and standard deviation of three independent experiments. Treatment means are compared along the line i.e., mean cell counts of *Salmonella* on pet food compared within treatment times; Treatment means with different letters are significantly different ($P< 0.05$) along the line.

6.3.4 Effect of a_w and storage on inactivation of *Salmonella* by ACP treatment

Considerable decrease in *Salmonella* cell counts on pet food was observed during inoculation and equilibration to specific a_w, depending on the initial population and a_w (Table 6.2 & 6.3). The *Salmonella* reduction during ACP treatment and post-treatment storage was dependent on the initial population (Table 6.2 & 6.3). The decrease in *Salmonella* cell counts were 0.94, 1.4, and 1.31 log (CFU/cm^2) on pet food with a_w of 0.13, 0.34, and 0.54, respectively, when the initial population was 9.1 log (CFU/cm^2). When the initial population was 8.2 log (CFU/cm^2), the decrease in *Salmonella* cell counts were 1.83, 1.82 and 2.03 log (CFU/cm^2) on pet food with a_w of 0.13, 0.34, 0.54, respectively, which were considerably higher compared to the reductions observed when the initial population was 9.1 log (CFU/cm^2). For *Salmonella* inactivation, the three-way interaction effect between ACP treatment time, a_w, and post-treatment storage time was not significant ($P>0.05$). There were significant two-way interactions between a_w and storage time, and between ACP treatment time and a_w ($P<0.05$). This means that the *Salmonella* reduction levels after specific ACP treatment times or post-treatment storage were dependent on the a_w of the pet food and vice versa. *Salmonella* cell counts were significantly different ($P< 0.05$) among water activity (a_w) groups, irrespective of treatment time. Post-treatment storage reduced the cell counts of *Salmonella* on pet food compared to untreated samples depending on the initial cell count, storage time, and a_w ($P < 0.05$) (Table 6.2 & 6.3). For instance, the reductions in *Salmonella* after 7 days were 0.9, 0.67 and 0.78 log CFU/cm^2 for untreated pet food with 0.13, 0.34, and 0.54 a_w, respectively when the initial cell count was 9.1 log CFU/cm^2 (Table 6.3). When the initial cell population was 8.2 log CFU/cm^2, the reductions in *Salmonella* cells in untreated pet food after 7 days of storage were 0.76, 0.92, and 0.76 log CFU/cm^2, respectively (Table 6.2).

Table 6.2: Mean log counts of *Salmonella* on freeze- dried pet foods equilibrated to different a_w and treated with ACP for different times and sampled immediately, and after 7 days of post ACP-treatment storage. Freeze-dried pet food surface was inoculated with initial cell population of 8.2 log_{10} (CFU/cm^2) of *Salmonella*.

a_w	Time (min)	**Log_{10} (CFU/cm^2)**	
		Storage (days)	
		0	7
0.13	0	6.37 ± 0.10^{Aa}	5.61 ± 0.05^{Ab}
	2.5	5.47 ± 0.08^{Ba}	4.50 ± 0.22^{Bb}
	5	5.29 ± 0.08^{Ba}	4.15 ± 0.29^{Bb}
	7.5	4.95 ± 0.41^{Ca}	3.31 ± 0.03^{Cb}
	10	4.66 ± 0.67^{Ca}	2.74 ± 0.23^{Cb}
0.34	0	6.38 ± 0.20^{Aa}	5.46 ± 0.15^{Ab}
	2.5	5.36 ± 0.16^{Ba}	4.58 ± 0.33^{Bb}
	5	4.97 ± 0.21^{BCa}	4.04 ± 0.63^{BCb}
	7.5	4.42 ± 0.21^{Ca}	3.54 ± 0.12^{Cb}
	10	3.24 ± 0.34^{Da}	2.21 ± 0.88^{Db}
0.54	0	6.17 ± 0.05^{Aa}	5.41 ± 0.06^{Ab}
	2.5	4.74 ± 0.09^{Ba}	3.01 ± 0.96^{Bb}
	5	3.86 ± 0.40^{Ca}	2.92 ± 0.53^{Bb}
	7.5	3.48 ± 0.21^{DC}	ND
	10	3.14 ± 0.27^{D}	ND

Data are shown as means of triplicate independent experiments. Lower case letters $^{a, b}$ represent significantly different ($P< 0.05$) mean cell counts of *Salmonella*, between storage groups for the same treatment times. Upper case letters $^{A-D}$ represent significantly different mean cell counts of *Salmonella*, among treatment times for the same a_w of pet food. ND: Cell counts below the limit of detection (1.5 log CFU/cm^2). 0 min**:** Mean cell counts of *Salmonella* on pet food after equilibration and packaging i.e., before ACP treatment.

The two-way interaction between ACP treatment time and storage time was not significant ($P>0.05$). During post-treatment storage, the highest reduction in *Salmonella* cell count was observed on pet food with 0.54 a_w followed by 0.34 a_w and 0.13 a_w, respectively (Table 6.2 & 6.3).

Table 6.3: Mean log counts of *Salmonella* on freeze-dried pet foods equilibrated to different a_w and treated with ACP for different times and sampled immediately and after 7 days of post ACP-treatment storage. Freeze-dried pet food surface was inoculated with 9.1 log_{10} (CFU/cm^2) of initial cell population of *Salmonella*.

a_w	Time (min)	Log_{10} (CFU/cm^2) Storage (days)		
		0	**7**	**14**
0.13	0	8.16 ± 0.50^{Aa}	7.26 ± 0.49^{Ab}	6.54 ± 0.17^{Ac}
	2.5	7.69 ± 0.41^{ABa}	6.66 ± 0.27^{Bb}	5.94 ± 0.03^{ABc}
	5	7.28 ± 0.63^{BCa}	$6.40\pm0.27B^{Cb}$	5.86 ± 0.07^{Bc}
	7.5	6.96 ± 0.73^{CDa}	6.22 ± 0.30^{Cb}	5.68 ± 0.18^{BCb}
	10	6.29 ± 0.65^{Da}	5.95 ± 0.16^{Ca}	5.01 ± 0.32^{Cb}
0.34	0	7.70 ± 0.51^{Aa}	7.03 ± 0.56^{Aa}	6.49 ± 0.19^{Ab}
	2.5	7.22 ± 0.36^{ABa}	6.34 ± 0.83^{ABb}	5.85 ± 0.26^{ABb}
	5	6.82 ± 0.29^{Ba}	6.19 ± 0.75^{Bab}	5.65 ± 0.30^{Bbc}
	7.5	6.61 ± 0.31^{Ba}	5.66 ± 0.40^{BCb}	4.68 ± 0.32^{Cc}
	10	6.22 ± 0.70^{Ba}	5.07 ± 0.26^{Cb}	4.23 ± 0.41^{Cc}
0.54	0	7.79 ± 0.38^{Aa}	$7.01\pm0.52A^{ab}$	6.33 ± 0.17^{Ac}
	2.5	7.05 ± 0.68^{ABa}	5.82 ± 0.87^{Bb}	4.87 ± 0.37^{ABc}
	5	6.80 ± 0.68^{Ba}	4.82 ± 0.73^{Cb}	4.40 ± 0.16^{Bb}
	7.5	6.46 ± 0.21^{BCa}	4.38 ± 0.89^{CDb}	$3.78\pm0.03B^{Cc}$
	10	5.64 ± 0.23^{Ca}	3.58 ± 0.62^{Db}	3.19 ± 0.39^{Cb}

Data are shown as means of triplicate independent experiments. Lower case letters $^{a, b, c}$ represents significantly different ($P< 0.05$) mean cell counts of *Salmonella*, among storage groups for the same treatment time. Upper case letters $^{A-D}$ represent significantly different mean cell counts of *Salmonella*, among treatment times for the same a_w of pet food. 0 min**:** Mean cell counts of *Salmonella* on pet food after equilibration and packaging i.e., before ACP treatment.

When the initial inoculum cell count was 9.1 log CFU/cm^2, the *Salmonella* reductions on pet food with 0.13, 0.34, and 0.54 a_w, after 10 min ACP treatment followed by 14 days post-treatment storage were 3.05, 3.47 and 4.6 log CFU/cm^2, respectively compared to untreated control at 0 day post-treatment storage (Table 6.3). When the initial inoculum cell count was 8.2 log CFU/cm^2, 10

min ACP treatment reduced *Salmonella* cells by 1.71, 3.14, and 3.03 log CFU/cm^2 on pet food with a_w of 0.13, 0.34, and 0.54, respectively (Table 6.2). Post-treatment storage further reduced the number of *Salmonella* cells on pet food, regardless of the a_w (Table 6.2). For instance, the *Salmonella* reductions in pet food with 0.13, 0.34, and 0.54 a_w were 3.63, 4.17 and >4.5 log (below the limit of detection), after 10 min ACP treatment followed by 7 days of post-treatment storage, respectively when the initial inoculum cell count was 8.2 log CFU/cm^2 (Table 6.2).

6.3.5 Effect of in-package ACP treatment on the quality of pet food

To assess the effect of a_w, ACP treatment time, and storage on quality, peroxide value (PV) and TBARS value of pet food with 0.13 a_w or 0.54 a_w were determined. Regardless of the a_w of pet food, ACP treatment significantly increased the PV of pet food samples compared to the untreated control samples (Figure 6.4). No significant two-way interaction between ACP treatment time and a_w was observed. Among the main effects, only ACP treatment time had significant influence on the PV of pet food samples. TBARS method was used to estimate the secondary lipid oxidation products, represented as mg MDA/kg of pet food. The combined effect of ACP treatment time and storage on TBARS was evaluated on pet food with 0.13 (Figure 6.5A) and 0.54 a_w (Figure 6.5B). ACP treatment time ($F(3, 35) = 263.17$; $P < 0.05$), a_w ($F(1, 35) = 60.85$; $P < 0.05$), and storage time ($F(1, 35) = 631.02$; $P < 0.05$) significantly influenced the TBARS value of pet food. Regardless of a_w of pet food, ACP treatment time significantly increased the TBARS values of pet food compared to untreated control (Figure 6.5 A&B). The mixed model ANOVA analysis revealed that significant two-way interactions between ACP treatment time and a_w ($F(3, 35) = 8.33$; $P <0.05$), between storage time and a_w ($F(1, 35) = 14.05$), and between ACP treatment time and storage time ($F(3,35) = 37.5$, $P < 0.05$). The TBARS values of pet food with 0.13 a_w were generally higher compared to those for 0.54 a_w pet food, especially after storage. Overall, among

main effects, post-treatment storage had significantly higher influence on TBARS values and among interaction effects, the interaction between ACP treatment time and storage had more adverse effects on lipid oxidation.

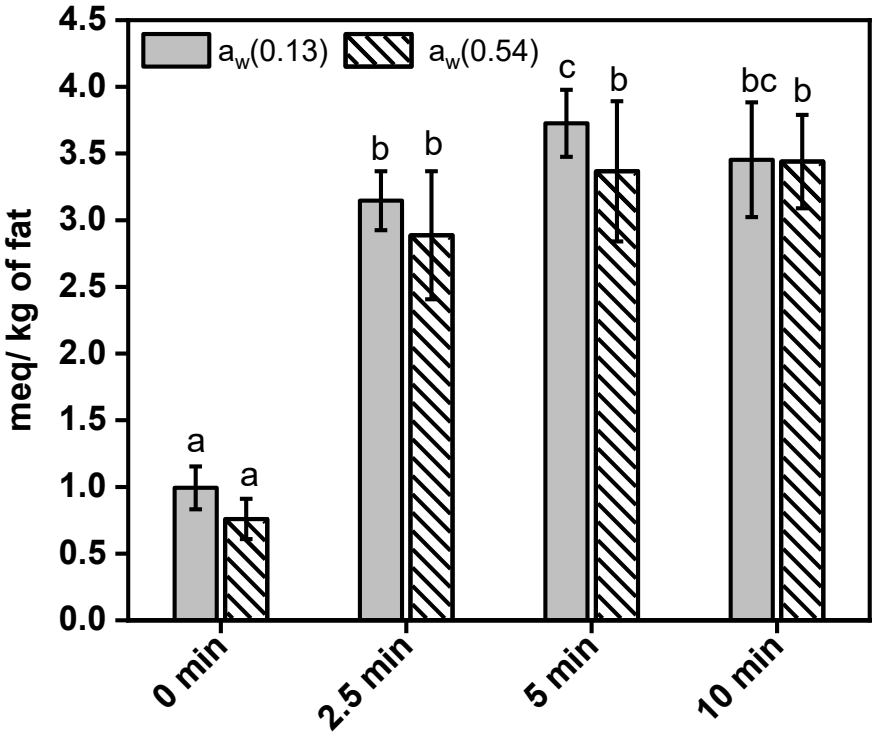

Figure 6.4: Effect of in-package ACP treatment on peroxide value (PV) of pet food equilibrated to target a_w of 0.13 (solid grey column) or 0.54 (hatched column). 0 min: PV of equilibrated pet food to target a_w and after packaging with no ACP treatment. Data shown as means± standard deviations (n=3). Treatment means are compared across the panel i.e., means PV of pet food compared within treatment time and a_w; Treatment means with different letters are significantly different ($P< 0.05$).

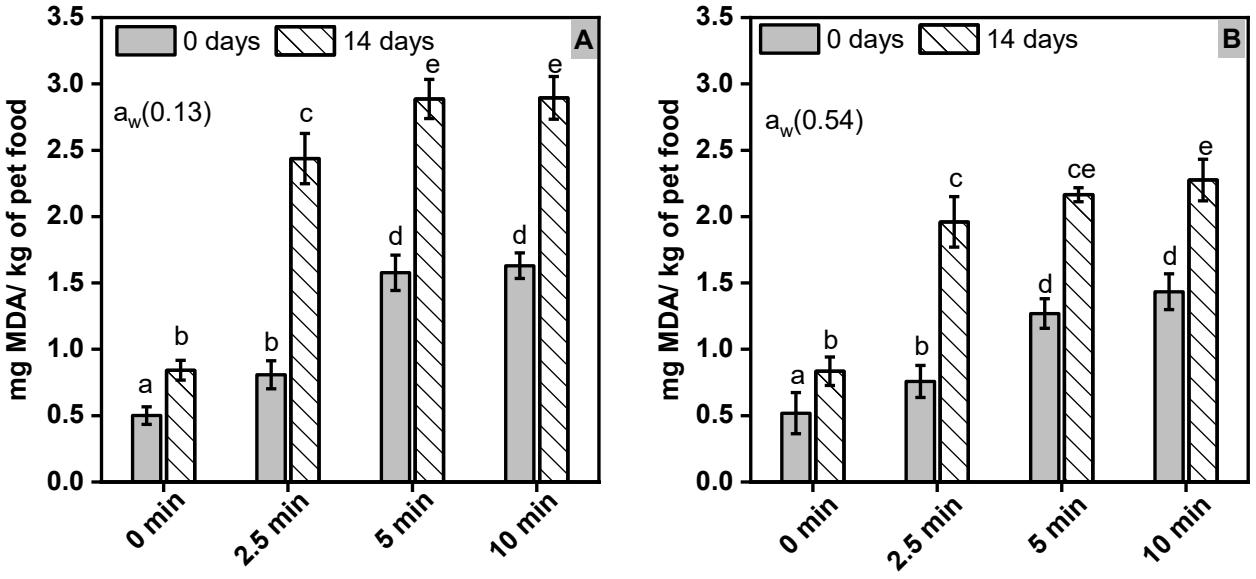

Figure 6.5: Effect of in-package ACP treatment on lipid oxidation of pet food equilibrated to target a_w of (A) 0.13 and (B) 0.54 in terms of mg malonaldehyde (MDA)/kg of pet food. 0 min: TBARS of equilibrated pet food after packaging. TBARS of pet food after 0 days of storage at 21 ± 2 °C: Solid grey column. TBARS of pet food after 14 days of storage at 21±2 °C: Hatched column. Data are shown as means ± standard deviations (n=3). Treatment means are compared across the panel i.e., mean TBARS of pet food compared within treatment time and a_w; Treatment means with different letters are significantly different ($P< 0.05$).

6.4 Discussion

The ACP discharge in atmospheric air or in-package filled with nitrogen and oxygen produces various reactive oxygen and nitrogen species (RONS), including free radicals, superoxides, and long-lived species including ozone, hydrogen peroxide, nitrates and nitrites that participate in microbial inactivation (Misra et al., 2018). Among the generated plasma reactive species, ozone, hydrogen peroxide and nitrites are mainly responsible for the decontamination of microorganisms (Toyokawa et al., 2017;Wang et al., 2018). The concentrations of these major reactive species in ACP discharge greatly are dependent on the ACP treatment time, temperature, and gas composition inside the package (Al-Abduly & Christensen, 2015; Chapter 4). In DBD ACP

discharge, ozone formation is an extremely fast process and proceeds in a few microseconds by a two step reaction, that starts with the dissociation of O_2 molecules and a subsequent three body reaction (6 R1-R2) (Eliasson, Hirth, & Kogelschatz, 1987). Possibly due to the fast ozone production inside the confined package, the saturation concentrations of ozone were reached within 30 s of ACP discharge (Table 6.1). The saturation concentration of ozone and the further depletion during extended period of ACP discharge depend on a number of reactions involving ozone formation (6 R1-R2) and the destruction process (6 R3-R5) (Chang & Wu, 1997; Eliasson et al., 1987). If ozone molecules are already present in the discharge medium, very fast destruction reactions take place (6 R3-R5), compared to ozone formation reactions.

$$e + O_2 \rightarrow 2O + e \qquad (6\ R1)$$

$$O + O_2 + M \rightarrow O_3 + M \qquad (6\ R2)$$

where M = O, O_2 or O_3 is a third collision partner

Major ozone decomposition process includes fast reaction of excited states of singlet oxygen atom with O_3.

$$O(^1D) + O_3 \rightarrow 2O_2 \qquad (6\ R3)$$

Reaction of ozone with vibrationally excited oxygen molecules and by electron impact.

$$O_2(v) + O_3 \rightarrow O_2 + O_3^* \qquad (6\ R4)$$

$$e + O_3 \rightarrow e + O_2 + O \qquad (6\ R5)$$

It is believed that the listed reactions (6 R10) could be the major reactions involving NO_x formation (Al-Abduly & Christensen, 2015). During the extended duration of ACP discharge, the measured

concentration of $NO+NO_2$ decreased with increased ACP exposure (Table 6.1). One possible reason could be the further reaction of NO and NO_2 with $H^{\cdot}$ and that may lead to the formation of HNO_x (Moiseev et al., 2014). A detailed discussion on NO, NO_2, and O_3 dissociation reactions during ACP discharge in a closed environment can be found in Moiseev et al. (2014).

Major reactions involved in the formation of NO_x and H_2O_2 are:

$$e + N_2 \rightarrow N + N + e \quad \text{(6 R6)}$$

$$N+O + M \rightarrow NO + M \quad \text{(6 R7)}$$

$$N + O_2 \rightarrow NO + O \quad \text{(6 R8)}$$

$$NO + O + M \rightarrow NO_2 + M \quad \text{(6 R9)}$$

$$NO_2 + O + M \rightarrow NO_3 + M \quad \text{(6 R10)}$$

The presence of a high concentration of N_2 and a trace amount of water vapor as an impurity in the package could also lower the ozone formation through the production of various NO_X (6 R11-R13) and OH (6 R14) as by-products (Al-Abduly & Christensen, 2015; Chang & Wu, 1997; Eliasson et al., 1987).

$$O_3 + NO \rightarrow NO_2 + O_2 \quad \text{(6 R11)}$$

$$O_3 + N \rightarrow NO + O_2 \quad \text{(6 R12)}$$

$$O_3 + NO_2 \rightarrow NO_3 + O_2 \quad \text{(6 R13)}$$

$$H + O_3 \rightarrow OH + O_2 \quad \text{(6 R14)}$$

In DBD ACP discharge, H_2O_2 could be mainly generated through the dissociation and recombination reaction (6 R14-R19) in oxygen rich environment (Machala et al., 2019).

$$e + H_2O \rightarrow e + {}^{\cdot}OH + {}^{\cdot}H \quad \text{(6 R15)}$$

$$O\left({}^{1}D\right) + H_2O \rightarrow {}^{\cdot}OH + {}^{\cdot}OH \quad \text{(6 R16)}$$

$${}^{\cdot}OH + {}^{\cdot}OH \rightarrow H_2O_2 \quad \text{(6 R17)}$$

$$HO_2^{\cdot} + HO_2^{\cdot} \rightarrow H_2O_2 + O_2 \quad \text{(6 R18)}$$

$$HO_2^{\cdot} + H \rightarrow H_2O_2 \quad \text{(6 R19)}$$

Overall, the results of this study indicated that the concentrations of O_3, NO + NO_2, and H_2O_2 were greatly influenced by ACP treatment time. Other factors such as an increase in temperature during ACP discharge (Table 6.1) and small headspace volume inside the package (~ 20 cm^3) could also have played an important role in the generation and depletion of O_3, NO + NO_2, and H_2O_2.

The results of this study demonstrated that the antimicrobial efficacy of in-package ACP discharge on pet food significantly depended on bacterial growth condition, initial inoculum population, a_w, ACP treatment time and post-treatment storage. Yu et al. (2006) reported that the bacteria growth phase affected the inactivation of *Escherichia coli* K12 by ACP. Cuny, Lesbats, & Dukan (2007) demonstrated that *E. coli* grown as lawn on solid agar medium induced sufficient stress to trigger global stress responses such as heat tolerance and oxidative stress regulation. Hildebrandt et al. (2016) reported that *Salmonella* grown as a lawn showed significantly higher resistance to heat treatment compared to broth culture in various low a_w foods. Similarly, in this study, *Salmonella* cells grown as lawn experienced more competitive and stressed environment compared to liquid media grown *Salmonella* with comparable initial inoculum population (~9.3 log CFU/cm^2).

Possibly due to stress induction during growth phase, *Salmonella* grown in lawn had higher resistance to ACP treatment than the culture grown in broth. Hildebrandt et al. (2016) studied five different frequently used inoculation methods in determining the heat resistance of *Salmonella* in low a_w foods. They concluded that the *Salmonella* grown in lawn produced more stable, consistent, and repeatable results.

Previous studies reported that the initial inoculum population may be a relevant parameter in determining the inactivation rate of microorganisms by ACP (Fernández, Shearer, Wilson, & Thompson, 2012; Yu et al., 2006). The results revealed that increasing the initial inoculum population of *Salmonella* from 10^8 to 10^{10} (CFU/cm^2) resulted in significantly lower inactivation efficacy of in-package ACP treatment (Figure 6.3). Even 10 min of ACP treatment did not significantly reduce *Salmonella* cells count on pet food inoculated with higher initial cell population (~ 10 log (CFU/cm^2) (Figure 6.3). This might be due to the formation of multiple layers of *Salmonella* cells on the food surface, when inoculated with higher initial cell population (Figure 6.6). In this scenario, the top layer of *Salmonella* cell may be inactivated, but they exist as a physical barrier to the plasma reactive species, thus protecting to the cells beneath them (Fernández et al., 2012; López et al., 2019) (Figure 6.6). Additionally, a layer of dry crust formation of *Salmonella* cells was visually observed on the inoculated dry pet food after 4 days of equilibration, when samples were inoculated with higher initial inoculum population (~ 10 log (CFU/cm^2) (Figure 6.6). The crust layer of *Salmonella* cells on pet food surface could further restrict the diffusion of the reactive species and reduce the decontamination efficacy of ACP treatment (Figure 6.6). Fernández et al. (2012) used nitrogen plasma jet (N_2: 12 slpm, 1 kHz, 1 W output power) to demonstrate that the addition of heat killed cells to healthy cells, acted as a physical barrier to plasma reactive species and protected *Salmonella* from inactivation by ACP treatment. There may

be a significant reduction in the microbial population occurring during the drying/desiccation and storage (equilibration) for the preparation of low a_w foods, as observed in this study. So, it is worthwhile to note that *Salmonella* inoculum population of ~10 or 9 log CFU/cm^2 may not be present in processed food products in real environments, especially in low a_w pet foods. Also, it is important to mention that the food itself might offer some protection to microorganisms, especially those foods with high surface roughness, as it might avoid the plasma to reach the microbial cells, for instance, when bigger volumes of foods are treated.

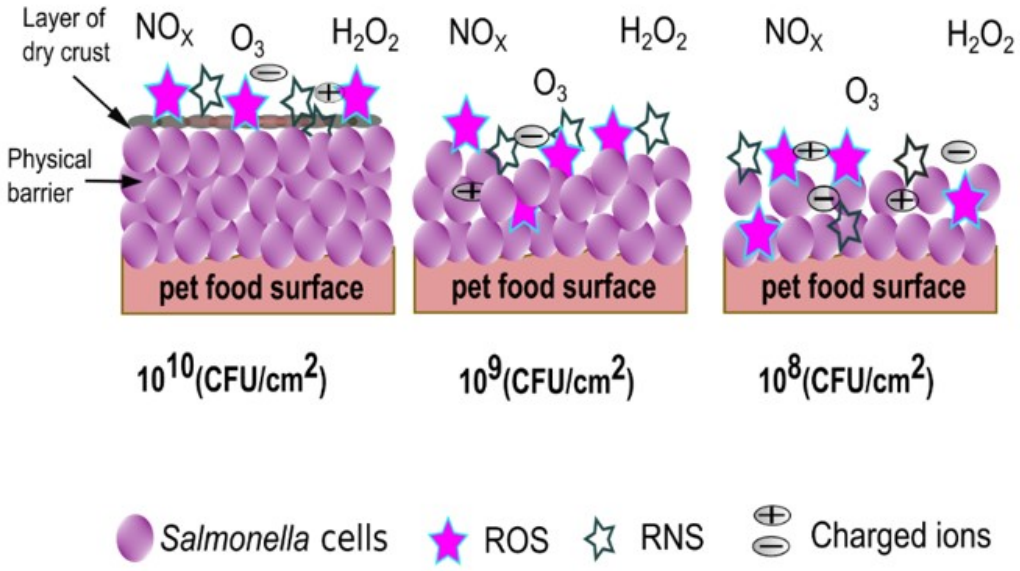

Figure 6.6 Schematic diagram presenting the *Salmonella* cells with higher inoculum levels as a physical barrier to the diffusion of plasma reactive species

A longer duration of ACP discharge resulted in significantly higher reduction in *Salmonella* cell counts, on pet food inoculated with lower cell population (Figure 6.3). The longer duration of ACP exposure might have led to the accumulation of reactive species in the confined environment.

Interaction of these concentrated reactive species with *Salmonella* cells could cause more intense multiple damage, during the extended period of ACP discharge. The antimicrobial effects of ACP discharge was attributed to the cumulative effects, resulting in the mechanical damage to cell envelope and cell wall structure, intracellular oxidative damage by RONS, and oxidative damage of DNA and RNA (López et al., 2019). Possibly, this damage is irreversible and beyond the limits of physiological repair during the extended duration of ACP exposure and resulted in reduced number of *Salmonella*.

In foods with $a_w < 0.85$, bacterial cells quickly respond to attain their turgor pressure by increasing intracellular concentration of compatible solutes (Finn et al., 2013). The mechanisms through which *Salmonella* respond to desiccation stress in low a_w foods includes but not limited to, filamentation of cells, the accumulation of osmoprotectant metabolites/molecules and shifting to a metabolically dormant stage (Finn et al., 2013). In low-a_w foods, the *Salmonella* adapted to desiccation stress was shown to provide cross protection against thermal treatment, UV irradiation, exposure to LED, and exposure to various disinfectants (Du, Jaya Prasad, Gänzle, & Roopesh, 2020; Finn et al., 2013; Prasad et al., 2019; Syamaladevi et al., 2016). Prasad et al. (2019) studied the effect of 365 nm and 395 nm LED treatments against lawn grown *Salmonella* culture suspended in PBS buffer or equilibrated to a_w 0.75. They reported 8 log reduction in *Salmonella* cells suspended in PBS buffer compared to a maximum of 2 log reduction in dry equilibrated (a_w 0.75) *Salmonella* (Prasad et al., 2019). In this study, *Salmonella* cells on pet food samples with 0.13 a_w showed highest resistance to ACP treatment, followed by 0.34 a_w and 0.54 a_w, respectively (Table 6.2&6.3). Further studies are required to understand the effect of desiccation stress response of *Salmonella* on ACP treatment efficacy in low a_w foods. Apart from *Salmonella* desiccation stress response to ACP treatment, different relative humidity of gas within the package due to

product a_w by altering the generation of plasma reactive species could have influenced the ACP inactivation efficacy. A detailed discussion on plasma discharge at different relative humidity conditions and their influence on ROS and RNS generation was provided by Moiseev et al., (2014). Pet food with higher a_w of 0.54 might have produced a higher relative humidity of filled gas inside the package compared to 0.13 and 0.34 a_w, leading to higher inactivation (Table 6.2&6.3). The enhanced inactivation effect of plasma discharge at the high relative humidity environment was extensively studied and reviewed by several authors (Bourke et al., 2017; Kim & Min, 2018)

Results of this study demonstrated that regardless of a_w of pet food, ACP treatment in combination with post-treatment storage resulted in significant decrease in total *Salmonella* cell counts (Table 6.2&6.3). This additional *Salmonella* reduction during storage could be due to the inactivation of sublethally damaged *Salmonella* cells and the extended interaction of long-lived reactive species (RONS) such as H_2O_2, even after 18 h ACP treatment (Figure 6.7A). Reduction in *Salmonella* cells during post ACP treatment storage can be due to the effect of storage time and the presence of long-lived ROS such as H_2O_2 on pet food surface within the package (Figure 6.7 A&B) (Table 6.1). Several different reaction mechanisms have been discussed in the literature to explain the interaction of plasma reactive species with bacterial cell components and the inactivation of sublethally-damaged bacterial cells during storage. Han, et al. (2016) used DBD plasma discharge inside air filled package (80 kV) to treat *Staphylococcus aureus* and *E. coli* cells suspended in PBS buffer and reported that the reduction in bacterial cell population during post ACP treatment storage was due to the effect of long-lived plasma reactive species produced by ACP discharge.

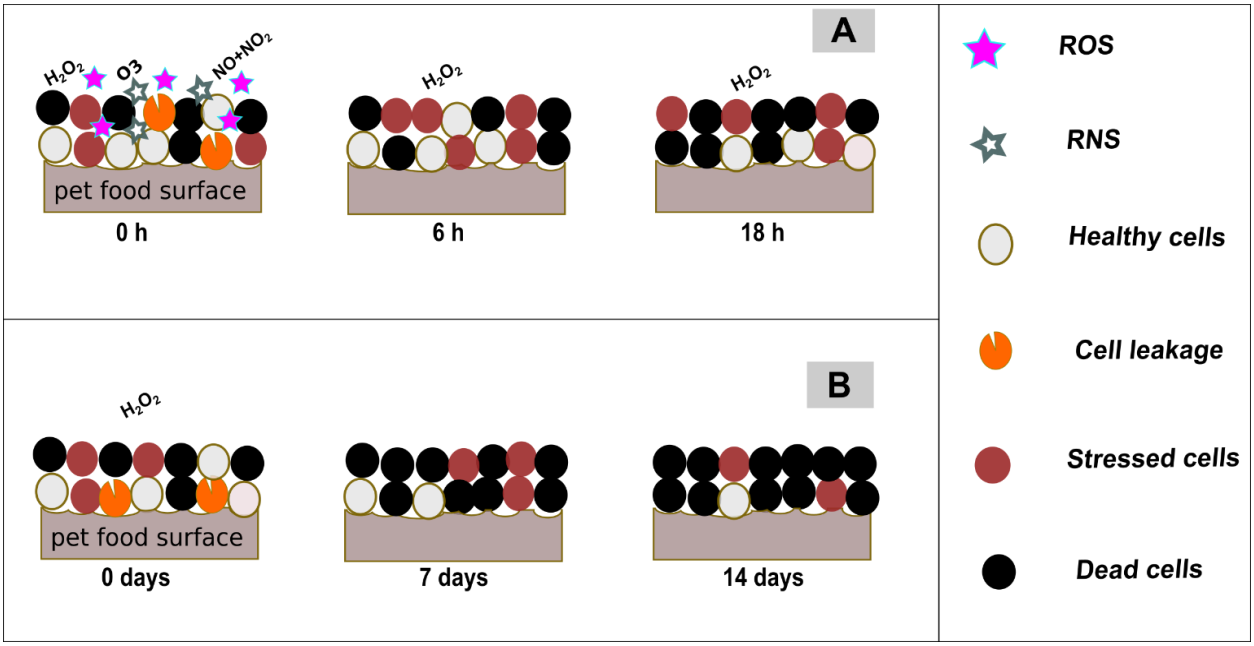

Figure 6.7: Schematic diagram presenting the *Salmonella* inactivation during post treatment storage. A: Induction of stress and cell damage in *Salmonella* cells due to the interaction of long-lived reactive species such as H_2O_2 for extended period (18 h) during post treatment storage, possibly resulting in their inactivation during storage. B**:** Schematic shows the stressed and sub-lethally damaged *Salmonella* cells with cell leakage are inactivated during 7 and 14 days post treatment storage, with little recovery.

The interaction of generated long-lived ROS and RNS with bacterial cell wall, generation of intracellular oxidative stress, and the destruction of DNA inside bacterial cell were reported during storage (Han, et al., 2016). Other mechanisms that could influence the bacterial cell death during storage include breakdown of membrane potential and the destruction of the lipid-bilayer. These mechanisms could lead to an increased inactivation rate of *Salmonella* cells as presented in this study. However, further investigation is required to understand the effects of generated ROS and RNS on cell damage after ACP treatments in low a_w food. The longer duration of storage may support the prolonged action of plasma reactive species on bacterial cell components due to confinement of ACP generated reactive species in the package (Ziuzina et al., 2014) (Figure 6.7A&B). Also, the diffusion of long-lived reactive species into bacterial cells could be increased,

causing a series of chemical reactions in bacterial cells and leading to cell damage (Ziuzina et al., 2014). Additionally, the impact of post-treatment storage on *Salmonella* reduction was higher for longer duration of ACP treatments (Table 6.2&6.3). This was expected, as longer duration of ACP treatment could produce more damage to bacterial cells due to the exposure of increased concentration of generated reactive species for extended times. Huang et al. (2018) studied the effect of in-package ACP treatment (80 kV) using air against *Salmonella* suspended in PBS, NaCl solution, and on gelatin surface and reported that increased ACP treatment time resulted in significantly higher percentage of sub-lethally damaged *Salmonella* cells. In addition, Han et al. (2016) assessed the effect of in-package ACP treatment against *Listeria monocytogenes* and *S. aureus* in meat model (beef extract 3 % or 12 %) followed by post-treatment storage using a cell recovery model and proposed a treatment time dependent response of cell recovery after post-treatment storage. The results also indicated a similar treatment time dependent *Salmonella* cells recovery during the post-treatment storage (Table 6.2&6.3). Additionally, the influence of ACP treatment on *Salmonella* cell damage during storage was more severe on pet food with higher a_w (0.54) followed by 0.34 and 0.13 a_w (Table 6.2&6.3).

The generated reactive species and free radicals can initiate oxidation chain reactions, especially in food with high fatty acids, by abstracting hydrogen ions from unsaturated fatty acid groups (Gavahian et al., 2018). Dry pet foods used in this study contained 40 % fat and is highly susceptible to primary and secondary oxidation during ACP treatment. The peroxide value (PV) was measured as a primary marker for lipid oxidation in pet food immediately after ACP treatment. In addition, TBARS value was measured as a secondary marker for lipid oxidation in pet foods after ACP treatment followed by 0 and 14 days storage. In-package ACP treatment of pet food resulted in increased PV and TBARS values, irrespective of a_w of samples (Figure 6.4 A&B). Gas

composition used in this study contained 21 % O_2, 78 % N_2, and 1 % CO_2. ACP discharge in the presence of 21 % O_2 led to the formation of various reactive species including O_3, NO+NO_2, and H_2O_2 (Figure 6.1). Owing to the high oxidative potential of ozone, an irreversible degradation happened to the unsaturated free fatty acid compounds in pet food (Cho et al., 2014). The oxidation of lipids by ACP obey the criegee mechanism, i.e., direct interaction of O_3 to produce ozonide, and the typical by-products of oxidation includes aldehydes, hydroperoxides, and carboxylic acid (Sarangapani et al., 2017). Other than ozone, other plasma-generated reactive species such as H_2O_2, NO + NO_2, and superoxide also caused lipid oxidation, either directly or acted as a precursor (Amaral et al., 2018). In the current study, increase in TBARS values during storage could be due to the presence of long-lived plasma reactive species such as hydrogen peroxide (Table 6.1) inside the package for an extended duration (Figure 6.5 A &B). Furthermore, the reaction of ROS with food lipids and formation of TBARS, a stable by-product of lipid peroxidation, is not an instantaneous reaction (Gavahian et al., 2018). Therefore, low TBARS value was recorded immediately after ACP treatment and an increase in lipid oxidation was observed after 14 days storage. Results of this study suggested a long-term monitoring of TBARS after ACP treatment could provide a better assessment of the quality of in-package ACP treated foods.

In-package cold plasma technology could be an effective treatment for food decontamination. Some of the major known reactive species produced by cold plasma discharge are used for food decontamination within the concentration limits. Also, the reactive species produced in plasma are short-lived, so the presence of any chemical residues is not anticipated after plasma treatments. However, more studies are required to evaluate the adverse changes in food components and any formation of toxic by-products after plasma treatment that can cause any health concerns; such knowledge is essential for obtaining regulatory approval.

6.5 Conclusions

This study demonstrated that the decontamination effects of in-package ACP treatment of freeze-dried pet food depended on product and process conditions, including the microbial counts, bacterial growth conditions, a_w, and post-treatment storage. Pet food inoculated with lawn-grown *Salmonella* presented significantly higher resistance to ACP treatment compared to broth-grown *Salmonella*. ACP treatment significantly reduced the *Salmonella* counts on pet food when the initial inoculum population was <10 log CFU/cm^2. The total cell counts of *Salmonella* were not changed significantly on pet food inoculated with higher microbial counts (>10 log CFU/cm^2) during ACP treatment. *Salmonella* reduction efficacy of in-package ACP treatment on pet food was affected by a_w. ACP treatments were significantly more effective for *Salmonella* reduction on pet food with 0.54 a_w compared to other studied a_w. ACP treatment for 10 min in combination with 7 days post-treatment storage at 21 °C reduced the *Salmonella* cell counts to below the limit of detection (>4.5 log reduction) for pet food with 0.54 a_w inoculated with 8.2 log CFU/cm^2 of *Salmonella.* ACP treatments and post-treatment storage for 14 days increased the lipid oxidation of pet food, irrespective of a_w of samples. Overall, the level of *Salmonella* inactivation achieved by ACP treatment was considerable, showing the potential of this technology to improve low a_w food safety.

Chapter 7: Synergistically Enhanced *Salmonella* Typhimurium Reduction by Sequential Treatment of Organic Acids and Atmospheric Cold Plasma and the Mechanism Study

7.1 Introduction

Foodborne illnesses associated with the consumption of contaminated meat products, particularly poultry meat is a growing concern for public health agencies and the food industries. Major food pathogens responsible for food contamination include pathogenic strains of *Salmonella* serovars, *Campylobacter jejuni*, *Listeria monocytogenes*, *Yersinia enteerocolitica*, *Escherichia coli* O157:H7, *Staphylococus aureus* and *Clostridium perfringens* (Nair & Johny, 2019; Dinçer & Baysal, 2004). Among all, *Salmonella* is more often associated with poultry meat contamination (Gonçalves-Tenório, Nunes Silva, Rodrigues, Cadavez, & Gonzales-Barron, 2018). Preventive measures based on physical and chemical methods are used to control *Salmonella* outbreaks. Physical methods such as hot water, steam, irradiation, UV light, and high pressure can be used to decontaminate meat, where different stresses induced by these methods cause rapid inactivation of food pathogens (Albert et al., 2021; Dinçer & Baysal, 2004). However, applications of some of these physical processes to decontaminate foods can have significant negative effects on the sensory and nutritional attributes (Csapó, Prokisch, Albert, & Sipos, 2019; Guyon, Meynier, & de Lamballerie, 2016).

Chemical antimicrobials such as chlorine compounds, salt, and organic acids are also used for the decontamination of meat products (Dinçer & Baysal, 2004; Mani-López et al., 2012; Sohaib et al., 2016). However, the stringent regulatory restrictions on the allowable concentration of these chemical antimicrobials in meat products and the dependence of their antimicrobial efficacy on the factors such as residence time, temperature, and pH limit their antimicrobial efficacy (Berdejo et al., 2019; Dinçer & Baysal, 2004; Mani-López et al., 2012). To overcome these limitations,

generally, chemical antimicrobials have been used after mild levels of physical treatments to achieve enhanced and rapid inactivation of microorganisms (Berdejo et al., 2019; Cossu et al., 2016). Recently, synergistic effects of various combinations of antimicrobial compounds and non-thermal processes such as atmospheric cold plasma, high pressure, irradiation, and UV-light on microbial inactivation were reported (Berdejo et al., 2019; Cap et al., 2020; Chaplot et al., 2019; Maherani, Ayari, & Lacroix, 2018; Sohaib et al., 2016; Wang, Oliveira, Alborzi, Bastarrachea, & Tikekar, 2017; Wu et al., 2017).

Atmospheric cold plasma (ACP) is an emerging non-thermal microbial inactivation method. The antimicrobial effects of ACP discharge are due to the generation of a diverse range of reactive species, including reactive oxygen species (ROS), reactive nitrogen species (RNS), ions, and free radical, all of which possess great potential to injure and inactivate bacteria, spores, and other pathogenic organisms (Liao et al., 2017; López et al., 2019). Several studies reported the potential antimicrobial action of ACP against a range of microorganisms on different surfaces (Liao et al., 2017; López et al., 2019; Misra et al., 2019). However, the decontamination effect of ACP discharge in combination with organic acids has rarely been investigated. Previously, the potential application of peroxyacetic acid, combined with ACP to increase *S.* Typhimurium inactivation on raw poultry meat was evaluated (Chaplot et al., 2019). The results of that study demonstrated the ability of this combined treatment to achieve up to 5 log reductions in *S.* Typhimurium. Recently, a few other studies also reported the synergistic activity of organic acids, including lactic acid, when combined with ACP on the reduction of microbial load. However, there is still a lack of understanding on the biological impacts of these treatments on bacterial cells and the reason behind the synergistic antimicrobial action of organic acids and ACP treatments (Qian, Wang, Zhuang, Zhang, & Yan, 2020; Trevisani et al., 2017; Wu et al., 2017)

This study evaluated a synergistic action of food-grade organic acids, i.e., lactic acid (LA) or gallic acid (GA), with ACP treatments to enhance *S.* Typhimurium inactivation. Additionally, the major mechanisms underlying the synergistic action of organic acids and ACP treatment were evaluated. The changes in bacterial membrane permeability, intracellular oxidative stress, membrane lipid peroxidation, and metabolic activity of cells were determined to understand the synergistic action of organic acids and ACP on *S.* Typhimurium at different treatment conditions. The applicability of this hurdle approach to inactivate *S.* Typhimurium on poultry meat was also assessed. Finally, a continuous cooling, misting, and ACP treatment system was developed, and its antimicrobial efficacy was tested. Poultry meat is estimated to cause 14 % of *Salmonella* outbreak-associated foodborne illnesses among food commodities (Vieira and Boyer, 2019). According to the Centre for Disease Control and Prevention (CDC), *Salmonella* cause about 1.35 million foodborne illnesses in the United States every year. The top 3 *Salmonella* serotypes causing salmonellosis are Enteritidis, Newport, and Typhimurium (CDC, 2021; Tack et al., 2019).

7.2 Materials and methods

7.2.1 Bacteria culture cultivation

Frozen stock culture of *Salmonella enterica serovar* Typhimurium ATCC 13311™ was streaked on tryptic soy agar (TSA) plates and kept at 37 °C for 24 h to obtain individual isolated colonies. Single isolated colonies were picked, transferred in 5 mL tryptic soy broth (TSB), and incubated for 18 h at 37 °C in an orbital shaker. Then, 50 µL of aliquots was withdrawn, added to 5 mL of fresh TSB broth, and aerobically incubated for 18 h at 37 °C in an orbital shaker at 200 rpm. The broth grown culture was centrifuged (3,500 × *g*, 10 min), the supernatant was discarded, and cells were resuspended in 5 mL 0.1 % peptone water (Fisher Scientific, Fair Lawn, NJ, USA).

7.2.2 ACP treatment system

A Dielectric Barrier Discharge (DBD) ACP system was used to study *S.* Typhimurium inactivation, similar as described in Chapter 3, section 3.2.3 of this thesis. The DBD system was operated at a frequency of 3.5 kHz and a duty cycle 70 % to generate plasma using atmospheric air as the working gas at atmospheric pressure. The discharge gap between the high voltage electrode and a ground electrode was kept at approximately 5 mm for all the experiments. The DBD discharge system used a ~ 300 W input power and produce DC voltage and current output in the range of 0 – 30 kV. The distribution of excited state reactive species and the concentration of the major reactive species in DBD discharge was previously characterized for this system using optical emission spectroscopy and Dragger tube (Chaplot et al., 2019; Chapter 4).

7.2.3 Sequential treatments using organic acids and ACP

The antimicrobial activity of treatments using lactic acid (LA) (Sigma Life science, Sigma-Aldrich. Co, Oakville, ON, Canada), gallic acid (GA) (Sigma Life science, Sigma-Aldrich Co, Oakville, ON, Canada) in the concentration ranges of 5, 10, and 15 mM, and ACP alone (15, 30, and 60 s) and in combination (10 mM LA/GA + 30 s ACP) were evaluated against *S.* Typhimurium inoculated on Whatman polycarbonate membrane filter paper (25 mm diameter, 0.2 µm pore size, Whatman Inc., NJ, USA) surface. An aliquot of 50 µL of the *S.* Typhimurium cells suspension was spot inoculated and carefully spread with a micropipette tip on the polycarbonate membrane filter paper surface to achieve a final mean cell density ~ 8 log CFU/cm^2. Inoculated filter papers were kept in a laminar flow biosafety cabin for 5 min for bacterial cell attachment and dispersion on the filter paper surface. After that, samples were subjected to organic acid treatment by spraying either LA or GA solution of desired concentration (5,10, and 15 mM) as described by Chaplot et al. (2019). In brief, 50 mL of acid solution was prepared in sterile deionized water and transferred

into a 250 mL spray bottle (Bel-Art SP Scienceware Spray Pump Bottles, Fisher Scientific, ON, Canada). The acid solution was sprayed (~ 0.5 mL per spray, n=1) on samples from approximately 10 cm to cover the entire outer surface. Immediately after spraying, sample weight gain was measured to calculate the fraction of sprayed solution deposited on the sample surface. The final volume deposited on samples was 35 ± 5 µL per sample. Within 5 min of acid treatment, the samples were transferred onto a glass slide and placed directly beneath the plasma discharge region on the ground electrode platform. The discharge gap between the high voltage and ground electrode was maintained at approximately 5 mm. After ACP treatment, samples were stored for 10 min at room temperature (22 ± 2 °C) to enable the interaction of plasma-treated acid solution with *S.* Typhimurium cells. To prepare untreated control, inoculated samples were sprayed with sterile deionized water and stored as treated samples.

7.2.4 Microbial enumeration

Treated and untreated samples after 10 min storage inside biosafety cabin were transferred to a sterile 50 mL falcon tube containing 3 mL of sterile 0.1 % peptone water and vortexed for 30 s to detach the *S.* Typhimurium cells from filter paper surface. An aliquot of 100 µL was withdrawn, serially diluted in 0.1 % peptone water, and was spread on TSA plates in duplicate for each dilution. The plates were incubated at 37 °C for 24 h before counting the colonies. The surviving cell counts of *S.* Typhimurium were expressed as $\log_{10}$ CFU/cm^2.

7.2.5 Cell membrane damage assessment

Cell membrane damage of *S.* Typhimurium after exposure to 10 mM LA or GA alone and in combination with ACP treatment was assessed using propidium iodide (PI), a membrane impermeant fluorescence dye, that can only penetrate damaged membrane. PI has a weak red fluorescence in its native form, but extremely intense fluorescence is produced upon binding with

DNA and RNA of compromised bacterial cells (Stiefel, Schmidt-Emrich, Maniura-Weber, & Ren, 2015). For cell membrane damage analysis, the staining procedure as described by Stiefel et al. (2015) with slight modifications. To harvest cells, treated and untreated samples were transferred in 50 mL falcon tube containing 1 mL of sterile 0.85 % NaCl and vortexed for 30 s at 3000 rpm. Suspended cells were transferred into 1.5 mL sterile Eppendorf tube and centrifuged (12, 500 × g for 3 min). The supernatants were discarded, and the harvested cells were resuspended in 1 mL of sterile 0.85 % NaCl solution. After vortexing gently, an aliquot of 150 µL was transferred into a 96- well flat-bottom clear polystyrene plate. Then, an aliquot of 25 µL of PI was added into each well to reach a final concentration of 20 µM and incubated in dark at room temperature for 15 min. The fluorescence reading was taken with fluorescence microplate reader (Variskon flash, Thermo Electro Corporation, Nepean, ON, Canada) with excitation and emission wavelengths of 488 nm and 645 nm, respectively. The recorded data were normalised with respect to positive control samples. To prepare positive control samples, cells of *S.* Typhimurium with final density of 8 log CFU/cm^2 was suspended in 70 % isopropanol for 60 min at room temperature. After incubation, washing, and resuspension, PI was added to the bacterial suspension and incubated for 15 min, and fluorescence intensity was recorded. The recorded fluorescence intensity was corrected by subtracting background fluorescence and results were normalised with respect to positive control samples.

7.2.6 Intracellular oxidative stress assessment

Intracellular oxidative stress of *S.* Typhimurium after exposure to LA, and GA alone or sequential combination with ACP treatment was assessed using 6-carboxy-2',7-dichlorodihydrofluorescin diacetate (H_2DCFDA), a membrane permeable fluorescence dye. The cell staining procedure was adapted from Qian et al. (2020) with minor modification. Treated and untreated cells were

harvested from filter paper surface in phosphate buffer saline (PBS) buffer as described in section 2.5. A 150 µL aliquot was transferred into a 96-well flat-bottom clear polystyrene plate and incubated with 50 µL H_2DCFDA (Invitrogen by Thermo Fisher Scientific, Life Technologies Corporation Eugene, OR, USA) at a final concentration 20 µM in PBS for 15 min at 37 ^{o}C in dark. The fluorescence reading was measured with fluorescence microplate reader (Variskon flash, Thermo Electro Corporation, Nepean, Canada) with excitation and emission wavelengths of 485 nm and 525 nm, respectively.

7.2.7 Metabolic activity

Metabolic activity was determined using a Vybrant Cell Metabolic Assay Kit (V-23110, Molecular Probe, Inc., OR, USA), following the manufacturer's instructions. Treated and untreated cells were harvested from the filter paper surface in 1 mL sterile deionized water as described in section 2.5 and transferred into 1.5 mL Eppendorf tube. A tube containing cells was centrifuged at 12,500 × g for 3 min, the supernatant was discarded. The cell pellets were resuspended in 200 µL TSB culture media and 2 µL C-12 resazurin was added to achieve a final concentration 20 µM. After vortexing, culture media along with 20 µM C-12 resazurin was transferred into 96-well plate and incubated for 15 min at 37 °C. Fluorescence was measured with a microplate reader with set excitation and emission wavelengths of 563 and 587 nm, respectively. After blank subtraction, results were normalised with respect to untreated control samples.

7.2.8 Membrane lipid peroxidation

Lipid peroxidation was determined using TBA test methods, modified from previous studies (Dolezalova & Lukes, 2015; Chapter 3 section 3.2.6 of this thesis). Briefly, pelletized cells were resuspended in 125 µL 20 % TCA containing 1.6 % phosphoric acid, vortexed, and the mixture was cooled to -20 °C for 20 min. Bacterial cells were removed by centrifugation at 12,500 × *g* for

3 min. The supernatant 100 µL was mixed with 200 µL TBA (10 mM) and placed in a water bath for 45 min at 90 °C. After cooling on ice for 10 min, 200 µL aliquot into 96 well plate and the absorbance were measured at 532 nm in a microplate reader (Variskon flash). The TBARS concentration was presented equivalent to malondialdehyde (MDA) using a molar absorption coefficient of 1.57×10^5 M^{-1} cm^{-1} (Dolezalova & Lukes, 2015).

7.2.9 Inactivation of *S.* Typhimurium on poultry meat surface

Fresh, raw, skinless, and boneless poultry meat was purchased from a local grocery store (Edmonton, AB, Canada) and stored at 4 °C until use. The package was aseptically opened inside the biosafety cabinet and the meat surface was cut into a square shape (1 × 1 cm) and approximately 3 mm thickness. Poultry meat surfaces were spot inoculated with 50 µL of *S.* Typhimurium cells suspension containing approximately 8 log CFU/cm^2 and kept inside a biosafety cabinet for 15 min. After the attachment of cells, desired concentrations of LA or GA were sprayed on inoculated samples, following the procedure described by Chaplot et al. (2019). The control samples were sprayed with sterile deionized water. Within 5 min of acid treatment, the samples were transferred to a sterile glass slide and exposed to ACP discharge for 30 s and 2 min. Treated samples were stored for 10 min inside the biosafety cabinet. After storage, samples were transferred to a sterile 50 mL falcon tube containing ten glass beads in 3 mL of sterile 0.1 % peptone water and vortexed for 30 s to detach the *S.* Typhimurium cells from the meat surface. An aliquot of 100 µL was withdrawn, serially diluted in 0.1 % peptone water, and was spread on TSA plates. The plates were then incubated at 37 °C for 24 h before counting the colonies. The cell counts of *S.* Typhimurium were expressed as $\log_{10}$ CFU/cm^2.

7.2.10 Simultaneous cooling and decontamination process development for poultry meat

To study the simultaneous cooling and decontamination of fresh poultry meat, a cooling system with organic acid mist was developed with a DBD electrode inside it, to create ACP. This ACP integrated cooling system's main component includes a 19.82 L airtight acrylic chamber, a vortex tube (Figure 7.1; Nex flow Air Product Corp, Richmond hill, ON, CA) to generate cold air, and a mist generator (Vicks Mini Filter Free humidifier, Katz Inc., ON, Canada). A compressed gas cylinder supplied air at 1516 kPa into a vortex tube through a hose tube. The vortex tube generated cold air with a temperature as low as -22 ℃, and through a hose tube, it was discharged into the treatment chamber. The hose tube had small perforations to distribute the cold air inside the chamber efficiently. The cold air leaves the chamber through the outlet provided at the other end of the chamber. For temperature measurement, a type K thermocouple connected to a high accuracy handheld thermometer with a 0.1 ℃ resolution and a range of -200 to 260 ℃ (Omega Engineering, Saint-Eustache, QC, Canada) was placed at three different locations inside the chamber. The temperature was recorded every minute during the cooling process and averaged for three locations to determine the cooling time to reach chamber temperature of approximately 4 ^{o}C. For ACP discharge inside the chamber at atmospheric pressure, a steel platform was embedded at the bottom surface of the chamber to serve as a ground electrode; the power electrode was hanging inside the chamber through an opening provided at the top surface. The water mist was discharged inside the chamber near the sample (~1 cm) through a hose pipe outlet for the duration of ACP treatment.

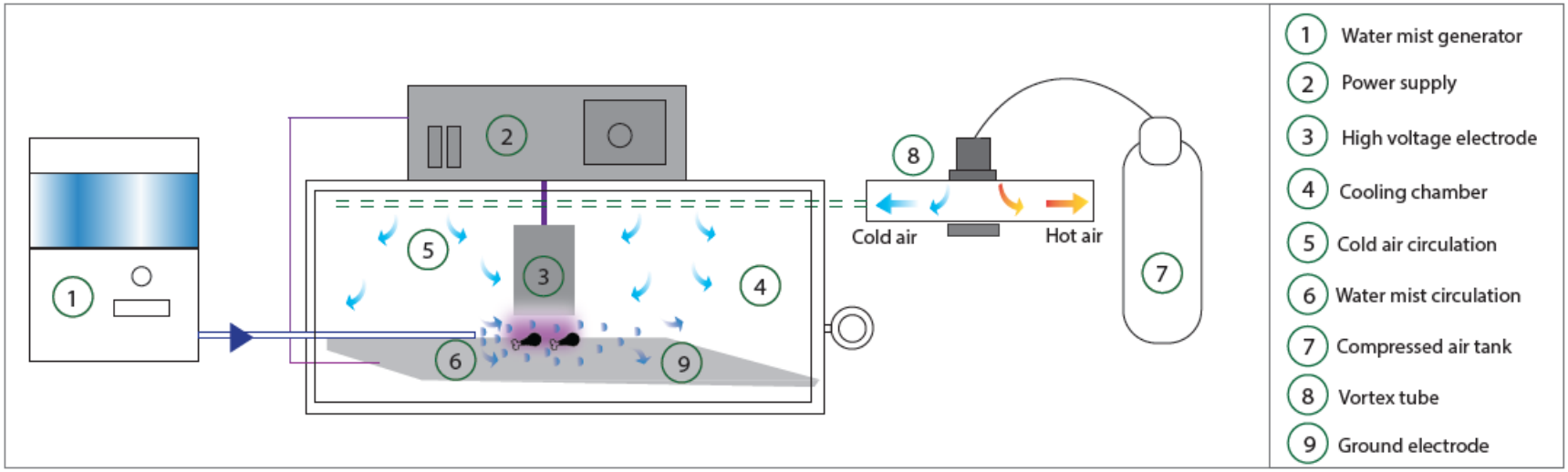

Figure 7.1: Schematic diagram featuring the main components of the plasma integrated simultaneous cooling and misting system for decontamination of poultry meat.

The cold air (-22 °C) from the vortex tube was supplied for 12 min to pre-cool the chamber from room temperature to 4 °C. After pre-cooling, the poultry meat sample on the glass slide was carefully placed on the ground electrode. During this process, the cabinet chamber temperature increased to 8-10 °C. Before misting and ACP treatment, the chamber temperature was cooled down to 4 °C. For misting, 500 mL of LA solution with a final concentration of 50 mM was prepared in sterile deionized water and transferred into the misting chamber. The organic acid mist was activated by ACP by simultaneous generation of ACP and organic acid misting (ACP activated mist) inside the chamber for 2 min to inactivate *S.* Typhimurium on the poultry meat surface. During the continuous misting and ACP treatment, the chamber temperature was increased to 8 °C. For the control sample, sterile deionized water misting was used. The poultry meat sample preparation, inoculation, and microbial enumeration were carried out, following the procedure described in the previous sections 7.2.9.

7.2.11 Statistical Analysis

All the experiments were independently performed in triplicate unless specified. The data was statistically analyzed using proc ANOVA procedure of SAS® University edition software (SAS institute inc., Cary, NC, USA, 2018). The pairwise difference was evaluated using Tukey' s honest test to identify significant difference between each samples group ($P < 0.05$)

7.3 Results

7.3.1 Inactivation of *S.* Typhimurium on membrane filter surface

Reductions in *S.* Typhimurium cell counts on polycarbonate membrane filter surface by separate ACP and LA/GA treatments are presented in (Figure 7.2A & B). The results indicated a significant decrease in *S.* Typhimurium cell counts compared to untreated control for all the tested ACP treatment times (Figure 7.2A). For instance, after 30 and 60 s ACP treatments, *S.* Typhimurium cell counts were reduced by 1.3 ± 0.5 and 4.6 ± 0.3 log CFU/cm^2, respectively, compared to untreated control (Figure 7.2A). For tested acid concentrations, no significant difference in cell counts of *S.* Typhimurium was observed among the samples exposed to 5 mM LA/GA and control samples treated with sterile deionized water (Figure 7.2B). Irrespective of acid treatments (LA/GA), a significant decrease in *S.* Typhimurium cell counts was observed only after the samples were exposed to acids with concentrations equal to or more than 10 mM (Figure 7.2B). However, the highest observed reduction in cell counts of *S.* Typhimurium was even less than 0.8 log CFU/cm^2 (Figure 7.2B) for the sample treated with 15 mM LA. No significant difference in the antibacterial activity between LA and GA was observed (Figure 7.2B). Based on this finding, a mild treatment condition of 30 s ACP treatment and 10 mM concentration of LA and GA was selected for the next set of experiments to evaluate the synergistic antimicrobial effect of the combined treatment.

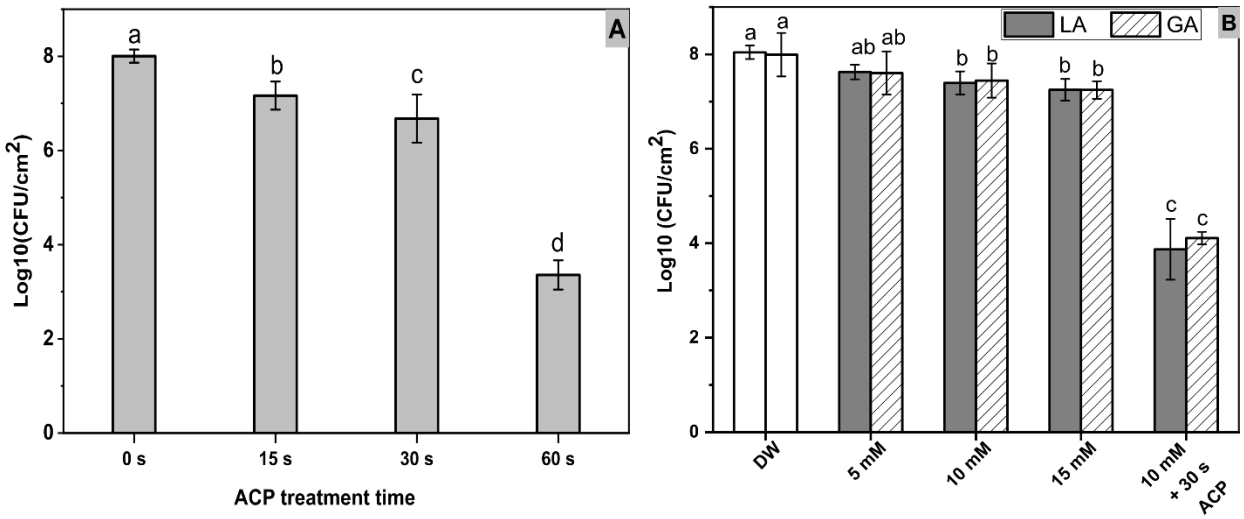

Figure 7.2: Mean log cell counts of *S.* Typhimurium treated with acids and ACP alone or sequentially treated with 10 mM acids followed by 30 s ACP. Individual effect of (A) atmospheric cold plasma treatment (ACP) time and (B) selected concentrations of lactic acid (LA) and gallic acid (GA) treatments alone and sequential combination of 10 mM LA or GA + 30 s ACP on the inactivation of S. Typhimurium inoculated on filter paper. DW stands for sterile deionized water. Data are means ± standard deviations (n = 3). Results with different lower-case letters are significantly different.

The inactivation results of *S.* Typhimurium treated with LA, GA, and ACP are presented in (Figure 7.2B). The samples treated with 10 mM LA followed by 30 s ACP showed a 3.9 ± 0.4 log CFU/cm^2 reduction compared to 1.2 ± 0.1 log CFU/cm^2 reduction in samples treated with 30 s ACP alone. Similarly, 10 mM GA treatment followed by 30 s ACP treatment increased the inactivation of *S.* Typhimurium by more than 2 log compared to samples subjected to ACP treatment alone (Figure7.2B). In the absence of ACP treatment, cells subjected to LA and GA showed no significant reduction in *S.* Typhimurium cell counts (< 0.5 log CFU/cm^2). Therefore, the results indicated that the sequential combination of these two treatments resulted in synergistic inactivation of *S.* Typhimurium.

7.3.2 Inactivation of *S.* Typhimurium on the poultry meat surface

The poultry meat samples which showed the absence of background microorganisms' growth on TSA plate were selected for the experiments. Poultry meat surfaces were inoculated with an average cell counts 8 log CFU/cm^2 of *S.* Typhimurium. A relatively higher concentration (50 mM) of LA and GA in combination with 30 s ACP was required to obtain 2.5 log CFU/cm^2 reduction in *S.* Typhimurium on poultry meat surfaces, compared to the reduction of *S.* Typhimurium on filter paper. The reductions in *S.* Typhimurium on poultry meat surfaces treated with 30 s and 2 min ACP in the presence of sterile deionized water (DW) (without LA/GA) were 0.3 ± 0.1 and 0.8 ± 0.1 log CFU/cm^2, respectively. The treatments using organic acids (LA or GA) with concentrations of 10 mM and 50 mM without ACP treatment only resulted in < 0.20 and < 0.8 log CFU/cm^2 reductions in cell counts respectively, regardless of the type of acid used. Regardless of the type of acid and the concentration used, with the increase in ACP treatment time from 30 s to 120 s further increased the reduction of *S.* Typhimurium cells (Figure 7.3A-B). Irrespective of the acid used (LA or GA), a significantly higher synergistic effect between ACP treatment and acid was observed in the presence of 50 mM acid compared to 10 mM acid concentration (Figure 7.3A-B). For instance, after 120 s of ACP treatment in the presence of 10 mM and 50 mM LA, the cell counts of *S.* Typhimurium were reduced by 1.2 and 3.1 log CFU/cm^2, respectively (Figure 7.3A). Regardless of treatment time, ACP with LA was more effective to reduce the *S.* Typhimurium cell counts on poultry meat surface compared to that of ACP with GA. These results suggest the synergistic antimicrobial activity of LA/GA and ACP in reducing cell counts of *S.* Typhimurium on poultry meat surfaces.

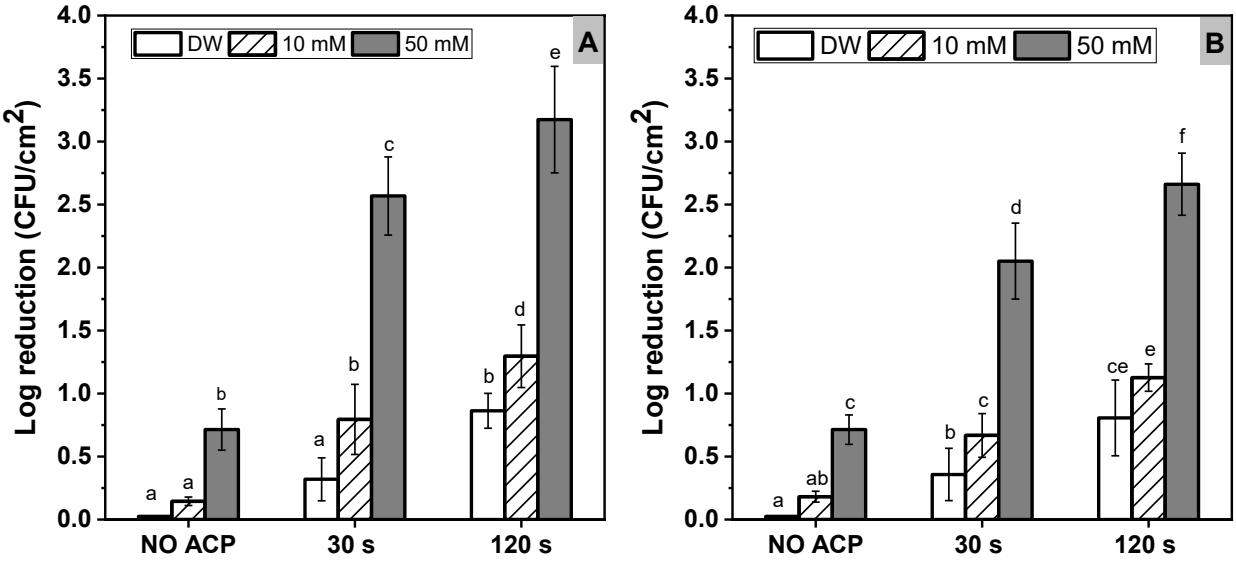

Figure 7.3: Inactivation of *S.* Typhimurium cells on raw poultry meat surface, treated with either (A) 10 mM and 50 mM of lactic acid (LA) or (B) 10 mM and 50 mM of gallic acid (GA) and exposed to atmospheric cold plasma (ACP) discharge alone for 30 s and 2 min or in sequential combination with these organic acids. Data are means ± standard deviations (n = 3). Results with different lower-case letters are significantly different in each figure ($P < 0.05$).

7.3.3 Simultaneous cooling and decontamination of poultry meat by ACP integrated cooling and misting

The observed reduction in cell counts of *Salmonella* on poultry meat surface after ACP treatment with lactic acid (LA) mist integrated with cooling to 4-8 ºC are presented in (Figure 7.4). The 50 mM LA mist treatment at 4-8 ºC for 2 min without ACP reduced the *S.* Typhimurium cell counts by 0.47 ± 0.39 log CFU/ cm^2. At the same time, simultaneous ACP, and deionized water mist treatment at 4-8 ºC for 2 min resulted in a reduction of 1.41 ± 0.39 log CFU/cm^2 in *S.* Typhimurium cell counts. However, the simultaneous LA mist and ACP treatment at 4-8 ºC for 2 min, the observed reduction in S. Typhimurium cell counts was significantly higher with reduction of 2.1

± 0.46 log CFU/cm^2. These results suggest the potential benefits of integrating ACP treatment with organic acid solution to decontaminate poultry meat surface. The sequence of treatment may influence the antimicrobial efficacy of the proposed integrated treatment. Recently, Adam et al. (2021) reported that the antimicrobial efficacy of a low-pressure plasma treatment system integrated with vacuum cooling showed a higher efficacy, when the product was first cooled and then subjected to ACP treatment. In another study, Chaplot et al. (2019) demonstrated that the ACP treatment followed by peracetic acid treatment was significantly more effective in reducing S. Typhimurium cell counts on poultry meat surface compared to peracetic acid treatment followed ACP treatment. Only preliminary experiments were completed, and the results obtained were able to prove the concept. The effect of product and process parameters such as treatment time, type and concentration of organic acid, temperature, process sequence, type of microorganism, and type and dimensions of product matrix on microbial inactivation and cooling efficacy of this integrated process need to be evaluated. More research in the future is required to optimize this integrated process for simultaneous cooling and decontamination of fresh meat products.

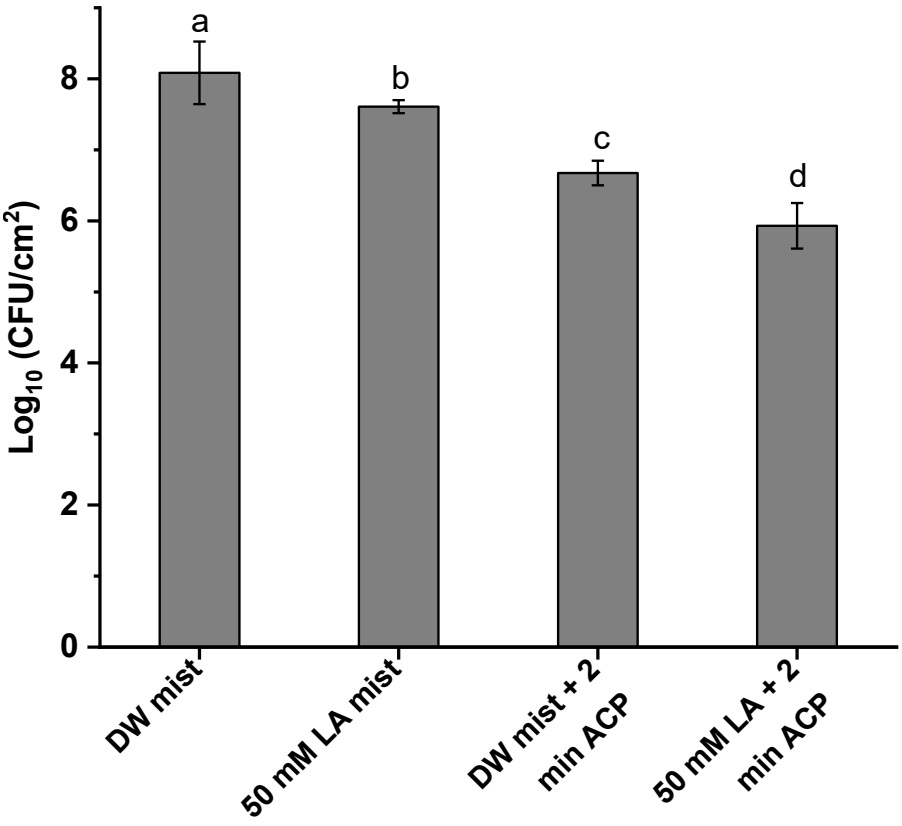

Figure 7.4: Inactivation effects of ACP integrated organic acid misting and cooling against *S.* Typhimurium on poultry meat surface at 4 to 8 °C. DW mist for 2 min; 50 mM LA mist for 2 min; ACP + (DW or 50 LA) mist for 2 min at 4 to 8 °C. Data are means ± standard deviations (n = 3). Results with different lower-case letters are significantly different ($P < 0.05$). DW: sterilized deionized water

7.3.4 Inactivation mechanisms of ACP on *S.* Typhimurium on a membrane filter

7.3.4.1 Cell membrane damage

The increase in permeation of propidium iodide (PI) dye into *S.* Typhimurium cells was determined to evaluate the changes in cell membrane permeability after LA, GA, ACP, and sequential LA/GA + ACP treatments (Figure 7.5A). The permeation of PI in untreated control and various treatment groups was normalized with respect to observed fluorescence signal for 70 % isopropanol treated cells, which represents the maximum PI permeation (100 %).

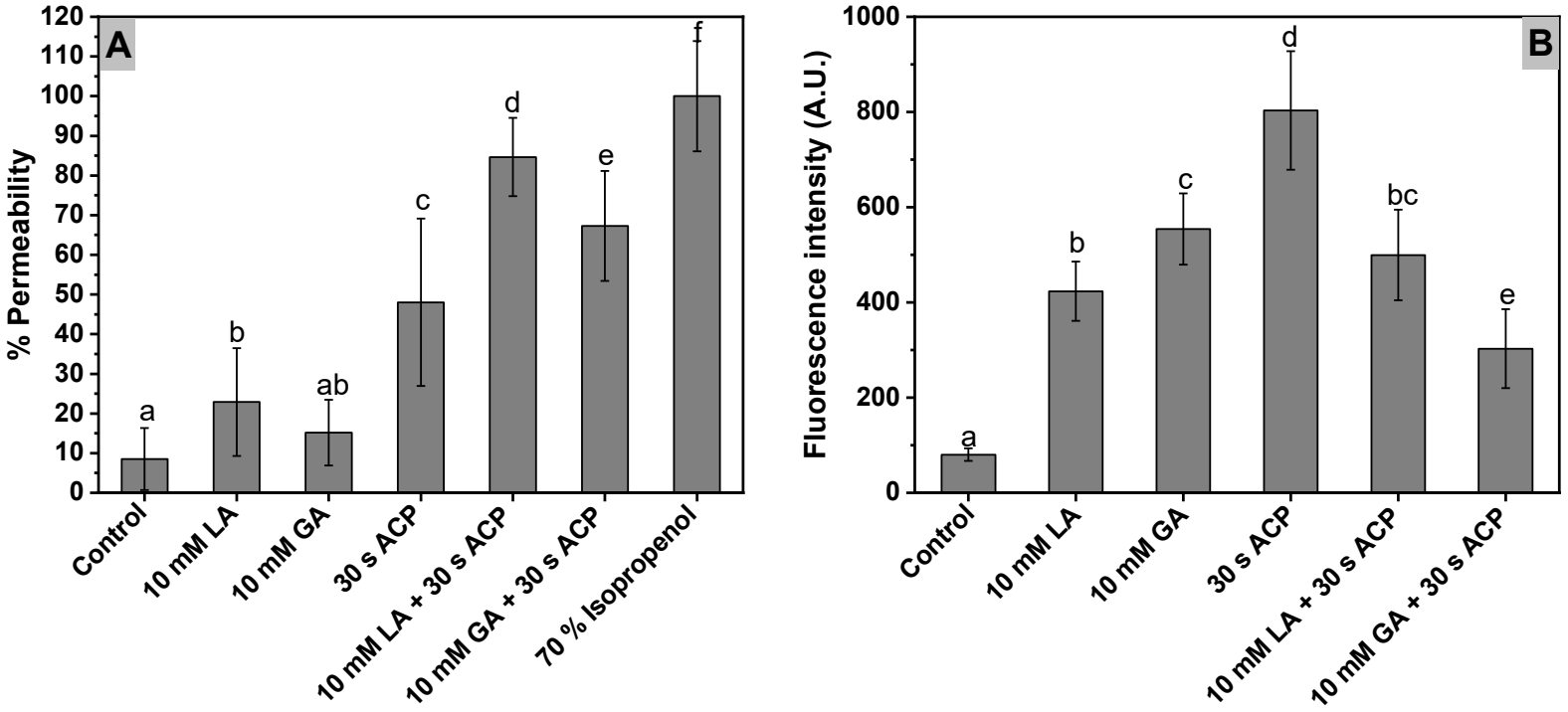

Figure 7.5: Measurement of (A) permeation of propidium iodide (PI) and (B) intracellular ROS density in *S.* Typhimurium cells treated with 30 s atmospheric cold plasma (ACP), 10 mM lactic acid (LA), 10 mM gallic acid (GA) alone, and in sequential combination of 10 mM LA or GA + 30 s ACP. To evaluate the relative increase in cell permeability at different treatment conditions, the results were normalized with respect to 70 % isopropanol treated cells, representing 100 % permeation of the PI dye. Data are means ± standard deviations (n = 3). Results with different lower-case letters are significantly different ($P < 0.05$).

The results showed a low level of PI permeation (9 %) in untreated control samples. LA and GA treatments without ACP increased PI permeation to approximately 22 % and 15 %, respectively. ACP treatment of control samples significantly ($P < 0.05$) increased the permeability of cells to PI (48 %). For the sequential treatment with 30 s ACP, further changes in the cell permeability were dependent on the type of organic acids (LA or GA). The sequential treatment using LA followed by ACP significantly increased the cell permeability to more than 80 %. Whereas, when GA was used with ACP, the cell permeability to PI increased significantly to more than 65 %. Thus, a synergistic interaction of organic acids in combination with ACP treatment increased the extent of *S.* Typhimurium cell membrane damage.

7.3.4.2 Intracellular oxidative stress

Changes in the intracellular ROS level of *S.* Typhimurium cells after treatments were characterized using fluorescence signals, which were correlated with ROS density levels (Figure 7.5B). Untreated *S.* Typhimurium cells, which were not exposed to either GA/LA or ACP had the lowest level of ROS compared to treated cells. Once cells were treated with either 10 mM GA or LA, a significant increase in the intracellular ROS level was observed (Figure 7.5B). Among the organic acids, GA treated *S.* Typhimurium cells showed a significantly higher ROS level compared to LA treated cells. When *S.* Typhimurium cells were treated with ACP for 30 s without acids, the intracellular ROS level of cells was the highest. However, for the *S.* Typhimurium cells treated with the sequential combination of LA and ACP, the observed ROS level was reduced approximately by 1.6 times compared to the cells treated with ACP alone. The ROS level in *S.* Typhimurium cells treated by a sequential combination of LA and ACP was comparable to that in the cells treated by LA or GA alone. While in the case of cells treated by the sequential combination of GA and ACP, the ROS level was reduced by 2.6 times, compared to those treated by ACP alone.

7.3.4.3 Membrane lipid peroxidation

Oxidative stress caused by intracellular ROS was assessed by measuring changes in concentrations of MDA as a biomarker for cell membrane lipid peroxidation. When samples were treated with 10 mM LA or GA acid alone, no significant increase in the membrane lipid peroxidation was observed (Figure 7.6A). After 30 s ACP treatment, a significant increase with more than 2 times in the lipid peroxidation was observed compared to that of untreated control. Regardless of the type of acid, the combination treatment of 10 mM LA or GA with 30 s ACP caused a significantly higher level of lipid peroxidation in *S.* Typhimurium cells compared to individual treatments. Among acids, GA in sequential combination with ACP showed a slightly higher level of lipid peroxidation compared to LA+ACP treatment, but results were not statistically different (Figure 7.6A). For instance, for *S.* Typhimurium cells treated with ACP in the presence of LA or GA, the observed lipid peroxidation level was increased approximately 1.5 and 1.8 times compared with that of ACP alone (Figure 7.6A), respectively.

7.3.4.4 Metabolic activity

Metabolic activity was evaluated using the C-12 resazurin assay, a fluorescent dye that can be reduced by viable cells to red fluorescent resorufin. Cell metabolism was determined after individual and sequential treatments, and the results were normalized with respect to untreated control. No significant reduction (< 10 %) in metabolic activity was observed after 10 mM LA or GA treatment alone compared to untreated control (Figure 7.6B).

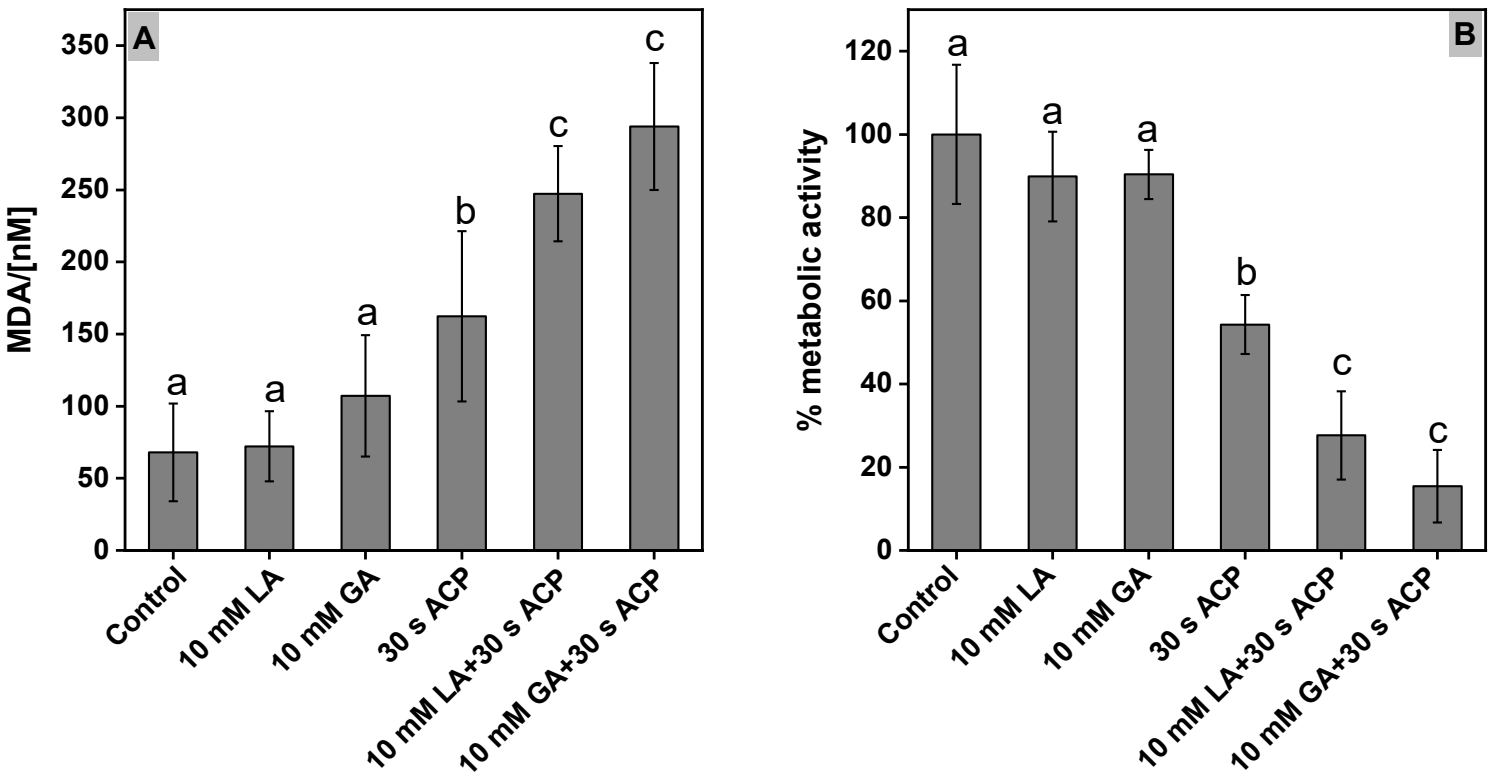

Figure 7.6 Measurement of (A) membrane lipid peroxidation and (B) metabolic activity of *S.* Typhimurium cells treated with 30 s atmospheric cold plasma (ACP), 10 mM lactic acid (LA), 10 mM gallic acid (GA) alone, and in sequential combination of 10 mM LA or GA + 30 s ACP. Data are means ± standard deviations (n = 6 for these sets of experiments). Results with different lower-case letters are significantly different ($P < 0.05$).

While after 30 s ACP treatment, a significant reduction in the metabolic activity was observed with more than 40 % reduction compared to untreated control (Figure 7.6B). The metabolic activity of cells was further reduced by 73 % and 85 % after the sequential combination of 10 mM LA + 30 s ACP and 10 mM GA + 30 s ACP treatments compared to control, respectively. These results indicated a synergistic effect of combined treatment on the reduction of *S.* Typhimurium metabolic activity.

7.4 Discussion

Although the decontamination efficacy of ACP treatment is well reported, ACP mediated biological effects in bacterial cells are not yet fully understood (López et al., 2019). The exposure to lethal levels of ACP causes several key changes in bacterial cells (Figure 7.7), such as membrane depolarisation and permeabilization, membrane lipid oxidation, oxidative damage of intracellular lipids, proteins, carbohydrates, DNA, and RNA (Liao et al., 2017). The observed reduction in *S.* Typhimurium population in this study did not correlate to the percentage of permeable cells, probably due to the presence of relatively higher proportion of slightly permeabilized cells, compared to completely permeabilized cells (Surowsky et al., 2014). Fröhling et al. (2012) demonstrated that the ACP treatment for 4 min caused 55 % permeabilization in *E. coli* cells on solid gel surface. In this study, the 30 s ACP treatment of *S.* Typhimurium cells on filter paper resulted in 40 % permeabilized cells (Figure 7.5A). This higher percentage of permeabilized cells in a short duration of ACP treatment may be due to the smoother filter paper surface and the presence of moisture in the form of fine droplets. The smoother surface and the presence of moisture in the products or in the ACP discharge produced greater damage to cells at both intracellular and extracellular levels (López et al., 2019).

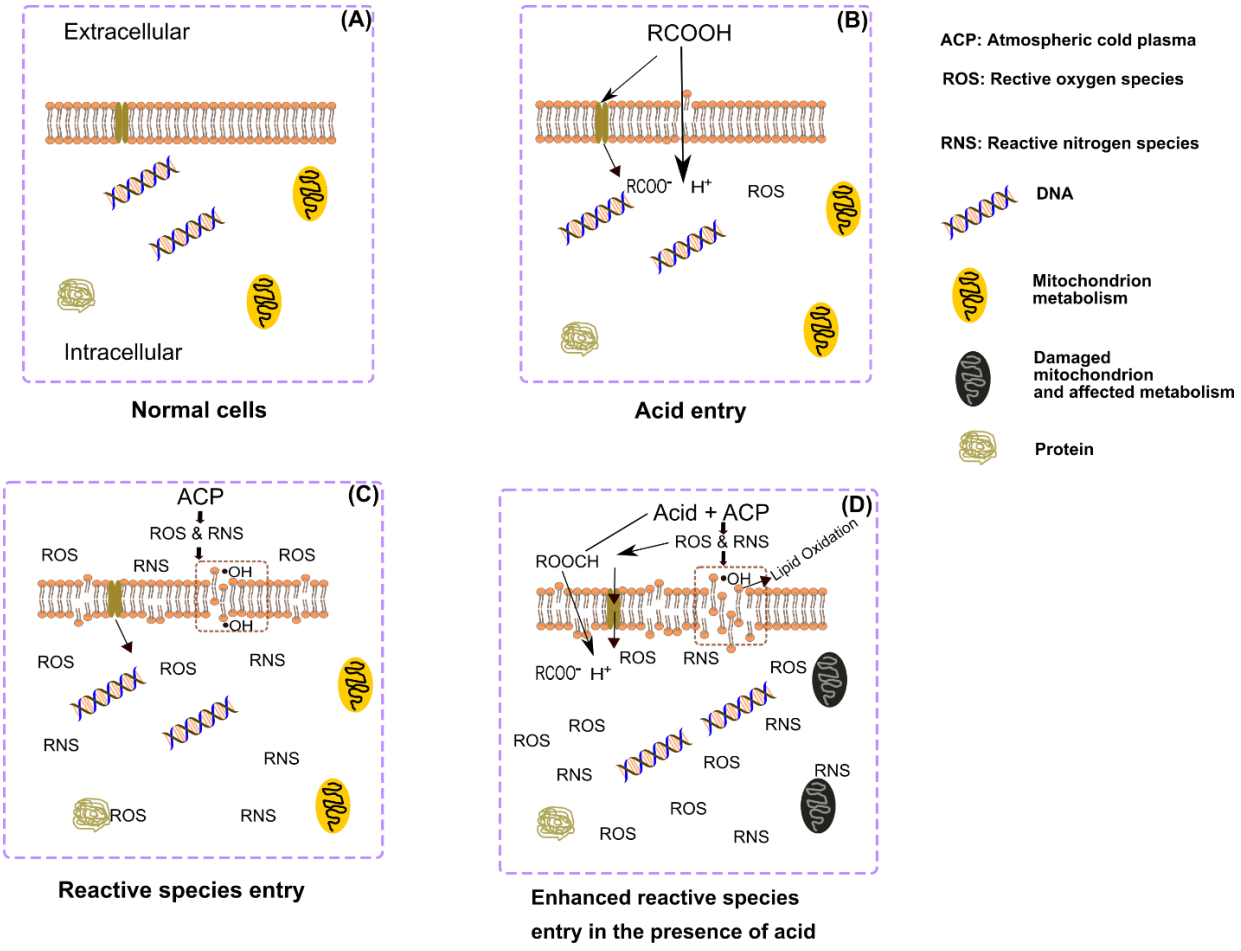

Figure 7.7: Schematic diagram of the enhanced *S.* Typhimurium cell damage by ACP treatment in the presence of acids. (A) Normal cells; (B) Slight membrane permeabilization by acid treatment; (C) Membrane permeabilization by ACP reactive species including ROS & RNS; (D) Sequential treatment of acid followed by ACP may enable higher diffusion of ACP generated reactive species including ROS & RNS across the previously damaged cells membrane due to organic acid exposure, that led to higher permeabilization and accumulation of intracellular ROS & RNS, enhanced membrane lipid oxidation, and compromised cell mitochondrial metabolism

The ACP discharge produces cocktails of reactive species, and the interaction of these reactive species cause oxidative stress to cell membrane at intracellular as well as extracellular levels (Liao, Liu & Xiang, 2017). The 6-carboxy-2',7'-dichlorodihydrofluorescin diacetate (H_2DCFDA) is a widely used biomarker to measure intracellular reactive oxygen species level and other peroxides (Gomes, Fernandes, & Lima, 2005). The intracellular ROS level was increased more than 8 folds

after 30 s ACP treatment compared to that of untreated control (Figure 7.5B). During ACP treatment, the generated and accumulated intracellular ROS could react with both outer membranes of lipopolysaccharide and inner thin layer of peptidoglycan of bacterial cell wall (Figure 7.7D), leading to molecular structure breakage by oxidation of C-O, C-N, and C-C bonds (Yusupov et al., 2013). The higher lipid peroxidation by-products (MDA) after 30 s ACP treatment (Figure 7.6A) indicate lipid oxidation of bacterial cell membrane (Figure 7.7D). The correlation between lipid oxidation and positive PI staining and compromised metabolic activity further supports the cell membrane damage during ACP treatment, as PI can penetrate only into bacteria with damaged cells wall (Figure 7.5 & Figure 7.6).

The individual treatment using 10 mM LA and GA did not exhibit a large reduction in *S.* Typhimurium with less than a 0.5 log CFU/cm^2 of cells reduction. The low level of antibacterial activity of the selected acids was likely due to the short exposure time, and low concentrations of GA and LA (10 mM). Similarly, previous studies reported the lack of antibacterial activity of LA (5 mM) and GA (15 mM), when exposed to *E. coli* for 30 min (Oliveira et al., 2017; Wang et al., 2017). They suggested that the bacteria exposed to lower concentrations of LA/GA require extended incubation time or exposure to higher concentrations in order to exhibit antimicrobial activity (Borges, Ferreira, Saavedra, & Simões, 2013; Cossu et al., 2016; Oliveira et al., 2017; Wang et al., 2017). The antimicrobial activity of lactic and gallic acid is attributed to their ability to cross the bacterial cell membrane by passive diffusion in their undissociated form (C. Wang, Chang, Yang, & Cui, 2015; Wang et al., 2017). Although LA and GA showed low levels of antibacterial activity, the selected concentration caused a significant increase in the intracellular ROS level (Figure 7.5B). The *S.* Typhimurium cells exposed to LA and GA (10 mM) showed 2.8 and 1.8 times higher permeation of PI dye respectively, compared to control cells. Previous studies

reported that 10 mM LA and GA caused cellular damage, increase in intracellular ROS, and cell permeabilization (Oliveira et al., 2017; Mani-López et al., 2012; Wang, Chang, Yang, & Cui, 2015; Wang et al., 2017). A recent study showed that the incubation of *S.* Enteritidis for 30 min with plasma activated LA (0.2 %) resulted in an additional 3 log reduction in *S.* Typhimurium population compared to plasma activated water (Qian et al., 2020). The exposure of *S. aureus* suspension to plasma activated hydrogen peroxide (100 mM H_2O_2, 5 min plasma jet treatment of H_2O_2 solution) increased the cell reduction by more than 2 log (Wu et al., 2017). However, it is worthwhile to highlight that the LA (0.2 %) and H_2O_2 (100 mM) concentrations, and ACP treatment time (between 1.5 to 5 min) used in these previous studies are comparatively higher than those in the present study. The temperature of the sample treated by the same ACP system was less than 27 °C after 6 min treatment as reported previously by Chaplot et al. (2019), hence the impact of temperature on *S.* Typhimurium inactivation can be neglected. The observed higher synergistic antibacterial effects within the short duration of ACP treatment in this study was likely due to the application of acid solutions in the form of fine droplets by spraying. The method of plasma activated liquid production and liquid volume can significantly affect the chemical composition of the plasma activated liquid (Zhou et al., 2020; Rathore & Nema, 2021). In this study, more than 3.5 log CFU/cm^2 reduction in *S.* Typhimurium was achieved by the application of sublethal concentration (10 mM) of LA/GA after a relatively short duration of ACP exposure for 30 s.

The antibacterial mechanisms of a combination treatment using organic acids with ACP is still not well understood. In this study, a synergistically increased cell membrane permeability of *S.* Typhimurium cells was observed after exposure to LA/GA in sequential combination with ACP, compared to individual treatments using LA, GA, or ACP. The acid treatment alone increased the

cell permeability (10-15 %), and the subsequent exposure of these permeabilized cells to ACP discharge probably increased the accessibility of plasma reactive species to cellular membrane. This is likely due to the easy diffusion and transport of plasma reactive species including but not limited to ROS, RNS, OH, peroxynitrites, and H_2O_2 through the membranes of cells permeabilized by organic acid treatment before ACP exposure. The interaction of these reactive species with the cell membrane can increase the cell permeability due to the oxidation of lipid bilayer (Herianto, Hou, Lin, & Chen, 2021). In addition, ACP generated reactive species are known to increase intracellular oxidative stress, disruption of enzyme activity, and cause DNA and protein fragmentation, finally leading to leakage of intracellular cell contents and cell death (Fröhling, Baier, et al., 2012; Herianto et al., 2021; López et al., 2019; Qian et al., 2020; Wu et al., 2017). In this study, the intracellular ROS level of cells decreased significantly after combined LA/GA and ACP treatments. Recently, Qian et al. (2020) reported that the intracellular ROS level of *S.* Enteritids treated with plasma activated LA solution (0.05 %) reached the highest, then decreased with increasing LA concentrations (0.10 – 0.20 %). Although the concentration of intracellular ROS decreased significantly after combined LA/GA and ACP treatments, a significant increase in cell membrane lipid oxidation by-products (MDA) was observed. This increase in MDA concentration indicated that the lipid bilayer was oxidised, and eventually, compromised the cell structure and integrity.

The experimental evidence in this study indicated that the sequential combination of organic acids (i.e., LA or GA) and ACP treatment synergistically reduced the *S.* Typhimurium cell metabolic activity. A significant decrease in cell metabolic activity during the combined treatment compared to the individual treatments suggests that the combined treatment may have compromised several key mitochondrial enzyme activities including NADH oxidase, which is directly correlated with

the resazurin metabolism and cell metabolic activity (E. F. De Oliveira et al., 2017). Previous studies reported that the cold plasma treatment reduced the activity of key metabolic enzyme, esterase, and increased the membrane permeability of *E. coli* and *S. aureus* cells on abiotic surfaces (Carré et al., 2018; Fröhling et al., 2012). However, the effect of plasma treatment is influenced by operating gas, power, and treatment time (Carré et al., 2018; Fröhling et al., 2012). In this study, bacterial cells exposed to organic acids could experience sublethal acid stress and partially damaged membrane (Oliveira et al., 2017; Wang et al., 2017), making them hypersensitive to the subsequent ACP treatment. The interaction of ACP generated reactive species with *S.* Typhimuirium cells resulted in reduced metabolic activity. To further understand the other underlaying mechanisms resulting in the synergistic antibacterial activity of ACP in the presence of organic acids, more detailed molecular analysis using advanced approaches, such as proteomics, genomics, and metabolomic analyses are required.

7.5 Conclusions

This study demonstrated that the sequential combination of organic acids (lactic acid or gallic acid) with atmospheric cold plasma (ACP) treatment led to enhanced and rapid inactivation of *S.* Typhimurium. Sublethal concentrations of LA/GA (10 mM) with a short duration (30 s) of ACP treatment synergistically reduced *S.* Typhimurium. The major mechanisms associated with the increased *S.* Typhimurium inactivation during a sequential combination of organic acids and ACP treatments were investigated. The findings of this study revealed that the combination of LA or GA with ACP treatment synergistically enhanced the membrane permeabilization and membrane lipid oxidation. In addition, the sequential treatment of LA or GA with ACP significantly reduced the cell metabolic activity and affected the intracellular reactive oxygen species level of *S.* Typhimurium. The significantly greater inactivation of *S.* Typhimurium on poultry meat surface

by the sequential combination of organic acids and ACP treatments compared to individual treatments demonstrates the potential application of this method to improve microbial food safety. In addition, the simultaneous cooling, misting, and ACP treatment process showed promising results and significantly reduced the *S.* Typhimurium cell counts on poultry meat. The proposed strategies effectively control the *S.* Typhimurium on the poultry meat surfaces. However, the antibacterial efficacy of these strategies could be influenced by the type of bacterial strain, cell attachment time on sample surfaces, physiological state of bacterial cells, and internalization of bacteria in poultry meat. In addition, the changes in important poultry meat quality attributes including, color, texture, and lipid oxidation, need to be evaluated in the future. Further, more studies are required to address the influence of microbial, product, and processing factors, including the optimum concentration of organic acids, ACP exposure time, and other underlying mechanisms of bacterial inactivation, in order to develop this method for different food product surface decontamination.

Chapter 8: General Conclusions and Future Recommendations

8.1 General conclusions

This research focused on the application of atmospheric cold plasma (ACP) based integrated processes to enhance meat-based food product safety by inactivating the pathogens associated with them. The research reported in this thesis focused on the antimicrobial efficacy of open and in-package ACP treatments to inactivate bacterial pathogens, associated with RTE ham, freeze-dried pet foods, and fresh poultry meat. The additives/ingredients presented in processed meat did not significantly influence the bacterial inactivation efficacy of ACP. The ACP treatment can inactivate *L. monocytogens* to below the limit of detection on ham surfaces. The sequential integrated treatment of organic acid (lactic acid or gallic acid) with ACP confirmed the enhancement of *S.* Typhimurium inactivation efficacy in poultry meat, compared to individual treatments. This research also focused on the probable *S.* Typhimurium inactivation mechanisms during the sequential integrated treatment of organic acids followed by ACP and the *L. monocytogens* inactivation mechanisms during post-ACP treatment storage.

In chapter 3, to evaluate the interaction effects of ACP treatment with ham ingredients on bacterial inactivation, the ham was formulated with NaCl (1 % & 3 %) and with or without rosemary extract. Irrespective of the % NaCl and the rosemary extract content of ham, ACP treatment showed promising antibacterial effects in a short exposure time against *L. innocua* on the ham surface. The % NaCl content and the presence of rosemary extract on the ham surface did not influence the antimicrobial efficacy of ACP treatment. Significant increases in lipid oxidation, product weight loss, and color changes were the major limitations of open atmospheric cold plasma treatment.

Although, the open ACP treatment effectively reduced the *L. innocua* counts on the ham surface, the observed reductions were limited to less than 2 log. In Chapter 4, ACP treatment was integrated

with modified atmosphere packaging to achieve a higher antimicrobial efficacy, and the ham was formulated with preservatives and bacteriocins. The in-package gas composition had significant influence on antimicrobial efficacy of ACP. A significantly higher reduction in *L. monocytogenes* counts was observed, when the in-package gas mixture contained oxygen. The presence of preservatives or bacteriocin in ham did not enhance the inactivation of *L. monocytogenes* during ACP treatment. This study suggested that post-ACP treatment storage time was an important parameter to achieve a higher inactivation efficacy.

Since a significantly higher reduction in bacterial cell counts was observed after post-ACP treatment storage, the possible bacterial inactivation mechanisms during post-ACP treatment storage were explored in Chapter 5. The study revealed that the *L. monocytogenes* cells were under high oxidative stress conditions with permeabilized membranes, during post-ACP treatment storage. In the first 24 h of storage, a significant percentage of the cell population lost their membrane integrity, but the cells were metabolically active. After 7 days of post-ACP treatment storage, a high percentage of cells lost their esterase activity and membrane integrity. During long-term post-treatment storage, cell membrane permeabilization was one of the major causes of the loss of culturability. A significant fraction of permeabilized cells lost their ability to grow on a nutrient agar plate.

Chapter 6 of this research evaluated the potential applicability of in-package ACP treatment to inactivate *Salmonella* in low a_w pet foods. The antimicrobial efficacy of ACP treatment against *S.* Typhimurium in low a_w freeze-dried pet foods was affected by bacterial growth condition, microbial load, treatment time, post-ACP treatment storage time, and a_w, with some key interactive effects between these parameters. *S.* Typhimurium equilibrated to 0.13 a_w pet food exhibited the

greatest resistance to ACP treatment. Extended post-ACP treatment storage reduced the *S.* Typhimurium cell counts to below the detection limit in 0.54 a_w pet foods.

Chapter 7 focused on developing a sequential integrated treatment of organic acids and ACP to reduce *S.* Typhimurium in fresh poultry meat. The sequential treatment of organic acids (lactic acid or gallic acid) followed by ACP led to significantly enhanced and rapid inactivation of *S.* Typhimurium. The probable mechanisms associated with the inactivation of *S.* Typhimurium could be due to the synergistically enhanced membrane permeabilization and membrane lipid oxidation. In addition, the sequential integrated treatment of LA or GA with ACP significantly reduced the cell metabolic activity and affected the intracellular reactive oxygen species level of *S.* Typhimurium. The significantly greater inactivation of *S.* Typhimurium on poultry meat surface by the sequential combination of organic acids and ACP treatments compared to individual treatments demonstrates the potential application of this method to improve the microbial safety of fresh poultry meat. An ACP integrated organic acid misting and cooling process was designed and tested for its simultaneous cooling and decontamination efficacies on fresh poultry meat. The results showed that this integrated treatment significantly increased the inactivation of *Salmonella* on poultry meat surface, while achieving rapid cooling.

Overall, several plasma processing and meat product parameters have been investigated to optimize the decontamination effects of ACP treatments, by considering the effects of plasma treatment time, in-package gas mixtures, post-plasma treatment storage, RTE meat ingredients, and integrated treatment with organic acids. The in-package ACP treatment showed significant effectiveness in reducing pathogens in low and high a_w foods, possibly due to the confinement of reactive species inside the package. However, due to the same reason, significant oxidation of fats in meat occurred, limiting the use of this technology for fat-rich food products. This indicates the

need for future optimization of in-package ACP treatment for industrial processing of meat products. The study on synergistic antimicrobial efficacy of integrated treatments using selected organic acids and ACP indicates the potential of an industrial treatment development using organic acid and ACP mist/spray in a single system for surface sanitation. The results of this thesis laid the foundation for the development of ACP processes for meat product decontamination.

8.2 Recommendations

This thesis research demonstrated the antibacterial efficacy of open and in-package ACP treatment against pathogens associated with meat products. These investigations will provide insight to develop the ACP-based processes in the food industry and provide a basic understanding on the possible integration of this technology with other decontamination techniques, which are used in the food industry. In addition, the following aspects of the ACP treatments can be further explored:

- Significant drying, lipid oxidation, and color changes of meat products during open ACP treatment were observed. Future research can focus on tailoring plasma process parameters to optimize treatment conditions and preserve the quality of meat products.
- Selection of specific gas composition inside the package is crucial for achieving the required level of microbial inactivation. Future research may examine the different combinations of gas ratios to enhance bacterial inactivation and reduce treatment time.
- Post-ACP treatment storage time emerged as a critical parameter to enhance bacterial inactivation. Future studies can consider the meat products supply chain environmental conditions and product shelf-life effects to evaluate ACP antimicrobial efficacy.
- Although this research elucidated the major underlying mechanisms of bacterial inactivation during post-ACP treatment storage, a more detailed understanding on the

bacterial inactivation mechanisms during storage could help in reducing ACP exposure time.

- This research showed the potential of ACP treatment to inactivate bacteria in low a_w meat-based pet food products. More detailed research on the antibacterial efficacy of ACP treatment and their modes of action against pathogens at low a_w conditions can be explored.
- This research finding demonstrated the significant advantage of in-package ACP treatment to reduce bacterial cell counts in low a_w and high a_w meat products. However, the changes in the packaging material properties and any residual toxic effects on food products need to be investigated in the future studies.
- The proposed strategies based on ACP integrated treatments with organic acids effectively reduced the *S.* Typhimurium on the poultry meat surface. However, the antibacterial efficacy of these strategies could be influenced by the type of organic acids and their application (washing/dipping vs. spraying), treatment time, process sequence, type and dimensions of product matrix, bacterial strain, cell attachment time on sample surfaces, physiological state of bacterial cells, and internalization of bacteria in poultry meat. Therefore, future research should explore the influences of these parameters on overall antimicrobial efficacy. More research in the future is required to optimize this integrated process for simultaneous cooling and decontamination of fresh meat products.
- In addition, the ACP treatment effects on important poultry meat quality attributes including, color, texture, and lipid oxidation, need to be evaluated in the future.
- More studies are required to address the influence of microbial, product, and processing factors, including the optimum concentration of organic acids, ACP exposure time, and

other underlying mechanisms of bacterial inactivation, to develop this novel method for different food product surface decontamination applications.

Bibliography

Ahn, J., Lee, H. Y., Knipe, L., & Balasubramaniam, V. M. (2014). Effect of a post-packaging pasteurization process on inactivation of a *Listeria innocua* surrogate in meat products. *Food Science and Biotechnology*, *23*(5), 1477–1481. https://doi.org/10.1007/s10068-014-0202-5

Al-Abduly, A., & Christensen, P. (2015). An in situ and downstream study of non-thermal plasma chemistry in an air fed dielectric barrier discharge (DBD). *Plasma Sources Science and Technology*, *24*(6). https://doi.org/10.1088/0963-0252/24/6/065006

Albert, T., Braun, P. G., Saffaf, J., & Wiacek, C. (2021). Physical Methods for the Decontamination of Meat Surfaces. *Current Clinical Microbiology Reports*, *8*, 9–20. https://doi.org/10.1007/s40588-021-00156-w

Albertos, I., Martín-Diana, A. B., Cullen, P. J., Tiwari, B. K., Ojha, S. K., Bourke, P., … Rico, D. (2017). Effects of dielectric barrier discharge (DBD) generated plasma on microbial reduction and quality parameters of fresh mackerel (*Scomber scombrus*) fillets. *Innovative Food Science and Emerging Technologies*, *44*(April), 117–122. https://doi.org/10.1016/j.ifset.2017.07.006

Amaral, A. B., Solva, M. V. Da, & Lannes, S. C. D. S. (2018). Lipid oxidation in meat: Mechanisms and protective factors - a review. *Food Science and Technology*, *38*, 1–15. https://doi.org/10.1590/fst.32518

Arjunan, K. P., Sharma, V. K., & Ptasinska, S. (2015). Effects of atmospheric pressure plasmas on isolated and cellular DNA—a review. *International Journal of Molecular Sciences*, *16*(2), 2971–3016. https://doi.org/10.3390/ijms16022971

Attri, P., Kim, Y. H., Park, D. H., Park, J. H., Hong, Y. J., Uhm, H. S., … Choi, E. H. (2015). Generation mechanism of hydroxyl radical species and its lifetime prediction during the plasma-initiated ultraviolet (UV) photolysis. *Scientific Reports*, *5*, 1–8. https://doi.org/10.1038/srep09332

Balay, D. R., Gänzle, M. G., & McMullen, L. M. (2018). The effect of carbohydrates and bacteriocins on the growth kinetics and resistance of *Listeria monocytogenes*. *Frontiers in Microbiology*, *9*(March), 1–12. https://doi.org/10.3389/fmicb.2018.00347

Barbosa-Cánovas, G. V., Medina-Meza, I., Candoğan, K., & Bermúdez-Aguirre, D. (2014). Advanced retorting, microwave assisted thermal sterilization (MATS), and pressure assisted thermal sterilization (PATS) to process meat products. *Meat Science*, *98*(3), 420–434. https://doi.org/10.1016/j.meatsci.2014.06.027

Bedinghaus, A. J., & Ockerman, H. W. (1995). Antioxidative Maillard Reaction-Products From Reducing Sugars and Free Amino-Acids in Cooked Ground Pork Patties. *Journal of Food Science*, *60*(5), 992–995. https://doi.org/10.1111/j.1365-2621.1995.tb06277.x

Behravesh, C. B., Ferraro, A., Deasy, M., Dato, V., Moll, M., Sandt, C., … Alexander, S. (2010). Human *Salmonella* infections linked to contaminated dry dog and cat food, 2006-2008. *Pediatrics*, *126*(3), 477–483. https://doi.org/10.1542/peds.2009-3273

Berdejo, D., Pagán, E., García-Gonzalo, D., & Pagán, R. (2019). Exploiting the synergism among physical and chemical processes for improving food safety. *Current Opinion in Food Science*, *30*(December), 14–20. https://doi.org/10.1016/j.cofs.2018.08.004

Beresford, M. R., Andrew, P. W., & Shama, G. (2001). *Listeria monocytogenes* adhers to many

materials found in food-processing environments. *Journal of Applied Microbiology*, *90*(6), 1000–1005. https://doi.org/10.1046/j.1365-2672.2001.01330.x

Beuchat, L., Komitopoulou, E., Betts, R., Beckers, H., Bourdichon, F., Joosten, H., … Kuile, B. (2011). *Survival of Pathogens in Dry Foods and Dry Food Processing Environments*.

Boler, D. D., & Woerner, D. R. (2017). What is meat? A perspective from the American Meat Science Association. *Animal Frontiers*, *7*(4), 8–11. https://doi.org/10.2527/af.2017.0436

Borges, A., Ferreira, C., Saavedra, M. J., & Simões, M. (2013). Antibacterial activity and mode of action of ferulic and gallic acids against pathogenic bacteria. *Microbial Drug Resistance*, *19*(4), 256–265. https://doi.org/10.1089/mdr.2012.0244

Bourke, P., Ziuzina, D., Han, L., Cullen, P. J., & Gilmore, B. F. (2017). Microbiological interactions with cold plasma. *Journal of Applied Microbiology*, *123*(2), 308–324. https://doi.org/10.1111/jam.13429

Bourke, Paula, Ziuzina, D., Boehm, D., Cullen, P. J., & Keener, K. (2018). The Potential of Cold Plasma for Safe and Sustainable Food Production. *Trends in Biotechnology*, *36*(6), 615–626. https://doi.org/10.1016/j.tibtech.2017.11.001

Boxhammer, V., Morfill, G. E., Jokipii, J. R., Shimizu, T., Klämpfl, T., Li, Y.-F., … Zimmermann, J. L. (2012). Bactericidal action of cold atmospheric plasma in solution. *New Journal of Physics*, *14*(11), 113042. https://doi.org/10.1088/1367-2630/14/11/113042

Brisset, J. L., & Hnatiuc, E. (2012). Peroxynitrite: A re-examination of the chemical properties of non-thermal discharges burning in air over aqueous solutions. *Plasma Chemistry and Plasma Processing*, *32*(4), 655–674. https://doi.org/10.1007/s11090-012-9384-x

Brunner, T. A., van der Horst, K., & Siegrist, M. (2010). Convenience food products. Drivers for consumption. *Appetite*, *55*(3), 498–506. https://doi.org/10.1016/j.appet.2010.08.017

Cap, M., Cingolani, C., Lires, C., Mozgovoj, M., Soteras, T., Sucari, A., … Leotta, G. (2020). Combination of organic acids and low-dose gamma irradiation as antimicrobial treatment to inactivate Shiga toxin-producing *Escherichia coli* inoculated in beef trimmings: Lack of benefits in relation to single treatments. *PLoS ONE*, *15*(3), 1–13. https://doi.org/10.1371/journal.pone.0230812

Carré, G., Charpentier, E., Audonnet, S., Terryn, C., Boudifa, M., Doliwa, C., … Gelle, M. P. (2018). Contribution of fluorescence techniques in determining the efficiency of the non-thermal plasma treatment. *Frontiers in Microbiology*, *9*(SEP), 1–12. https://doi.org/10.3389/fmicb.2018.02171

CDC. (2012). Notes from the field: Human *Salmonella* infantis infections linked to dry dog food--United States and Canada, 2012. *MMWR. Morbidity and Mortality Weekly Report*, *61*(23), 436. Retrieved from https://www.cdc.gov/mmwr/preview/mmwrhtml/mm6123a4.htm

CDC. (2014). Foodborne Diseases Active Surveillance Network FoodNet 2014 Surveillance Report.

CDC. (2021). Centre for Diseases Control and Prevention. Retrieved October 10, 2021, from https://www.cdc.gov/*Salmonella*/

Chang, M. B., & Wu, S. J. (1997). Experimental study on ozone synthesis via dielectric barrier discharges. *Ozone: Science and Engineering*, *19*(3), 241–254. https://doi.org/10.1080/01919519708547304

Chaplot, S., Yadav, B., Jeon, B., & Roopesh, M. S. (2019). Atmospheric cold plasma and peracetic acid-based hurdle intervention to reduce *Salmonella* on raw poultry meat. *Journal of Food Protection*, *82*(5), 878–888. https://doi.org/10.4315/0362-028X.JFP-18-377

Chizoba Ekezie, F. G., Sun, D. W., & Cheng, J. H. (2017). A review on recent advances in cold plasma technology for the food industry: Current applications and future trends. *Trends in Food Science and Technology*, *69*(November), 46–58. https://doi.org/10.1016/j.tifs.2017.08.007

Cho, Y., Muhlisin, M., Choi, J. H., Hahn, T. W., & Lee, S. K. (2014). Effect of gaseous ozone exposure on the bacteria counts and oxidative properties of ground hanwoo beef at refrigeration temperature. *Korean Journal for Food Science of Animal Resources*, *34*(4), 525–532. https://doi.org/10.5851/kosfa.2014.34.4.525

Choi, E. J., Yang, H. S., Park, H. W., & Chun, H. H. (2018). Inactivation of *Escherichia coli* O157:H7 and *Staphylococcus aureus* in red pepper powder using a combination of radio frequency thermal and indirect dielectric barrier discharge plasma non-thermal treatments. *Lwt*, *93*(March), 477–484. https://doi.org/10.1016/j.lwt.2018.03.081

Cossu, A., Ercan, D., Wang, Q., Peer, W. A., Nitin, N., & Tikekar, R. V. (2016). Antimicrobial effect of synergistic interaction between UV-A light and gallic acid against *Escherichia coli* O157:H7 in fresh produce wash water and biofilm. *Innovative Food Science and Emerging Technologies*, *37*, 44–52. https://doi.org/10.1016/j.ifset.2016.07.020

Csapó, J., Prokisch, J., Albert, C., & Sipos, P. (2019). Effect of UV light on food quality and safety. *Acta Universitatis Sapientiae, Alimentaria*, *12*(1), 21–41. https://doi.org/10.2478/ausal-2019-0002

Cui, H., Wu, J., Li, C., & Lin, L. (2017). Promoting anti-listeria activity of lemongrass oil on pork loin by cold nitrogen plasma assist. *Journal of Food Safety*, *37*(2). https://doi.org/10.1111/jfs.12316

Cullen, P. J., Misra, N. N., Han, L., Bourke, P., Keener, K., O'Donnell, C., … Milosavljević, V. (2014). Inducing a dielectric barrier discharge plasma within a package. *IEEE Transactions on Plasma Science*, *42*(10), 2368–2369. https://doi.org/10.1109/TPS.2014.2321568

Cuny, C., Lesbats, M., & Dukan, S. (2007). Induction of a global stress response during the first step of *Escherichia coli* plate growth. *Applied and Environmental Microbiology*, *73*(3), 885–889. https://doi.org/10.1128/AEM.01874-06

Currie, A., Farber, J. M., Nadon, C., Sharma, D., Whitfield, Y., Gaulin, C., … Sierpinska, U. (2015). Multi-Province Listeriosis Outbreak Linked to Contaminated Deli Meat Consumed Primarily in Institutional Settings, Canada, 2008. *Foodborne Pathogens and Disease*, *12*(8), 645–652. https://doi.org/10.1089/fpd.2015.1939

De Oliveira, E. F., Cossu, A., Tikekar, R. V., & Nitin, N. (2017). Enhanced antimicrobial activity based on a synergistic combination of sublethal levels of stresses induced by UV-A light and organic acids. *Applied and Environmental Microbiology*, *83*(11), 1–14. https://doi.org/10.1128/AEM.00383-17

Dezest, M., Bulteau, A.-L., Quinton, D., Chavatte, L., Le Béchec, M., Cambus, J. P., … Cousty, S. (2017). Oxidative modification and electrochemical inactivation of *Escherichia coli* upon cold atmospheric pressure plasma exposure. *PloS One*, *12*(3), 0173618.

Dinçer, A. H., & Baysal, T. (2004). Decontamination techniques of pathogen bacteria in meat

and poultry. *Critical Reviews in Microbiology*, *30*(3), 197–204. https://doi.org/10.1080/10408410490468803

Dobrynin, D., Fridman, G., Friedman, G., & Fridman, A. (2009). Physical and biological mechanisms of direct plasma interaction with living tissue. *New Journal of Physics*, *11*. https://doi.org/10.1088/1367-2630/11/11/115020

Dolezalova, E., & Lukes, P. (2015). Membrane damage and active but nonculturable state in liquid cultures of *Escherichia coli* treated with an atmospheric pressure plasma jet. *Bioelectrochemistry*, *103*, 7–14. https://doi.org/10.1016/j.bioelechem.2014.08.018

Du, L., Jaya Prasad, A., Gänzle, M., & Roopesh, M. S. (2020). Inactivation of *Salmonella spp.* in wheat flour by 395 nm pulsed light emitting diode (LED) treatment and the related functional and structural changes of gluten. *Food Research International*, *127*(June 2019), 108716. https://doi.org/10.1016/j.foodres.2019.108716

Eliasson, B., Hirth, M., & Kogelschatz, U. (1987). Ozone synthesis from oxygen in dielectric barrier discharges. *Journal of Physics D: Applied Physics*, *20*(11), 1421–1437. https://doi.org/10.1088/0022-3727/20/11/010

Farber, J. M. (1990). Microbiological Aspects of Modified-Atmosphere Packaging Technology - A Review. *Journal of Food Protection*, *54*(1), 58–70. https://doi.org/10.4315/0362-028x-54.1.58

Farber, Jeffrey M., Zwietering, M., Wiedmann, M., Schaffner, D., Hedberg, C. W., Harrison, M. A., … Gummalla, S. (2021). Alternative approaches to the risk management of *Listeria monocytogenes* in low risk foods. *Food Control*, *123*, 107601.

https://doi.org/10.1016/j.foodcont.2020.107601

Fernández, A., Shearer, N., Wilson, D. R., & Thompson, A. (2012). Effect of microbial loading on the efficiency of cold atmospheric gas plasma inactivation of *Salmonella enterica serovar* Typhimurium. *International Journal of Food Microbiology*, *152*(3), 175–180. https://doi.org/10.1016/j.ijfoodmicro.2011.02.038

Field, D., Ross, R. P., & Hill, C. (2018). Developing bacteriocins of lactic acid bacteria into next generation biopreservatives. *Current Opinion in Food Science*, *20*(April), 1–6. https://doi.org/10.1016/j.cofs.2018.02.004

Finn, S., Condell, O., McClure, P., Amézquita, A., & Fanning, S. (2013). Mechanisms of survival, responses, and sources of *Salmonella* in low-moisture environments. *Frontiers in Microbiology*, *4*(NOV), 1–15. https://doi.org/10.3389/fmicb.2013.00331

Food, E., & Authority, S. (2015). The 2013 joint ECDC/EFSA report on trends and sources of zoonoses, zoonotic agents and food-borne outbreaks published. *Euro Surveillance : Bulletin Européen Sur Les Maladies Transmissibles = European Communicable Disease Bulletin*, *20*(4), 3991. https://doi.org/10.2903/j.efsa.2015.3991

Fridman. (2012). Characterization of dielectric barrier discharge in air applying current measurement, numerical simulation and emission spectroscopy. *Measurement Science and Technology*, *23*(8), 085605. https://doi.org/10.1088/0957-0233/23/8/085605

Fröhling, A., Baier, M., Ehlbeck, J., Knorr, D., & Schlüter, O. (2012). Atmospheric pressure plasma treatment of *Listeria innocua* and *Escherichia coli* at polysaccharide surfaces: Inactivation kinetics and flow cytometric characterization. *Innovative Food Science and*

Emerging Technologies, *13*(JANUARY), 142–150. https://doi.org/10.1016/j.ifset.2011.11.002

Fröhling, A., Durek, J., Schnabel, U., Ehlbeck, J., Bolling, J., & Schlüter, O. (2012). Indirect plasma treatment of fresh pork: Decontamination efficiency and effects on quality attributes. *Innovative Food Science and Emerging Technologies*, *16*(October), 381–390. https://doi.org/10.1016/j.ifset.2012.09.001

Fröhling, Antje, & Schlüter, O. (2015). Flow cytometric evaluation of physico-chemical impact on Gram-positive and Gram-negative bacteria. *Frontiers in Microbiology*, *6*(SEP), 1–21. https://doi.org/10.3389/fmicb.2015.00939

Gaunt, L. F., Beggs, C. B., & Georghiou, G. E. (2006). Bactericidal action of the reactive species produced by gas-discharge nonthermal plasma at atmospheric pressure: A review. *IEEE Transactions on Plasma Science*, *34*(4 II), 1257–1269. https://doi.org/10.1109/TPS.2006.878381

Gavahian, M., Chu, Y. H., Mousavi Khaneghah, A., Barba, F. J., & Misra, N. N. (2018). A critical analysis of the cold plasma induced lipid oxidation in foods. *Trends in Food Science and Technology*, *77*(March), 32–41. https://doi.org/10.1016/j.tifs.2018.04.009

Gök, V., Aktop, S., Özkan, M., & Tomar, O. (2019). The effects of atmospheric cold plasma on inactivation of *Listeria monocytogenes* and *Staphylococcus aureus* and some quality characteristics of pastırma—A dry-cured beef product. *Innovative Food Science and Emerging Technologies*, *56*(November 2018), 102188. https://doi.org/10.1016/j.ifset.2019.102188

Gomes, A., Fernandes, E., & Lima, J. L. F. C. (2005). Fluorescence probes used for detection of reactive oxygen species. *Journal of Biochemical and Biophysical Methods*, *65*(2–3), 45–80. https://doi.org/10.1016/j.jbbm.2005.10.003

Gonçalves-Tenório, A., Nunes Silva, B., Rodrigues, V., Cadavez, V., & Gonzales-Barron, U. (2018). Prevalence of pathogens in poultry meat: A meta-analysis of European published surveys. *Foods*, *7*(5). https://doi.org/10.3390/foods7050069

Guyon, C., Meynier, A., & de Lamballerie, M. (2016). Protein and lipid oxidation in meat: A review with emphasis on high-pressure treatments. *Trends in Food Science and Technology*, *50*, 131–143. https://doi.org/10.1016/j.tifs.2016.01.026

Guzel-Seydim, Z. B., Greene, A. K., & Seydim, A. C. (2004). Use of ozone in the food industry. *LWT - Food Science and Technology*, *37*(4), 453–460. https://doi.org/10.1016/j.lwt.2003.10.014

Han, L., Boehm, D., Amias, E., Milosavljević, V., Cullen, P. J., & Bourke, P. (2016). Atmospheric cold plasma interactions with modified atmosphere packaging inducer gases for safe food preservation. *Innovative Food Science and Emerging Technologies*, *38*(December), 384–392. https://doi.org/10.1016/j.ifset.2016.09.026

Han, L., Patil, S., Boehm, D., Milosavljević, V., Cullen, P. J., & Bourke, P. (2016). Mechanisms of inactivation by high-voltage atmospheric cold plasma differ for *Escherichia coli* and *Staphylococcus aureus*. *Applied and Environmental Microbiology*, *82*(2), 450–458. https://doi.org/10.1128/AEM.02660-15

Han, Lu, Ziuzina, D., Heslin, C., Boehm, D., Patange, A., Sango, D. M., … Bourke, P. (2016).

Controlling microbial safety challenges of meat using high voltage atmospheric cold plasma. *Frontiers in Microbiology*, *7*(JUN), 1–12. https://doi.org/10.3389/fmicb.2016.00977

Health Canada. (2011). Policy on *Listeria monocytogenes* in Ready-to-Eat Foods Bureau of Microbial Hazards Food Directorate Health Products and Food Branch, 1–49. Retrieved from https://www.canada.ca/content/dam/hc-sc/migration/hc-sc/fn-an/alt_formats/pdf/legislation/pol/policy_listeria_monocytogenes_2011-eng.pdf

Health Canada. (2012). Illnesses related to *Salmonella* and pet food. Retrieved April 12, 2020, from https://www.canada.ca/en/public-health/services/food-safety/public-health-notice/public-health-notice-illnesses-related-*salmonella*-food.html

Health Canada. (2015). *Sodium Reduction in Processed Foods in Canada: An evaluation of Progress toward Voluntary Targets from 2012 to 2016 2*. Retrieved from https://www.canada.ca/content/dam/hc-sc/documents/services/food-nutrition/legislation-guidelines/guidance-documents/guidance-food-industry-reducing-sodium-processed-foods-progress-report-2017/pub1-eng.pdf

Health Canada. (2016). Food-related illnesses, hospitalizations and deaths in Canada. Retrieved April 12, 2018, from https://www.canada.ca/en/public-health/services/publications/food-nutrition/infographic-food-related-illnesses-hospitalizations-deaths-in-canada.html

Heredia, N., & García, S. (2018). Animals as sources of food-borne pathogens: A review. *Animal Nutrition*, *4*(3), 250–255. https://doi.org/10.1016/j.aninu.2018.04.006

Herianto, S., Hou, C. Y., Lin, C. M., & Chen, H. L. (2021). Nonthermal plasma-activated water:

A comprehensive review of this new tool for enhanced food safety and quality. *Comprehensive Reviews in Food Science and Food Safety*, *20*(1), 583–626. https://doi.org/10.1111/1541-4337.12667

Hernandez-Milian, A., & Payeras-Cifre, A. (2014). What is new in Listeriosis? *BioMed Research International*, *2014*, 358051. https://doi.org/10.1155/2014/358051

Hertwig, C., Reineke, K., Ehlbeck, J., Knorr, D., & Schlüter, O. (2015). Decontamination of whole black pepper using different cold atmospheric pressure plasma applications. *Food Control*, *55*, 221–229. https://doi.org/10.1016/j.foodcont.2015.03.003

Hertwig, C., Reineke, K., Rauh, C., & Schlüter, O. (2017). Factors involved in *Bacillus* spore's resistance to cold atmospheric pressure plasma. *Innovative Food Science and Emerging Technologies*, *43*(May), 173–181. https://doi.org/10.1016/j.ifset.2017.07.031

Hildebrandt, I. M., Marks, B. P., Ryser, E. T., Villa-Rojas, R., Tang, J., Garces-Vega, F. J., & Buchholz, S. E. (2016). Effects of inoculation procedures on variability and repeatability of *Salmonella* thermal resistance in wheat flour. *Journal of Food Protection*, *79*(11), 1833–1839. https://doi.org/10.4315/0362-028X.JFP-16-057

Hoffmann, C., Berganza, C., & Zhang, J. (2013). Cold Atmospheric Plasma: Methods of production and application in dentistry and oncology. *Medical Gas Research*, *3*(1), 1–15. https://doi.org/10.1186/2045-9912-3-21

Horita, C. N., Baptista, R. C., Caturla, M. Y. R., Lorenzo, J. M., Barba, F. J., & Sant'Ana, A. S. (2018). Combining reformulation, active packaging and non-thermal post-packaging decontamination technologies to increase the microbiological quality and safety of cooked

ready-to-eat meat products. *Trends in Food Science and Technology*, *72*(September), 45–61. https://doi.org/10.1016/j.tifs.2017.12.003

Huang, M., Zhuang, H., Wang, J., Yan, W., Zhao, J., & Zhang, J. (2018). Inactivation kinetics of *Salmonella typhimurium* and *Staphylococcus aureus* in different media by dielectric barrier discharge non-thermal plasma. *Applied Sciences (Switzerland)*, *8*(11), 1–15. https://doi.org/10.3390/app8112087

Jayasena, D. D., Kim, H. J., Yong, H. I., Park, S., Kim, K., Choe, W., & Jo, C. (2015). Flexible thin-layer dielectric barrier discharge plasma treatment of pork butt and beef loin: Effects on pathogen inactivation and meat-quality attributes. *Food Microbiology*, *46*(April), 51–57. https://doi.org/10.1016/j.fm.2014.07.009

Jiang, J., & Xiong, Y. L. (2015). Technologies and Mechanisms for Safety Control of Ready-to-eat Muscle Foods: An Updated Review. *Critical Reviews in Food Science and Nutrition*, *55*(13), 1886–1901. https://doi.org/10.1080/10408398.2012.732624

Joshi, S. G., Cooper, M., Yost, A., Paff, M., Ercan, U. K., Fridman, G., … Brooks, A. D. (2011). Nonthermal dielectric-barrier discharge plasma-induced inactivation involves oxidative DNA damage and membrane lipid peroxidation in *Escherichia coli*. *Antimicrobial Agents and Chemotherapy*, *55*(3), 1053–1062. https://doi.org/10.1128/AAC.01002-10

Jung, S., Lee, J., Lim, Y., Choe, W., Yong, H. I., & Jo, C. (2017). Direct infusion of nitrite into meat batter by atmospheric pressure plasma treatment. *Innovative Food Science and Emerging Technologies*, *39*, 113–118. https://doi.org/10.1016/j.ifset.2016.11.010

Kananub, S., Pinniam, N., Phothitheerabut, S., Krajanglikit, P., 2020. Contamination factors

associated with surviving bacteria in Thai commercial raw pet foods. Vet. World 13, 1988–1991. doi:10.14202/vetworld.2020.1988-1991

Kang, M. H., Hong, Y. J., Attri, P., Sim, G. B., Lee, G. J., Panngom, K., … Park, G. (2014). Analysis of the antimicrobial effects of nonthermal plasma on fungal spores in ionic solutions. *Free Radical Biology and Medicine*, *72*, 191–199. https://doi.org/10.1016/j.freeradbiomed.2014.04.023

Kim, B., Yun, H., Jung, S., Jung, Y., Jung, H., Choe, W., & Jo, C. (2011). Effect of atmospheric pressure plasma on inactivation of pathogens inoculated onto bacon using two different gas compositions. *Food Microbiology*, *28*(1), 9–13. https://doi.org/10.1016/j.fm.2010.07.022

Kim, H. J., Jayasena, D. D., Yong, H. I., & Jo, C. (2016). Quality of Cold Plasma Treated Foods of Animal Origin. *Cold Plasma in Food and Agriculture: Fundamentals and Applications*, 273–291. https://doi.org/10.1016/B978-0-12-801365-6.00011-1

Kim, Hyun Joo, Yong, H. I., Park, S., Choe, W., & Jo, C. (2013). Effects of dielectric barrier discharge plasma on pathogen inactivation and the physicochemical and sensory characteristics of pork loin. *Current Applied Physics*, *13*(7), 1420–1425. https://doi.org/10.1016/j.cap.2013.04.021

Kim, J. H., & Min, S. C. (2018). Moisture vaporization-combined helium dielectric barrier discharge-cold plasma treatment for microbial decontamination of onion flakes. *Food Control*, *84*, 321–329. https://doi.org/10.1016/j.foodcont.2017.08.018

Klockow, P. A., & Keener, K. M. (2009). Safety and quality assessment of packaged spinach treated with a novel ozone-generation system. *LWT - Food Science and Technology*, *42*(6),

1047–1053. https://doi.org/10.1016/j.lwt.2009.02.011

Lang, E., Guyot, S., Peltier, C., Alvarez-Martin, P., Perrier-Cornet, J. M., & Gervais, P. (2018). Cellular injuries in *Cronobacter sakazakii* CIP 103183T and *Salmonella enterica* exposed to drying and subsequent heat treatment in milk powder. *Frontiers in Microbiology*, *9*(MAR), 1–10. https://doi.org/10.3389/fmicb.2018.00475

Laroque, D. A., Seó, S. T., Valencia, G. A., Laurindo, J. B., & Carciofi, B. A. M. (2022). Cold plasma in food processing: Design, mechanisms, and application. *Journal of Food Engineering*, *312*(April 2021), 110748. https://doi.org/10.1016/j.jfoodeng.2021.110748

Laroussi, M., & Leipold, F. (2004). Evaluation of the roles of reactive species, heat, and UV radiation in the inactivation of bacterial cells by air plasmas at atmospheric pressure. *International Journal of Mass Spectrometry*, *233*(1–3), 81–86. https://doi.org/10.1016/j.ijms.2003.11.016

Laroussi, M., Mendis, D. A., & Rosenberg, M. (2003). Plasma interaction with microbes. *New Journal of Physics*, *5*. https://doi.org/10.1088/1367-2630/5/1/341

Laroussi, Mounir. (2002). Nonthermal decontamination of biological media by atmospheric-pressure plasmas: Review, analysis, and prospects. *IEEE Transactions on Plasma Science*, *30*(4 I), 1409–1415. https://doi.org/10.1109/TPS.2002.804220

Lee, G. J., Sim, G. B., Choi, E. H., Kwon, Y., Kim, J. Y., Jang, S., & Hwan, S. (2015). Optical and structural properties of plasma-treated Cordyceps bassiana spores as studied by circular dichroism , absorption , and fluorescence spectroscopy Optical and structural properties of plasma-treated Cordyceps bassiana spores as studied by circula. *Journal of Applied Physics*,

023303(2), 023303. https://doi.org/10.1063/1.4905194

Lee, J., Lee, C. W., Yong, H. I., Lee, H. J., Jo, C., & Jung, S. (2017). Use of atmospheric pressure cold plasma for meat industry. *Korean Journal for Food Science of Animal Resources*, *37*(4), 477–485. https://doi.org/10.5851/kosfa.2017.37.4.477

Liao, X., Cullen, P. J., Muhammad, A. I., Jiang, Z., Ye, X., Liu, D., & Ding, T. (2020). Cold Plasma–Based Hurdle Interventions: New Strategies for Improving Food Safety. *Food Engineering Reviews*, *12*(3), 321–332. https://doi.org/10.1007/s12393-020-09222-3

Liao, X., Liu, D., Xiang, Q., Ahn, J., Chen, S., Ye, X., & Ding, T. (2017). Inactivation mechanisms of non-thermal plasma on microbes: A review. *Food Control*, *75*, 83–91. https://doi.org/10.1016/j.foodcont.2016.12.021

Liao, X., Xiang, Q., Liu, D., Chen, S., Ye, X., & Ding, T. (2017). Lethal and Sublethal Effect of a Dielectric Barrier Discharge Atmospheric Cold Plasma on *Staphylococcus aureus*. *Journal of Food Protection*, *80*(6), 928–932. https://doi.org/10.4315/0362-028X.JFP-16-499

Limcharoenchat, P., Buchholz, S. E., James, M. K., Hall, N. O., Ryser, E. T., & Marks, B. P. (2018). Inoculation protocols influence the thermal resistance of *Salmonella Enteritidis* PT 30 in fabricated almond, wheat, and date products. *Journal of Food Protection*, *81*(4), 606–613. https://doi.org/10.4315/0362-028X.JFP-17-297

Lis, K. A., Boulaaba, A., Binder, S., Li, Y., Kehrenberg, C., Zimmermann, J. L., … Ahlfeld, B. (2018). Inactivation of *Salmonella Typhimurium* and *Listeria monocytogenes* on ham with nonthermal atmospheric pressure plasma. *PLoS ONE*, *13*(5), 1–21.

https://doi.org/10.1371/journal.pone.0197773

Liu, X., Miller, P., Basu, U., & Mcmullen, L. M. (2014). Sodium chloride-induced filamentation and alternative gene expression of *fts*, *murZ*, and *gnd* in *Listeria monocytogenes* 08-5923 on vacuum-packaged ham. *FEMS Microbiology Letters*, *360*(2), 152–156. https://doi.org/10.1111/1574-6968.12599

López, M., Calvo, T., Prieto, M., Múgica-Vidal, R., Muro-Fraguas, I., Alba-Elías, F., & Alvarez-Ordóñez, A. (2019). A review on non-thermal atmospheric plasma for food preservation: Mode of action, determinants of effectiveness, and applications. *Frontiers in Microbiology*, *10*(APR), 622. https://doi.org/10.3389/fmicb.2019.00622

Machala, Z., Tarabová, B., Sersenová, D., Janda, M., & Hensel, K. (2019). Chemical and antibacterial effects of plasma activated water: Correlation with gaseous and aqueous reactive oxygen and nitrogen species, plasma sources and air flow conditions. *Journal of Physics D: Applied Physics*, *52*(3). https://doi.org/10.1088/1361-6463/aae807

Maherani, B., Ayari, S., & Lacroix, M. (2018). The Use of Natural Antimicrobials Combined with Nonthermal Treatments to Control Human Pathogens. *ACS Symposium Series*, *1287*, 149–169. https://doi.org/10.1021/bk-2018-1287.ch008

Mani-López, E., García, H. S., & López-Malo, A. (2012). Organic acids as antimicrobials to control *Salmonella* in meat and poultry products. *Food Research International*, *45*(2), 713–721. https://doi.org/10.1016/j.foodres.2011.04.043

Martin-Visscher, L. A., Gong, X., Duszyk, M., & Vederas, J. C. (2009). The three-dimensional structure of carnocyclin A reveals that many circular bacteriocins share a common structural

motif. *Journal of Biological Chemistry*, *284*(42), 28674–28681. https://doi.org/10.1074/jbc.M109.036459

Martin-Visscher, L. A., Van Belkum, M. J., Garneau-Tsodikova, S., Whittal, R. M., Zheng, J., McMullen, L. M., & Vederas, J. C. (2008). Isolation and characterization of carnocyclin A, a novel circular bacteriocin produced by *Carnobacterium maltaromaticum* UAL307. *Applied and Environmental Microbiology*, *74*(15), 4756–4763. https://doi.org/10.1128/AEM.00817-08

Matan, N., Nisoa, M., & Matan, N. (2014). Antibacterial activity of essential oils and their main components enhanced by atmospheric RF plasma. *Food Control*, *39*(1), 97–99. https://doi.org/10.1016/j.foodcont.2013.10.030

Mataragas, M., Skandamis, P. N., & Drosinos, E. H. (2008). Risk profiles of pork and poultry meat and risk ratings of various pathogen/product combinations. *International Journal of Food Microbiology*, *126*(1–2), 1–12. https://doi.org/10.1016/j.ijfoodmicro.2008.05.014

Mattick, K. L., Jørgensen, F., Legan, J. D., Cole, M. B., Porter, J., Lappin-Scott, H. M., & Humphrey, T. J. (2000). Survival and filamentation of *Salmonella enterica serovar enteritidis* PT4 and *Salmonella enterica serovar typhimurium* DT104 at low water activity. *Applied and Environmental Microbiology*, *66*(4), 1274–1279. https://doi.org/10.1128/AEM.66.4.1274-1279.2000

Mbandi, E., & Shelef, L. A. (2002). Enhanced antimicrobial effects of combination of lactate and diacetate on *Listeria monocytogenes* and *Salmonella spp.* in beef bologna. *International Journal of Food Microbiology*, *76*(3), 191–198. https://doi.org/10.1016/S0168-1605(02)00026-0

Mehlhorn, H. (2015). Food-Borne Disease Burden Epidemiology Reference Group. *Encyclopedia of Parasitology*, 1–1. https://doi.org/10.1007/978-3-642-27769-6_3884-1

Min, B., & Ahn, D. U. (2005). Mechanism of Lipid Peroxidation in Meat and Meat Products -A Review. *Food Science and Biotechnology*, *14*(1), 152–163.

Min, S. C., Roh, S. H., Boyd, G., Sites, J. E., Uknalis, J., Fan, X., & Niemira, B. A. (2017). Inactivation of *Escherichia coli* O157:H7 and Aerobic Microorganisms in Romaine Lettuce Packaged in a Commercial Polyethylene Terephthalate Container Using Atmospheric Cold Plasma. *Journal of Food Protection*, *80*(1), 35–43. https://doi.org/10.4315/0362-028X.JFP-16-148

Min, S. C., Roh, S. H., Niemira, B. A., Boyd, G., Sites, J. E., Fan, X., … Jin, T. Z. (2018). In-package atmospheric cold plasma treatment of bulk grape tomatoes for microbiological safety and preservation. *Food Research International*, *108*(December), 378–386. https://doi.org/10.1016/j.foodres.2018.03.033

Min, S. C., Roh, S. H., Niemira, B. A., Boyd, G., Sites, J. E., Uknalis, J., & Fan, X. (2017). In-package inhibition of *E. coli* O157:H7 on bulk Romaine lettuce using cold plasma. *Food Microbiology*, *65*(Auguest), 1–6. https://doi.org/10.1016/j.fm.2017.01.010

Misra, N. N., & Jo, C. (2017). Applications of cold plasma technology for microbiological safety in meat industry. *Trends in Food Science and Technology*, *64*, 74–86. https://doi.org/10.1016/j.tifs.2017.04.005

Misra, N. N., Kaur, S., Tiwari, B. K., Kaur, A., Singh, N., & Cullen, P. J. (2015). Atmospheric pressure cold plasma (ACP) treatment of wheat flour. *Food Hydrocolloids*, *44*, 115–121.

https://doi.org/10.1016/j.foodhyd.2014.08.019

Misra, N. N., Koubaa, M., Roohinejad, S., Juliano, P., Alpas, H., Inácio, R. S., … Barba, F. J. (2017). Landmarks in the historical development of twenty first century food processing technologies. *Food Research International*, *97*(February), 318–339. https://doi.org/10.1016/j.foodres.2017.05.001

Misra, N. N., Tiwari, B. K., Raghavarao, K. S. M. S., & Cullen, P. J. (2011). Nonthermal Plasma Inactivation of Food-Borne Pathogens. *Food Engineering Reviews*, *3*(3–4), 159–170. https://doi.org/10.1007/s12393-011-9041-9

Misra, N. N., Yadav, B., Roopesh, M. S., & Jo, C. (2019). Cold Plasma for Effective Fungal and Mycotoxin Control in Foods: Mechanisms, Inactivation Effects, and Applications. *Comprehensive Reviews in Food Science and Food Safety*. https://doi.org/10.1111/1541-4337.12398

Misra, N. N., Yepez, X., Xu, L., & Keener, K. (2018). In-package cold plasma technologies. *Journal of Food Engineering*, *244*(May), 21–31. https://doi.org/10.1016/J.JFOODENG.2018.09.019

Misra, N. N., Ziuzina, D., Cullen, P. J., & Keener, K. M. (2013). Characterization of a Novel Atmospheric air Cold Plasma System for Treatment of Packaged Biomaterials. *American Society of Agricultural and Biological Engineers*, *56*(3), 1011–1016.

Moisan, M., Barbeau, J., Moreau, S., Pelletier, J., Tabrizian, M., & Yahia, L. (2001). Low-temperature sterlization using gas plasmas: a review of the experiment and an analysis of the inactivation mechanisms. *International Journal of Pharmaceutics*, *226*, 1–21.

Moiseev, T., Misra, N. N., Patil, S., Cullen, P. J., Bourke, P., Keener, K. M., & Mosnier, J. P. (2014). Post-discharge gas composition of a large-gap DBD in humid air by UV-Vis absorption spectroscopy. *Plasma Sources Science and Technology*, *23*(6), 065033. https://doi.org/10.1088/0963-0252/23/6/065033

Moreau, M., Orange, N., & Feuilloley, M. G. J. (2008). Non-thermal plasma technologies: New tools for bio-decontamination. *Biotechnology Advances*, *26*(6), 610–617. https://doi.org/10.1016/j.biotechadv.2008.08.001

Nair, D. V. T., & Johny, A. K. (2019). Food Safety in Poultry Meat Production. *Food Safety in Poultry Meat Production*, 1–24. https://doi.org/10.1007/978-3-030-05011-5

Neyts, E. C., Ostrikov, K., Sunkara, M. K., & Bogaerts, A. (2015). Plasma Catalysis: Synergistic Effects at the Nanoscale. *Chemical Reviews*, *115*(24), 13408–13446. https://doi.org/10.1021/acs.chemrev.5b00362

Niemira, B. A. (2012). Cold plasma decontamination of foods. *Annual Review of Food Science and Technology*, *3*(1), 125–142. https://doi.org/10.1146/annurev-food-022811-101132

Niemira, Brendan A. (2012). Cold Plasma Reduction of *Salmonella* and *Escherichia coli O157: H7* on Almonds Using Ambient Pressure Gases. *Journal of Food Science*, *77*(3), 171–175. https://doi.org/10.1111/j.1750-3841.2011.02594.x

Noriega, E., Shama, G., Laca, A., Díaz, M., & Kong, M. G. (2011). Cold atmospheric gas plasma disinfection of chicken meat and chicken skin contaminated with *Listeria innocua*. *Food Microbiology*, *28*(7), 1293–1300. https://doi.org/10.1016/j.fm.2011.05.007

Ojeda-Sana, A. M., van Baren, C. M., Elechosa, M. A., Juárez, M. A., & Moreno, S. (2013).

New insights into antibacterial and antioxidant activities of rosemary essential oils and their main components. *Food Control*, *31*(1), 189–195. https://doi.org/10.1016/j.foodcont.2012.09.022

Oliveira, S. (2014). Canadian Pet Market Outlook. *Consumer Corner - Alberta Agriculture and Rural Development*, (28), 4. Retrieved from http://www1.agric.gov.ab.ca/$department/deptdocs.nsf/all/sis14914/$file/sarah_pet_june20_2014.pdf?OpenElement

Painter, J. A., Hoekstra, R. M., Ayers, T., Tauxe, R. V., Braden, C. R., Angulo, F. J., & Griffin, P. M. (2013). Attribution of foodborne illnesses, hospitalizations, and deaths to food commodities by using outbreak data, United States, 1998-2008. *Emerging Infectious Diseases*, *19*(3), 407–415. https://doi.org/10.3201/eid1903.111866

Park, S., Choe, W., & Jo, C. (2018). Interplay among ozone and nitrogen oxides in air plasmas: Rapid change in plasma chemistry. *Chemical Engineering Journal*, *352*(July), 1014–1021. https://doi.org/10.1016/j.cej.2018.07.039

Patange, A., O'Byrne, C., Boehm, D., Cullen, P. J., Keener, K., & Bourke, P. (2019). The Effect of Atmospheric Cold Plasma on Bacterial Stress Responses and Virulence Using *Listeria monocytogenes* Knockout Mutants. *Frontiers in Microbiology*, *10*(December), 1–12. https://doi.org/10.3389/fmicb.2019.02841

Phillips, C. A. (1996). Review: Modified atmosphere packaging and its effects on the microbiological quality and safety of produce. *International Journal of Food Science and Technology*, *31*(6), 463–479. https://doi.org/10.1046/j.1365-2621.1996.00369.x

Pietrasik, Z., Pierce, D. L., Zhang, J., & Mcmullen, L. M. (2012). Effect of Post-Packaging Steam Pasteurization on Quality and Consumer Acceptance of Fully Cooked Vacuum-Packaged Sliced Turkey Breast. *International Congress of Meat Science and Technology*, (August), 2–5.

Pignata, C., D'Angelo, D., Fea, E., & Gilli, G. (2017). A review on microbiological decontamination of fresh produce with nonthermal plasma. *Journal of Applied Microbiology*, *122*(6), 1438–1455. https://doi.org/10.1111/jam.13412

Pothakos, V., Devlieghere, F., Villani, F., Björkroth, J., & Ercolini, D. (2015). Lactic acid bacteria and their controversial role in fresh meat spoilage. *Meat Science*, *109*, 66–74. https://doi.org/10.1016/j.meatsci.2015.04.014

Prasad, A., Gänzle, M., & Roopesh, M. S. (2019). Inactivation of *Escherichia coli* and *Salmonella* using 365 and 395 nm high intensity pulsed light emitting diodes. *Foods*, *8*(12). https://doi.org/10.3390/foods8120679

Qian, J., Wang, C., Zhuang, H., Zhang, J., & Yan, W. (2020). Oxidative stress responses of pathogen bacteria in poultry to plasma-activated lactic acid solutions. *Food Control*, *118*(May), 107355. https://doi.org/10.1016/j.foodcont.2020.107355

Qian, J., Zhuang, H., Nasiru, M. M., Muhammad, U., Zhang, J., & Yan, W. (2019). Action of plasma-activated lactic acid on the inactivation of inoculated *Salmonella Enteritidis* and quality of beef. *Innovative Food Science and Emerging Technologies*, *57*(March), 102196. https://doi.org/10.1016/j.ifset.2019.102196

Ramamurthy, T., Ghosh, A., Pazhani, G. P., & Shinoda, S. (2014). Current perspectives on

viable but non-culturable (VBNC) pathogenic bacteria. *Frontiers in Public Health*, *2*(JUL), 1–9. https://doi.org/10.3389/fpubh.2014.00103

Rathore, V., & Nema, S. K. (2021). Optimization of process parameters to generate plasma activated water and study of physicochemical properties of plasma activated solutions at optimum condition. *Journal of Applied Physics*, *129*(8). https://doi.org/10.1063/5.0033848

Ricci, A., Allende, A., Bolton, D., Chemaly, M., Davies, R., Fernández Escámez, P. S., … Lindqvist, R. (2018). *Listeria monocytogenes* contamination of ready-to-eat foods and the risk for human health in the EU. *EFSA Journal*, *16*(1), 5134. https://doi.org/10.2903/j.efsa.2018.5134

Rød, S. K., Hansen, F., Leipold, F., & Knøchel, S. (2012). Cold atmospheric pressure plasma treatment of ready-to-eat meat: Inactivation of *Listeria innocua* and changes in product quality. *Food Microbiology*, *30*(1), 233–238. https://doi.org/10.1016/j.fm.2011.12.018

Ryu, Y. H., Kim, Y. H., Lee, J. Y., Shim, G. B., Uhm, H. S., Park, G., & Choi, E. H. (2013). Effects of Background Fluid on the Efficiency of Inactivating Yeast with Non-Thermal Atmospheric Pressure Plasma. *PLoS ONE*, *8*(6), 1–9. https://doi.org/10.1371/journal.pone.0066231

Santillana Farakos, S. M., Frank, J. F., & Schaffner, D. W. (2013). Modeling the influence of temperature, water activity and water mobility on the persistence of *Salmonella* in low-moisture foods. *International Journal of Food Microbiology*, *166*(2), 280–293. https://doi.org/10.1016/j.ijfoodmicro.2013.07.007

Sarangapani, C., Ryan Keogh, D., Dunne, J., Bourke, P., & Cullen, P. J. (2017). Characterisation

of cold plasma treated beef and dairy lipids using spectroscopic and chromatographic methods. *Food Chemistry*, *235*(November), 324–333. https://doi.org/10.1016/j.foodchem.2017.05.016

Scholtz, V., Pazlarova, J., Souskova, H., Khun, J., & Julak, J. (2015). Nonthermal plasma - A tool for decontamination and disinfection. *Biotechnology Advances*, *33*(6), 1108–1119. https://doi.org/10.1016/j.biotechadv.2015.01.002

Schottroff, F., Fröhling, A., Zunabovic-Pichler, M., Krottenthaler, A., Schlüter, O., & Jäger, H. (2018). Sublethal injury and Viable but Non-culturable (VBNC) state in microorganisms during preservation of food and biological materials by non-thermal processes. *Frontiers in Microbiology*, *9*(NOV), 1–19. https://doi.org/10.3389/fmicb.2018.02773

Sekhon, R. K., Schilling, M. W., Phillips, T. W., Aikins, R. M. J., Hasan, M. M., Nannapaneni, R., & Mikel, W. B. (2010). Effects of Carbon Dioxide and Ozone Treatments on the Volatile Composition and Sensory Quality of Dry-Cured Ham. *Journal of Food Science*, *75*(5), 452–458. https://doi.org/10.1111/j.1750-3841.2010.01646.x

Shunying, Z., Yang, Y., Huaidong, Y., Yue, Y., & Guolin, Z. (2005). Chemical composition and antimicrobial activity of the essential oils of *Chrysanthemum indicum*. *Journal of Ethnopharmacology*, *96*(1–2), 151–158. https://doi.org/10.1016/j.jep.2004.08.031

Smet, C., Baka, M., Steen, L., Fraeye, I., Walsh, J. L., Valdramidis, V. P., & Van Impe, J. F. (2019). Combined effect of cold atmospheric plasma, intrinsic and extrinsic factors on the microbial behavior in/on (food) model systems during storage. *Innovative Food Science and Emerging Technologies*, *53*(May 2018), 3–17. https://doi.org/10.1016/j.ifset.2018.05.016

Sohaib, M., Anjum, F. M., Arshad, M. S., & Rahman, U. U. (2016). Postharvest intervention technologies for safety enhancement of meat and meat based products; a critical review. *Journal of Food Science and Technology*, *53*(1), 19–30. https://doi.org/10.1007/s13197-015-1985-y

Song, H. P., Kim, B., Choe, J. H., Jung, S., Moon, S. Y., Choe, W., & Jo, C. (2009). Evaluation of atmospheric pressure plasma to improve the safety of sliced cheese and ham inoculated by 3-strain cocktail *Listeria monocytogenes*. *Food Microbiology*, *26*(4), 432–436. https://doi.org/10.1016/j.fm.2009.02.010

Stiefel, P., Schmidt-Emrich, S., Maniura-Weber, K., & Ren, Q. (2015). Critical aspects of using bacterial cell viability assays with the fluorophores SYTO9 and propidium iodide. *BMC Microbiology*, *15*(1), 1–9. https://doi.org/10.1186/s12866-015-0376-x

Surowsky, B., Fröhling, A., Gottschalk, N., Schlüter, O., & Knorr, D. (2014). Impact of cold plasma on *Citrobacter freundii* in apple juice: Inactivation kinetics and mechanisms. *International Journal of Food Microbiology*, *174*, 63–71. https://doi.org/10.1016/j.ijfoodmicro.2013.12.031

Surowsky, B., Schlüter, O., & Knorr, D. (2014). Interactions of Non-Thermal Atmospheric Pressure Plasma with Solid and Liquid Food Systems: A Review. *Food Engineering Reviews*, *7*(2), 82–108. https://doi.org/10.1007/s12393-014-9088-5

Syamaladevi, R. M., Tang, J., Villa-Rojas, R., Sablani, S., Carter, B., & Campbell, G. (2016). Influence of Water Activity on Thermal Resistance of Microorganisms in Low-Moisture Foods: A Review. *Comprehensive Reviews in Food Science and Food Safety*, *15*(2), 353–370. https://doi.org/10.1111/1541-4337.12190

Syamaladevi, R. M., Tang, J., & Zhong, Q. P. (2016). Water Diffusion from a Bacterial Cell in Low-Moisture Foods. *Journal of Food Science*, *81*(9), R2129–R2134. https://doi.org/10.1111/1750-3841.13412

Tack, D. M., Marder, E. P., Griffin, P. M., Cieslak, P. R., Dunn, J., Hurd, S., … Geissler, A. L. (2019). Preliminary incidence and trends of infections with pathogens transmitted commonly through food — Foodborne Diseases Active Surveillance Network, 10 U.S. sites, 2015–2018. *American Journal of Transplantation*, *19*(6), 1859–1863. https://doi.org/10.1111/ajt.15412

Teixeira, J., Repková, L., Gänzle, M., & McMullen, L. M. (2018). Effect of pressure, reconstituted meat microbiota, and antimicrobials on survival and post-pressure growth of *Listeria monocytogenes* on ham. *Frontiers in Microbiology*, *9*(August), 1979. https://doi.org/10.3389/FMICB.2018.01979

Thomas-Popo, E., Mendonça, A., Misra, N. N., Little, A., Wan, Z., Moutiq, R., … Keener, K. (2019). Inactivation of Shiga-toxin-producing *Escherichia coli*, *Salmonella enterica* and natural microflora on tempered wheat grains by atmospheric cold plasma. *Food Control*, *104*(December 2018), 231–239. https://doi.org/10.1016/j.foodcont.2019.04.025

Thomas, M. K., Murray, R., Flockhart, L., Pintar, K., Fazil, A., Nesbitt, A., … Pollari, F. (2015). Estimates of Foodborne Illness–Related Hospitalizations and Deaths in Canada for 30 Specified Pathogens and Unspecified Agents. *Foodborne Pathogens and Disease*, *12*(10), 820–827. https://doi.org/10.1089/fpd.2015.1966

Thomas, M. K., Vriezen, R., Farber, J. M., Currie, A., Schlech, W., & Fazil, A. (2015). Economic Cost of a *Listeria monocytogenes* Outbreak in Canada, 2008. *Foodborne*

Pathogens and Disease, *12*(12), 966–971. https://doi.org/10.1089/fpd.2015.1965

Timoshkin, I. V., MacLean, M., Wilson, M. P., Given, M. J., MacGregor, S. J., Wang, T., & Anderson, J. G. (2012). Bactericidal effect of corona discharges in atmospheric air. *IEEE Transactions on Plasma Science*, *40*(10 PART 1), 2322–2333. https://doi.org/10.1109/TPS.2012.2193621

Toyokawa, Y., Yagyu, Y., Misawa, T., & Sakudo, A. (2017). A new roller conveyer system of non-thermal gas plasma as a potential control measure of plant pathogenic bacteria in primary food production. *Food Control*, *72*(852), 62–72. https://doi.org/10.1016/j.foodcont.2016.07.031

Trevisani, M., Berardinelli, A., Cevoli, C., Cecchini, M., Ragni, L., & Pasquali, F. (2017). Effects of sanitizing treatments with atmospheric cold plasma, SDS and lactic acid on verotoxin-producing *Escherichia coli* and *Listeria monocytogenes* in red chicory (radicchio). *Food Control*, *78*, 138–143. https://doi.org/10.1016/j.foodcont.2017.02.056

Ulbin-Figlewicz, N., Brychcy, E., & Jarmoluk, A. (2013). Effect of low-pressure cold plasma on surface microflora of meat and quality attributes. *Journal of Food Science and Technology*, *52*(2), 1228–1232. https://doi.org/10.1007/s13197-013-1108-6

Vieira, A., & Boyer, M. (2019). Foodborne Illness Source Attribution Estimates for *Salmonella* , *Escherichia coli O157* , *Listeria monocytogenes*, and *Campylobacter* using Outbreak Surveillance Data Report Interagency Food Safety Analytics Collaboration (IFSAC). *Interagency Food Safety Analytics Collaboration*, *157*(February), 1–12.

Vinnikova, L., Synytsia, O., & Kyshenia, A. (2019). the Problems of Meat Products Thermal

Treatment. *Food Science and Technology*, *13*(2), 44–57. https://doi.org/10.15673/fst.v13i2.1386

Wang, C., Chang, T., Yang, H., & Cui, M. (2015). Antibacterial mechanism of lactic acid on physiological and morphological properties of *Salmonella Enteritidis*, *Escherichia coli* and *Listeria monocytogenes*. *Food Control*, *47*, 231–236. https://doi.org/10.1016/j.foodcont.2014.06.034

Wang, J. M., Zhuang, H., Lawrence, K., & Zhang, J. H. (2018). Disinfection of chicken fillets in packages with atmospheric cold plasma: effects of treatment voltage and time. *Journal of Applied Microbiology*, *124*(5), 1212–1219. https://doi.org/10.1111/jam.13637

Wang, J., Zhuang, H., Hinton, A., & Zhang, J. (2016). Influence of in-package cold plasma treatment on microbiological shelf life and appearance of fresh chicken breast fillets. *Food Microbiology*, *60*(December), 142–146. https://doi.org/10.1016/j.fm.2016.07.007

Wang, J., Zhuang, H., & Zhang, J. (2016). Inactivation of Spoilage Bacteria in Package by Dielectric Barrier Discharge Atmospheric Cold Plasma - Treatment Time Effects. *Food and Bioprocess Technology*, *9*(10), 1648–1652. https://doi.org/10.1007/s11947-016-1746-6

Wang, Q., De Oliveira, E. F., Alborzi, S., Bastarrachea, L. J., & Tikekar, R. V. (2017). On mechanism behind UV-A light enhanced antibacterial activity of gallic acid and propyl gallate against *Escherichia coli* O157:H7. *Scientific Reports*, *7*(1), 1–11. https://doi.org/10.1038/s41598-017-08449-1

Warner, R. D. (2017). *The Eating Quality of Meat-IV Water-Holding Capacity and Juiciness*. *Lawrie's Meat Science: Eighth Edition*. Elsevier Ltd. https://doi.org/10.1016/B978-0-08-

100694-8.00014-5

Weis, T. (2013). The meat of the global food crisis. *Journal of Peasant Studies*, *40*(1), 65–85. https://doi.org/10.1080/03066150.2012.752357

Whitnall, T., & Pitts, N. (2019). Global trends in meat consumption. *Agricultural Commodities*, *9*(1), 96.

WHO. (2015). Global Burden of Foodborne Diseases. Retrieved April 12, 2018, from https://www.who.int/activities/estimating-the-burden-of-foodborne-diseases

Wu, S., Zhang, Q., Ma, R., Yu, S., Wang, K., Zhang, J., & Fang, J. (2017). Reactive radical-driven bacterial inactivation by hydrogen-peroxide-enhanced plasma-activated-water. *European Physical Journal: Special Topics*, *226*(13), 2887–2899. https://doi.org/10.1140/epjst/e2016-60330-y

Yong, H. I., Han, M., Kim, H. J., Suh, J. Y., & Jo, C. (2018). Mechanism Underlying Green Discolouration of Myoglobin Induced by Atmospheric Pressure Plasma. *Scientific Reports*, *8*(1), 1–9. https://doi.org/10.1038/s41598-018-28096-4

Yong, H. I., Lee, H., Park, S., Park, J., Choe, W., Jung, S., & Jo, C. (2017). Flexible thin-layer plasma inactivation of bacteria and mold survival in beef jerky packaging and its effects on the meat's physicochemical properties. *Meat Science*, *123*(January), 151–156. https://doi.org/10.1016/j.meatsci.2016.09.016

Yu, H., Perni, S., Shi, J. J., Wang, D. Z., Kong, M. G., & Shama, G. (2006). Effects of cell surface loading and phase of growth in cold atmospheric gas plasma inactivation of *Escherichia coli* K12. *Journal of Applied Microbiology*, *101*(6), 1323–1330.

https://doi.org/10.1111/j.1365-2672.2006.03033.x

Yusupov, M., Bogaerts, A., Huygh, S., Snoeckx, R., Van Duin, A. C. T., & Neyts, E. C. (2013). Plasma-induced destruction of bacterial cell wall components: A reactive molecular dynamics simulation. *Journal of Physical Chemistry C*, *117*(11), 5993–5998. https://doi.org/10.1021/jp3128516

Zhang, H., Kong, B., Xiong, Y. L., & Sun, X. (2003). Antimicrobial activities of spice extracts against pathogenic and spoilage bacteria in modified atmosphere packaged fresh pork and vacuum packaged ham slices stored at 4 °C. *Environmental Health Perspectives*, *111*(13), 686–692. https://doi.org/10.1016/j.meatsci.2008.11.011

Zhang, Y., Mao, Y., Li, K., Luo, X., & Hopkins, D. L. (2019). Effect of Carcass Chilling on the Palatability Traits and Safety of Fresh Red Meat. *Comprehensive Reviews in Food Science and Food Safety*, *18*(6), 1676–1704. https://doi.org/10.1111/1541-4337.12497

Zhou, G. H., Xu, X. L., & Liu, Y. (2010). Preservation technologies for fresh meat - A review. *Meat Science*, *86*(1), 119–128. https://doi.org/10.1016/j.meatsci.2010.04.033

Zhou, R., Zhou, R., Prasad, K., Fang, Z., Speight, R., Bazaka, K., & Ostrikov, K. (2018). Cold atmospheric plasma activated water as a prospective disinfectant: The crucial role of peroxynitrite. *Green Chemistry*, *20*(23), 5276–5284. https://doi.org/10.1039/c8gc02800a

Zhou, R., Zhou, R., Wang, P., Xian, Y., Mai-Prochnow, A., Lu, X., … Bazaka, K. (2020). Plasma-activated water: Generation, origin of reactive species and biological applications. *Journal of Physics D: Applied Physics*, *53*(30). https://doi.org/10.1088/1361-6463/ab81cf

Zhu, M., Du, M., Cordray, J., & Ahn, D. U. (2005). Control of *Listeria monocytogenes*

contamination in ready-to-eat meat products. *Comprehensive Reviews in Food Science and Food Safety*, *4*(2), 34–42. https://doi.org/10.1111/j.1541-4337.2005.tb00071.x

Ziuzina, D., Misra, N. N., Han, L., Cullen, P. J., Moiseev, T., Mosnier, J. P., … Bourke, P. (2020). Investigation of a large gap cold plasma reactor for continuous in-package decontamination of fresh strawberries and spinach. *Innovative Food Science and Emerging Technologies*, *59*(April 2019), 102229. https://doi.org/10.1016/j.ifset.2019.102229

Ziuzina, D., Patil, S., Cullen, P. J., Keener, K. M., & Bourke, P. (2013). Atmospheric cold plasma inactivation of *Escherichia coli* in liquid media inside a sealed package. *Journal of Applied Microbiology*, *114*(3), 778–787. https://doi.org/10.1111/jam.12087

Ziuzina, D., Patil, S., Cullen, P. J., Keener, K. M., & Bourke, P. (2014). Atmospheric cold plasma inactivation of *Escherichia coli*, *Salmonella enterica serovar* Typhimurium and *Listeria monocytogenes* inoculated on fresh produce. *Food Microbiology*, *42*(September), 109–116. https://doi.org/10.1016/j.fm.2014.02.007

Appendices

Appendix A

Supplemental figures S5

(A) 1 h

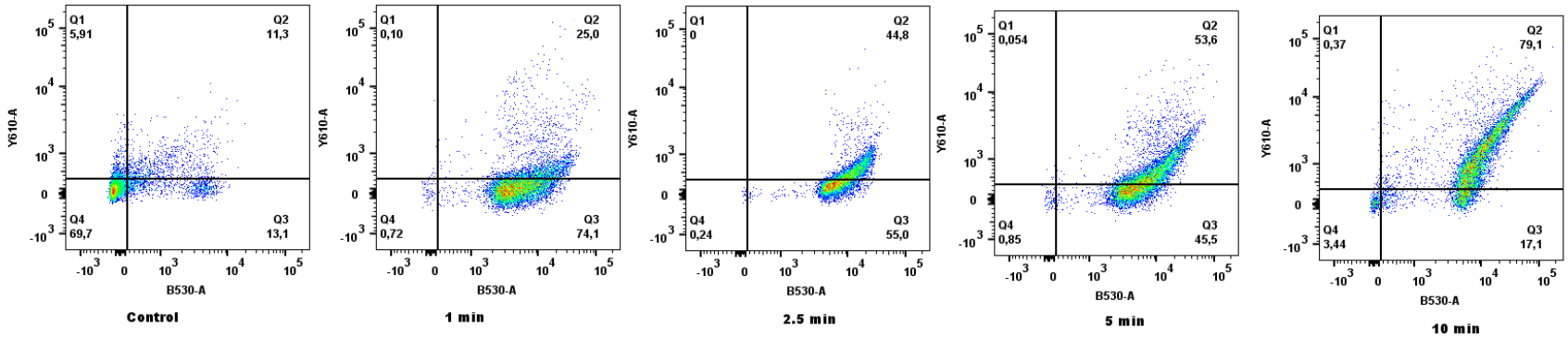

(B) 24 h

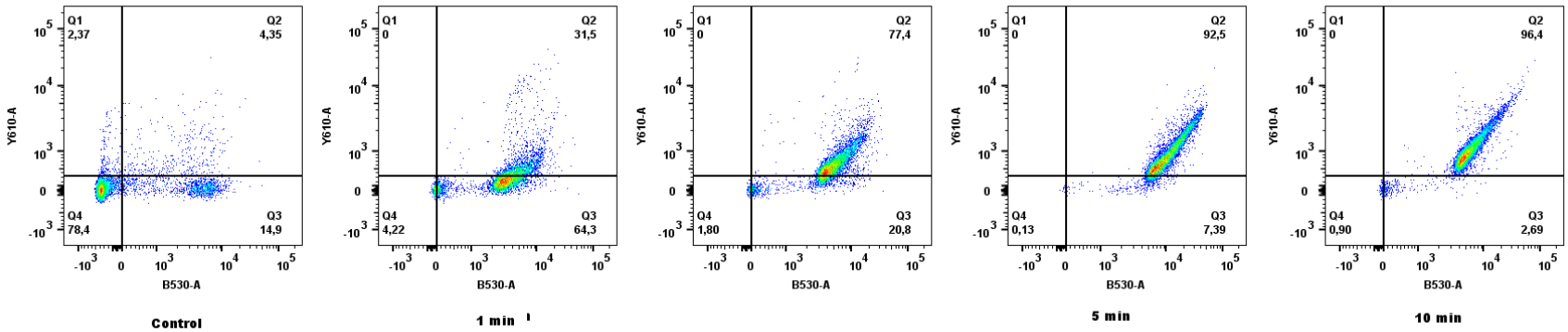

(C) 7 days

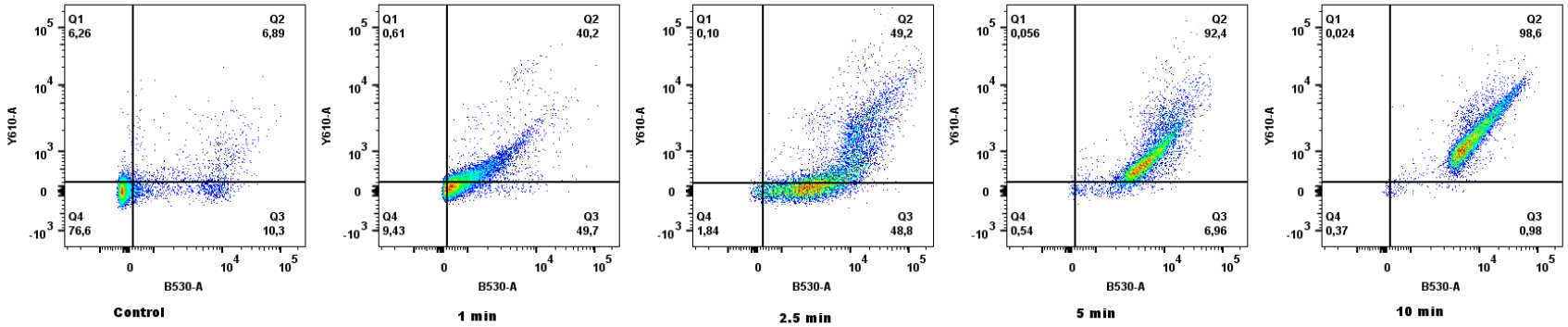

Figure S5.1**:** Flow Cytometry density plot of *L. monocytogenes* after ACP treatment and post-ACP treatment storage to measure membrane integrity. (A) post-treatment storage for 1 h at 4 °C, (B) post-treatment storage for 24 h at 4 °C, (C) post-treatment storage for 7 days at 4 °C. Q1 represents permeabilized cells (PI- fluorescence; Q2 represents slightly permeabilized cells (SYTO9 + PI fluorescence); Q3 represents intact cells (SYTO 9 fluorescence); Q4 represents cells without fluorescence. The horizontal axis represents the SYTO9-green fluorescence intensity of cells. The vertical axis represents the PI-red fluorescence intensity of cells.

Supplementary figures S5

(A) 1 h

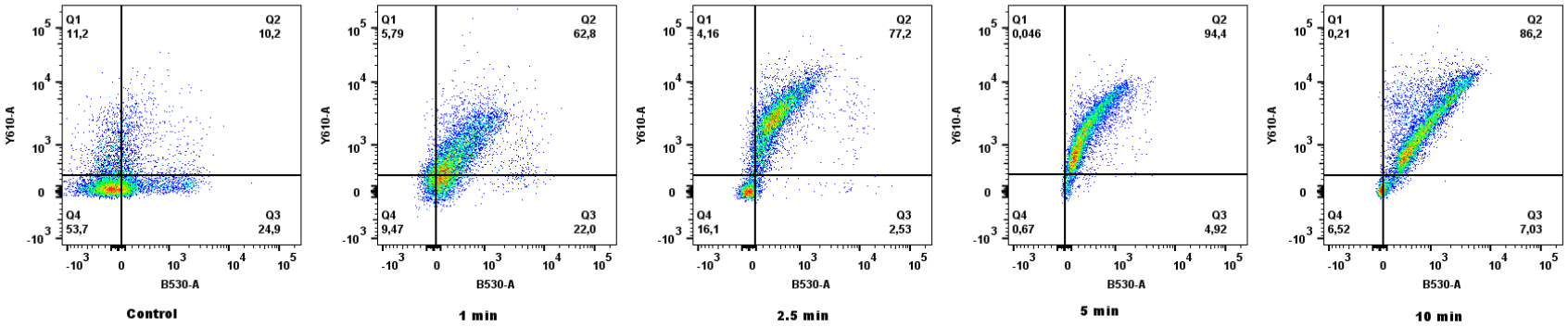

(B) 24 h

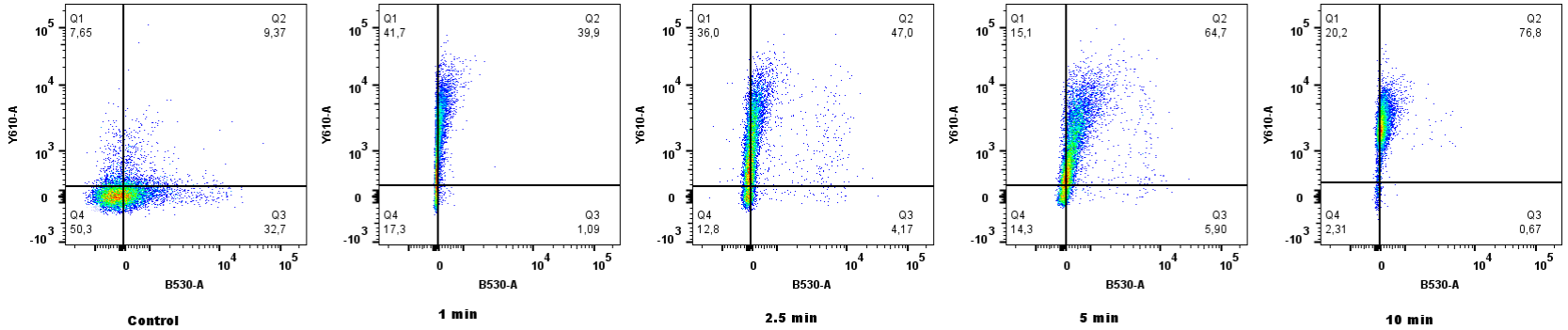

(C) 7 days

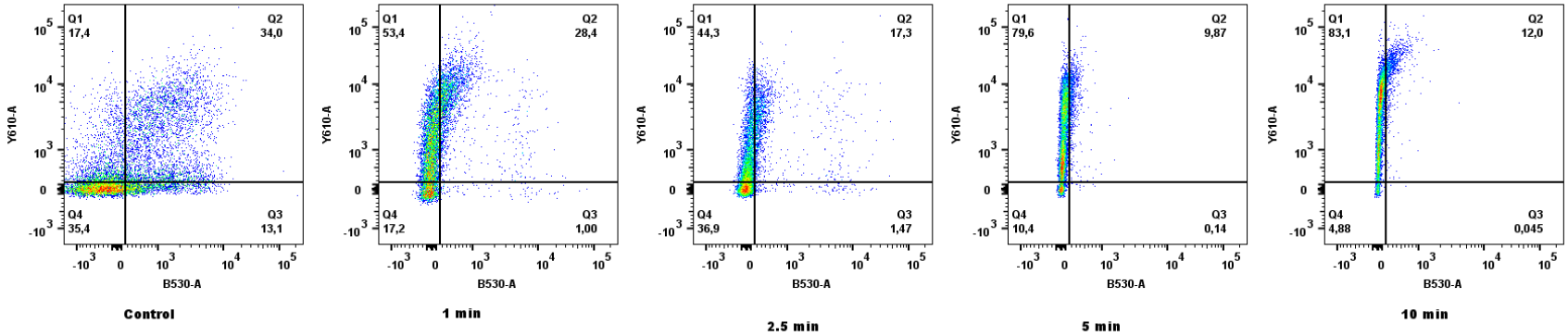

Figure S5.2**:** Flow Cytometry density plot of *L. monocytogenes* after ACP treatment and post-ACP treatment storage to measure esterase activity and membrane integrity. (A) post-treatment storage for 1 h at 4 °C, (B) post-treatment storage for 24 h at 4 °C, (C) post-treatment storage for 7 days at 4 °C. Q1 represents permeabilized cells (PI- fluorescence; Q2 represents slightly permeabilized cells with esterase activity (cFDA + PI fluorescence); Q3 represents intact cells with esterase activity (cFDA fluorescence); Q4 represents cells without fluorescence. The horizontal axis represents cFDA-green fluorescence intensity of cells. The vertical axis represents PI-red fluorescence intensity of cells.

Supplementary Figure S5

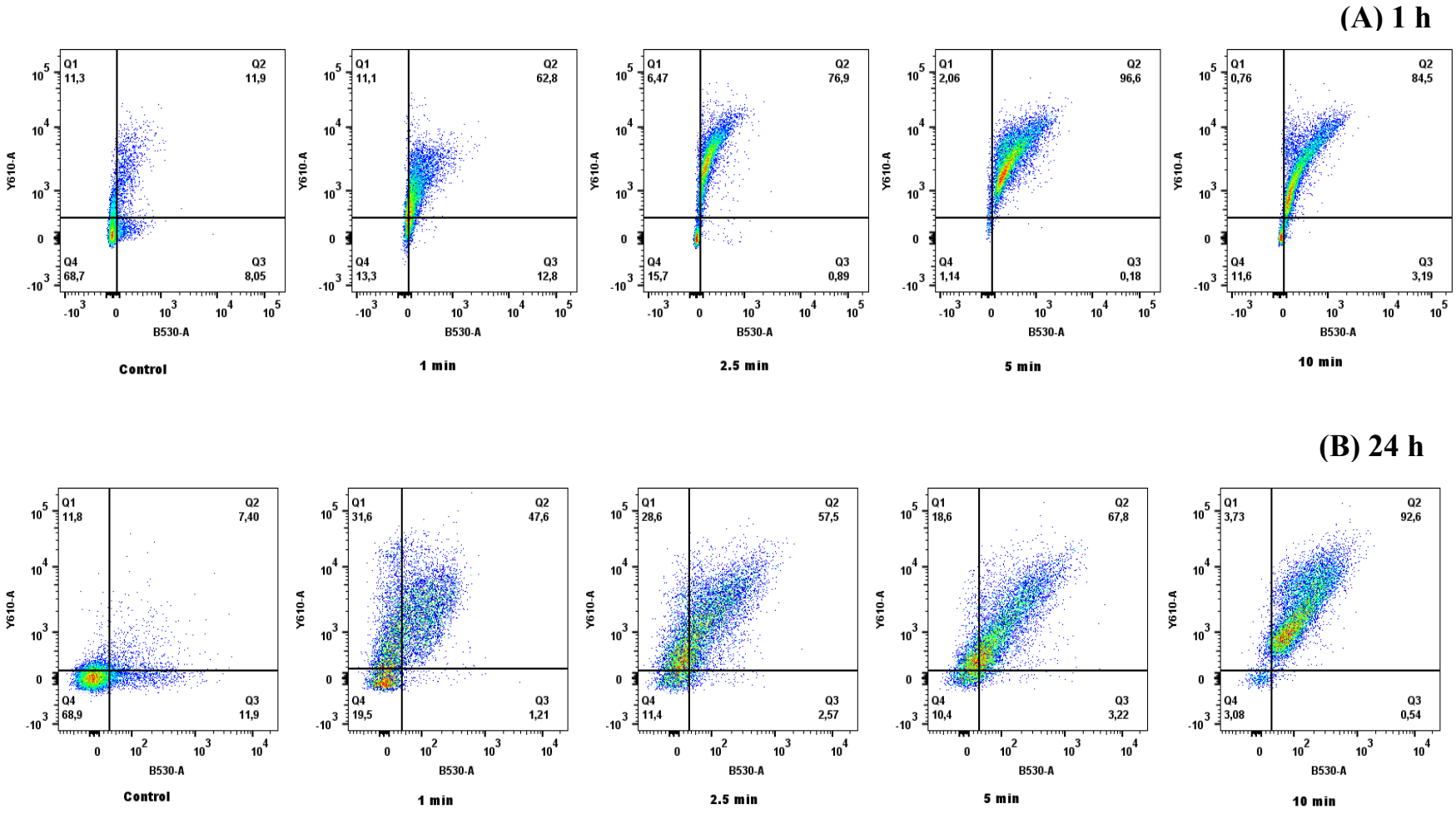

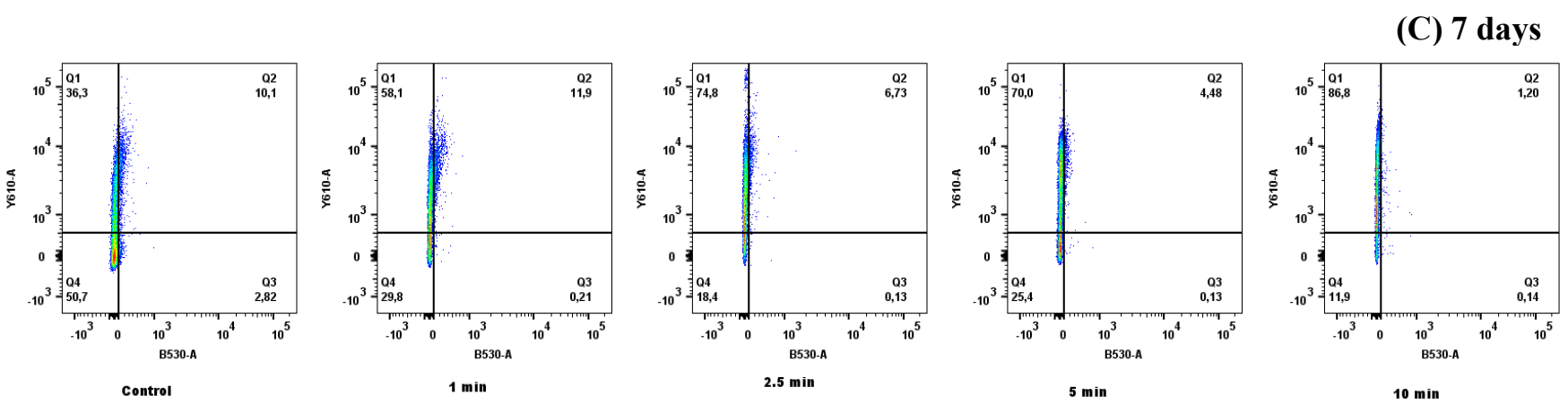

Figure S5. 3**:** Flow Cytometry density plot of *L. monocytogenes* after ACP treatment and post-ACP treatment storage to measure oxidative stress and membrane integrity. (A) post-treatment storage for 1 h at 4 °C, (B) post-treatment storage for 24 h at 4 °C, (C) post-treatment storage for 7 days at 4 °C. Q1 represents permeabilized cells (PI- fluorescence; Q2 represents slightly permeabilized cells with oxidative stress (H2DCFDA + PI fluorescence); Q3 represents intact cells with oxidative stress (H2DCFDA fluorescence); Q4 represents cells without fluorescence. The horizontal axis represents H2DCFDA-green fluorescence intensity of cells. The vertical axis represents PI-red fluorescence intensity of cells.